FINAL PROGRAM

ICMOVPE XV

15th International Conference on Metal Organic Vapor Phase Epitaxy

May 23 – 28, 2010

Hyatt Regency Lake Tahoe
Incline Village, Nevada, USA

Sponsored by:

TMS

LEARN • NETWORK • ADVANCE

http://www.tms.org/Meetings/Specialty/icmovpe-xv/home.aspx/

Welcome to the 15th International Conference on Metal Organic Vapor Phase Epitaxy!

May 23 – 28, 2010 • Hyatt Regency Lake Tahoe • Incline Village, Nevada, USA

Your presence will help build a new chapter in the tradition established by previous conferences on metal organic vapor phase epitaxy (MOVPE) where the latest advances in science, technology and applications of MOVPE and related growth techniques are presented.

This engaging forum features a grand spectrum of specialists from industry, commerce, academia, and national laboratories who are sharing their most recent endeavors in the fundamental and applied aspects of MOVPE technology. You will have the opportunity to engage in a wide range of formal and informal discussions, as well as enjoy diverse technical presentations.

CONFERENCE ORGANIZERS

ICMOVPE-XV has been organized by the following individuals in association with the organizing committees:

- **Conference Chair:**
  Christine Wang, *Massachusetts Institute of Technology-Lincoln Laboratory*
- **Program Co-Chairs:**
  Rajaram Bhat, *Corning*
  Dave Bour, *Alta Devices*
- **Publications:**
  Catherine Caneau, *Corning*
  Thomas Kuech, *University of Wisconsin-Madison*
- **Sponsorship:**
  Russell Dupuis, *Georgia Institute of Technology*
- **Local Arrangements:**
  Steve Denbaars, *University of California-Santa Barbara*
- **Exhibits:**
  Bob Biefeld, *Sandia National Laboratories*

TABLE OF CONTENTS

About the Conference 3
Programming/Proceedings/Policies 3
Schedule of Events 4
Networking & Social Events 4
Floor Plan 5
Optional Tours 6
Technical Program 7

ABOUT THE CONFERENCE

On-Site Registration & Advance Registrant Badge Pick-up

Regency Foyer

Sunday, May 23	3 to 9 p.m.
Monday, May 24	7 a.m. to 5 p.m.
Tuesday, May 25	8 a.m. to 5 p.m.
Wednesday, May 26	8 a.m. to 1 p.m.
Thursday, May 27	8 a.m. to 5 p.m.
Friday, May 28	8 a.m. to noon

Your value-packed registration includes:

- Admission to technical sessions
- Welcome Reception
- Refreshment breaks
- Poster Sessions
- Panel Discussion
- Conference proceedings
- Banquet dinner (included with Full Conference registration only)
- Admission to the exhibition

PROGRAMMING NOTES

Plenary Speakers:

"SSL: The Killer III-V Epi Application"
Jeff Tsao, Sandia National Laboratories, USA

"Recent Progress in Indium Gallium Nitride Based LEDs and LDs"
Takashi Mukai, Nichia, Japan

Invited Papers:

"Wurtzite–Zinc Blende Transition in InAs Nanowires"
Jonas Johansson, Lund University, Sweden

"MOVPE Growth of Lattice Matched III/V Materials on Silicon Substrate for Optoelectronics" **Bernardette Kunert**, Philipps-University Marburg, Germany

"Metamorphic MOVPE Growth for High Quality Lattice-Mismatched III-V Solar Cells Junctions" **John Geisz**, National Renewable Energy Laboratories, USA

"III-V Semiconductor Nanowires-from Crystal Growth to Device Applications" **Takashi Fukui**, Hokkaido University, Japan

"InGaN Based True Green Laser Diodes on Novel Semi-Polar {20-21} GaN Substrates" **Masaki Ueno**, Sumitomo Electric, Japan

"Growth and Characterization of Polar and Nonpolar Nitride Quantum Well Structures" **Menno Kappers**, University of Cambridge, UK

"Impact of Gas-*Phase* and Surface Chemistry during InGaN MOVPE"
J. Randall Creighton, Sandia National Laboratories, USA

"Various Embedded Structures of InGaN LED Employing Selective MOCVD Growth" **Chang-Hee Hong**, Chonbuk National University, Korea

TECHNICAL SESSIONS

(see program details page 8)

All technical programming and conference functions will take place at the Hyatt Regency Lake Tahoe in Incline Village, Nevada.

PROCEEDINGS

One copy of the CD-ROM proceedings is included with each full or student registration. Additional copies may be purchased for $55 each at the TMS registration desk.

POLICIES

Badge Policy
Conference badges must be worn for admission to technical sessions, exhibition and all conference events. Advance registrants must check in at the TMS registration desk to obtain their conference badges.

Audio/Video Recording Policy
TMS reserves the right to all audio and video reproductions of presentations at TMS sponsored meetings. Recording of sessions (audio, video, still photography, etc…) intended for personal use, distribution, publication or copyright without the express written consent of TMS and the individual authors is strictly prohibited.

Photography Notice
By registering for the conference, all attendees acknowledge that they may be photographed by TMS personnel while at events and that those photos may be used for promotional purposes.

Americans with Disabilities Act
TMS strongly supports the Federal Americans with Disabilities Act (ADA) which prohibits discrimination against, and promotes public accessibility for those with disabilities. In support of and in compliance with this act, we ask attendees requiring specific equipment or services to contact TMS personnel at the registration desk.

SCHEDULE OF EVENTS

Sunday, May 23

Registration	3 to 9 p.m.
Welcome Reception	*(Sponsored by Akzo Nobel)* 7 to 9 p.m.

Monday, May 24

Registration	7 a.m. to 5 p.m.
Continental Breakfast	7 to 8:00 a.m.
Plenary Session	8:20 to 9:50 am.
Break	*(Sponsored by Veeco)* 9:50 to 10:20 a.m.
Sessions	10:20 a.m. to noon
Lunch on Own	Noon to 1:30 p.m.
Sessions	1:30 to 3:30 p.m.
Break	3:30 to 4 p.m.
Sessions	4 to 5:20 p.m.
Exhibitors Reception	5:30 to 6:30 p.m.
Dinner on Own	

Tuesday, May 25

Continental Breakfast	7 to 8:30 a.m.
Registration	8 a.m. to 5 p.m.
Invited Talks	8:30 to 9:30 a.m.
Break	*(Sponsored by Dow Chemical)* 9:30 to 10 a.m.
Sessions	10 a.m. to noon
Exhibits Open	9:30 a.m. to 5 p.m.
Lunch on Own	Noon to 1:30 p.m.
Sessions	1:30 to 3:30 p.m.
Break	3:30 to 4 p.m.
Poster Session	4 to 6 p.m.
Panel Discussion/Pizza Party	*(Sponsored by SAFC HiTech)* 6:30 to 9:30 p.m.

Wednesday, May 26

Continental Breakfast	7 to 8:30 a.m.
Registration	8 a.m. to 5 p.m.
Invited Talks	8:30 to 9:30 a.m.
Break	9:30 to 10 a.m.
Sessions	10 a.m. to noon
Exhibits Open	9:30 a.m. to 1 p.m.
Optional Tour Activities	12:30 to 5:30 p.m.
Dinner on Own	

Thursday, May 27

Continental Breakfast	7 to 8:30 a.m.
Registration	8 a.m. to 5 p.m.
Invited Talks	8:30 to 9:30 a.m.
Break	9:30 to 10 a.m.
Sessions	10 a.m. to noon
Exhibits Open	9:30 a.m. to 5 p.m.
Lunch on Own	Noon to 1:30 p.m.
Sessions	1:30 to 3:30 p.m.
Break	3:30 to 4 p.m.
Posters	4 to 6 p.m.
Conference Reception	*(Sponsored by SAFC HiTech)* 6:30 to 7:30 p.m.
Conference Banquet	*(Sponsored by AIXTRON)* 7:30 to 9:30 p.m.

Friday, May 28

Continental Breakfast	7 to 8:30 a.m.
Registration	8 a.m. to noon
Invited Talks	8:30 to 9:30 a.m.
Break	9:30 to 10 a.m.
Sessions	10 a.m. to noon

NETWORKING & SOCIAL EVENTS

WELCOME RECEPTION
(Sponsored by Akzo Nobel)
Sunday, May 23
7 to 9 p.m. .... Lakeside Ballroom

Reconnect with colleagues or network with other professionals and form new alliances at this kickoff event.

EXHIBITORS' RECEPTION
Monday, May 24
5:30 to 6:30 p.m. .... Regency A,B,D,E and Corridor

Browse among the exhibitors and discover the latest services and groundbreaking products in the world of MOVPE and related growth technology in a casual setting.

PANEL DISCUSSION/PIZZA PARTY

The topic of discussion will be "The Role of III-Vs in SSL and Terrestrial PV"
(Sponsored by SAFC HiTech)
Tuesday, May 25
6:30 to 9:30 p.m. .... Lakeside Ballroom

CONFERENCE RECEPTION/BANQUET
Thursday, May 27 .... Lakeside Ballroom
Reception .... *(Sponsored by SAFC HiTech)* 6:30 to 7:30 p.m.
Banquet .... *(Sponsored by AIXTRON)* 7:30 to 9:30 p.m.

HYATT REGENCY LAKE TAHOE

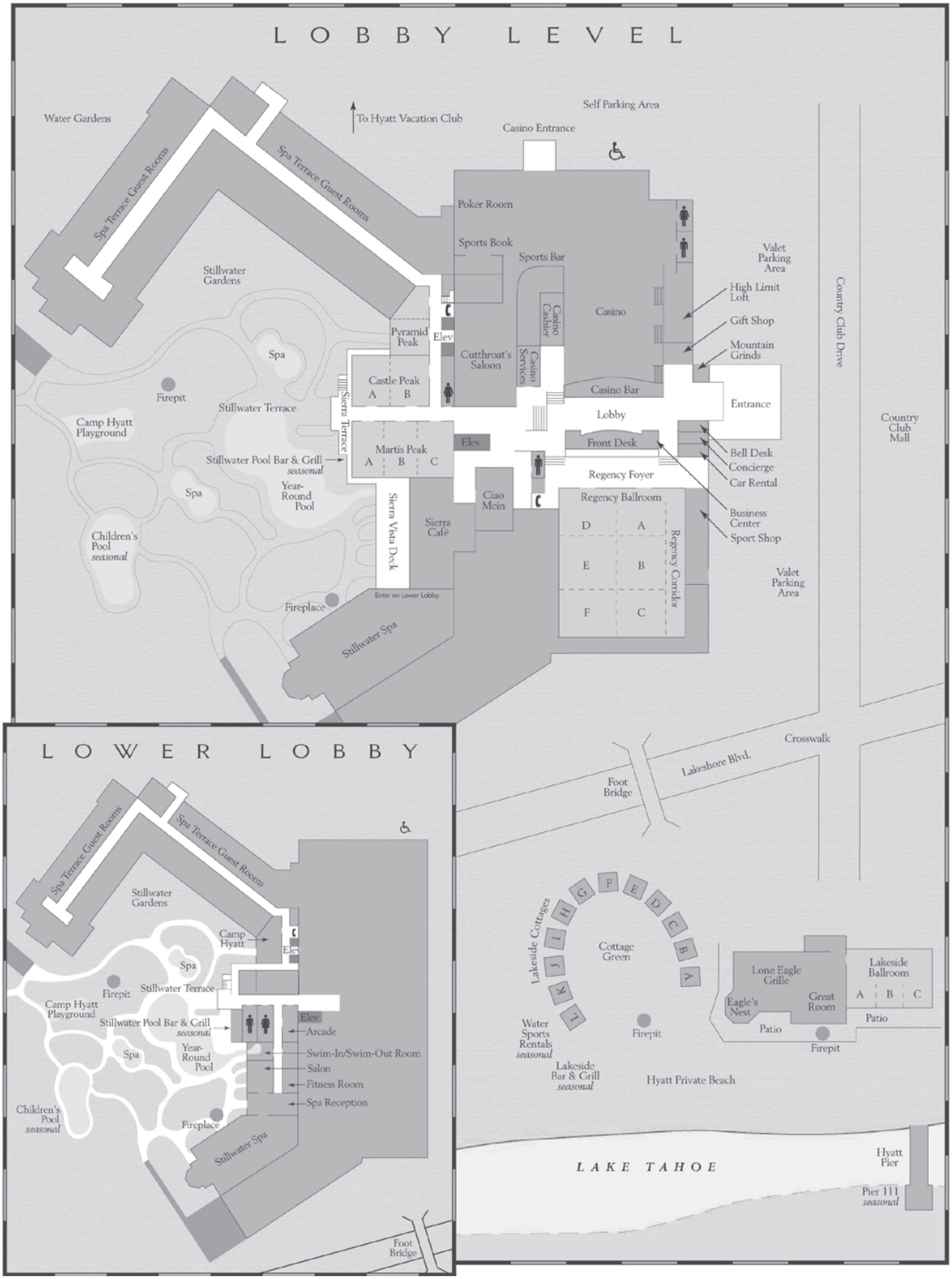
LOBBY LEVEL
Water Gardens
To Hyatt Vacation Club
Self Parking Area
Casino Entrance
Spa Terrace Guest Rooms
Spa Terrace Guest Rooms
Poker Room
Sports Book
Sports Bar
Valet Parking Area
Stillwater Gardens
Casino Cashier
Casino
High Limit Loft
Gift Shop
Mountain Grinds
Country Club Drive
Pyramid Peak
Elev
Spa
Cutthroat's Saloon
Casino Services
Castle Peak
A
B
Casino Bar
Entrance
Firepit
Stillwater Terrace
Sierra Terrace
Lobby
Country Club Mall
Camp Hyatt Playground
Martis Peak
A
B
C
Elev
Front Desk
Stillwater Pool Bar & Grill
seasonal
Bell Desk
Concierge
Car Rental
Regency Foyer
Spa
Year-Round Pool
Ciao Mein
Regency Ballroom
D
A
Business Center
Sport Shop
Sierra Café
Sierra Vista Deck
Children's Pool
seasonal
E
B
Regency Corridor
Valet Parking Area
Fireplace
Enter on Lower Lobby
F
C
Stillwater Spa
Crosswalk
Lakeshore Blvd.
Foot Bridge
LOWER LOBBY
Spa Terrace Guest Rooms
Spa Terrace Guest Rooms
Stillwater Gardens
Camp Hyatt
Elev
Spa
Firepit
Stillwater Terrace
Camp Hyatt Playground
Stillwater Pool Bar & Grill
seasonal
Elev
Arcade
Spa
Year-Round Pool
Swim-In/Swim-Out Room
Salon
Fitness Room
Spa Reception
Children's Pool
seasonal
Fireplace
Stillwater Spa
Foot Bridge
Lakeside Cottages
G
F
E
D
C
B
A
H
I
J
K
L
Cottage Green
Lone Eagle Grille
Lakeside Ballroom
A
B
C
Eagle's Nest
Great Room
Patio
Patio
Water Sports Rentals
seasonal
Firepit
Firepit
Lakeside Bar & Grill
seasonal
Hyatt Private Beach
LAKE TAHOE
Hyatt Pier
Pier 111
seasonal

OPTIONAL TOURS

VIRGINIA CITY HISTORICAL TOUR

Wednesday, May 26	12:30 to 5:30 p.m.
Cost	$70 Per Person

Virginia City was once one of the most prominent cities in the western United States, a place where you can still find fortune and glory today. Gold and silver buried in the mountain, once attracted people from the world over. Follow in the footsteps of the "Bonanza Kings," the mine owners who played an important role in shaping America's economy. Discover the place where Mark Twain took his pen name and began his writing career. Virginia City is a one-of-a-kind destination where you can get your hands on the Wild West on this walking tour. If all the old time shops and saloons are not enough, there are museum tours, mine tours and stagecoach rides available to purchase.

Additional Attractions

- Virginia City Trolley Tour
- Ponderosa Mine Tour
- Historic Fourth Ward School & Museum
- Comstock Gold Mill
- Stagecoach Thrill Ride
- Piper's Opera House
- Western Historic Radio Museum
- Way it Was Museum
- Lunch available at the local saloons or watering holes on Main Street at own expense

(*$2-$10 additional fee for each attraction available at own expense)*

Tour Timing

• Depart Hotel (Meet in main lobby)	12:30 p.m.
• Arrive in Virginia City	1:30 p.m.
• Depart Virginia City	4:30 p.m.
• Guests arrive at hotel	5:30 p.m.

Tour Notes

- Wear comfortable walking shoes, casual attire, light jacket

THE TAHOE QUEEN LAKE CRUISE

Wednesday, May 26	1 to 4:15 p.m.
Cost	$70 per person

Enjoy a memorable experience on the illustrious Tahoe Queen. This famous paddle wheeler was built on the Mississippi River in 1983, then trucked to Lake Tahoe and reassembled. This magnificent boat is 144 feet long and 33 feet wide and features three decks. On this 2.5 hour cruise, just relax, take in the beautiful views, and mingle with others while enjoying a beverage or light appetizers. Comfortable shoes and casual attire with a light jacket are recommended.

Tour Timing

• Board Tahoe Queen from the Hyatt dock	1 p.m.
• Cruise departs	1:30 p.m.
• Arrive back at the Hyatt dock	4 p.m.
• Return from Tahoe Queen excursion	4:15 p.m.

Food and Beverage

- Hosted open bar- Includes beer, wine, bottled water, soft drinks, coffee, and tea
- Light appetizer will be provided

Registration Deadline is Tuesday, May 25, 2010

(Cancellations must be confirmed prior to this date. No refunds will be given for cancellations received after May 25, 2010).

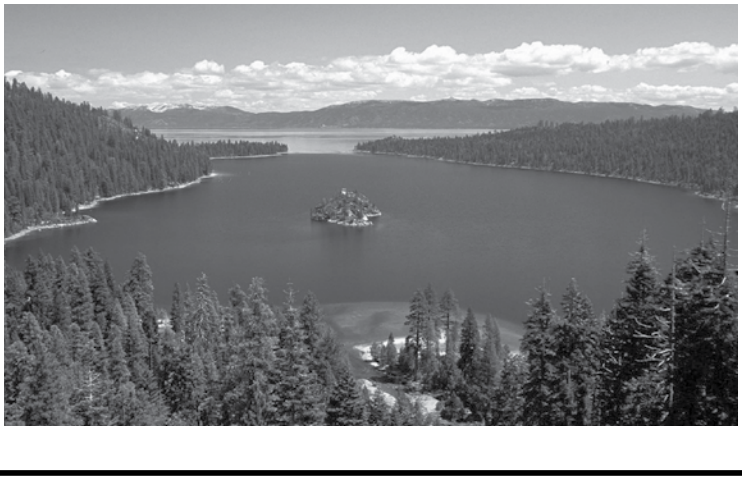

At-A-Glance

Session	Time	Room	Page
Sunday, May 23			
Welcome Reception	7:00-9:00 PM	Lakeside Ballroom	
Monday, May 24			
Opening Remarks	8:00-8:20 AM	Lakeside Ballroom	8
Plenary Session	8:20-9:50 AM	Lakeside Ballroom	8
Coffee Break	9:50-10:20 AM	Regency ABDE	
Nitrides I	10:20 AM-Noon	Lakeside Ballroom	8
Arsenides, Phosphides, Antimonides and Dilute Nitrides	10:20 AM-Noon	Regency C&F	9
Lunch on Own	Noon-1:30 PM		
Patterned and Selective Area Growth	1:30-3:30 PM	Regency C&F	11
In Situ Monitoring and Process Control	1:30-3:30 PM	Lakeside Ballroom	12
Coffee Break	3:30-4:00 PM	Regency ABDE	
Nitrides (LEDs)	4:00-5:20 PM	Lakeside Ballroom	14
Devices I	4:00-5:20 PM	Regency C&F	15
Exhibitors' Reception	5:30-6:30 PM	Regency ABDE	
Tuesday, May 25			
Tuesday Invited Talks	8:30-9:30 AM	Lakeside Ballroom	17
Coffee Break	9:30-10:00 AM	Regency ABDE	
Energy Technology (Solid State Lighting, PV, Thermoelectrics, etc)	10:00 AM-Noon	Lakeside Ballroom	17
Heteroepitaxy - Nanostructures	10:00 AM-Noon	Regency C&F	19
Lunch on Own	Noon-1:30 PM		
Nitrides (Nonpolar and Semipolar)	1:30-3:30 PM	Lakeside Ballroom	20
Characterization	1:30-3:30 PM	Regency C&F	21
Coffee Break	3:30-4:00 PM	Regency ABDE	
Poster Session I	4:00-6:00 PM	Regency ABDE	23
Panel Discussion	6:30-9:30 PM	Lakeside Ballroom	23
Wednesday, May 26			
Wednesday Invited Talks	8:30-9:30 AM	Lakeside Ballroom	24
Coffee Break	9:30-10:00 AM	Regency ABDE	
Nitrides II	10:00 AM-Noon	Lakeside Ballroom	24
Devices II	10:00 AM-Noon	Regency C&F	26
Virginia City Historical Tour	12:30-5:30 PM		
Tahoe Queen Lake Cruise	1:00-4:15 PM		
Thursday, May 27			
Thursday Invited Talks	8:30-9:30 AM	Lakeside Ballroom	28
Coffee Break	9:30-10:00 AM	Regency ABDE	
Nitrides (Devices)	10:00 AM-Noon	Lakeside Ballroom	28
Nanowires	10:00 AM-Noon	Regency C&F	30
Lunch on Own	Noon-1:30 PM		
Novel Materials	1:30-3:30 PM	Regency C&F	31
Arsenides, Phosphides	1:30-3:30 PM	Lakeside Ballroom	33
Coffee Break	3:30-4:00 PM	Regency ABDE	
Poster Session II	4:00-6:00 PM	Regency ABDE	34
Reception	6:30-7:30 PM	Lakeside Ballroom	
Banquet	7:30-9:30 PM	Lakeside Ballroom	
Friday, May 28			
Friday Invited Talks	8:30-9:30 AM	Lakeside Ballroom	35
Coffee Break	9:30-10:00 AM	Regency ABDE	
Nitrides III	10:00 AM-Noon	Lakeside Ballroom	35
Nanostructures	10:00 AM-Noon	Regency C&F	37
Posters			
Poster Session I	Tuesday, 4:00-6:00 PM	Regency ABDE	39-45
Poster Session II	Thursday, 4:00-6:00 PM	Regency ABDE	45-51

Plenary Session

Monday AM May 24, 2010
Room: Lakeside Ballroom
Location: Hyatt Regency Lake Tahoe

Session Chair: Gerald Stringfellow, University of Utah, USA

8:00 AM Opening Remarks

8:20 AM Plenary
SSL: The Killer III-V Epi Application: *Jeffrey Tsao*[1]; [1]Sandia National Laboratories

Throughout its history, lighting technology has made tremendous progress: the efficiency with which power is converted into usable light has increased 2.8 orders of magnitude over three centuries. This progress has, in turn, fueled large increases in the consumption of light and productivity of human society. In this talk, we review an emerging new technology, solid-state lighting: its frontier performance potential; the underlying advances in physics and materials that might enable this performance potential; the resulting energy consumption and human productivity benefits; and the impact on worldwide III-V epi manufacture.

9:05 AM Plenary
Recent Progress in Indium Gallium Nitride Based LEDs and LDs: *Takashi Mukai*[1]; Y. Narukawa[1]; M. Sano[1]; T. Miyoshi[1]; S. Nagahama[1]; [1]Nichia Corporation

The efficiency of white light emitting diodes (LEDs) is growing higher and higher. We demonstrate some kinds of high efficiency white light LEDs. The first one has an extremely high luminous efficiency (η_L) of 249 lm/W and a high radiant flux (ϕ_v) of 14.4 lm at forward current of 20 mA. This η_L is roughly three times as high as that of a tri-phosphor fluorescent lamp (90 lm/W). The blue LED, used for this white LED as an excitation light source, has a light output power (ϕ_e) of 47 mW and an external quantum efficiency (η_{ex}) of 84%. The second one is middle power type white LEDs, by using larger size blue LED. ϕ_v and η_L of this white LED are 203 lm and 183 lm/W at 350 mA, respectively. The blue LED used for this emits 756 mW blue light at 350 mA. Last one is high power white LED using 4 larger size blue LED dies. ϕ_v and η_L are 1913 lm and 135 lm/W at 1 A, respectively. Thus, recent remarkable progress in efficiency makes 'eco LED lighting' possible. Today, longer wavelength laser diodes (LDs) occupy the interest of nitride laser diodes (LDs) research. We introduce InGaN based 488 nm and 518 nm LDs. 488 nm LDs are useful in mainly bio-science equipments. Needless to say, 518 nm LDs are for display applications. The threshold currents and threshold voltages are 45 mA and 5.5 V in 518 nm LDs, 30 mA and 4.5 V in 488 nm LDs, respectively. Lifetime testing showed an estimated lifetime of over 5,000 hours, operating at 5 mW and at 80°C in 515-518 nm LDs. 488 nm LDs had over 10,000 hours estimated lifetime, operated under 60mW and 60°C. These LDs are very promising to replace Ar+ ion laser and SHG green laser.

9:50 AM Break

Nitrides I

Monday AM May 24, 2010
Room: Lakeside Ballroom
Location: Hyatt Regency Lake Tahoe

Session Chairs: Andrew Allerman, Sandia National Laboratories, Albuquerque, NM, USA; Hilde Hardtdegen, Research Center Juelich, Jülich, Germany

10:20 AM
Quaternary AlInGaN Layers Deposited by Pulsed Metal-Organic Vapor-Phase Epitaxy for High Efficient Light Emission: *Michael Jetter*[1]; Clemens Wächter[1]; Alexander Meyer[1]; Peter Michler[1]; [1]Universität Stuttgart

Quaternary nitride alloys offer the possibility to separately adjust the lattice constant and the band gap [1], allowing for example lattice matched growth on GaN with reduced dislocation densities or significant reduction of piezoelectric fields at the GaN/AlInGaN interfaces. AlInGaN epilayers have shown enhanced luminescence emission at room temperature compared to ternary compounds at similar wavelength. This has been associated to the existence of In-rich nanoclusters which were predicted because of an unstable mixing region in the quaternary nitride compounds. More recent ab inito calculations determined that the presence of aluminum in InGaN catalyzes the phase separation process to form In-rich phases [2]. In the past, we have reported on the growth and optical characterization of AlInGaN thick layers, quantum wells [3] and low-dimensional nanostructures [4] deposited by conventional low-pressure metal-organic vapor phase epitaxy (MOVPE). The quaternary structures were controlled varying the precursor flows. A special modification of the vapor phase deposition technique for depositing thin films is to pulse the precursors as for example in the pulsed atomic layer epitaxy. This allows a simple control of the film thickness, sharp interfaces, uniformity over large areas, good reproducibility, and high film qualities at relatively low deposition temperatures. In this contribution we present this growth method of pulsed MO precursor deposition to fabricate AlInGaN layers (nanostructures and quantum wells) and their characterization by x-ray diffraction and photoluminescence spectroscopy. The emission wavelength of the QWs was varied from 370 nm up to 470 nm. The quantum efficiency of the quaternary layers was approx. 5 times higher than comparable ternary QWs. Furthermore we have embedded InGaN quantum wells in quaternary barriers and compare their optical properties to conventional InGaN/GaN quantum wells. [1] Y. Kobayashi, Y. Yamauchi, and N. Kobayashi, Jpn. J. Appl. Phys. 42, 2300 (2003). [2] M. Marques, L. K. Teles, L. M. R. Scolfaro, L. G. Ferreira, and J. R. Leite, Phys. Rev. B 70, 073202 (2004). [3] V. Pérez-Solórzano, A. Gröning, R. Härle, H. Schweizer, and M. Jetter, J. Crystal Growth 272, 386 (2004).[4] A. Gröning,V. Pérez-Solórzano, M. Jetter, and H. Schweizer, Advances in OptoElectronics 2007, 69568 (2007).

10:40 AM
High Quality AlGaN Epilayers Grown Directly on Sapphire without GaN Buffer Layer: *Kamran Forghani*[1]; Martin Klein[1]; Frank Lipski[1]; Stephan Schwaiger[1]; Joachim Hertkorn[1]; Ferdinand Scholz[1]; Martin Feneberg[2]; Benjamin Neuschl[2]; Robert A. R. Leute[2]; Kim Fujan[2]; Ingo Tischer[2]; Klaus Thonke[2]; Oliver Klein[3]; Ute Kaiser[3]; Thorsten Passow[4]; Richard Gutt[4]; [1]Institute of Optoelectronics, University of Ulm; [2]Institut of Semiconductor Physics, University of Ulm; [3]Transmission Electron Microscopy Group, University of Ulm; [4]Fraunhofer-Institut für Angewandte Festkörperphysik

The AlGaN metalorganic vapor phase epitaxy (MOVPE) growth has attracted strong research interests due to the applicability of AlGaN for UV-laser diodes and UV-LEDs. For the latter, a high quality GaN buffer layer on the commonly used sapphire substrate should be avoided in order to minimize internal absorption of the generated UV light. Unfortunately, direct growth of AlGaN on sapphire typically leads to layers with high dislocation density. Poor crystal quality is one of the main reasons for generally low efficiency of optical devices. Therefore, we have investigated the optimization of AlGaN layers directly grown on sapphire by MOVPE. The AlGaN epi-layers with 20% and 30% Al content are the main focus in this work.The quality of the AlGaN epilayers was improved by in-situ nano-masking employing ultra-thin SiNx interlayers. TEM investigations reveal enormous reduction of edge-type dislocation by SiN nano-masking; besides formation of bundles of dislocations is visible converging the surface, leading to large areas up to 1 µm in size on the surface which is almost dislocation free. The SiN surface coverage was carefully optimized resulting in narrower peaks of XRD (102) reflection down to FWHM values of 570 arcsec, followed by a narrow symmetric XRD reflection down to FWHM of 150 arcsec. Furthermore, the SiN interlayers were deposited at different distances from the nucleation layer. Double SiN interlayer structures revealed even higher quality of the epilayers e.g. FWHM of 440 arcsec for (102) XRD reflection. These AlGaN epilayers also have a very smooth surfaces yielding sub-nanometer surface roughness (Rms-value) in AFM investigations. A series of GaN-AlGaN multi quantum wells were grown on samples with different SiN modifications, taking their CL signal as a figure of merit in order to investigate the influence of the AlGaN layer improvements obtained by the SiN interlayers on device-relevant structures. The best MQW structures in regard of the luminescence signal show also very good properties in HRXRD and TEM investigations.These templates have been used as buffer layers for UV LEDs emitting at 355 nm, which demonstrated an output power of 1 mW at 50 mA measured on-wafer.

11:00 AM
Investigation of AlN Buffer Layers on 6H-SiC for AlInN HEMT Grown by MOVPE: *H. Behmenburg*[1]; C. Giesen[2]; U. Heinle[3]; M. Kunze[3]; H. Kalisch[1]; M. Heuken[2]; R. H. Jansen[1]; [1]RWTH Aachen University; [2]Aixtron AG; [3]microGaN GmbH

Silicon carbide (SiC) is at present the reference substrate material for growth of GaN-based high electron mobility transistors (HEMT), mainly due to its relatively small lattice mismatch to GaN and a high thermal conductivity. The usually employed AlN starting layer on SiC further reduces this lattice mismatch. However, AlN thickness, surface morphology and crystal quality play an important role since they strongly influence the quality and insulating properties of the subsequent GaN buffer. In our contribution, a series of four samples was grown on semi-insulating 6H-SiC substrates in AIXTRON metal-organic vapor phase epitaxy reactors. Each sample consists of an AlN starting layer of 270 nm – 350 nm thickness and a 2 µm GaN layer. NH_3 fluxes of 100, 500, 2000 and 3500 sccm were applied during AlN growth in order to investigate the impact on growth mode, coalescence and crystal quality. The GaN layer was grown at identical conditions for all samples. For detailed investigations of surface morphology and coalescence, growth was interrupted after the AlN starting layer as well as after ~200 nm of the GaN layer to enable atomic force microscopy measurements (AFM) at this stage. AFM pictures of the AlN surface indicate a significant change from two-dimensional growth mode for low NH_3 fluxes to three-dimensional growth for high NH_3 fluxes which is attributed to a reduced diffusion length of the Al adatoms. For low NH_3 flux, partial cracking occurred and the formation of holes is observed. X-ray diffraction Omega/2Theta scans show an increasing c lattice constant for the AlN with decreasing NH_3 indicating strain relaxation due to crack formation. The same series was regrown without interruption. This time, a 1 nm AlN interlayer and a 7 nm AlInN barrier layer were added to form a HEMT structure. Buffer breakdown voltage measurements on these samples show a significant decrease with increasing NH_3 flux indicating an impact of the AlN growth conditions. Hall measurements on unpassivated processed wafers show high average electron mobilites exceeding 2100 $cm^2V^{-1}s^{-1}$ at room temperature at a sheet carrier concentration of $1.5 \cdot 10^{13}$ cm^{-2}. Further investigations are ongoing and will be presented in the paper.

11:20 AM
AlN/GaN Heterostructures Grown by Metal Organic Vapour Phase Epitaxy with In Situ Si_3N_4 Passivation: Kai Cheng[1]; Stefan Degroote[1]; *Maarten Leys*[1]; Farid Medjdoub[1]; Joff Derluyn[1]; Bram Sijmus[1]; Marianne Germain[1]; Gustaaf Borghs[1]; [1]IMEC

AlN/GaN heterostructures are very attractive because their 2DEG density may exceed $5\times10^{13}/cm^2$. Recently, AlN/GaN HEMTs with very low sheet resistance (<200 Ω/□) have been demonstrated by MBE [1]. However, there are few reports on AlN/GaN heterostructures grown by MOVPE. The difficulty in growing AlN/GaN heterostructures by MOVPE first results from the large lattice mismatch between AlN and GaN (2.5%) so the critical thickness of AlN on GaN is limited up to 6-8 nm [1]. In addition, the large discrepancy between the optimized growth parameters of AlN and GaN may lead to either strong decomposition of GaN or 3D growth of AlN. GaN is grown preferably at 1000-1100°C with V/III above 1000 while AlN needs to be grown at a very high temperature >1200°C and extremely low V/III ratio ~ 10 [2]. In this work, we show that good quality AlN layers can be grown on GaN at relatively low growth temperatures when TMIn is added to the carrier gas flow. First, 1.3 µm GaN buffers are grown on 4" Si(111) substrates with AlGaN intermediate layers. After the TMGa flow is switched off, the substrate temperature is decreased and the hydrogen ambient is replaced by nitrogen. Then, both TMAl and TMIn are introduced. Analysis by XPS and TEM revealed that at a growth temperature of 900°C or higher no Indium is actually incorporated. Then, various thicknesses of AlN are grown from 2 to 8 nm. Finally, in-situ Si_3N_4 is deposited in order to protect the AlN surface and thus prevent stress relaxation. AFM revealed that the root-mean-square roughness in a 2×2 μm^2 area is 0.25 nm. When the AlN thickness is increased from 2nm to 6nm, the sheet resistance is reduced from 368 down to 181 Ω/□. Van de pauw Hall measurements show the electron density is about $2.5\times10^{13}/cm^2$ in a 4nm AlN/GaN heterostructure. This thus demonstrates that it is possible to grow AlN/GaN HEMT structures by MOVPE with excellent electrical characteristics. [1] Y. Cao and D. Jena, Appl. Phys. Lett. 90, 182112 (2007)[2] Y. Ohba, et al, Jpn. J. Appl. Phys. 36, L1565 (1997).

11:40 AM
MOVPE Growth and Characterization of Non-Polar a-Plane $Al_xGa_{1-x}N$ ($0 \leq x \leq 1$) on r-Plane Sapphire: *Masihhur Laskar*[1]; Tapas Ganguli[2]; A. A. Rahman[1]; M.R. Gokhale[1]; A. P. Shah[1]; Arnab Bhattacharya[1]; [1]Tata Institute of Fundamental Research; [2]Raja Ramanna Centre for Advanced Technology

We report MOVPE growth and characterization of non-polar (11-20) a-plane $Al_xGa_{1-x}N$ epilayers on (1-102) r-plane sapphire substrates over the entire aluminum composition range (0=x=1). The epilayers were grown in a 3x2" close-coupled showerhead reactor using TMGa, TMAl and NH_3 precursors. All epilayers were 0.8 µm thick and were deposited at 50 Torr using a 3-stage AlN nucleation layer and appropriate V/III ratio switching following nucleation to improve crystalline quality. Smooth, uniform and specular layers are obtained for all Al compositions. Optical interference contrast and atomic force microscopy imaging show a striated morphology for a:GaN with a progressive increase in island growth and rms roughness with increasing Al content. The epitaxial relationship $[0001]_{AlGaN} \parallel [-1\ 101]_{Sapphire}$, $[-1100]_{AlGaN} \parallel [11\text{-}20]_{Sapphire}$ was confirmed by high-resolution x-ray diffraction. For comparison, AlGaN epilayers were also deposited on c-plane sapphire substrates in the same run. For c-plane samples biaxial strain from the buffer layer is isotropic; whereas for a-plane oriented films, anisotropic lattice mismatch results in an anisotropic biaxial strain in the epilayer which causes distortion of the hexagonal unit cell. This was confirmed by measuring 'a' and 'c' lattice parameters using several symmetric and asymmetric reflections. It was thus not possible to accurately determine the solid-phase Al composition (x_{solid}) in a-AlGaN using x-ray measurements alone. Thus, we have estimated x_{solid} for both c-AlGaN and a-AlGaN films by fitting the optical transmission data using an appropriate bowing parameter. The variation of x_{solid} as a function of gas phase Al content (x_{gas}) is almost linear. For the same x_{gas} the Al incorporation for a-AlGaN deposited on r-sapphire is lower than that for c-AlGaN deposited on c-sapphire. Further, all a-plane AlGaN films show an in-plane anisotropy in the crystalline mosaicity as revealed from the (11-20) rocking curve width as a function of in-plane rotation. This anisotropy is strongly influenced by Al incorporation and the growth parameters. This anisotropy arises from different types and densities of dislocations that contribute to the x-ray broadening along c- and m-directions and will be discussed in detail. Data for the above results can be viewed online at www.tifr.res.in/~arnab/a_AlGaN.pdf.

12:00 PM Lunch

Arsenides, Phosphides, Antimonides and Dilute Nitrides

Monday AM	Room: Regency C&F
May 24, 2010	Location: Hyatt Regency Lake Tahoe

Session Chairs: Simon Watkins, Simon Fraser University, Vancouver, Canada; Wolfgang Stolz, Philipps-Universität Marburg, Marburg, Germany

10:20 AM
Influence of Sb Surfactant on Carrier Concentration in Heavily Zn-Doped InGaAs Grown by MOVPE: *Tomonari Sato*[1]; Manabu Mitsuhara[1]; Ryuzo Iga[1]; Shigeru Kanazawa[1]; Yasuyuki Inoue[1]; [1]NTT Photonics Labs.

Zn-doped InGaAs layers have been widely used as contact layers in InP-based optoelectronic devices such as lasers and modulators. Increasing the carrier concentration of Zn-doped InGaAs layers is useful for reducing the contact resistance of these devices, which results in high-speed operation. In MOVPE growth, the carrier concentration can be increased by reducing the growth temperature, but it commonly saturates at 2-3 × 10^{19} cm^{-3}. The saturation is attributed to the low incorporation efficiency of Zn atoms into an InGaAs layer. The Zn incorporation depends on the structure of the growing surface, while the surface structure is known to be influenced by the addition of surfactants. In this study, we investigated the effect of Sb surfactant in increasing the carrier concentration in Zn-doped InGaAs layers grown by MOVPE. Zn-doped InGaAs layers were grown on InP (100) substrates in a horizontal MOVPE reactor. Zn and Sb precursors were diethyl-zinc (DEZn) and tris-dimethyl-amino-antimony (TDMASb), respectively. The growth temperature was varied from 500 to 620°C. Zn and carrier concentrations were measured by secondary ion mass spectroscopy (SIMS) and electrochemical capacitance-voltage depth profiling, respectively. For InGaAs layers grown without the TDMASb supply, the carrier concentration increased with reducing growth temperature and/or increasing DEZn flow rate, but it was difficult to obtain a value of more than 3 × 10^{19} cm^{-3}. On the other hand, for InGaAs layers grown with the TDMASb supply, the carrier concentration increased with increasing TDMASb flow rate even when the DEZn was kept at a constant flow rate. SIMS measurements revealed that the Zn concentration in the InGaAs layer was increased significantly with the incorporation of a small amount of Sb. Therefore, increasing in the carrier concentration by supplying TDMASb could be attributed to the surfactant effect of Sb on the Zn incorporation. As a result, we obtained the heavily Zn-doped InGaAs layers with a carrier concentration of 6.5 × 10^{19} cm^{-3}. To the best of our knowledge, this is the highest value ever reported for Zn-doped InGaAs layers grown by MOVPE.

10:40 AM

A Comparative Precursor Study of the Growth Behavior of InSb Using Metal–organic Vapor Phase Epitaxy: *Smita Jha*[1]; Monika Wiedmann[1]; Thomas Kuech[1]; [1]University of Wisconsin-Madison

InSb has become increasingly important for a wide range of infrared and high-speed devices due to its low bandgap and highest electron mobility among III-V compound semiconductors. The growth of high quality InSb films is therefore important to realize the full potential of these InSb-based devices. The MOVPE growth of InSb is however complicated due to several factors. The range of accessible growth temperatures is limited by its low melting point of 525°C. Additionally due to low vapor pressure of all constituents, a precise control of the V/III ratio is required to grow InSb films with good surface morphology. Despite the considerable interest in epitaxial growth of InSb, there are few studies that report the growth mechanism and behavior of InSb using MOVPE. In this study, we have carried out a comparative study of the ethyl and methyl-based sources for InSb growth: TEIn/TESb and TMIn/TMSb with varying precursor mole fractions and growth temperatures. InSb films were grown on both InSb {100} as well as SI GaAs {100} substrates for electrical measurements. The growth temperature was varied from 300-480° C using both precursor chemistries. InSb films grown at 465°C using TEIn and TESb showed indium droplets on the film surface for V/III ratios < 8.5. Films grown at TESb/TEIn ratio ~ 8.5 had good surface morphology with RMS roughness < 1 nm. The growth rate of InSb using TEIn and TESb was constant in the temperature range (430-480°C) at a fixed TEIn mole fraction and V/III ratio. The growth of InSb using TMIn and TMSb however was temperature activated. InSb films grown at 465°C using TMIn and TMSb had mirror smooth surface for a V/III ratio of 6 with no undesired additional phase. This ratio is much higher than the V/III ratio employed for the growth of single-phase GaSb using methyl precursors as unlike TMGa, TMIn is fully decomposed at these temperatures. The properties and kinetics of InSb films grown using both precursor chemistries will be discussed in the context of the Langmuir-Hinshelwood mechanism proposed for the analogous systems in GaSb.

11:00 AM

Cooperative Effects in the Incorporation of Nitrogen into GaAsN Using Mixed Nitrogen Sources: *Thomas Kuech*[1]; Claudio Canizares[1]; Luke Mawst[1]; [1]University of Wisconsin

The growth of the dilute nitride material, GaAs$_{1-x}$N$_x$ has been studied extensively using 1,1-dimethylhydrazine (unsymmetrical dimethylhydrazine, UDMH) as the nitrogen source. The incorporation of nitrogen into these alloys during metal organic vapor phase epitaxy is generally inefficient due to the high nitrogen activity required in order to incorporate small amounts of nitrogen, $x \leq 0.03$ in GaAs$_{1-x}$N$_x$, and the low equilibrium solubility of nitrogen in GaAs. The incorporation of nitrogen from UDMH is thought to follow from the absorption of the molecule through the two N-atoms on adjoining surface sites with its subsequent decomposition. Other sources, such as tertiary butyl hydrazine (TBHy), ammonia and tertiary butyl amine (TBAm) have also been studied but to a lesser extent. A common feature of proposed decomposition and incorporation schemes is the formation at or near the surface of NH or NH$_2$ radicals as a precursor to nitrogen incorporation. The radical reactions are known in MOVPE to create secondary reactive species. This is the case with the presence of methyl radicals which can abstract hydrogen from surface absorbed carbon-containing species which leads to carbon incorporation. This study looks to the cooperative reactions between ammonia and alternative nitrogen sources, such as UDMH, TBHy and TBAm. In particular, the cooperative reactions between radicals produced by these secondary nitrogen sources and excess ammonia can be expected to lead to the formation of NH and NH$_2$ from the ammonia and enhance the incorporation of nitrogen. The combined use of UDMH and ammonia leads to an increase in the nitrogen incorporation above that of UDMH alone with a slight change in growth rate at 515°C when growing GaAsN based superlattices. Ammonia as a single source leads to very low or minimal nitrogen incorporation over a wide range of growth conditions. We will present a comparative study of nitrogen incorporation using ammonia with UDMH, TBHy or TBAm. The combined use of ammonia and a secondary N-source can be a means to increase nitrogen incorporation while minimizing the use of organo-nitrogen compounds. Chemical mechanisms will be discussed for these effects which will discuss the role of radical reactions on nitrogen incorporation.

11:20 AM

Narrow Band Gap Material Grown by Metal Organic Vapor Phase Epitaxy (MOVPE) for Solar Cell Applications: *Toby Garrod*[1]; Peter Dudley[1]; Jeremy Kirch[1]; Sangho Kim[1]; Luke Mawst[1]; Thomas Kuech[1]; [1]University of Wisconsin-Madison

Much work has been reported on the quaternary alloy GaInNAs lattice matched to GaAs, although short minority carrier diffusion lengths, structural defects and high carbon incorporation have limited the performance in MOVPE grown solar cell devices. It has been shown by molecular beam epitaxy (MBE), that the addition of antimony, in dilute amounts to GaInNAs, can improve the internal quantum efficiencies (IQE) of these devices, while maintaining the lattice matched condition to the GaAs substrate [D. B. Jackrel, et al. JAP, 101, 114916 (2007)]. To date, there are no reports on the MOVPE growth of bulk GaInNAsSb alloys. The ability to produce such materials using high throughput MOVPE is an essential requirement for effective commercial exploitation of these new materials in solar cells. Material studies are in progress on GaInNAsSb thin film (bulk) alloys, grown on GaAs (001) substrates utilizing liquid metal organic precursors in a Thomas Swan, close coupled showerhead MOVPE reactor. Confirmed by high-resolution x-ray diffraction (HRXRD) and temperature dependent photoluminescence (PL) measurements, we have successfully grown GaInNAsSb material with band gaps in the range 1.13 to 1.29eV, nominally lattice matched to the GaAs substrate. Van der Pauw-Hall measurements show background carrier concentrations are on the order of 2×10^{17} cm^{-3} for material grown at 525C (200 torr) with growths rates of approximately 1.1 µm/hr. Secondary ion mass spectroscopy (SIMS) has been utilized on selected GaInNAs and GaInNAsSb samples in order to determine the actual compositions of constituent elements. Nominally lattice matched, bulk films have compositions of GaIn$_{(0.07)}$N$_{(0.03)}$As (1eV) and GaIn$_{(0.02)}$N$_{(0.012)}$AsSb$_{(0.01)}$ (1.29eV), respectively. Preliminary annealing studies show a similar blue shift in PL wavelength with the GaInNAsSb material as seen with GaInNAs, on the order of 0.035eV. Studies have also been done on GaInAsSbP as an alternative material, with potential for 1.0 eV bandgap. GaInAsSbP lattice-matched to GaAs with a band gap of 1.37 eV (600C, 100torr and 0.9 µm/hr) has been achieved. We are interested in engineering this material to lower band gap energy and to study the addition of nitrogen. Acknowledgement: This work is funded by Army Research Lab (ARL), contract number W911NF-09-2-0008.

11:40 AM

MOVPE Grown InGaAsN Quantum Wires/Wells Emitting at 1.3µm: Dan Fekete[1]; Romain Carron[1]; *Alok Rudra*[1]; Benjamin Dwir[1]; Pascal Gallo[1]; Eli Kapon[1]; [1]EPFL

Dilute nitride GaInAsN/GaAs alloys are promising for fabricating lasers and single photon emitters at telecom wavelengths(1). Here, we report significant progress on MOVPE of GaInAsN quantum wells (QWs) and V-groove quantum wires (QWRs). A systematic study of incorporation dependence with substrate misorientation is performed, confirming the paramount importance of surface related effects on growth(2). Successful nitrogenation of GaInAs V-groove QWRs is also presented, with emission wavelength of 1200nm at low temperature. Incorporation of N is especially challenging in MOVPE. In order to overcome N desorption, we grow our QWs at low temperature, typically 520°C. Usually such low temperatures are detrimental for the optical quality of QWs. We managed to increase dramatically the N content from 1.4% to 1.7%, which corresponds to an emission red-shift from 1180nm to 1250nm, by using 5° off –(100) substrates. This red-shift is accompanied with a slight linewidth increase, from 20meV to 40meV, which is better than the state of the art, to our knowledge (especially without post-growth annealing). We explain the better results by preferential incorporation at step-edges. Indeed, it is already known that Ga-N bonds are favored in a GaInAsN quaternary. At step edges, Ga concentration is larger; increasing the density of steps thus increases the density of the incorporation sites of N. Another challenge addressed here is the nitrogenation of QWRs. Our GaInAsN V-groove QWRs are grown on patterned on GaAs (100) substrates. Incorporation of N is evidenced by emission redshift to 1200nm at 77K, corresponding to 1300nm at room temperature. The observed linewidth at low excitation power is 20meV, and an excited state appears at higher powers, providing evidence for 2D quantum confinement. Preliminary results show that N experiences capillarity effects like group III adatoms. Thanks to our technology of InGaAs/GaAs pyramidal QDs growth(3) and the successful nitrogenation of QWRs, we are confident that the fabrication of dilute nitride, site controlled QDs on patterned (111)B GaAs substrate can be achieved. (1) M .Henini, Dilute Nitride Semiconductors (Elsevier, Oxford 2005) (2) A. Albo et al. private communication(3) M. Felici et al. Small 5, 938 (2009).

12:00 PM Lunch

Patterned and Selective Area Growth

Monday PM — Room: Regency C&F
May 24, 2010 — Location: Hyatt Regency Lake Tahoe

Session Chairs: Robert Biefeld, Sandia National Laboratories, Albuquerque, NM, USA; Wsevolod Lundin, Ioffe Institute, St. Petersburg, Russia

1:30 PM

Optimization of Selective Area Growth Mask Shape for Fine Band-Gap Tuning in Photonic Integrated Circuits: *Jean Decobert*[1]; Nicolas Dupuis[2]; Alexandre Garreau[1]; Ronan Guillamet[1]; Christophe Kazmierski[1]; [1]Alcatel-Thales III-V Lab; [2]Bell Laboratories, Alcatel-Lucent

The AlGaInAs/InP quaternary system has demonstrated its high potential as an alternative to InGaAsP and has gained a growing industrial acceptance for the new generation of low-cost telecommunication components. In this work, this material system was thoroughly investigated in the selective area growth regime by MOVPE. Computational analysis with a systematic comparison with experiments was conducted to evaluate the growth rate enhancement and compositional variations of ternary or quaternary alloys. These materials were deposited as thin layers or staked in MQW structures, with a specific mask design corresponding to a real opto-electronic device integration scheme. In these integrated components, the high cell density is a requirement and important interferences or proximity effects occur between the different masks. Complex stacking like MQW requires barrier and well strain calculation, not only in the middle of the opened area, where the waveguide ridge is generally placed, but everywhere and especially at the edge of the dielectric masks, where large and uncompensated strain appears. As well, the emitting wavelength, related to the transition splitting between the heavy hole and light hole sub-bands, must be calculated not only for each individual component section but to all the transition area between the different components. This can be of critical importance in devices such as electro-absorption modulators, where low polarization dependency is required. In the classical scheme of multi-component integration along the waveguide ridge, constant characteristics, such as strain or wavelength, are highly desired in each specific component section, while continuous but abrupt transitions of these characteristics are wanted in the interconnection sections. In the case of high mask density, particular attention was paid to interferences between neighboring cells due to the long-range effect of aluminum and gallium species. Therefore, the dielectric masks cannot keep the classical rectangular shape but should integrate specific curvatures to take into account the different specie diffusion lengths and to compensate their effects in specific areas. In this work, different micro and submicro-characterization techniques were used for precise layer analysis and model tuning. Using this approach, we have demonstrated a new 10-Gb/s reflective electro-absorption modulator monolithically integrated with a semiconductor optical amplifier.

1:50 PM

The Growth Behavior of III-V Semiconductor Nanostructures Grown by Nanoscale Selective Area MOCVD: *Hyung-Joon Chu*[1]; Ting Wei Yeh[1]; Lawrence Stewart[1]; P. Dapkus[1]; [1]University of Southern California

III-V semiconductor nanostructures are a unique material phase because of their large surface area and strong quantum confinement. This affords the opportunity to control charge transport and optical properties for applications such as nanoscale transistors, lasers, and detectors. In this regime, the size of structure plays an important role in the materials properties as well as the growth behavior. In this work, InP, GaP, InAs, and GaAs nanostructure arrays are grown by nano-scale selective area MOCVD growth (NS-SAG) to maximize control of the nanostructure size and location. Uniform InP, GaP, InAs, and GaAs nanowire arrays are observed on GaAs and InP (111) substrates by NS-SAG. Extensive transmission electron microscopy shows that the crystal structure of the nanowires has a high density of stacking faults (SFs), which indicates a competition between crystal phases. This is particularly true for InP nanowires that show a strong tendency to grow in the Wurtzite structure. We find the competition is affected by surface kinetics of NS-SAG as well as thermodynamic stability of the crystal phases and this competition can be controlled by the growth rate of the nanowires. We observe that SF density in a nanowire is inversely proportional to the growth rate of nanowires. Because NS-SAG relies on the growth suppression on non-polar planes, precursor concentration must be regulated to achieve the maximum suppression. For precise control, a model was developed which describes the spatial precursor concentration profile as well as complex diffusion mechanisms in NS-SAG. We employ a vapor phase diffusion model with average adsorption approximation which dramatically reduces the computation cost. It predicts the growth rate of nanowires with an error less than 9% and illustrates the effect of the threshold precursor concentration on SF disorder in nanowire growth. *This work was supported in part by the Center for Energy Nanoscience, an Energy Frontier Research Center funded by the U.S. Department of Energy, Office of Science, Office of Basic Energy Sciences under Award Number DE-SC0001013 and by the National Science Foundation under Grant Number ECCS-0901867.

2:10 PM

Growth Behavior and Defect Reduction in Hetero-Epitaxial InAs and GaSb Using Block Copolymer Lithography: *Smita Jha*[1]; Monika Wiedmann[1]; T. Kuan[2]; Susan Babcock[1]; Thomas Kuech[1]; [1]University of Wisconsin-Madison; [2]University at Albany

Defect reduction in hetero-epitaxial growth of lattice-mismatched materials was achieved using nano-patterned GaAs substrates generated by block copolymer lithography. This method is based on the self-assembly of block co-polymer Polystyrene-block-Polymethylmethacrylate to produce full wafer patterning at the 20-nm length scale. The pattern is transferred to an underlying SiO2 mask layer using reactive ion etching. The efficacy of these patterns in reducing defects in lattice-mismatched growths was investigated through the growth of GaSb and InAs. The growth of these lattice-mismatched materials initiates in the nanoscale holes and proceeds laterally over the SiO2 layer. For the case of GaSb growth, film coalescence occurs at nanoscopic island size due to the small 20 nm separation between the growth windows. These coalescing islands are almost fully relaxed and result in a film with reduced threading dislocation density as shown by X-ray and TEM. InAs films were also grown on such nano-patterned GaAs substrates. In order to reduce the indium adatom diffusion at the employed growth temperatures (450-650°C), a thin ~ 1nm thick layer of Al0.07Ga0.93As was grown prior to InAs growth. This thin Al0.07Ga0.93As layer enhances the InAs nucleation within the nanoscopic holes resulting in a uniform array of InAs dots. Unlike GaSb, the increased surface mobility of indium at high growth temperatures (>450°C) does not readily result in a coalesced film. The addition of incoming atoms to fully relaxed islands over islands with some residual strain was observed, resulting in formation of large islands as opposed to a film on the substrate. This behavior is attributed to the increase in surface migration length of the adatoms at higher temperatures wherein the incoming atom would choose to attach to the most strain-relaxed island. When the growth temperature was reduced to 450°C a coalesced InAs film was observed. These initial results of InAs growth on nano-patterned substrates suggest that the balance between surface diffusion and the rate of adatom attachment must be balanced through choice of growth temperature in order to achieve a uniform InAs film with a reduced defect density.

2:30 PM

Void Shape Control in GaN Re-Grown on Hexagonally Patterned Maskless GaN: *Muhammad Ali*[1]; Alexei Romanov[2]; Sami Suihkonen[1]; Olli Svensk[1]; Pekka Törmä[1]; Markku Sopanen[1]; Harri Lipsanen[1]; Maxim Odnoblyudov[2]; Vlad Bougrov[2]; [1]Helsinki University of Technology; [2]Optogan

We present the experimental findings on the void formation and control of the void shape in the process of GaN re-growth on hexagonally patterned GaN templates using sapphire as substrate. Formation of voids is known to be typical for the re-growth on patterned GaN [1]. However, controlling the shape of the voids has not been addressed as yet. The knowledge of the void configurations in GaN layers and a possibility to control their shape could potentially help in enhancing the light extraction from the light emitting structures [2]. Metal organic vapor phase epitaxy is used as the primary growth technique and inductively couple plasma (ICP) etching is used to define hexagonal patterns in the GaN layers. The etching of GaN layers inside the hexagonal holes is performed down to GaN/sapphire interface using the Ar/Cl2 etch chemistry. The sidewall angle of the voids can be controlled from near vertical to fully inclined (angles of about 60 degrees) configurations. It was found out that the initial aspect ratio (etch depth / hexagon hole diameter) of the hexagonal patterns plays a key role in determining the final shape of the voids. Backed by our experimental results, we propose a growth model pertaining the mechanism of void shape formation. The x-ray diffraction analysis of the re-grown layers shows that the re-grown material is either comparable or of improved crystalline quality depending upon the size and shape of voids. The measure of twist angle is often considered to be connected to the density of edge type threading dislocations [3]. For comparison, we present the twist angle measurement results from the re-grown layers that contain voids of different shape. [1] T.S. Zheleva, S.A. Smith, D.B. Thomson, K.J. Linthicum, P. Rajagopal and R.F. Davis, J. Elect. Mat. 28 (1999) L5-L8. [2] T. Kaneko, K. Horimo, H. Yamamoto, H. Ito and A. Kuramata, J. Light Vis. Env. 32 (2008) 124-128. [3] H. Heinke, V. Kirchner, S. Einfeldt and D. Hommel, Appl. Phys. Lett. 14 (2000) 2145-2147.

2:50 PM

Growth of High Quality InP Layers in Si STI Trenches on Si (001) Substrates: *Gang Wang*[1]; Duy Nguyen[2]; Maarten Leys[2]; Roger Loo[2]; Olivier Richard[2]; Guy Brammertz[2]; Marc Meuris[2]; Marc Heyns[1]; Matty Caymax[2]; [1]IMEC/KULeuven; [2]IMEC

Epitaxial growth of III-V compound semiconductor materials has been extensively studied in the past decades. To integrate III-V materials on Si substrates for CMOS device fabrication, extended defect free thin layers are required. Selective epitaxial growth (SEG) in shallow trench isolation (STI) structures on Si (001) provides a solution. The advantage of SEG in submicron STI trenches is the extended defect necking effect, which provides the feasibility of making extended defect free materials in device regions despite the large lattice mismatch between the epitaxial layers and the Si substrates. However, STI side walls often induce undesired stacking faults and microtwins. In this work, we report the defect formation mechanism of InP layers in STI trenches on exact and offcut Si (001) substrates. In SEG, The stacking fault formation is strongly associated with several factors, such as the local growth rates, the shape of STI walls, and the trench orientation on offcut substrates. The local growth rates change with pattern size and pattern density due to the loading effect. The STI wall plays an important role in stacking fault formation because of the steric hindrance effect. On offcut substrates toward (111), the trench orientation has an impact on stacking fault formation and high quality InP layers were obtained in the [110] oriented trenches as confirmed by our XTEM images. Photoluminescence measurement showed the InP peak despite the broader peak compared with the InP reference substrate due to the defects close to the InP/Ge interface. We also obtained similar good quality InP layers in trenches narrower than 100 nm on Si (001) exact substrates. The details of stacking fault and microtwin formation mechanism in STI trenches will be presented in the conference. In summary, we investigated the stacking fault formation mechanism of InP SEG in STI trenches on offcut and on-axis Si (001) substrates. This study gives some insights for optimizing InP SEG on Si(001) substrates.The authors acknowledge the support of the European Commission from the project DUALLOGIC for part of this work.

3:10 PM

Highly Lateral Growth of InGaAs on Si(111) with Reduced Size of Selective Growth Window: *Yoshiyuki Kondo*[1]; Momoko Deura[1]; Mitsuru Takenaka[1]; Shinichi Takagi[1]; Yoshiaki Nakano[2]; Masakazu Sugiyama[1]; [1]Department of Electrical Engineering and Information Systems, School of Engineering, The University of Tokyo; [2]Research Center for Advanced Science and Technology, The University of Tokyo

InGaAs growth on a selected part of Si wafer is an essential technology for implementation of high-speed and/or low-operation-power MISFETs on a Si platform; InGaAs is a desirable material for an electron channel because of its high electron mobility and moderate bandgap. By using micro-channel selective area growth (MC-SAG) with MOVPE, we have successfully obtained dislocation-free InGaAs lateral micro-discs on patterned Si surface. In order to implement MISFETs on such micro-discs, a diameter of the disc should be more than a couple of micrometers and a height should preferably be smaller than 0.1 µm. A key issue for obtaining dislocation-free InGaAs discs is a single InAs island in a single growth window, which leads to a single-domain crystal. In addition, the height of an InGaAs disc is primarily determined by that of the initial island. In order to obtain a small InAs island on a growth window, it is effective to reduce the diameter of the window. We here try to use the growth windows with 1 µm in diameter, as compared with our previous 2-µm-in-diameter windows. Growth windows were patterned on a Si(111) surface with thermal oxide and electron beam lithography. InAs islands were initially grown on the windows with TMIn and TBAs. TMGa was then introduced to initiate lateral growth of InGaAs. We first focused on the growth of InAs islands. Uniform nucleation was difficult to achieve in the 1-µm-in-diameter windows. We modulated TBAs partial pressure: initial low partial pressure to obtain a single nucleus selectively in a window, and high partial pressure after nucleation to obtain flat InAs islands. As a result, we obtained a single InAs island in a growth window with 0.1 µm in height, which is 3 times smaller than conventional InAs islands with the 2-µm-in-diameter windows. Subsequent growth of InGaAs on such small islands resulted in InGaAs discs with the average height of 320 nm and average diameter of 4.8 µm, which is a significant progress compared with the InGaAs islands (430 nm in height and 3.6 µm in diameter) using the 2-µm-in-diameter windows. Smaller growth window is indeed better for highly-lateral InGaAs.

3:30 PM Break

In Situ Monitoring and Process Control

Monday PM	Room: Lakeside Ballroom
May 24, 2010	Location: Hyatt Regency Lake Tahoe

Session Chairs: Nigel Mason, ORS, Ltd., St. Asaph, Denbighshire, UK; Thomas Zettler, LayTec GmbH, Berlin, Germany

---

1:30 PM

Reflectance Anisotropy Spectroscopy Assessment of the MOVPE Growth of III-V Compounds on Germanium: *Enrique Barrigon*[1]; Beatriz Galiana[1]; Ignacio Rey-Stolle[1]; [1]Solar Energy Institute - Politechnical University of Madrid

During the last decades there has been an increasing interest in the heteroepitaxy of III-V semiconductors on germanium (Ge). Nowadays, Ge wafers are mostly used in the manufacture of solar cells though there are other emerging applications which are starting to gather momentum, such as photodetectors, LEDs, magnetoresistive sensors and even HEMTs. The basic knowledge of the state at atomic level of the surface of the Ge wafer during the pre-growth steps and of the initial monolayers of the heteroepitaxial growth of the III-V on Ge can be advantageous in order to be able to understand the nucleation of III-V on Ge and therefore optimize the process [1]. In this way, reflectance anisotropy spectroscopy (RAS) [2] turns out to be a non-destructive powerful tool to monitor surface preparation before growth and characterize the surface reconstruction prior and during growth, among others [3]. This work will present and analyze the in-situ RAS measurements of the Ge wafer prior to and during MOVPE epitaxial growth of a GaInP nucleation layer. Particularly, different aspects of the growth will be studied: a) RAS spectra of Ge wafers at different prenucleation conditions (group V partial pressure; pre-growth anneal temperature and time,...); b) RAS signal during the growth of GaInP nucleation layer at different growth conditions (V/III, growth rate, growth temperature, ...); and c) RAS signal of Ge substrates with different characteristic (as received, aged,...). In summary, this work will outline the potential of this tool to explore, and therefore optimize, the nucleation routine within MOVPE environment that leads to high quality III-V semiconductor layers on Ge. [1] J. Olson, W.E.McMahon, Proc. of the 2nd world conference and exhibition on photovoltaic solar energy conversion, 1998. [2] D. E. Aspnes, A. A. Studna, Physical Review Letters. 54 (17) (1985) [3] W. Richter, J.-T. Zettler, Applied Surface Science 100-101 (1996).

1:50 PM

Watching the Formation of Si(100) Surfaces via In-Situ RDS for Subsequent III-V-MOVPE Preparation: Sebastian Brueckner[1]; Anja Dobrich[1]; Peter Kleinschmidt[1]; Henning Doescher[1]; *Thomas Hannappel*[1]; [1]Helmholtz-Centre Berlin for Materials and Energy

The technological interest in the superior electronic and opto-electronic properties of III-V compounds advances the research for their integration on standard silicon substrates. Hence, the formation of III-V films on silicon with significantly reduced defect concentration is a great task not only for multi junction solar cells, but for opto- and micro-electronic devices in general. In particular, the reduction of undesirable anti-phase disorder necessitates the formation of double atomic steps instead of the typical two-domain (2x1)/(1x2) surface reconstruction of Si(100) associated to single atomic steps. MOVPE is technologically well-established for III-V growth, but there is much less experience in the preparation and analysis of qualified Si(100) surfaces via MOVPE. It will be shown here that in-situ reflectance difference spectroscopy (RDS) can identify already in the MOVPE reactor the complete removal of intrinsic silicon oxides for different types of substrates' off-cut orientations (0°, 2°, 6° toward <111>), the generation of a suitable atomic surface structure as well as the H-termination. The in-situ signals have been benchmarked via a contamination-free transfer system from MOVPE to UHV and employing surface science tools like Fourier Transform Infrared Spectroscopy, Scanning Tunneling Microscopy, and

Low Energy Electron Spectroscopy. In addition, X-ray Photoelectron Spectroscopy provided direct observation of the oxide layers on native and wet-chemical prepared substrates as well as their removal under specific process parameters. Besides the critical influence of the realized surface temperature, the results also depended on the pressure and choice of the process gas (H2, N2, or Ar). Our RD spectra measured in the MOVPE reactor were consistent with results reported in the literature that were derived from UHV studies. The oxidized surfaces of Si(100) with 6° off-cut did not exhibit any reflection anisotropy. After the complete oxide removal at a surface temperature below 1000°C, we obtained the typical spectrum of the clean Si(100) surface. Benchmarking of the RDS signals enabled us to prove the oxide removal from the surface in situ by transient RAS measurements. Transient measurements at the characteristic energy of the clean Si spectrum show the change from oxidized to clean Si(100) surface for different preparation parameters.

2:10 PM

In Situ Quantification of III-V/Si(100) Anti-Phase Domains for the Indirect Evaluation of Substrate Surfaces: *Henning Döscher*[1]; Sebastian Brückner[1]; Jens Ohlmann[2]; Andreas Beyer[2]; Anja Dobrich[1]; Oliver Supplie[1]; Kerstin Volz[2]; Wolfgang Stolz[2]; Thomas Hannappel[1]; [1]Helmholtz-Zentrum Berlin für Materialien und Energie; [2]Phillips University Marburg

Beyond the in situ identification of the well-established atomic GaP(100) surface structures, in situ reflection anisotropy spectroscopy (RAS) was applied as a quantitative probe of anti-phase domains (APDs) in heteroepitaxial films deposited on Si(100). The precise interpretation of the in situ data with respect to the APD content required specific experiments to identify the different origins of changes in the RAS measurement: The shape and intensity of the RA spectra taken on homoepitaxial GaP(100) surfaces in the MOVPE reactor already varied significantly with measurement conditions. In particular, we considered the temperature, reconstruction and atomic order of the surfaces. Due to the presence of anti-phase disorder, we expected a linear reduction of the RAS signal measured at heteroepitaxial GaP films deposited on Si(100) in comparison to the established RA spectrum of the P-rich GaP(100) surface typical for MOVPE preparation. Beyond that, we observed characteristic deviations between these RA spectra which originated from reflections at the additional GaP/Si(100) hetero-interface. Simple interference affecting the normalization of the RAS signal was found as a major source of the deviations and, thus, corresponding corrections were applied on the RA spectra. This operation improved the agreement of the GaP/Si(100) RA spectra with the homoepitaxially grown GaP(100) reference significantly and is essential for the accuracy and reliability of the in situ APD quantification via RAS. This provided several advantages over the established methods of APD characterization techniques, including transmission electron microscopy (TEM) and atomic force microscopy (AFM), which are not applicable in situ and principally only cover relatively small sample areas. Statistical AFM and TEM evaluations of the homogeneity of APD distributions on typical GaP/Si(100) samples revealed that the implicit lateral integration during RAS measurement is a key advantage of the presented APD quantification method. Its application was even beneficial for the indirect non-destructive in situ characterization of the step structure of Si(100) substrate surfaces prior to heteroepitaxy. If specific growth conditions forced the propagation of the anti-phase boundaries (APBs) perpendicular to the surface, the APD structure of the GaP film reflected the surface reconstruction terraces on the Si(100) substrate, since single layer steps initiate the APBs.

2:30 PM

In-situ Monitoring of GaAs Grown on Si(100) by Metal Organic Chemical Vapor Deposition: *Zhenyu Zhong*[1]; Kei May Lau[1]; [1]Hong Kong University of Science and Technology

Reflectance anisotropic(RA)/difference(RD) techniques have been utilized for in-situ monitoring of the MOCVD process for many years. Surface reconstruction of the growing epitaxial layers can be interpreted from the signature of the RA Spectrum (RAS). However, most of the reports have been focused on either homoepitaxial processes or growth after nucleation in heteroepitaxy. Very few studies involved a discussion of the initial/nucleation stage in heteroepitaxy, which is extremely critical to the subsequent epi-layer quality. In this paper, RAS study of MOCVD grown GaAs on Si(100) substrates is described. A two-step growth technique involving low and high temperatures was successfully developed for the process. Smooth high quality GaAs layers on Si(100) substrates with no miscut can be used as templates for subsequent growth of metamorphic device structures, including those lattice-matched to InP. The RA signal was monitored by an EpiRAS 2000 system. During the low temperature nucleation process, the time resolved RA signal at 2.55eV shows a damped oscillation profile. The amplitude of the first period of the oscillation, somewhat larger than the RA signal originated from surface chemistry, is a result of 3-dimensional growth during the initial stage, where the anisotropic nuclei elongated along the [011] direction are being formed. This oscillation was used to precisely control the nucleation time, which is of critical importance to obtain high quality GaAs epi-layers on Si substrates. Experimental results suggest that the best end-point of nucleation is at the time when the RA signal reaches its first peak value. The coverage of the Si surface at this point is maximized, which is good for mismatch accommodation and surface morphology of the grown layer. The growth temperature was ramped up afterwards for subsequent high temperature growth.The RA signal changed dramatically once switched to high temperature growth, implying surface roughening. This signifies an 3-D to 2-D transition process during initial high temperature growth. In the final epi-layer, penetrated threading dislocations will lead to spiral growth, resulting in hillocks on the surface. This adverse surface roughening effect modifies the surface anisotropy. A RAS signature deviated from the well-known “As-terminated” indicates final undesirable epitaxial quality.

2:50 PM

Strain-Balanced MOVPE of InGaAs/GaAsP Multiple Quantum Wells Using *In Situ* Surface Reflectance, Anisotropy and Curvature Monitoring: *Masakazu Sugiyama*[1]; Kenichi Sugita[1]; Yunpeng Wang[1]; Yoshiaki Nakano[1]; [1]University of Tokyo

Strain-balanced pseudo-morphic growth of multiple quantum wells (MQWs), which is mandatory for high-efficiency solar cells and quantum cascade lasers, is indeed a challenge for MOVPE. In order to avoid lattice relaxation that leads to threading dislocations, we need elaborate strain balancing between a well and a barrier by controlling both layer thickness and atomic content. *In situ* monitoring is potentially a great aid for such growth conditioning. We here adopted typical optical *in situ* monitoring methods in order to observe strain behavior of InGaAs/GaAsP MQWs that is the heart of high-efficiency III-V tandem photovoltaic cells. Total reflectance of the surface is the simplest monitor. At the initial growth stage, reflectance exhibited steady Fabry-Perot oscillation due to existence of multiple interfaces within an optical penetration depth. With successful strain balancing, an average level of reflectance remained constant with large number of MQWs. If average strain was imbalanced, reflectance started to drop monotonically in the middle of the growth, indicating surface roughening. The total reflectance cannot detect lattice relaxation itself, but resultant surface roughening can be detected. In this sense, the total reflectance is an indirect but concise monitor of strain balancing. Reflectance anisotropy is potentially sensitive to the topmost surface in terms of both atomic content and strain, which we intend to use to obtain abrupt hetero interfaces. For MQWs, however, strain at hetero-interfaces causes interference and makes transient anisotropy signal quite complexed. Curvature of a wafer is a direct measure of accumulated strain. An issue is whether or not we can detect subtle strain values, which is roughly ±1% in each ~10-nm-thick layer resulting in an average strain of less than 1000 ppm. With a novel high-sensitivity curvature sensor, we have successfully observed periodic linear oscillation of curvature. When strain balancing is quite successful, one period of InGaAs and GaAsP resulted in no shift of curvature baseline; a drift in the baseline is a measure of an averaged strain. If strain balancing is unsuccessful, such a periodic behavior collapsed indicating lattice relaxation. Curvature is, therefore, a direct and quite sensitive measure of strain.

3:10 PM

Uniformity of the Wafer Surface Temperature and Emission Wavelength during MOVPE Growth of GaN-Based Laser Diodes: *Veit Hoffmann*[1]; Arne Knauer[1]; Frank Brunner[1]; Sven Einfeldt[1]; Markus Weyers[1]; Günther Tränkle[1]; Kolja Haberland[2]; J.-Thomas Zettler[2]; Michael Kneissl[3]; [1]Ferdinand-Braun-Institut für Höchstfrequenztechnik; [2]LayTec GmbH; [3]Technische Universität Berlin

GaN-based laser diodes (LDs) are usually epitaxially grown on GaN substrates. However, for cost reasons the development of growth processes for these devices is often conducted on sapphire substrates which have different thermal properties compared to GaN substrates. In this work the influence of the substrate material on the emission wavelength distribution of LDs around 405 nm is investigated. The LD structures were grown on sapphire and GaN substrate in a multi-wafer *AIX2400G3-HT* MOVPE reactor equipped with a *EpiCurveTT* in-situ sensor capable of measuring wafer curvature, pocket temperature and 405 nm reflectance and a *Pyro 400* system measuring the 400 nm emission light from the GaN layer. By this the real temperature at the wafer surface is measured and not only the temperature of the pocket. Because of the susceptor rotation in the planetary reactor, the wafer moves under the viewport allowing to measure the spatial uniformity of the temperature across the wafer. Since the indium incorporation in the quantum wells of the active region is strongly influenced by the temperature on the wafer surface, we can directly correlate the active region growth conditions and the properties of the substrate material with the absolute value and the spatial uniformity of the emission wavelength of the LDs.On both substrates the lattice mismatch induced stress results in a strong wafer bow before deposition of the active region. Due to the differences in thermal expansion coefficients the bow of the sapphire-based wafer is reduced during cool down to the InGaN growth temperature while the bow of the GaN-based wafer remains almost unchanged. Consequently, the different thermal coupling to the hot pocket and the different thermal conductivities of the substrates result in different surface temperatures and temperature distributions across the wafer. A multi-layer model is used to simulate the lattice mismatch and thermal stress-induced wafer bow for the different substrates. Furthermore, strategies to increase the surface temperature uniformity on GaN substrates will be shown using the*Pyro 400* sensor.

3:30 PM Break

Nitrides (LEDs)

Monday PM — Room: Lakeside Ballroom
May 24, 2010 — Location: Hyatt Regency Lake Tahoe

Session Chairs: Maarten Leys, IMEC, Belgium; Kei May Lau, Hong Kong University of Science and Technology, Hong Kong

---

4:00 PM

InAlN Electron Blocking Layer in Visible Light-Emitting Diodes Grown by Metalorganic Chemical Vapor Deposition: *Hee Jin Kim*[1]; Suk Choi[1]; Seong-Soo Kim[1]; Jae-Hyun Ryou[1]; P. Yoder[1]; Russell Dupuis[1]; Kewei Sun[2]; Alec Fischer[2]; Fernando Ponce[2]; [1]Georgia Institute of Technology; [2]Arizona State Univeristy

In the present study, we describe the growth and properties of InAlN layers which are lattice-matched to GaN and act as an electron blocking layer (EBL) for visible III-nitride-based light-emitting diodes (LEDs), and report on the development of high-quality InAlN EBLs for the improvement of the quantum efficiencies of the LEDs. EBLs and visible LED epitaxial structures were grown by low-pressure MOCVD in a Thomas Swan Scientific Equipment 6×2" reactor system on c-plane sapphire substrates. The LED structures consist of a 3-µm-thick Si-doped GaN layer with an electron concentration of n~5×10^{18} cm^{-3}, a five-period $In_{0.25}Ga_{0.75}N$/GaN (2.5/11 nm) multiple QW (MQW) active region, a 20-nm-thick Mg-doped $In_{0.18}Al_{0.92}N$ EBL, a Mg-doped $In_{0.03}Ga_{0.97}N$ layer with a hole concentration of p~2×10^{18} cm^{-3}, and a Mg-doped $In_{0.04}Ga_{0.96}N$ contact layer with a doping concentration of [Mg]~1×10^{20} cm^{-3}. We employed two kinds of lattice-matched $In_{0.18}Al_{0.82}N$ EBL layers with different growth conditions. One was grown at 840°C and 300 Torr (labeled as HT-InAlN EBL) and the other was grown at 780°C and 75 Torr (labeled as LT-InAlN EBL). The growth rates are 0.013 nm/s and 0.065 nm/s for the HT-EBL and LT-EBL, respectively. The low growth temperature, high conduction band offset, and lattice-matching capability of these InAlN layers are believed to enhance the quantum efficiency of the LEDs by reducing the thermal damage of the active-layer during EBL growth, providing a greater electron confinement effect, and reducing strain-induced defect generation. We demonstrate higher electroluminescence intensities and improvement in quantum efficiencies in green LEDs with InAlN EBLs compared with those without one, which we attribute to better confinement of electrons in the active region. Improvement in the quantum efficiencies of LEDs with an InAlN EBL grown at LT (~780°C) is particularly pronounced in comparison with devices having InAlN EBLs grown at HT (~840°C). Since growth at low temperatures happens at higher rates and shorter times, our observations suggest that thermal damage in the active layer may have a significant influence on the device efficiency.

4:20 PM

Single Quantum Well Deep-Green Leds with Buried InGaN/GaN Short-Period Superlattice: *Wsevolod Lundin*[1]; Andrey Nikolaev[1]; Alexey Sakharov[1]; Evgeniy Zavarin[1]; Gleb Valkovskiy[1]; Maria Yagovkina[1]; Sergei Usov[1]; Natalia Kryzhanovskaya[1]; Viktor Sizov[1]; Andrey Tsatsulnikov[1]; Nikolay Cherkashin[2]; M. Hytch[2]; Evgeniy Yakovlev[3]; Denis Bazarevskiy[3]; [1]Ioffe Institute; [2]CEMES/CNRS; [3]STR Group - Soft-Impact Ltd.

In spite of the great progress in III-N technology, LEDs with wavelength >535 nm still demonstrate low efficiency comparing to blue and short-wavelength green ones. Here we report on significant improvement of deep-green LED properties by modifications of structure design. The structures were grown in AIX2000HT system with 6 X 2" planetary reactor. An optimized structure consists of 5 µm n-GaN, 12-period InGaN/GaN short-period superlattice (SPSL) with 2 nm period fabricated by InGaN-conversion technique, 25 nm n-GaN barrier grown at reduced temperature (LT GaN), 2.5 nm InGaN QW, 4 nm undoped GaN upper barrier, 15 nm p-AlGaN, and 120 nm p-GaN. It was observed that InGaN/GaN SPSL followed by LT GaN are the key elements of high-efficiency deep-green LED. If InGaN QW is grown directly on the top of high-temperature n-GaN layer, EL efficiency is 15-30 times lower and wavelength is ~ 10 nm shorter in comparison with the optimized structure. HRTEM and HR X-ray reciprocal space mapping were used for structural characterization. It was revealed that the used InGaN/GaN SPSL prevents inheritance of GaN buffer layer mosaic structure by the consequent layers. Moreover, InGaN/GaN SPSL and LT GaN barrier improve LED properties only if implemented together and does not effect if used alone. A special attention will be given to the procedure of InGaN/GaN SPSL formation by InGaN-conversion technique: repeating of 2 nm thick InGaN growth followed by growth interruption (GI) with hydrogen admixing into the carrier gas. During SPSL formation, indium concentration on the surface is governed by an interplay between InGaN decomposition at the stage of GI, indium segregation, desorption, and incorporation into InGaN during subsequent growth. Modeling has been used to study the effect of operating parameters on these processes. Thicknesses and growth conditions of the other layers forming the structure should be carefully optimized too. For example, EL efficiency is very sensitive to GaN upper barrier thickness; p-GaN contact layer should be grown in the hydrogen-free ambient. For the LEDs processed and assembled in a simple flip-chip geometry, external quantum efficiency of 16% (545 nm) and 20% (535 nm) were achieved.

4:40 PM

Phosphor-Free White Light-Emitting Diodes with Height-Controlled InGaN Quantum Dots: *Il-Kyu Park*[1]; Seong-Ju Park[2]; [1]LED-IT Fusion Technology Research Center and Department of Electronic Engineering, Yeungnam University; [2]Gwangju Institute of Science and Technology

White light-emitting diodes (LEDs) fabricated by combining a phosphor wavelength converter with a blue or ultra-violet LED have been commercially available. However, this method has some limitations, such as, the degradation of phosphor materials during long-term optical pumping, unavoidable Stokes-shift energy loss and complex packaging steps in phosphor-based white LEDs. To circumvent these problems, phosphor-free white LEDs with vertically or laterally stacked blue and green InGaN/GaN multiple quantum wells (MQWs) inserted between the n-GaN and p-GaN layers have been widely investigated. However, it has been known to be difficult to grow InGaN MQWs emitter with longer wavelength than green spectral range and to get color stability with variation of input current. In this paper, we report on the fabrication of white LEDs with InGaN height-controlled quantum dots (QDs) emitting long and short wavelength spectral ranges simultaneously.White light-emitting InGaN QDs were grown by alternately depositing In0.4Ga0.6N QDs and In0.2Ga0.8N spacer layers on a seed In0.4Ga0.6N QD layer using a metal-organic chemical vapor deposition system. Transmission electron microscope results showed that the In0.4Ga0.6N QDs were surrounded by In-poor In0.2Ga0.8N spacer layer. The electroluminescence (EL) spectra of the LED showed a peak between the orange and red wavelength spectral range at low input current, indicating that the carriers recombine only at the potential minima of the In0.4Ga0.6N QDs embedded in the In0.2Ga0.8N spacer layer when the input current is low. As the input current increases, the dominant peak of the QD shifted to the higher energy side, which is attributed to the distribution of depth of potential wells caused by variation in the indium composition or the size of the QDs. At the input current above 100 mA, another peak appeared simultaneously at the higher energy side around 450 nm which corresponds to a recombination of carriers in the In0.2Ga0.8N spacer layer, finally resulting in white emission spectrum. These results indicate that the InGaN height-controlled QDs are promising to create long wavelength or white light-emitting single active layer.

5:00 PM

III-Nitride LEDs Grown on Porous Si Substrates: *Dongmei Deng*[1]; Naisen Yu[1]; Yong Wang[1]; Xinbo Zou[1]; Peng Chen[1]; Kei May Lau[1]; [1]HKUST

With the potential for high volume manufacturing and integration with main stream electronics, growth of III-N based devices on silicon substrates is being intensively investigated. However, due to the large lattice and thermal mismatch, hetero-epitaxy of GaN on Si usually results in high-density of defects and residual strain, which in turn degrade both the electrical and optical performances of devices. Although epitaxial lateral overgrowth (ELO) techniques can alleviate some of these problems to a certain extent, the quality of GaN-based films grown on Si is still inferior to those obtained on conventional substrates such as sapphire and SiC. The typical dislocation density in GaN grown on Si is 10^{9}-10^{11}/cm^2. Both theoretical and experimental studies have suggested that it is possible to further reduce the defect density when the ELO approach is extended to the nanoscale. LED structures grown on nanoscale patterned sapphire substrates already showed a reduced dislocation density and an increased output power in LEDs. In practice, the patterned structure dimension relies on the limitation of photolithography. Reducing such dimensions to sub-micron is costly in both equipment and production throughput.In this paper, anodized aluminum oxide (AAO) and inductively coupled plasma (ICP) etching techniques were used for the preparation of nano-scale porous Si substrates. Nano-pores were uniformly distributed on the entire 2-inch Si substrate with an average pore diameter of ~150nm, inter-pore distance of ~120nm, and an etched depth of ~250nm. LEDs were grown by MOCVD in an Aixtron 2000HT system. For comparison, the same LED structures were also grown on the patterned Si substrates of micron dimensions, namely, 340×340μm^2 grid-patterned. After the growth, with optical microscopy, Crack-free surface was observed across the whole wafer, and the morphology was mirror-like. Typical cross-sectional transmission electron microscopy images indicated a reduction of dislocation density in the LED grown on porous Si substrates. Room temperature Raman backscattering measurements showed that the LEDs on porous Si substrate endure less tensile stress. These results demonstrate the feasibility of using porous Si for the growth of high power LEDs on Si substrates.

5:30-6:30 PM Exhibitor's Reception (Regency ABDE)

Devices I

Monday PM | Room: Regency C&F
May 24, 2010 | Location: Hyatt Regency Lake Tahoe

Session Chairs: Chris Ebert, Veeco Turbodisc, Somerset, NJ, USA; Alok Rudra, EPFL, Lausanne, Switzerland

4:00 PM

Growth and Characterization of Electrically Pumped Red-Emitting VCSEL with Embedded InP/AlGaInP Quantum Dots: *Marcus Eichfelder*[1]; Wolfgang-Michael Schulz[1]; Matthias Reischle[1]; Michael Wiesner[1]; Robert Rossbach[1]; Michael Jetter[1]; Peter Michler[1]; [1]Institut für Halbleiteroptik und Funktionelle Grenzflächen

Highly efficient solid-state emitters have already proven to be very attractive light sources as they can be easily fabricated by using e.g. metal-organic vapor-phase epitaxy (MOVPE) and operated by electrical pumping in an elegant and cheap way. By using zero-dimensional quantum dots (QDs) as active media of such devices and embedding them in a pin-diode structure with distributed Bragg reflectors (DBR), theory has predicted splendid properties like ultra-low threshold and high-speed modulation capability. The sample structure was fabricated by MOVPE. The complete growth was in-situ monitored with an in-situ reflection measurement setup. This allows precise growth control of the n- and p-type DBR. The single layer of self-assembled InP QDs was grown using the Stranski-Krastanow growth mode by depositing 2.1 monolayers (ML) of InP at 650°C and a growth rate of 1.05 ML/s. The QDs were embedded in intrinsic $(Al_{0.20}Ga_{0.80})_{0.51}In_{0.49}P$ as barrier material which is surrounded by $(Al_{0.55}Ga_{0.45})_{0.51}In_{0.49}P$ cladding layers building up a 1-λ cavity. The p-type DBR with linearly graded interfaces allows for lower the series resistance and an $Al_{0.98}Ga_{0.02}As$ oxidation layer enables current constriction for electrical pumping. Atomic force microscope and scanning electron microscope measurements were used to investigate the semiconductor chip. Post-growth standard laser processing was carried out to fabricate single laser devices. Besides room temperature lasing with almost temperature independent ultra-low thresholds we will demonstrate first attempts of stacking several layers of InP QDs to increase the gain material. In order to shift the emission energy to around 650 nm, the attenuation minimum of commercial polymer optical fibers, the growth temperature for both layers of QDs has to be decreased. Additionally, we minimize the growth rate of the second QD layer to ensure a narrow ensemble electroluminescence spectra.

4:20 PM

Realization of Monolithic Electro-Optically Modulated Vertical Cavity Surface Emitting Lasers: *Tim Germann*[1]; Jan-Hindrik Schulze[1]; Alex Mutig[1]; Sergey Blokhin[1]; James Lott[2]; Vitaly Shchukin[2]; Nikolay Ledentsov[2]; Udo Pohl[1]; Dieter Bimberg[2]; [1]Berlin Institute of Technology; [2]VI-Systems GmbH

The steadily growing data traffic requires high-speed and low-cost laser diodes. Conventional current modulated vertical-cavity surface-emitting lasers (VCSEL) are limited in speed due to a quadratic increase in the current density with the bit rate leading to device degradation. The concept of the vertical monolithic integration of an electro-optic modulator (EOM) and a VCSEL was proposed precisely to solve this problem[1]. The light modulation in the EOM-VCSEL is caused by a reflectivity modulation of the top distributed-Bragg-reflector (DBR), while the VCSEL section is run continuously, in contrast to a conventional current-modulated VCSEL. The first successful proof of concept of an EOM-VCSEL was recently presented by us[2]. In this work we report the growth, fabrication and characterization of advanced 850 nm EOM-VCSELs suitable for data transmission with industry-acceptable parameters. Our present devices include an EOM section within the top DBR consisting of multiple quantum wells (QW) separated by $Al_{0.2}Ga_{0.8}As$ barriers. By applying a reverse bias to the EOM part the refractive index of the EOM is altered up to 0.01, sufficient to modulate the properties of the top DBR. Doping-related effects are compensated by specifically tuning DBR growth parameters to achieve a perfect match of the QW emission wavelength with the EOM operational wavelength. A variety of EOM-VCSEL designs, each with close to 400 epitaxial layers, are grown on (100) GaAs substrates using metalorganic vapor-phase epitaxy. Good uniformity of the laser parameters across the wafer is achieved. Record low modulation voltages (<2V) are needed to reach -3dB extinction ratio for a broad temperature range from 25 to 85°C. A similar extinction ratio was revealed in large-signal modulation experiments at frequencies up to 3 GHz. Thus for the first time the potential of high-bit rate data transmission by an EOM-VCSEL is really demonstrated. Analysis of our present results indicates possibilities for next generation devices with one order of magnitude larger bit rates by further improvements of the growth process. [1] V. A. Shchukin et al., Proc. of SPIE Vol. 6889, 68890H, (2008). [2] T. D. Germann et al., Proc. of ISCS 2009 Santa Barbara.

4:40 PM

Properties of MOVPE-Grown Vertical External Cavity Surface Emitting Laser (VECSEL) for High Power Applications in the Emission Regime from 950 nm up to 1200 nm: Bernardette Kunert[1]; Alexej Chernikow[2]; Sangam Chatterjee[2]; Kerstin Volz[2]; Stephan Koch[2]; *Wolfgang Stolz*[2]; Jörg Hader[3]; Jerome Moloney[4]; [1]NAsP III/V GmbH; [2]Philipps University; [3]Nonlinear Control Strategies Inc.; [4]University of Arizona

A vertical external cavity surface emitting laser (VECSEL) is a semiconductor disk laser with a high quality output beam. The vertical external cavity ensures a low-divergence and circular laser beam and allows for second harmonic generation and mode-locking by installing additional optical components into the external resonator. Optical pumping of the gain region shows potential for power scaling whereas an optimized heat management allows for achieving high continuous wave (cw) output powers of several tens of watts. A closed-loop design concept of microscopic modeling, epitaxial realization by metal organic vapour phase epitaxy (MOVPE) and device characterization of optical pumped disk lasers is applied to (GaIn)As/Ga(PAs)-based multi-quantum well heterostructures (MQWHs) in the emission wavelength range from about 960 nm up to 1200 nm. The defect-free deposition of highly strain-compensated MQWHs requires specific low-temperature MOVPE growth conditions using the more efficiently decomposing liquid metal organic sources tertiarybutylarsine (TBAs) and tertiarybutylphosphine (TBP). The emission wavelength is determined by the gain spectrum of the active material system (GaIn)As and the thickness of the resonant periodic gain region (RPG). In order to achieve high output powers the optical pumped VECSEL chip is mounted on either a copper or a diamond heat sink. The focus of the paper is the detailed study of the MOVPE growth conditions in correlation to the structural as well as the optoelectronic properties of the laser chip. The influence of V/III ratios and growth temperatures for the highly compressively strained (GaIn)As-MQW in particular for long emission wavelengths as well as the design of the tensile-strained Ga(PAs)-barrier layers will be presented and discussed. Furthermore, the experimental characteristics of the realized VECSEL-chips with emission wavelengths of 960 nm, 1040 nm and 1180 nm will be compared to the predictive microscopic modeling results. Cw output powers of more than 40 Watts have been achieved for an emission wavelength of 1040 nm.

5:00 PM

Pulsed Single-Photon Resonant Cavity Quantum Dot LED: *Wolfgang-Michael Schulz*[1]; Marcus Eichfelder[1]; Matthias Reischle[1]; Christian Kessler[1]; Robert Roßbach[1]; Michael Jetter[1]; Peter Michler[1]; [1]Universität Stuttgart

Single-photon sources using quantum dots (QDs) are an important element in quantum information applications. From the viewpoint of practical application, an electrically driven photon source is favored. As current Si-based single-photon detectors have their highest photon detection efficiency in the red spectral range it is preferable to fabricate single QDs emitting at such wavelengths. We concentrated our efforts on the growth of electrically driven InP-QDs embedded in (Al, Ga)InP barrier material that is lattice-matched to GaAs to achieve QD luminescence in the red spectral region [1]. Previously, the authors demonstrated single-photon emission of cw-operated InP QDs up to at least 80 K in a simple light emitting diode (LED) configuration [2]. A common technique to increase the luminescence yield and the extraction efficiency is the use of so called resonant-cavity LEDs RCLEDs) [3]. We demonstrate the growth of an AlAs/$Al_{0.50}GaAs$-RCLED in which our self-assembled QDs were placed in a lambda cavity. The sample structure was grown by metal-organic vapor phase epitaxy with standard sources (TMGa, TMIn, TMAl, DMZn, SiH4, CBr4, arsine, and phosphine) at low pressure (100 mbar) on (100) GaAs substrates oriented by 6° toward the [111]A direction. The single-layer of self-assembled InP-QDs was grown using the Stranski-Krastanow growth mode by depositing 2.1 ML of InP and a growth rate of 1.05 ML/s. A high Al containing $Al_{0.98}GaAs$ layer allows the implementation of a current restricting oxide aperture. The RCLED was mounted on a high frequency mount to allow electrical pumping with sub-nanosecond pulses. In this way we could achieve pulsed single photon emission at a repetition rate of 200 MHz. To proof that single photons are emitted, we performed second-order autocorrelation measurements. A fourfold suppression of multi-photon events compared to a Poissonian source with same average intensity was found. [1] W.-M. Schulz et al., Phys. Rev. B, 79, 035329 (2009) ; [2] M. Reischle, et al. Opt. Express 16, 12771 (2008).; [3] E. F. Schubert et al., Science, Vol. 265, No. 5053, 66, (1992).

5:30-6:30 PM Exhibitor's Reception (Regency ABDE)

Tuesday Invited Talks

Tuesday AM Room: Lakeside Ballroom
May 25, 2010 Location: Hyatt Regency Lake Tahoe

Session Chair: Abdallah Ougazzaden, Georgia Institute of Technology, Georgia Tech Lorraine, Metz, France

8:30 AM Invited
Metamorphic Growth for High Quality Lattice-Mismatched III-V Solar Cell Junctions: *John Geisz*[1]; [1]NREL

Multi-junction solar cells overcome some of the fundamental efficiency limitations of single junction photovoltaics by splitting the solar spectrum into smaller regions that can be more efficiently converted to electric power. Optically concentrated sunlight on these devices further improves efficiency, as well as the economics of solar energy generation. MOVPE-grown, monolithic, lattice-matched GaInP / GaInAs / Ge solar cells have exceeded 41% efficiency under concentrated light, but the band gaps are not optimized for typical spectral, concentration, and temperature conditions. Lattice-MISmatched compositions of III-V semiconductors open the possibility for more junctions and optimized band gaps in monolithic devices that could significantly increase efficiencies. Low defect densities are required to prevent loss mechanisms that defeat the efficiency gains in optimized band gaps. Gradually increasing the lattice constant within a graded III-V buffer layer allows the strain to be relieved with threading dislocations gliding to the edges so that the dislocation density in the active "metamorphic" junction is minimized. Overshooting the lattice constant and stepping back provides a technique to engineer the strain within the active metamorphic junction. Inverting the growth direction allows the highest power-producing junctions to be grown lattice-matched for the lowest defect densities. Using these techniques, we have demonstrated defect densities of $2x10^{6}$ cm^{-2} in 2.6% misfit Ga$_{.63}$In$_{.37}$As solar cell junctions grown on GaAs. Currently, the efficiencies of prototype inverted metamorphic (IMM) and non-inverted metamorphic triple-junction solar cells are comparable to the best lattice matched solar cells, with further potential as the quality of metamorphic junctions improves. In this talk, I will discuss MOVPE growth strategies and characterization techniques to achieve low defect densities and low strain within metamorphic solar cell junctions while maintaining optical transparency and electrical conductivity within necessary buffer layers.

9:00 AM Invited
III-V Semiconductor Nanowires - From Crystal Growth to Device Applications: *Takashi Fukui*[1]; Katsuhiro Tomioka[1]; Shinjiro Hara[1]; Kenji Hiruma[1]; Junichi Motohisa[1]; [1]Hokkaido University

Semiconductor nanowires have stimulated extensive interest in recent years because of their unique properties and potential applications as building blocks for nanoscale electronic and photonic devices. We report on the systematically controlled growth of IIII-V nanowire arrays by catalyst-free selective area metalorganic vapor phase epitaxy (SA-MOVPE) on partially masked (111) oriented substrates. The length, diameter, shape and position of the nanowires were precisely controlled by optimization of the growth conditions and mask patterning. Manipulation of the growth conditions also enabled us to deliberately define the nanowire growth along either the axial or the radial direction, which has significant potential for the realization of novel nanostructures. We also grew vertically aligned InAs and GaAs nanowires on Si (111) substrates by modifying initial Si (111) surface. Cross-sectional transmission electron microscope showed that misfit dislocation with local strains was accommodated in InAs/Si interface, while no misfit dislocation was observed in GaAs/Si interface. Using this technology, we fabricated InAs vertical surrounding-gate FETs (VSGFETs) on a Si substrate. Fabricated VSGFET contained 50 NWs parallel in the channel. We observed n-type FET behavior in ID-VDS and ID-VG characteristics. The performances are threshold voltage ~ 0V, Gm,max = 0.26 mS, Ion / Ioff = 100, subthreshold slope, S = 1.87 V/decade. We also successfully fabricated single GaAs/GaAsP coaxial core-shell nanowire laser. Photoluminescence (PL) spectra from a single nanowire indicate that the obtained heterostructures can produce near-infrared (NIR) lasing under pulsed light excitation. The end facets of a single nanowire form natural mirror surface to create an axial cavity, which realizes resonance and give stimulated emission. This study is a considerable advance towards the realization of nanowire-based NIR light sources.A periodically aligned dense core–shell InP nanowire array was fabricated and used in photovoltaic device applications. As-grown nanowire solar cell covering 2.0x2.6mm2area exhibited open-circuit voltage (VOC), short-circuit current (ISC) and fill factor (FF) levels of 0.43 V, 13.72mA/cm2 and 0.57, respectively, which indicated a solar power conversion efficiency of 3.37% under AM1.5G illumination.

9:30 AM Break

Energy Technology
(Solid State Lighting, PV, Thermoelectrics, etc)

Tuesday AM Room: Lakeside Ballroom
May 25, 2010 Location: Hyatt Regency Lake Tahoe

Session Chairs: John Geisz, NREL, Boulder, CO, USA; Thomas Hannappel, Hahn Meitner Institute, Berlin, Germany

10:00 AM
MOVPE Growth of High Efficiency Inverted Metamorphic 1.1eV Solar Cell on Thin Ge Substrate: *XingQuan Liu*[1]; C. M. Fetzer[1]; R. R. King[1]; A. Boca[1]; D. Larrabee[1]; A. Zarkaria[1]; W. Hong[1]; J. Chang[1]; S. Mesropian[1]; D. Law[1]; D. Bhusari[1]; J. P. Krogen[1]; N. H. Karam[1]; [1]Spectrolab Inc.

The multiple junction solar cells based on GaInP, GaInAs, and Ge have achieved the highest conversion efficiencies so far. However, most of the designs are lattice matched structures to Ge substrate. The band gap combination is very limited due to the lattice matching requirement. By using lattice mismatched metamorphic materials, much more band gap combinations can be used to achieve even higher conversion efficiency. However, the highly lattice mismatched metamorphic materials normally give high defect density which will cause the low epitaxial quality for layers grown on top of it. Inverted multiple junction design overcomes this problem by growing the lattice matched top cell structures first and leaving the metamorphic cells the last. This paper focuses on the 1.1ev Ga0.77In0.23As inverted metamorphic solar cell grown with AlGaInAs quarternary step graded buffer on 6o miscut (001) thin Ge substrate. The performance of this inverted metamorphic 1.1eV solar cell on thin Ge substrate is found very sensitive to the wafer flatness, which is directly related to the strain relaxation and therefore active cell layer quality, particularly on the thin Ge substrate. The flattest wafer shows the best open circuit voltage (Voc) of 0.66V and nearly 100% internal quantum efficiency above the band gap. The band gap offset (Eg/q-Voc) of the best cell is 0.43V. Electron beam induced current (EBIC) analysis showed the threading dislocation density of the flattest wafer is 2.0x106cm-2, while the warped wafers showed higher threading dislocation density. The cell band gap depends on the wafer flatness, which is due to the different strain conditions in the active cell layers. Warped wafers show higher band gap, which is corresponded to the compressive strain. The high resolution XRD reciprocal space mapping (RSM) shows the strain is completely relaxed for the flattest wafer.

10:20 AM
Germanium Junctions Entirely Grown by MOVPE for Solar Cell Applications: *Roberto Jakomin*[1]; Gregoire Beaudoin[1]; Noelle Gogneau[1]; Olivia Mauguin[1]; Ludovic Largeau[1]; Cristophe Roblin[1]; Erik Johnson[2]; Pere Roca I. Cabarrocas[2]; Isabelle Sagnes[1]; [1]Laboratoire de Photonique et de Nanostructures; [2]Laboratoire de Physique des Interfaces et des Couches Minces, École Polytechnique

Triple-junction InGaP/(Ga,In)As/Ge solar cells with a conversion efficiency of 41% under concentration have been developed in the recent years. Although high efficiencies have been obtained by optimizing the material quality and the cell structures, today one of the limiting part is the Germanium (Ge) botton junction, which is usually realized by diffusion doping. In fact, this process may induce a reduction of Voc (open circuit voltage) due to the spread doping profiles. The improvement of the Ge-junction doping appears thus as an important issue to realize very high efficient cells.In this work, we realize Ge cells entirely grown by metalorganic vapour phase epitaxy (MOVPE). The cell structure is formed by a p-n Ge epitaxial junction grown on a n-doped Ge substrate. Iso-butyl germane (IBGe) is used as Ge source, Trimethylgallium is used for p-doping, while n-doping is either intrinsic or obtained by supplying Arsine. To develop the Ge-junction, we have studied and optimized the growth conditions by adjusting the growth parameters such as temperature, IBGe or doping flows… The memory effect and the interdiffusion mechanisms have been considered, since a low background doping in the base is a crucial point for photovoltaic applications.

Hence, we demonstrate the precise control of the growth of p and n-doped Ge layers, characterized by very good structural and crystallographic properties. By comparing the electrical characteristics of our entirely epitaxial Ge junctions with cells obtained by diffusion of Arsine into a p-doped base, we demontrate that the epitaxial Ge layers present better defined doping profiles. As a consequence, our entirely epitaxial Ge-cells (although they lack antireflection coatings and passivation layers which would reduce the surface losses) show a very good conversion efficiency of 4.7% For comparison, the best Germanium solar cells obtained by diffusion present an efficiency around 3.5% without passivation layer. This result demonstrates that our approach is very promising for further improvement of conversion efficiency. This work is supported by the European project 7th PCRD-APOLLON

10:40 AM

MOVPE Development of III/V Multijunction Terrestrial Solar Cells at Spectrolab: *Chris Fetzer*[1]; William Hong[1]; Xing-Quan Liu[1]; James Chang[1]; Maggy Lau[1]; Andreea Boca[1]; Diane Larrabee[1]; Richard King[1]; Peter Hebert[1]; James Ermer[1]; Aniruddh Parekh[2]; [1]Boeing-Spectrolab; [2]Veeco Tubodisk

Demonstrating the 41.6% efficiency world record [1] in concentrator photovoltaics (CPV) requires many areas of expertise. One key element is the metal-organic vapor phase epitaxial (MOVPE) growth of the crystalline device structure for III/V multijunction photovoltaics. This work gives an overview of the present status and future work of Spectrolab in MOVPE development for production III/V multijunction CPV cells. A new CPV product, C3MJ, with a target efficiency of 38.5% at maximum power (50.0 W/cm2, AM1.5D, ASTM G173-03 spectrum, 25ºC) is the current state-of-the-art in Spectrolab terrestrial production. Multiple in-situ tools in MOVPE such as real-time emissivity corrected pyrometry and wafer curvature add new capability to monitor the process which has improved key process capabilities (Cp) by up to 2x over previous processes, with expected further improvement in Cp attainable in certain areas. Among the various projects under development are the 6” (150 mm) diameter C3MJ epiwafer and the targeted 40.0% efficient C4MJ product. C3MJ cells based on a 7 x 6” configuration show efficiencies equal to those of C3MJ cells produced on 4” diameter wafers over most of the wafer. Thickness uniformity and composition uniformity are also equally attainable on 4” and 6” diameter wafers. Prototype 40% cells for C4MJ take advantage of the in-situ wafer curvature capability to repeatedly produce upright metamorphic GaInP/5%-InGaAs/Ge cells with 100% crystal lattice relaxation by 5-point maps of High Resolution X-ray Diffraction in run-to-run stability testing. These same epitaxial experiments have provided early builds averaging 39.6% efficiency at max power spanning multiple experimental runs. [1] R. R. King, et al. (2009). 24th European Photovoltaic Solar Energy Conference and Exhibition, Hamburg.

11:00 AM

High-Material-Efficiency MOVPE of GaAs without Degradation of Photovoltaic Performances: *Ryusuke Onitsuka*[1]; Takuo Tanemura[1]; Masakazu Sugiyama[1]; Yoshiaki Nakano[1]; [1]The University of Tokyo, Japan

III-V semiconductors have a great potential for high-efficiency photovoltaic (PV) cells. Although MOVPE is the most suitable for such an application, it has a disadvantage of low material efficiency: ~10% for group III and ~1% for group V, which has to be improved drastically in order to reduce burden to environment and to make III-V PV cells cost effective. Although fundamental improvement of the material efficiency necessitates novel reactor design and/or material recycling, there is a plenty of room for adjustment of growth conditions. In order to explore a high-material efficiency growth condition of GaAs with TMGa and TBAs, we have observed in situ surface reflectance anisotropy. GaAs surface reconstruction during growth seems to be dependent on V/III ratio and no significant change was observed until the V/III ratio was below 1.5. We, therefore, increased the partial pressure of TMGa with a constant TBAs partial pressure, resulting in an increase in growth rate from 9.5 to 55 nm/min and a decrease in V/III ratio from 15 to 2.2. In terms of impurity level, this high-efficiency condition resulted in 5 times larger amount of carbon (5x10^16 [/cm^3]) and 3 times larger amount of oxygen (1x10^17 [/cm^3]), which may lead to degraded minority-carrier diffusion length in the layer. In addition, the change in growth rate and V/III ratio altered vapor-solid relationship of dopant atoms (Zn and S) and obliged us tough process conditioning. We, therefore, have adopted p-i-n structure for a GaAs PV cell and applied the high-material efficiency growth condition to the intrinsic layer alone, which occupies most of the epi-layer thickness in the GaAs p-i-n cell. The advantages of the p-i-n structure are (1) carrier transport inside of the absorber (intrinsic) layer is enhanced by built-in potential even though a certain amount of carrier traps exist, and (2) there is no need to control the dopant concentration in the thickest intrinsic layer. Remarkably, both the standard growth condition and the high-material-efficiency condition resulted in the same PV characteristics of the p-i-n cell: VOC = 0.92V, ISC=24mA, FF=0.75, and conversion efficiency was 17%.

11:20 AM

Nanocomposite: The First Demonstration of MOCVD-Grown Rare Earth Monoantimonide Embedded in In(Ga)Sb(As) Matrices: *Takehiro Onishi*[1]; Tela Favaloro[1]; Ali Shakouri[2]; Nobuhiko Kobayashi[3]; Elane Coleman[4]; Gary Tompa[4]; [1]UCSC; [2]Bio-Info-Nano Research and Development Institute (BINRDI); [3]Nanostructured Energy Conversion Technology and Research (NECTAR), Advanced Studies Laboratories; [4]Structured Materials Industries, Inc.

In the continuing quest for ever more efficient and environmentally friendly energy sources, thermoelectrics (TE) is one of the “new” frontiers. However, in spite of more than five decades of material development there has been very little improvement in TE properties until very recently. The ability of tuning materials at nanometer scale has been a driving force for recent dramatic improvements in the performance of TE devices. One particular promising line of development follows the concept of nanocomposites in which two dissimilar materials having significantly different physical characteristics and dimensions are coupled coherently. In particular, our focus is to combine rare earth monoantimonide (semi-metal) in the form of nanoparticles with a bulk group III-antimonide (semiconductor) ternary or quaternary alloy. Such a nanocomposite can be tuned to optimize its overall electrical transport properties and Seebeck coefficient, and it can be made either p- or n-type. In addition, the nanoparticles introduce efficient phonon scattering centers, in particular for mid and long-wavelength phonon, resulting in thermal conductivity much lower than the alloy-limit. The net result is that a nanocomposite offers a significant enhancement in material’s ZT. We herein report on our recent efforts in the first demonstration of the growth of erbium monoantimonide nanoparticles embedded in group III-antimonide matrices by metal organic chemical vapor deposition (MOCVD). We developed a unique MOCVD tool and a reproducible low-pressure growth process for ErSb embedded in InSb, InGaSb and InAsSb alloys that are doped with Zn and grown on n-type InSb substrates. Structural analyses focus on surface morphology, crystallographic properties and chemical composition of the In(Ga)Sb(As) matrices, and crystallographic registry of ErSb. Techniques such as infrared-absorption, atomic force microscope, and x-ray scattering, are used to obtain information on the growth of ErSb on InSb surfaces. In addition, properties relevant to thermoelectrics such as the dependence of Seebeck and electrical transport properties on temperature will be reported. The latest characterization results indicate that the overall quality of MOCVD-grown ErSb-In(Ga)Sb(As) is comparable to that grown by MBE.

11:40 AM

MOVPE of High Performance Oxide Superconducting Films on Flexible Metal Substrates: *Venkat Selvamanickam*[1]; [1]University of Houston

Superconductors are quite likely a unique system that provides solutions for a broad spectrum of the looming problems in energy generation, transmission, conversion, storage, and use. Superconductors enable high efficiencies and power densities in generators, power transmission cables, motors, transformers and energy storage. The progress of superconductors in the form of practically useful wires/tapes has required the last 22 years primarily because of the immense fundamental challenges with weak links at grain boundaries, anisotropy, brittleness and incompatibility with most metals at processing temperatures. Several of these problems have been overcome by diligent research and superconducting tapes have come of age, enabled by a novel approach to create epitaxial, single-crystal-like thin films on polycrystalline substrates. In this technique, a thin film of materials with rock-salt crystal structure such as MgO is deposited by ion beam-assisted deposition (IBAD) over flexible, metal substrates. MOVPE has been used to grow heteroepitaxial oxide superconducting films on the IBAD-based metal substrates and critical current densities comparable to that of epitaxial films grown on single crystal substrates have been achieved. This IBAD-MOVPE approach has been successfully transitioned to pilot-scale manufacturing of kilometer-long, continuous superconducting films. MOVPE-based superconducting thin film tapes have been used to fabricate a power transmission cable that has been employed in the electric power grid. Several unique challenges with MOVPE of superconducting films are being addressed in our work. Since long tapes have to be fabricated, high growth rates (~ 30 microns/hour) need to be used, and epitaxy has to be preserved at these high rates over kilometer lengths over a deposition area of 1 m × 10 cm in process runs lasting over 30 hours! Higher critical currents require film thickness of about 3 microns and epitaxy needs to be maintained over such thickness without misoriented grains. High critical currents need to be achieved in the presence of magnetic fields, which are present in most applications. Recently, nanoscale columnar defects introduced in the superconductor film via self assembly process during MOVPE have enabled improved performance in high magnetic fields. Progress made in addressing these challenges will be discussed in this presentation.

12:00 PM Lunch

Heteroepitaxy - Nanostructures

Tuesday AM Room: Regency C&F
May 25, 2010 Location: Hyatt Regency Lake Tahoe

Session Chairs: Jeffrey Tsao, Sandia National Laboratories, Albuquerque, NM, USA; Eduard Hulicius, Institute of Physics, Czech Republic

10:00 AM
Heteroepitaxial Growth of InGaAs Nanowires Formed on GaAs(111)B by Selective-Area MOVPE: *Masatoshi Yoshimura*[1]; Katsuhiro Tomioka[1]; Kenji Hiruma[1]; Shinjiro Hara[1]; Junichi Motohisa[1]; Takashi Fukui[1]; [1]Hokkaido University

Semiconductor nanowires have attracted a lot of attention in the field of nanoscale electronic/photonic devices and bio-devices. We have focused on fabricating InGaAs FETs and quantum confinement structures for optical devices using InGaAs nanowires. To develop these devices, we have to control the size, atomic composition, and doping of the nanowires. In this work, we fabricated and analyzed the InGaAs nanowires in SiO_2 mask openings on a lattice mismatched GaAs(111)B substrate using catalyst-free selective-area metal-organic vapor phase epitaxy (SA-MOVPE). The SA-MOVPE growth of undoped InGaAs was carried out in a horizontal MOVPE system working at a pressure of 0.1 atm and at growth temperatures of between 600–700°C. The source materials were 5%-arsine diluted in hydrogen, trimethylgallium and trimethylindium. Scanning electron microscopy, transmission electron microscopy (TEM), and micro-photoluminescence (µ-PL) at 4.2 K were used to create the structural and optical characterizations of the InGaAs nanowires. We found from the PL measurement that the luminescence peak energy of InGaAs nanowires exhibited a blue shift when the growth temperature increased, indicating an increase in the Ga composition of the InGaAs nanowire. A clear PL spectrum with a strong peak at 1.09 eV was observed from the InGaAs nanowires grown on GaAs(111)B, while a planar InGaAs layer grown on GaAs(111)B or GaAs(100) indicated a very weak spectrum without a peak, which is thought to be caused by the lattice mismatch between InGaAs and GaAs. We think the crystal defect generated by the lattice mismatch between the nanowire and the substrate could be reduced by using the nanowire structure, and therefore, a strong PL peak from the nanowires was observed. Cross-sectional TEM images of the InGaAs nanowires showed that they were grown with a uniform diameter in the axial direction of <111>B without lateral growth onto the SiO_2 mask. Furthermore, an energy dispersive X-ray TEM analysis indicated that In atomic composition x was about 0.26 in $In_xGa_{1-x}As$, and that little change was observed in the composition along a 2 µm-long nanowire. The results show that a ternary alloy nanowire with a good crystal quality was successfully grown using SA-MOVPE.

10:20 AM
Selective-Area Growth of InGaAs Nanowires on Si Substrate: *Katsuhiro Tomioka*[1]; Masatoshi Yoshimura[1]; Junichi Motohisa[1]; Shinjiroh Hara[1]; Kenji Hiruma[1]; Takashi Fukui[1]; [1]Hokkaido University

Heteroepitaxy of III-V compound semiconductor nanowires (NWs) on Si is expected for the next- generation techniques for applications of III-V NWs-based electronics and photonics on Si platforms, such as vertical FETs, LEDs and solar cells because NWs can overcome mismatches in lattice constants and thermal coefficients of III-V/Si system by nm-scaled footprints. The control of the growth directions for III-V NWs, however, becomes a problem resulting from the polar materials on non-polar materials. Here, we report on growth of vertical-aligned InGaAs NWs on Si by using selective-area MOVPE. In this study, n-type Si(111) substrates were used. 20 nm-thick SiO_2 was formed using thermal oxidation. Then, openings were formed using lithography and wet etching. Finally, InGaAs NWs were grown on Si by MOVPE with H_2 carrier gas. The source materials were TMIn. TMGa, and AsH_3. The growth temperature was 690ºC with V/III = 80. The fraction of the TMGa/(TMIn+TMGa) was 0.38. The substrate was cooled down to 400ºC in H_2 ambient, and AsH_3 was supplied for 5 min to form (111)B-oriented surface. Then, we grew InGaAs buffer layer at 400ºC for 3 min. Finally, the temperature was increased to 690ºC, and the nanowire growth was resumed.The hexagonal-shaped uniform InGaAs NW array were grown on Si(111). In composition was about 62%. The growth direction of the InGaAs NWs were totally vertical <111> direction on Si(111) substrate. In case of large openings (diameter, $d_0 \geq 200$ nm), giant hillocks resulted from lattice mismatch were formed on the openings. As for small openings ($d_0 \approx 100$ nm), the vertical-aligned NWs were formed on Si. The average diameter of NWs was same as d_0. This means lateral-over growth was suppressed at this temperature. The NW height was linearly increased with decreased diameters. This relation is explained by surface diffusion of Group III atoms as reported in selective-area growth of InGaAs NWs. Growth of InGaAs NW on Si, therefore, virtually follows the growth mechanism although the system contains large lattice mismatch (lattice mismatch is 8.7%) Further characterization of optical properties and crystallographic structures for the NWs will be reported.

10:40 AM
Wurtzite GaAs Nanoneedles Epitaxially Grown on Highly Lattice-Mismatched Sapphire with Bright Luminescence: *Kar Wei Ng*[1]; Linus C. Chuang[1]; Thai-Truong D. Tran[1]; Wai Son Ko[1]; Michael Moewe[1]; Roger Chen[1]; Connie Chang-Hasnain[1]; [1]University of California Berkeley

Extensive work has been done on heterogeneous integration of dissimilar single crystalline materials to obtain functionalities and performance that cannot be achieved with one material system alone, e.g. III-V materials on Si or sapphire substrates. However, lattice mismatch has always been the greatest barrier to get high quality thin films. Nano-structures obtained by three-dimensional growth have recently been shown to be promising in overcoming this barrier. Here, we report a self-assembled, catalyst-free, single crystalline and ultra sharp GaAs nanoneedle (NN) epitaxially grown on a sapphire substrate with 46% lattice mismatch. GaAs NNs were spontaneously grown on a (0001) sapphire substrate by low temperature MOCVD without any ex-situ substrate surface treatment. Each NN has a hexagonal base, six slanted sidewalls and a sharp tip. In a 60-minute growth, a typical six-facet needle is ~600 nm in base diameter and ~3 µm in height. The taper angle, being growth-time-invariant, is typically ~11°. TEM analysis shows that the tip of a NN is only 3 nm wide. In addition, the NNs were found to be wurtzite crystalline instead of conventional zinc-blende GaAs structure. Single atomic steps composed of terraces of {1-100} and (0001) forms the slanted sidewalls. Our growth model shows that the large lattice mismatch gives rise to the high NN aspect ratio. The growth temperature of GaAs NNs is 400°C.In spite of the 46% lattice mismatch, the NNs show bright photoluminescence. The emission of this wurtzite NN structure peaks at 1.519 eV, which is 6.5 meV larger than that from zinc-blende GaAs. This agrees with what was previously reported. The linewidth of the peak is 18 meV. Such a narrow linewidth indicates that the NNs are of excellent crystal quality. These high-quality GaAs NNs open an opportunity for fabricating high-performance electronic and optoelectronic devices onto a highly lattice mismatched substrate.

11:00 AM
Axial pn-Junctions in Vapour-Liquid-Solid Grown GaAs Nanowires by MOVPE Using DEZn and TESn: Ingo Regolin[1]; Christoph Gutsche[1]; *Andrey Lysov*[1]; Kai Blecker[1]; Werner Prost[1]; Franz-Josef Tegude[1]; [1]University Duisburg-Essen

The control of carrier type and density in an extremely wide range is the unique advantage of semiconductors for (opto-)electronic device applications [1]. Therefore, the future of any semiconductor nanowire technology will inherently rely on their doping capability. However, the specific parameters for nanowire growth do often not favor the incorporation of doping atoms. This holds especially, if both n- and p-type doping shall be realized during one nanowire growth. In the few recent publications, very low current densities were reported. In addition, a combination of nanowire growth and layered growth enabling core-shell pn-junctions or a combination of doped substrate and nanowire have been selected in order to particularly overcome the doping problem. In this contribution, we report on axial pn-GaAs nanowires grown on (111)B GaAs substrate by MOVPE method, using the VLS mechanism in combination with an pervious evaporated Au layer. The nanowires were grown at 400 °C, to exclude almost completely additional growth on the nanowire sidewalls. For p-type doping diethylzinc (DEZn) was used as precursor material and lead to doping concentrations up to 2E19 cm-3, as recently published [2]. To realize the n-doped part, tetraethyltin (TESn) was introduced to the reactor, which generates an electron concentration above n = 1E18 cm-3. The n- as well as the p-type behaviour was in addition verified by processed MISFETs structures on single n- and p-doped wires using equal growth parameters. The whole pn-GaAs nanowires have length up to 20 µm and different diameters up to some 100 nm according to the evaporated Au layer. For electrical characterisation the nanowires were transferred to insulating carrier substrates and contacted via electron beam lithography. The device exhibits a diode-like I-V characteristics. The current in the 100 nA range is limited by the conductivity of the n-side. With the successful realization of both, n- and p-type doping in one wire, the requirements for electroluminescence are elaborated. To our knowledge this is the first axial GaAs pn-diode realised in single nanowires. [1] B. Tian et al., Chem. Soc. Rev. 38 (16), 2009. [2] C. Gutsche et al., J. Appl.. Phys. 105 (024305), 2009.

11:20 AM
Effect of Carbon Doping on Morphology and Structure of GaAs Nanowires: *Omid Salehzadeh*[1]; Simon Watkins[1]; [1]Simon Fraser University

Doping of semiconductor nanowires is still an area of high interest for potential device applications. Carbon is a well known p-type dopant in the growth of planar III-V materials such as GaAs, however its use has not yet been investigated for nanowire growth by the vapour-liquid-solid (VLS) growth mechanism. In this work we show that the morphology of the gold assisted catalyzed GaAs nanowires are significantly modified by the presence of CBr_4 vapour during growth by metalorganic vapour phase epitaxy (MOVPE). Nanowires grown in the presence of CBr_4 exhibit negligible tapering and a much lower level of gold catalyst migration loss than compared with nanowires grown in the absence of CBr_4 under the same conditions. Increasing the concentration of CBr_4 leads to increased linear growth rate and reduced nanowire diameter. We attribute this to the coverage of the GaAs by carbon adsorbates which greatly suppress wetting of GaAs by Au, resulting in increased contact angles for Au islands and a smaller nanowire diameter. In addition, we propose that carbon on the nanowire sidewalls suppresses the diffusion of Au down the nanowire, resulting in the observed dramatic reduction of tapering. Nanowires grown with CBr_4 show pure zincblende structure with no detectable stacking faults, in contrast to the wires grown in the absence of CBr_4 which show a high density of stacking faults and wurtzite structure. High resolution energy dispersive x-ray spectroscopy (EDS) measurements show that a significant amount of carbon can be incorporated into the nanowires by this technique, although it appears to reside primarily in a thin outer shell. Doping likely proceeds via sidewall surface reactions and bulk diffusion since the solubility of carbon in the Au droplet is probably too low for a doping mechanism involving the solid-liquid interface. This work suggests a simple method to fabricate free-standing, untapered, stacking faults-free nanowires which should be applicable to the other III-V nanowires.

11:40 AM
Dependence of III-V Nanowire Growth by Selective Area MOCVD on the Polarity of Substrates: Hyung-Joon Chu[1]; *Ting Wei Yeh*[1]; Lawrence Stewart[1]; P. Dapkus[1]; [1]University of Southern California

III-V nanowire arrays are potentially important structures for application to photovoltaic devices and light emitting diodes. In this work such arrays are grown by nano-scale selective area growth (NS-SAG). The formation of InP, GaAs, and GaP nanowires on (111) GaAs, InP or Si substrates or GaN nanostructures on (0001) GaN epitaxial substrates have been studied to determine the influence of substrate polarity and MOCVD growth conditions on the growth habit and morphology. Each type of nanostructure array is successfully grown on a specific substrate crystal polarity by nanoscale selective area metalorganic vapor phase deposition (MOCVD). Vertical InAs, GaAs, and GaP nanowire arrays can be grown on GaAs and InP (111)B, group V terminated, substrates. However, vertical InP nanowire arrays can only be grown on InP (111)A, group III terminated, substrates. In the latter case, there is a strong tendency to form wurtzite crystal structures. The morphology of GaN nanostructures selectively grown on Ga-polar and N-polar GaN layers show markedly different morphologies. Highly stable hexagonal GaN nanopyramid arrays are formed on Ga-polar surfaces while vertical GaN nanowires are observed on the N-polar surface. In the case of GaAs nanowires heteroepitaxially grown on Si (111) substrate, surface treatment prior to nanowire growth is found to be an important step to create a Si surface with an As-polar surface - the preferential growth plane for vertical GaAs nanowire growth. We explain the growth behavior difference on polarity of these substrates by a model that invokes the surface reconstruction and bond dissociation energy for each compound. The model successfully predicts the observed growth tendencies. In particular, it explains why InP easily forms the Wurtzite crystal phase in the nanowire form and why this phase can be easily disrupted by small amounts of As or Ga incorporation observed in InAsP and InGaP nanowire growth. *This work was supported in part by the Center for Energy Nanoscience, an Energy Frontier Research Center funded by the U.S. Department of Energy, Office of Science, Office of Basic Energy Sciences under Award Number DE-SC0001013 and by the National Science Foundation under Grant Number ECCS-0901867.

12:00 PM Lunch

Nitrides (Nonpolar and Semipolar)

Tuesday PM	Room: Lakeside Ballroom
May 25, 2010	Location: Hyatt Regency Lake Tahoe

Session Chairs: Russell Dupuis, Georgia Institute of Technology, Atlanta, GA, USA; Sung-Nam Lee, Korea Polytechnic University, South Korea

---

1:30 PM
Growth of Semipolar (10-13) InN on M Plane Sapphire by MOVPE: *Duc Dinh*[1]; Markus Pristovsek[1]; Raimund Kremzow[1]; Michael Kneissl[1]; [1]Technical University of Berlin

Growth of nonpolar and semipolar III-group nitride films has gained much interest due to suppression of spontaneous and strain-induced polarization effects. However, the growth of high quality InN is very challenging. Especially in MOVPE the growth window is very narrow. Thus, very few publications on nonpolar InN exist and there is no report about semipolar InN.We present the first semipolar InN layers grown on (10-10) *m*-plane sapphire substrates by metal-organic vapor phase epitaxy. In order to grow III-nitride layers on sapphire substrates, a nitridation process is employed to improve the crystalline quality and optical properties. In this study different nitridation times from 45s to 6min at 1050°C prior to InN epitaxy were investigated. At 2 to 4min nitridation, the InN layers showed exclusively (10-13) orientation in high-resolution X-ray diffraction (XRD), rotated 90° to the sapphire *m*-plane substrate. Similar to semipolar GaN on m-plane sapphire, also the (10-13) layers of InN show a strong twinning. However, the InN layers with the shorter and longer nitridation times showed additional (10-12), (11-20) and (11-22) orientations. Nitridation times of 2 and 4min resulted in improved values of full width at half maximum (about 0.6°) in the XRD symmetric $\omega/2\theta$ scan and smallest root-mean square roughness (rms~19nm for 10µmx10µm) determined by atomic force microscopy. Photoluminescence (PL) measurements at low temperature of the grown InN showed a maximum of near band-edge at energies between 0.7 - 0.75 eV.

1:50 PM
Growth of Planar Semipolar (10-11) GaN on Pre-Patterned Sapphire Substrates: *Stephan Schwaiger*[1]; Ilona Argut[1]; Thomas Wunderer[1]; Frank Lipski[1]; Rudolf Rösch[1]; Sebastian Metzner[2]; Jürgen Christen[2]; Frank Bertram[2]; Ferdinand Scholz[1]; [1]University of Ulm; [2]Otto-von-Guericke-University

Currently, there are many research activities to obtain devices on semipolar GaN due to the advantage of reduced piezoelectric fields compared to c-plane oriented material. In particular, the facets which form naturally are preferred due to a high surface quality. It has been shown that the (10-11) orientation fulfills these requirements very well [1]. Unfortunately, there is still no satisfying possibility to grow high quality planar semipolar (10-11) GaN on large scale up to now. We report on the growth of planar semipolar (10-11) GaN on pre-patterned (11-23) oriented sapphire substrates via metalorganic vapor phase epitaxy. The substrates were structured with grooves perpendicular to the c-direction of the crystal. Using appropriate growth parameters, GaN can be grown from the c-plane like sidewall of the patterned sapphire in c-direction of the GaN, resulting in a flat and planar semipolar surface. X-ray diffraction (XRD) \969-2\952-measurements only show peaks of the desired (10-11) GaN. In contrast to other experiments usually using facets to get semipolar (10-11) material [2] or growing on silicon [3], this method allows the planar growth of semipolar GaN on large areas on sapphire templates. Scanning electron, transmission electron and atomic force microscopy measurements show an atomically flat surface. Photoluminescence and cathodoluminescence spectroscopy spectra confirm the high quality of the material. The spectra are dominated by the near band edge emission (NBE) but still exhibit some defect related contributions. Furthermore, high resolution XRD rocking curve measurements result in small full widths at half maximum of less than 400arcsec for both, the symmetrical (10-11) and the asymmetrical (0002) and (10-12) reflections, respectively. [1] T. Iwahashi et al. Jap. J. Appl. Phys. 46 (2007), L103 [2] T. Wunderer et al. Appl. Phys. Lett. 89 (2006), 041121[3] T. Hikosaka et al. Appl. Phys. Lett. 84 (2004), 4717.

2:10 PM

Spatio-Time-Resolved Cathodoluminescence Microscopy of Semipolar InGaN SQW on Inverse GaN Pyramids: Correlation of Real Structure and Recombination Kinetics: *Sebastian Metzner*[1]; Frank Bertram[1]; Juergen Christen[1]; Thomas Wunderer[2]; Frank Lipski[2]; Stephan Schwaiger[2]; Ferdinand Scholz[2]; [1]Otto-von-Guericke-University Magdeburg, Germany; [2]University of Ulm, Germany

We present a direct microscopic correlation of the crystalline real structure and the recombination kinetics of a semipolar InGaN/GaN single quantum well (SQW) using highly spatially, spectrally and time-resolved cathodoluminescence microscopy (CL). The sample under investigation was grown using MOVPE. On top of a 2 µm thick GaN buffer a 200 nm thick SiO_2 mask was patterned into hexagonally shaped pads with 3µm space between by photolithography and reactive ion etching. Subsequent MOVPE overgrowth led to perfectly smooth {10-11} and {11-22} facets above the mask forming a surface structure of 3D inverse pyramids due to selective area growth. This structured surface of semipolar facets is used as a template for an InGaN SQW optimized for long wavelength emission. The spectrally resolved CL measurement at 4K reveals a gigantic shift of nearly 1eV of the SQW emission energy along the facet. At the center position of the inverted pyramid the InGaN emits at 380nm (3.26eV), going along the facet to the ridge the luminescence monotonously shifts towards longer wavelengths reaching 530 nm (2.34eV) at the very top. At exactly the same facet, the evolution of microscopic transient properties was investigated by time-resolved CL transient mapping. At the ridge the spectrally integral, the local transient directly shows a significantly slower recombination kinetic of the low energy emission at the onset as well as at the decay. The initial lifetime map quantifies the correlation to $\tau_{initial} < 0.4$ns at the center ($\lambda =$ 380nm) and $\tau_{initial} > 13$ns at the ridge ($\lambda = 530$nm).Additionally, local time-delayed spectra give access to the spectral and temporal characteristics of the InGaN SQW at a microscopic position. Especially the long wavelength SQW emission near the ridge exhibits a pronounced red-shift of the spectrum at the onset as well as at the decay. This implies that polarization fields do not have a dominating impact on the recombination kinetics, otherwise we would expect a blue-shift during onset due to screening of the quantum confined Stark effect. Moreover, localization in time and space can be observed as the main recombination mechanism in the semipolar green-emitting InGaN quantum structure.

2:30 PM

Heteroepitaxially Grown A-Plane GaN without Evidence of Basal Plane Stacking Faults in X-Ray Diffraction Measurements and Luminescence Spectra: *Matthias Wieneke*[1]; Martin Noltemeyer[1]; Thomas Hempel[1]; Hartmut Witte[1]; Armin Dadgar[1]; Juergen Blaesing[1]; Juergen Christen[1]; Alois Krost[1]; [1]Otto-von-Guericke-University Magdeburg

Growing non c-plane wurtzite III-N films, as, e. g., a-plane GaN, is a possibility to reduce or even to avoid polarization affected red shifting of luminescence and reduction of radiative recombination efficiency of GaN based light emitting quantum-wells. Therefore r-plane sapphire substrates are well-established to get non-polar a-plane GaN films. However, heteroepitaxially grown a-plane GaN films are characterized by poor crystal quality expressed in a high density of basal plane stacking faults and partial dislocations. For improving a lattice matched growth of Si doped GaN films on (1-102) r-plane sapphire substrates by metal organic vapor phase epitaxy high temperature AlGaN nucleation layers were used. FE-SEM images revealed three dimensionally grown GaN crystallites sized up to tenth micrometer in the basal plane and a few tenth micrometer along the c-axes. The micro structural properties were investigated by high resolution X-ray diffraction, photoluminescence and cathodoluminescence. The full width at half maxima (FWHMs) of the ω-scans at the in-plane GaN(1-100) and GaN(0002) Bragg reflections in the ranges of about 450 arcsec and 525 arcsec, respectively, exhibited a very high crystal quality. Furthermore, the luminescence spectra were dominated by near band gap emission, while there was no separated peak of the basal plane stacking faults. These results are in good agreement with the detailed evaluation of the ω-scan broadening. We will present heteroepitaxially grown a-plane GaN with a considerable reduced density of the basal plane stacking faults.

2:50 PM

Growth and Characterization of Green Emission A-Plane InGaN/GaN MQW Grown on Trench Epitaxial Lateral Overgrowth A-Plane GaN: *Shih-Pang Chang*[1]; Bo-Hang Chiang[1]; Chi-Chin Yang[1]; Tien-Chang Lu[1]; Hao-Chung Kuo[1]; [1]National Chiao Tung University

The growth of InGaN/GaN quantum wells (QWs) as an active region in light emitting diodes (LEDs) on non-polar GaN crystal planes is considered as a promising approach for improving quantum efficiency due to the absence of quantum-confined stark effect (QCSE). In this study, we characterized the structural and optical properties of a-plane MQWs grown on Trench Lateral Overgrowth (TELOG) a-plane GaN template [1]. The a-plane InGaN/GaN MQWs were grown on TELOG a-plane GaN template under growth temperature 750°, 730° and 710°. The total pressure was 100mbar for TELOG template and 400mbar for MQWs. After growth, the spatial luminescence properties were characterized by cathodoluninescence (CL). The polarization and photoluminescence (PL) properties were excited by He-Cd and Ti-sapphire laser, respectively. The crystalline quality was characterized by X-ray diffraction (XRD). The figure 1 shows the Omega-2Theta scan of the three samples, the satellite peaks became more obvious as decreasing the growth temperature. This could be due to the lower V/III ratio that will promote 2D growth of a-plane GaN. In the figure 2, the degree of polarizations at room temperature was 74%, 85% and 50% for UV, blue and green emission MQWs respectively. In figure 3, as the growth temperature was decreased from 750° to 710° the emission pattern became spotty and not uniform. This is suggested due to the phase separation of InGaN alloy under high In composition, and results in zero dimension InGaN clusters which reduce the degree of polarization of green emission MQWs. High crystalline and optical properties of blue emission MQWs had been developed with a strong polarization of 85% perpendicular to c-axis and uniform In distribution in the QWs. These results are encouraging for developing high In composition nonpolar InGaN/GaN MQWs to realize high efficiency green emitters.[1]T. C. Wang, T. C. Lu, T. S. Kuo, H. C. Kuo, H. G. Chen, M. Yu, C. C. Chuo, Z. H. Lee, S. C. Wang, phys. Stat. sol. (c) 3, 2519 (2007).

3:10 PM

Regrown High Quality A-Plane GaN on In Situ Etched GaN Template by MOCVD: *Hsiao-Chiu Hsu*[1]; Yan-Kuin Su[2]; Shyh-Jer Huang[1]; Shin-Hao Cheng[2]; Jia-Ming Cao[2]; [1]National Cheng Kung University; [2]Kun Shan University of Technology

In this paper, a high efficient method for reducing dislocation has been investigated to grow the a-plane GaN on in-situ etched GaN template. First, a 1µm a-plane GaN was deposited on the r-sapphire by MOCVD. Then, it is treated by in-situ etching in the mixture gas (H2/NH3) at high temperature. The ratio of mixture gas and the effect of temperature have been investigated. From scanning electron microscopy (SEM) images, it was shown that there has the stripe-like pattern along c-axis on the surface after in-situ thermal etching. Moreover, it was found that the inverse-pyramidal pits result in deeper wells. The possible explanation is the in-situ thermal etching method shows defect-selective etching property. Finally, high-resolution X-ray diffraction (HR-XRD) measurement shows that the crystal quality of re-grown GaN is better than the as-grown GaN. The mechanism of the re-grown process has been discussed. This paper provides a simple and short period process to grow a high quality a-GaN in MOCVD without any ex-situ process.

3:30 PM Break

Characterization

Tuesday PM
May 25, 2010

Room: Regency C&F
Location: Hyatt Regency Lake Tahoe

Session Chairs: J. Creighton, Sandia National Laboratories, Albuquerque, NM, USA; Kerstin Volz, Philipps University Marburg, Marburg, Germany

---

1:30 PM

Crystal Defect Topography of SK Dots Using Atomic Force Microscopy: Kamil Gradkowski[1]; Lorenzo Mereni[1]; Valeria Dimastrodonato[1]; Guillaume Huyet[1]; *Emanuele Pelucchi*[1]; [1]Tyndall National Institute

Understanding the defect formation during Stransky-Krastanov (SK) quantum dot (QD) epitaxy is a fundamental step towards the optimization of growth parameters.

Substantial defect formation processes are more easily found when longer wavelength QD are sought and care has to be put into both the QD deposition parameters and their capping. These are vitally important steps for obtaining defect-free QD layers. It has been reported that the ripening of the dots and the strain relaxation process can produce undesirable dislocations in the capping layer, which can provide localized heating as well as disrupt stacked QD layers, degrade performances and even destroy the waveguide in a laser device. So far the stacking fault dislocations have been observed and studied using Transmission Electron Microscopy (TEM), which is a costly, time-consuming and relatively impractical technique. We show that, provided appropriate capping growth protocols are implemented, Atomic Force Microscopy (AFM) can image SK dot sample defect densities, and therefore provides an excellent cheap, fast and, most importantly, non-invasive alternative to TEM, demonstrating itself as a perfect tool toward the optimization of SK dot growth parameters by metalorganic vapor phase epitaxy (MOVPE). We have grown single InAs/GaAs QD layer using low-pressure MOVPE in different conditions and optimized its emission properties, correlating them with the defect densities. We can show that AFM can image defects on the sample surface, which appear, variably, either as squares or linear defects. The defect density as a function of the estimated surface growth temperature (T_{QD}) shows rapid decline with increasing temperature: from 1.3×10^{7} cm^{-2} at 475°C to 1.85×10^{6} cm^{-2} at 530°C. The defect density for $T_{QD}>530°C$ is below our detection limit (1×10^{6} cm^{-2}), which is limited by our statistical analysis. On the other hand, since the Arrhenius plot shows two stages of the defect density evolution, it appears reasonable to speculate that two mechanisms (with two different activation energies) are responsible for their formation. We can also correlate the photoluminescence intensity with defect density. The photoluminescence is hindered by the presence of the defects and is getting better as the growth temperature increases.

1:50 PM

Characterization of III-V/Si(100) Anti-Phase Domains: *Henning Döscher*[1]; Peter Kleinschmidt[1]; Benjamin Borkenhagen[2]; Anja Dobrich[1]; Sebastian Brückner[1]; Oliver Supplie[1]; Ulrike Bloeck[1]; Gerhard Lilienkamp[2]; Winfried Daum[2]; Thomas Hannappel[1]; [1]Helmholtz-Zentrum Berlin für Materialien und Energie; [2]Clausthal University of Technology

The technological interest in superior electronic and opto-electronic properties of III-V semiconductors promotes the research for their heteroepitaxial integration on monocrystalline silicon substrates. However, interface-induced defect mechanisms still prohibit many of the desired applications. Anti-phase disorder according to the step structure of the substrate surface prior to III-V deposition is one of the major challenges in polar on non-polar epitaxy. Thin gallium phosphide films grown on Si(100) represent an important model system and anti-phase domains (APDs) have been identified by transmission electron microscopy (TEM) and atomic force microscopy (AFM) on a local scale. Due to the specific surface orientation of APDs, evaluations of the domain composition by surface sensitive probes like low energy electron diffraction (LEED) and reflectance anisotropy spectroscopy (RAS) is possible. These techniques integrate over surface areas in the mm to cm scale and, thus, provide quantitative access to the APD fraction. However, the lack of lateral resolution complicates the comparison to TEM results since the homogeneity of the APD distribution is not resolved. In contrast, scanning tunnelling microscopy (STM) maps the atomic structure of the P-rich GaP(100) surface typical for MOVPE preparation. It exhibited the predicted $p(2\times2)/c(4\times2)$ reconstruction formed by alternating, buckled phosphorus dimers stabilized by one hydrogen atom per dimer. We observed zigzag dimer chains which ran either parallel or anti-parallel over the surfaces and resulted in surface unit cells with $p(2\times2)$ and $c(4\times2)$, respectively.Where an anti-phase boundary (APB) intersects the surface, the dimer chains alternate between perpendicular orientations, explaining the potential for APD detection by surface sensitive instruments. We performed low energy electron microscopy (LEEM) on thin GaP films deposited on slightly off-oriented Si(100) substrates to evaluate this technique for systematic inspection of APD distributions. The specific MOVPE preparation for a P-rich sample surface ensured the formation of the well-defined (2x2)/c(4x2) reconstruction of GaP(100). Due to the presence of APDs, two perpendicular orientations superimpose in the LEED pattern. Since the half-order diffraction reflexes in the perpendicular directions were mainly generated by the respective domains, dark field LEEM imaging allowed us to distinguish between the APDs and the main phase.

2:10 PM

Time Resolved Measurement of Interfacial and Bulk Recombination of Solar Cell Materials: *Nadine Szabó*[1]; B. Sagol[1]; Marinus Kunst[1]; Klaus Schwarzburg[1]; Thomas Hannappel[1]; [1]Helmholtz Center Berlin for Materials and Energy

One of the most important properties in solar cells is the minority carrier lifetime. We will present time resolved measurements of low band gap III-V compounds. Time resolved photoluminescence (TRPL) and transient microwave conductivity (TRMC) measurements were performed to evaluate the lifetime in p-type absorber materials. With this method it is possible to analyze both the interface and the bulk properties. For this propose we have grown double hetero structures consisting of InP barriers embedding either an InGaAs and InGaAsP absorber layer, which could be part of a low bandgap tandem solar cell with InGaAs/InGaAsP absorber layers. This tandem cell could replace the Ge subcell of the current world record multi-junction solar. Hence, the most relevant injection level of TRPL corresponding to a solar cell at short circuit and the operating voltage and under modest concentration can be studied. To get meaningful results, a precise knowledge of the excess carrier density created by the pump pulse is necessary. Our single photon counting TRPL setup allows to quickly measure the spatial pulse profile as well as the pulse power at the sample position. Typical lifetimes range from 1 to several hundred ns. However a strong dependency on the minority carrier injection level was found. The lifetime was found to be controlled by Shockley-Read-Hall recombination in the low injection regime. Due to the arsenic transition in the InP layer the InGaAs/InP interface is reported to be critical regarding the sharpness of the interface. We have varied the preparation method of the InGaAs/InP interface. Two approaches are possible, a III-rich preparation and a V-rich preparation. We will show the dependency of the interface reconstruction on the interface recombination velocity. Furthermore, by scanning the sample, spatial inhomogeneities in the lifetime can be detected.

2:30 PM

Intrinsic Doping Characteristics of MOVPE-Grown InAs: *Magnus Wagener*[1]; Viera Wagener[1]; Reinhardt Botha[1]; [1]Nelson Mandela Metropolitan University

Besides the various technological application of InAs, the narrow bandgap arsenide compound is of great importance for the development and evaluation of III-V defect models. An interesting peculiarity of InAs is the positioning of the charge neutrality level above the conduction band minimum. This has been proposed as an explanation for the near-surface electron accumulation layer observed in intrinsic and nominally doped material [1]. As a result, the degenerate surface layer typically conceals the bulk transport characteristics of thin film material, greatly complicating the interpretation of even basic electrical measurements. Recent work by Wagener et al. [2,3] demonstrated the accurate determination of the transport properties of non-degenerate p-type InAs by employing variable temperature thermoelectrical measurements in conjunction with Hall effect measurements. In this paper, the electrical properties of undoped InAs grown by MOVPE on GaAs substrate, is presented. The free carrier density and mobility, as well as the level of compensation have been determined by comparing the transport characteristics before and after hydrogenation. Unlike other III-V compounds, where hydrogen behaves as an amphoteric impurity, hydrogen remains a donor in n-type InAs, preferentially passivating any acceptors. The extent by which hydrogenation increased the free carrier concentration of n-type InAs has therefore be used to deduce the level of compensation in the as-grown material. The shallow and deep level concentrations have also been obtained using steady-state and transient capacitance measurements performed on p-i-n diodes fabricated using various growth conditions. The effect the growth temperature and V/III ratio has on the intrinsic doping of InAs thin films, as well as the diode characteristics, will be presented. [1] L.F.T. Piper, T.D. Veal, M.J. Lowe, and C.F. McConville, Phys. Rev. B 73 (2006) 195321. [2] M.C. Wagener, V. Wagener, and J.R. Botha, Appl. Phys. Lett. 94 (2009) 262106. [3] M.C. Wagener, V. Wagener, and J.R. Botha, Physica B 404 (2009) 5038.

2:50 PM

Direct Microscopic Correlation of Real Structure and Recombination Kinetics in Semipolar Grown InGaN Quantum Well Grown on of Hexagonal GaN Pyramids: *Frank Bertram*[1]; Sebastian Metzner[1]; Juergen Christen[1]; Michael Jetter[2]; Clemens Wächter[2]; Peter Michler[2]; [1]University of Magdeburg; [2]University of Stuttgart

One principal problem in the nitrides is the quantum confined Stark effect as a consequence of the strong internal polarization fields in c-direction (QCSE). The most common strategy to overcome the QCSE-problem is the growth of heterostructures in other directions than the c-axis. One approach to reduce the polarization fields is the growth in semipolar directions. However, the epitaxial growth on such planes is by far less developed than the growth on the commonly used c-plane. Moreover, in ternary alloys and their heterostructures, nanoscale fluctuations of stoichiometry as well as interfaces have strong impact on the radiative recombination in light emitters. In this study we correlate the optical properties of hexagonal GaN pyramids overgrown by an InGaN single quantum well with the crystalline real structure using highly spatially, spectrally, and time resolved cathodoluminescence microscopy. The selective epitaxial growth of GaN was performed with MOVPE. First, a 1µm GaN buffer layer was deposited on sapphire using an AlN nucleation layer. Subsequently, a 60nm thick sputtered SiO2 mask was patterned by photolithography to form arrays of round windows. GaN was selectively grown on top of this mask creating periodic arrays of hexagonally shaped pyramids. The selfassembled pyramids exhibit perfectly formed semipolar {10-11} facets. The pyramids were covered by a nominal 6nm thick In0.18Ga0.82N quantum well followed by a 30nm thick GaN caplayer. The InGaN luminescence is exclusively emitted from the pyramids. A striation-like intensity contrast is observed at the pyramids' bases. Here, the stripes of high and low intensity directly correlate with the local emission wavelength: lower intensities are associated with shorter wavelengths, resulting in an average wavelength of 550nm. In the upper part of the pyramids two distinctly different wavelengths are emitted: while 590nm dominates at the edges and at the very top of the pyramids, the center of the facets is dominated by 530nm emission. These results directly visualize a higher indium incorporation and/or a thicker quantum well at the edges and tops of the pyramids, i.e. the self organized formation of quantum wires at the edges and quantum dots at the tips of the pyramids.

3:10 PM

Deep Structural Analysis of Novel BGaN Material Layers Grown by MOVPE: *Simon Gautier*[1]; Gilles Patriarche[2]; Tarik Moudakir[3]; Mohamed Abid[4]; Konstantinos Pantzas[4]; Gaëlle Orsal[1]; David Troadec[5]; Ali Soltani[5]; Abdallah Ougazzaden[4]; [1]University of Metz; [2]LPN- CNRS; [3]Supelec; [4]UMI - Georgia Tech CNRS 2958; [5]IEMN

The development (Al,Ga,In)N nitride materials has given rise to a new generation of opto- and micro-electronic devices. However, there is still room for innovation and improvement in this field. For instance, Boron Nitride (BN) has numerous unique properties, i.e. high-temperature-induced electrical conductivity, high mechanical resistance, exceptional chemical stability, short chemical bond length, radiation resistance and optical transparency in a wide spectral range. B(Al,Ga,In)N alloys have been recently proposed in order to take advantage of these properties. Specific applications of such alloys currently under development are: i) BAlGaN based UV-optoelectronic device active regions, possibly lattice matched on AlN or SiC substrates, ii) BAlGaN nuclear detectors, taking advantage of the high sensitivity of the boron atoms to gamma radiation and iii) BInGaN based third generation solar cells in the visible range lattice matched on GaN or ZnO template substrates. In spite of numerous interesting applications, there are several challenges involving the growth of B(Al,Ga,In)N alloys. Since BN is highly dissimilar to GaN, InN and AlN in terms of lattice constant or stable crystalline phase, it is commonly accepted that randomly distributed B(Al,Ga,In)N alloys are not attainable above a few percent of boron. Even if growth conditions can be optimized to limit the impact of immiscibility gaps and improve the material quality, a better understanding of the alloy structural properties will help to further improve boron incorporation with good material quality. In this work, we used High Resolution Transmission Electron Microscopy (HR-TEM) and aberration-corrected Scanning TEM (STEM) to investigate simple layer and multi-layer structures of BGaN and BInGaN grown by MOVPE on GaN template substrates. We used atomic resolution High Angle Annular Dark Field (HAADF) STEM images with EDX spectroscopy to determine their structural and chemical nature of grown films. At low bonron incorporation we observed a uniform composition with very sharp sixfold hexagonal pattern of electron diffraction. However, at high boron content we observed the formation compositional non-homogeneities in the structures. For example, c-BGaN clusters, nano-precipitates and material platelets formation at multi-layers structures interfaces have been identified. Results will be presented under the scope of the optimization of the layers quality.

3:30 PM Break

Poster Session I

Tuesday, 4:00-6:00 PM	Room: Regency Ballroom
May 25, 2010	Location: Hyatt Regency Lake Tahoe

Please see pages 39-45 for posters.

Panel Discussion:
The Role of III-Vs in SSL and Terrestrial PV

Tuesday, 6:30-9:30 PM	Room: Lakeside Ballroom
May 25, 2010	Location: Hyatt Regency Lake Tahoe

Session Chair: Robert Biefeld, Sandia National Laboratories, Albuquerque, NM, USA

Wednesday Invited Talks

Wednesday AM	Room: Lakeside Ballroom
May 26, 2010	Location: Hyatt Regency Lake Tahoe

Session Chair: Christine Wang, Massachusetts Institute of Technology, Lincoln Laboratory, Lexington, MA, USA

8:30 AM Invited

Impact of Gas-Phase and Surface Chemistry during InGaN MOVPE: *J. Creighton*[1]; Michael Coltrin[1]; Daniel Koleske[1]; Jeffrey Figiel[1]; [1]Sandia National Laboratories

During MOVPE the indium content of InGaN films is typically lower than expected and difficult to accurately control. In particular, indium content falls significantly as the growth temperature is raised above 700°C. The observed trends with temperature and other growth parameters are most often attributed to the limited thermodynamic stability of InGaN films and/or the kinetic stability of surface growth species. Some of our recent observations suggest that parasitic gas-phase reactions may also play a role in limiting indium incorporation. By using in situ laser light scattering, we have directly observed the formation of gas-phase nanoparticles during InN and InGaN metal-organic chemical vapor deposition. The angular dependence of the light scattering intensity suggests that the nanoparticles are predominately metallic In or InGa alloys, while ex situ TEM results indicate a composite In/InN composition. From the angle-resolved scattering profile, we determined that the particle diameters were in the range 20-50 nm, and particle densities were mostly in the 1e8-1e9 cm^{-3} range. Results indicate that for growth temperatures of ~800°C nearly 100% of the indium near the surface is converted into gas-phase nanoparticles and is no longer available for InGaN growth. However, MOVPE results as a function of platen spin rate (which controls residence time) suggest that the nanoparticles may only be a “downstream” consequence and play no significant role in limiting indium incorporation. In our talk we will review the potential impact of the parasitic gas-phase reactions and compare with the possible roles of surface kinetic and thin-film thermodynamic effects. Acknowledgement: This research was performed at Sandia National Laboratories, for the United States Department of Energy under contract No. DE-AC04-94AL85000.

9:00 AM Invited

MOVPE Growth of Lattice Matched III/V Materials on Silicon Substrate for Optoelectronics: *Bernardette Kunert*[1]; Kerstin Volz[2]; Wolfgang Stolz[2]; [1]NAsP III/V GmbH; [2]Philipps University

Nowadays the research activities for the growth of III/V-semiconductor materials on Si substrate are again gaining increasing interest. In particular the integration of III/V compound materials to Si based microelectronics but also the use of Si as a cheap substrate for III/V multi junction solar cells are in strong focus. The major advantages of III/V semiconductors over Si are their sophisticated optical properties and high electron mobilities due to the direct electronic band structure. In order to fully profit from these benefits it is necessary to preserve a high crystal quality of the III/V layer in the monolithic integration process. However, the main obstacle between Si and most standard III/V compound material systems such as GaAs, InP or InAs is the large lattice mismatch, which leads unavoidably to the formation of a threading dislocations restricting device lifetime specifically for lasers. The novel dilute nitride Ga(NAsP) allows for the first time the monolithic integration of a direct III/V band gap material lattice matched to Si substrate. The high As concentration of the quaternary compound material guarantees the direct band gap formation whereas the incorporation of N enables the adjustment of the lattice constant of Ga(NAsP) towards the one of Si. In this novel lattice matched approach of III/V integration on Si substrates no misfit or threading dislocations are formed being essential to ensure long device lifetime.After a short introduction about the active material system Ga(NAsP) the focus of this presentation is the monolithic integration scenario of Ga(NAsP) based laser diode on exactly oriented (001) Si substrate. MOVPE growth conditions will be discussed in line with structural as well as optical properties of deposited multi-quantum-well heterostructures and laser structures on Si. Since the successful integration of a laser source on Si microelectronics would open up a completely new field of application possibilities some future integration concepts will be suggested and discussed.

9:30 AM Break

Nitrides II

Wednesday AM	Room: Lakeside Ballroom
May 26, 2010	Location: Hyatt Regency Lake Tahoe

Session Chairs: Menno Kappers, University of Cambridge, Cambridge, UK; Uwe Rossow, TU Braunschweig, Braunschweig, Germany

10:00 AM

AlGaN Growth Rate and Composition in a Close-Coupled Showerhead MOVPE Reactor: *Joachim Stellmach*[1]; Özgür Savas[1]; Jessica Schlegel[1]; Markus Pristovsek[1]; Michael Kneissl[1]; Eugene Yakovlev[2]; [1]Technische Universität Berlin; [2]STR Group - Soft-Impact Ltd

For deep UV light emitters AlGaN layers with high aluminium content are needed. However, metalorganic vapour phase epitaxy of AlGaN is quite challenging due to gas-phase pre-reactions and the formation of nanoparticles. Therefore, the growth rate and composition depend non-linearly on temperature and growth pressure. The underlying mechanism is the formation of AlN particles, but interactions of gallium species with the particles must be considered under high growth rate conditions. We have investigated the growth of AlGaN layers on sapphire substrates in an Aixtron 3x2” close-coupled showerhead (CSS) MOVPE reactor. In case of a CSS MOVPE reactor the chamber height, i.e. the distance between gas inlet and susceptor, provides an additional growth variable to control gas phase reaction. To prevent gas phase reactions, AlGaN is typically grown at low total pressures to obtain a high velocity of the carrier gases and thus only a short residence time in the gas phase. We found that the chamber height is also a critical parameter to minimize the parasitic reactions. Reducing chamber height from 21 mm to 6 mm results in an increase of growth rate from 0.5 μm/h to 4 μm/h and an increase of aluminium content from 15% to 50%. With 6 mm chamber height, the growth rate of AlGaN over the entire composition range exceeded 3 μm/h for standard fluxes. The observed composition and growth rates could be reproduced by two models. The first is an analytical model assuming fixed rate coefficients for TMAl and TMGa loss via first order particle formation, with the rate constants being fitted to reproduce the AlGaN growth rate vs pressure and chamber height. The second model uses the CVDSim software package. It assumes formation of AlN particles and their additional growth at the expense of $Ga(CH_3)_x$ species. At this stage, the particle growth is kinetically limited by CH_3 desorption from the particle surface. Both models fit the data well, but an increase of Al content at chamber heights larger than 18 mm (visible in XRD data) is only predicted by the numerical model including nanoparticle formation.

10:20 AM

Investigation of Nitride MOVPE at High Pressure and High Growth Rates in Large Production Reactors by a Combined Modelling and Experimental Approach: *Martin Dauelsberg*[1]; Daniel Brien[1]; Roland Püsche[1]; Oliver Schön[1]; Eugene Yakovlev[2]; Alexandr Segal[2]; Roman Talalaev[2]; [1]AIXTRON AG; [2]STR Group - Soft Impact Ltd

The scope of this work is the analysis of gas phase processes during MOVPE of GaN at conditions of high pressure, high growth rates and large reactor volumes by growth experiments in a production scale reactor, refine our computational model based on these data and lead the way to capacity scaling while increasing growth rate and pressure at the same time. Usually difficulties arise at the above conditions due to parasitic gas-phase processes that ultimately result in gas phase nucleation, which is critical for deposition efficiency and uniformity on large substrates. An 8x4 inch Planetary reactor was used to investigate the parametric dependencies of gas phase nucleation and its effect on GaN growth rate profiles on stalled wafers. Pressure, MO precursor flow, residence time and wall temperatures were varied independently and over a wide range. Modelling includes the computation of flow, heat transfer and reaction chemistry. High pressure depletion is critically governed by nucleation of an over-saturated low volatile species and subsequent nano-particulate growth. Among our findings there is a critical pressure at otherwise fixed conditions when radial depletion of the growth rate curve increases due to the onset of gas phase nucleation. Likewise, there is a linear relation between mean growth rate on wafer and MO flow up to a point when this relation starts to saturate. Both critical values can be pushed out by increasing gas flow. The effect of increasing wall temperature, however, turned out rather ambiguous due to the competing effects of reduced thermophoretic particle drift to the colder walls and increased parasitic reaction kinetics in the hotter ambient. The modelling approach is validated and the typically obtained prediction accuracy is discussed in view of the complexity of the process. Understanding of the processes that control gas phase nucleation and intensive use of computational modelling enabled us to increase the chamber and optimise gas injection and chamber contours. We were able to obtain growth rates of GaN up to 8 µm/h at p=600 mbar on multiple 6 inch sapphire wafers before saturation started, with thickness standard deviation of 2% and layer quality judged by XRD FWHM.

10:40 AM

Strain Controlled Growth of Crack-Free GaN with Low Defect Density on Silicon (111) Substrate: *Philipp Drechsel*[1]; Henning Riechert[1]; [1]Paul-Drude-Institut für Festkörperelektronik

GaN growth of high thickness and good crystalline quality is desirable for applications in high-frequency electronics and optoelectronic devices. While GaN today is typically grown on sapphire and silicon-carbide it is desirable to establish growth on less expensive substrates. Despite a number of growth problems, mostly due to the high CTE mismatch, the availability of silicon wafers with large diameters, its low price as well as the good thermal conductivity makes silicon a promising candidate for future GaN heteroepitaxy. In our work GaN layers with a thickness of 4.5µm on Si (111) were achieved using a 400nm AlN/AlGaN nucleation layer and low temperature (LT) AlN inter-layers of approximately 20nm thickness. The conservation of compressive strain during growth of the GaN layers is essential; otherwise the high CTE mismatch between GaN and silicon will lead to crack formation during cool down to RT. The structural quality and properties were characterized by XRD, etch pit density (EPD), AFM and TEM. A comparison is made between GaN grown on sapphire and silicon. Typical values for x-ray diffraction ω-scans are 445” and 650” for the GaN on Si (0002) and (20-21) reflexions, respectively. EPD measurements indicate a dislocation density of approximately 5E8 cm^{-2}. However a threading dislocation density (TDD) of 1E9 cm^{-2} is observed in TEM-measurements. The surface roughness (RMS) of the GaN on Si is in the range of comparable samples grown on sapphire.We found a major dependency of compressive strain and crystalline quality on the properties of the LT-AlN interlayers and the silicon doping level. Adding a SiN interlayer, the amount of edge-type dislocations could be reduced significantly at the cost of compressive strain. Ex-situ bow-measurements clearly show that the compressive strain built up during growth is in good agreement with the final shape of the epitaxial wafers. Finally we will discuss the potential to optimize both strain and quality of the grown GaN layers on Si(111).

11:00 AM

Growth and Lift-off of High-Quality GaN Epitaxial Thin Films Using Self-Assembled Monolayers of Silica Microspheres: *Qiming Li*[1]; George Wang[1]; [1]Sandia National Laboratories

We demonstrate that self-assembled monolayers of silica microspheres can be used as inexpensive, selective growth masks for both significant threading dislocation density reduction and laser-free lift-off of GaN epilayers and devices. Silica microspheres self-assemble into a close-packed monolayer on the surface of an initial GaN epilayer on sapphire using a Langmuir-Blodgett method. In a subsequent GaN regrowth, the silica microspheres effectively terminate the propagation of threading dislocations. As a result, the threading dislocation density, measured by large area AFM and CL scans, is reduced from 3.3 × 109 cm-2 to 4.0 ×107 cm-2. This nearly two orders of magnitude reduction is attributed to a dislocation blocking and bending by the unique interface between GaN and silica microspheres. The sequential wet etching of the samples in HF solution removes the silica microspheres sandwiched between the GaN epilayers and the growth template. Further wet etching of the samples in KOH solution successfully detaches the GaN epilayers from the growth templates. Micro-channels are created on the GaN epilayers by plasma etching in order to facilitate the uniformity of the wet etches. This laser-free lift-off technique may be potentially applied to lift-off GaN homoepitaxial thin film device from GaN bulk substrates. Sandia is a multiprogram laboratory operated by Sandia Corporation, a Lockheed Martin Company, for the United States Department of Energy under contract DE-AC04-94AL85000.

11:20 AM

Measurement of Real Wafer Temperature during Gan Growth on Sapphire and SiC: *Marta Borasio*[1]; Kolja Haberland[1]; Thomas Zettler[1]; Tobias Schenk[1]; Frank Brunner[2]; Markus Weyers[2]; [1]LayTec GmbH; [2]Ferdinand-Braun-Institut für Höchstfrequenztechnik

The growth temperature is the most critical parameter to control during MOVPE growth. Especially for LED production of GaN LEDs the emission wavelength and uniformity and, therefore, the yield strongly depend on the temperature variation across the wafer. As infrared (IR) pyrometers can only measure the temperature of IR absorbing and emitting materials, for GaN epitaxy on sapphire and SiC only the pocket temperature of the susceptor under the wafer is accessible. Due to the strained growth and the evolving wafer curvature, the true wafer temperature significantly deviates from the pocket temperature. Up to now, only in-situ measurements of the wafer curvature during growth could be used to indirectly estimate the wafer temperature and its profile. A newly developed UV pyrometer takes advantage of the absorption of the GaN layer at 400 nm. Using the tool detecting thermal radiation of GaN at the wavelength of 400 nm, we were able to directly measure the surface temperature of GaN layers on a sapphire or SiC wafer during growth in production-line MOCVD systems. The growth of a full GaN MQW LED structure was studied on 3” and 4” wafers. True wafer surface temperature, pocket temperature, three wavelength reflectance and wafer curvature have been measured simultaneously and are discussed in comparison to ex-situ PL mapping of the wafers. All parameters have been measured at various positions across the wafers’ diameter, allowing for spatially resolved results on thickness uniformity, temperature and wafer curvature distribution. The different behavior of a 2” wafer in the same run will be discussed as comparison. We will show that many effects on the true wafer surface temperature are invisible to the conventional infrared pyrometer.

11:40 AM

Efficient Growth of InN Films by Separate Supply of TMIn and DMHy: *Quang Thieu*[1]; Takashi Tachikawa[1]; Yuki Seki[1]; Shigeyuki Kuboya[1]; Kentaro Onabe[1]; [1]University of Tokyo

It is highly desirable to realize high-quality InN films by MOVPE for the practical use of InN-based devices in an industrial scale. For the MOVPE growth of InN films, a growth temperature around 500-600°C is essential to avoid thermal dissociation of InN. In view of this, dimethylhydrazine (DMHy) is an advantageous precursor of nitrogen as it decomposes much more efficiently than widely used NH$_3$ at the temperatures compatible with the InN growth. On the other hand, DMHy will form low-vapor-pressure adducts with trimethylindium (TMIn) at room temperature, and will hinder the InN growth. In this study, the adduct-forming parasitic reactions were efficiently suppressed by adopting a separate supply of the precursors, leading to a successful growth of InN films. An rf-heated horizontal-type reactor is used, to which Gas 1 (TMIn or DMHy) is introduced from the inlet at the up-stream region, while Gas 2 (the rest of the precursors) is fed through a capillary to the susceptor region, so as to avoid the mixing of the precursors at low temperature. An N$_2$ carrier is used, avoiding H$_2$ which leads to gas-phase etching of InN. The TMIn flow was 0.57 µmol/min with the growth time of 40 min. When TMIn is fed through the capillary, the growth temperature, pressure and V/III ratio are optimized to 520°C, 160 Torr and 200, respectively, with a grown film thickness around 100 nm, for the standard position (x=0) of the capillary orifice as reported elsewhere [1]. Then, the orifice position x was varied to assess the growth characteristics in detail. In the range x= 0~10 cm, the growth of the InN films is assured by the distinct InN(0002) XRD peak. The decreasing InN(0002) diffraction with increasing x (departing from the susceptor) is interpreted by the effective decrease of the TMIn supply and the effective increase of V/III ratio due to the extending flow from the capillary orifice. The growth of InN films is also assured when DMHy is fed through the capillary. [1] Q.T. Thieu, Y. Seki, S. Kuboya, R. Katayama and K. Onabe, J. Cryst. Growth 311, 2802 (2009).

12:00 PM Lunch

12:30-5:30 PM Virginia City Historical Tour (Available at an additional charge)

1:00-4:15 PM Tahoe Queen Lake Cruise (Available at an additional charge)

Devices II

Wednesday AM Room: Regency C&F
May 26, 2010 Location: Hyatt Regency Lake Tahoe

Session Chairs: Anthony SpringThorpe, National Research Council, Ottawa, Canada; Yoshiaki Nakano, University of Tokyo, Tokyo, Japan

10:00 AM
Characterization and Optimization of 2-Step Epitaxial Growth for Single-Mode DFB or DBR Laser Diodes: *Frank Bugge*[1]; Anna Mogilatenko[2]; Ute Zeimer[1]; Olaf Brox[1]; Goetz Erbert[1]; Marcus Weyers[1]; [1]FBH; [2]HUB

GaAs based single-mode diode lasers are of great interest for a wide range of applications such as atomic clocks, absorption spectroscopy and LIDARs. One possibility for the realisation of such diodes is the integration of a Bragg grating directly into the internal laser cavity resulting in distributed feedback (DFB) or distributed Bragg reflector (DBR) lasers. Their fabrication requires a 2-step epitaxy process and special efforts have to be put into the overgrowth of the grating to prevent its deterioration and defect formation. The laser structure is an Alx1Ga1-x1As/Alx2Ga1-x2As heterostructure with different quantum wells for different emission wavelengths. The first epitaxy step ends with an InGaP/GaAs(P)/InGaP/GaAs layer sequence in which the grating is formed by holographic photolithography and wet chemical etching. The shape of the grating changes during the heating up procedure for the 2nd epitaxy due to surface diffusion effects which also result in compositional variations across the trench nominally filled with AlGaAs of one composition. During the heating up, indium migration occurs and under phosphine flow quaternary InGaAsP intermediate layers are formed on the sidewalls. As a result, the second epitaxy step starts on different surfaces, which can lead to defect formation. Additionally, the Al incorporation on different growth facets may vary leading to lateral inhomogeneities of the Al content in the overgrown waveguide layer. Local Al fluctuations result in variation of the refractive index which affects the coupling coefficient and thus the device efficiency. This was investigated in detail by transmission electron microscopy (TEM). Also the oxygen peak at the regrown interface, which is the result of chemical etching and cleaning procedures, depends on the aluminium content and the growth temperature of the 2nd epitaxy step. The influence of the growth start temperature and the composition of the GaAs(P) grating layer on crystal quality and composition of the overgrown layers will be discussed. The results of single-mode laser diodes with emission wavelengths between 800 nm and 1064 nm will be shown.

10:20 AM
InP/AlGaInP Quantum Dot Laser Emitting at 638 nm: Wolfgang-Michael Schulz[1]; Marcus Eichfelder[1]; *Robert Rossbach*[1]; Michael Jetter[1]; Peter Michler[1]; [1]Universität Stuttgart

High-power semiconductor laser diodes emitting in the visible red spectral range (630–710 nm) have attracted great interest e.g. for data storage, medical applications like photodynamic therapy (PDT), for pumping of solid state lasers and display applications for laser projection. The epitaxial layer structures usually applied for such lasers consist of Al(Ga)InP cladding layers and AlGaInP waveguide layers embedding GaInP quantum wells (QW). However, theory has predicted better laser properties using quantum dots (QDs) as the active medium of semiconductor lasers than for higher dimensional media. For example, lower threshold current density, higher differential gain, and higher temperature stability were expected. To obtain QD lasers that emit deep red light, it has been shown that a stack of five InP-QDs layers embedded in GaInP barriers are capable to produce lasing at 740 nm with a threshold current density of 190 A/cm^2 [1]. However, when using aluminum containing barriers (AlGaInP), the interdiffusion of Al out of the barrier into the QDs increases with growth temperature, leading to higher bandgap energies and therefore shorter emission wavelengths of the QDs. Our sample structure was fabricated by metal-organic vapor-phase epitaxy on (100) GaAs:Si substrates oriented 6° toward the [111]A direction. A single-layer of self-assembled InP-QDs was grown by depositing 2.1 monolayers of InP at 710°C and placed in the center of a 20 nm thick undoped $(Al_{0.20}Ga_{0.80})_{0.51}In_{0.49}P$ barrier surrounded by two 150 nm thick undoped $(Al_{0.55}Ga_{0.45})_{0.51}In_{0.49}P$ waveguide layers. Using doped AlInP and highly doped $Al_{0.95}Ga_{0.05}As$ cladding layers a separate confinement heterostructure (SCH) was formed. After standard postgrowth photolithography and evaporation of ohmic contacts, the structure was equipped with 64 µm wide and 2000 µm long broad area stripes. Electrically pulsed laser operation at room temperature with a low threshold current density of 870 A/cm^2 and a lasing wavelength of 638 nm could be achieved. Optical output powers of more than 55 mW per facet and lasing up to 313 K is demonstrated. [1] A.B. Krysa et al., JCG 298 (2007) 663.

10:40 AM
Growth and Properties of Light Emitting Diodes with an Incorporated InMnAs Ferromagnetic Layer: *Jozef Novak*[1]; Peter Telek[1]; Stanislav Hasenohrl[1]; Ivo Vavra[1]; Marian Reiffers[2]; [1]IEE SAS; [2]IEP SAS

Great advances in the development of III-V diluted magnetic semiconductors materials (DMS) allow for the incorporation of ferromagnetic epitaxial layers into advanced device structures. To integrate an InMnAs epitaxial layer into a GaAs based light emitting diode (LED) structure, it is necessary to reach an acceptable compromise between two contradictory conditions. One is the necessity to incorporate the highest possible MnAs content to obtain good magnetic properties. The second one is to prevent the creation of hexagonal MnAs clusters inside the InMnAs matrix. The presence of such clusters substantially damages the crystallographic quality of an epitaxial layer with drastic impact on the LED properties. In this paper, we report on the incorporation of InMnAs layers with various thickness into GaAlAs/GaAs multiquantum well LED structures. We studied the influence of InMnAs layer thickness, composition and its position inside the LED structure on the optical and electrical characteristics. The LED structures were grown by metalorganic vapour phase epitaxy (MOVPE) on n-GaAs (100) oriented substrates at a growth temperature Tg=500°C. All InMnAs layers were grown at a V/III ratio of 133. The composition of the ternary was controled by adjusting the ratio between the partial pressures of ((MeCp)2Mn and TMIn. The partial pressure of (MeCp)2Mn was kept constant at a value of 3.59x10-2 mbar and the partial pressure TMIn was decreased. The active region consists of three 9-nm thick undoped GaAs wells separated by 18 nm AlGaAs barriers sandwiched between two 40 nm thick undoped AlGaAs spacer layers. An AlGaAs silicon-doped epitaxial layer was grown between the buffer and MQW structure. On top of the MQW structure, a p-doped AlGaAs layer was grown followed by a GaAs p+ cap layer. The Curie temperature Tc obtained by the SQUID measurements after the subtraction of the diamagnetic contribution of the GaAs substrate was approximately 343K. The electroluminescence properties versus magnetic field in a (0-1) T range will be presented.

11:00 AM
MOVPE Grown GaAs/AlGaAs QCLs with GaInP Waveguide: Dmitry Revin[1]; Paul Commin[1]; John Cockburn[1]; Ken Kennedy[1]; *Andrey Krysa*[1]; [1]University of Sheffield

MOVPE grown quantum cascade lasers (QCLs) were first demonstrated in 2003. Since that time MOVPE has become one of the major epitaxial techniques for manufacturing high-performance InGaAs/InAlAs QCLs promoting these devices towards mass-production. Little attention has been paid to mid-IR GaAs based QCLs as they cannot compete with their InGaAs/InAlAs counterparts in terms of performance due to fundamental reasons. One of the problems of GaAs/AlGaAs QCLs is that in practice the choice of waveguides is limited to AlGaAs. Depending on the Al fraction, these waveguides provide a low optical confinement or weaken the resistibility of QCLs to degradation. On the other hand, manufacturing GaAs/AlGaAs QCLs has certain advantages. In contrast to InGaAs/InAlAs, only one reagent requires switching while growing the core and no attention required to its lattice matching with the substrate. Besides, large, 6-inch diameter substrates are commercially available. In this paper, we show that MOVPE can address the waveguide issue to realise the above advantages.High quality In0.49Ga0.51P can be easily grown by MOVPE and represents a better alternative to the previously reported waveguide materials. We have made a direct comparison of QCLs with identical core region designs and grown at identical conditions but having different waveguides, i.e. GaAs and GaInP. The calculated figure of merit is higher by factor of 3 for the lasers with InGaP waveguide. All lasers operated very close to the designed wavelength of 9µm. However, the laser performance differed dramatically. The devices with InGaP claddings operated above room temperature up to at least 320K. The output peak power for these lasers was more than 250mW at 240K and about 10mW at 320K. The lasers with GaAs claddings operated only up to 210K with much higher threshold current densities. The waveguide losses for InGaP contained QCLs are found to be ~15cm-1, less than 25-30cm-1 estimated for the lasers with GaAs waveguide. By optimizing the laser design and growth conditions, we expect the performance of the QCLs with InGaP claddings to be improved even further, making them affordable sources of coherent 9-10µm radiation and suitable for mass-production.

11:20 AM
Characterization of the Absorbance Bleaching in AlInAs/AlGaInAs Multiple-Quantum Wells for Semiconductor Saturable Absorbers: *Jeff Cederberg*[1]; Daniel Bender[1]; Michael Wanke[1]; Ines Waldmueller[1]; Darrell Alliman[1]; Karen Cross[1]; [1]Sandia National Laboratories

Semiconductor saturable absorbers (SESAs) introduce loss into a solid-state laser cavity until the cavity field bleaches the absorber producing a high-energy pulse. Multiple quantum wells (MQWs) of AlGaInAs grown lattice-matched to InP have characteristics that make them attractive for SESAs. The band gap can be tuned around the target wavelength, 1064 nm, and the large conduction band offset relative to the AlInAs barrier material helps reduces the saturation fluence, and transparent substrate reduces nonsaturable losses. We have characterized the lifetime of the bleaching process, the modulation depth, the nonsaturable losses, and the saturation fluence associated with SESAs. We compare different growth conditions and structure designs. These parameters give insight into the quality of the epitaxy and effect structure design has on SESA performance in a laser cavity. AlGaInAs MQWs were grown by MOVPE using a Veeco D125 machine using methyl-substituted metal-organics and hydride sources at a growth temperature of 660°C at a pressure of 60 Torr. A single period of the basic SESA design consists of approximately 130 to 140 nm of AlInAs barrier followed by two AlGaInAs quantum wells separated by 10 nm AlInAs. This design places the QWs near the nodes of the 1064-nm laser cavity standing wave. Structures consisting of 10-, 20-, and 30-periods were grown and evaluated. The SESAs were measured at 1064 nm using an optical pump-probe technique. The absorbance bleaching lifetime varies from 160 to 300 nsec. The nonsaturable loss was as much as 50% for structures grown on n-type, sulfur-doped InP substrates, but was reduced to 16% when compensated, Fe-doped InP substrates were used. The modulation depth of the SESAs increased linearly from 9% to 30% with the number of periods. We are currently investigating how detuning the QW transition energy impacts the bleaching characteristics. We will discuss how each of these parameters impacts the laser performance. Sandia is a multi-program laboratory operated by Sandia Corporation, a Lockheed Martin Company, for the United States Department of Energy's National Nuclear Security Administration under Contract DE-AC04-94-AL85000.

11:40 AM
Intersubband Absorption at 1.55 µm in AlN/GaN Multi Quantum Wells Grown at 770°C by Metal Organic Vapor Phase Epitaxy Using Pulse Injection Method: *Jungseung Yang*[1]; Sodabanlu Hassanet[1]; Masakazu Sugiyama[1]; Yoshiaki Nakano[1]; Yukihiro Shimogaki[1]; [1]The University of Tokyo

Intersubband transition (ISBT) in AlN/GaN multi quantum wells (MQWs) exhibits excellent property for the application to all optical switches such as ultrafast carrier relaxation time. ISB absorption at 1.55 µm realized by metal organic vapor phase epitaxy (MOVPE) system at room temperature, however, shows very weak compared with that by molecular beam epitaxy (MBE) system. This is mainly due to the insufficient carrier density in GaN well layer grown at low temperature due to the increase of carbon concentration which acts as an acceptor in GaN layer. Pulse injection (PI) method in which group III precursors are alternately supplied is considered to be effective in reducing carbon concentration in GaN layer due to reduction at NH_3 supply time without supply of group-III precursors. We have found that blue-shift of ISBT wavelength is clearly observed by lowering growth temperature of MQWs to 770°C and ISBT at 1.58 µm with 90 meV of full width at half maximum (FWHM) value was observed. In this study, we have fabricated 40-pairs AlN/GaN MQWs with different well thickness at 770°C using PI method for the purpose of observing ISBT at 1.55 µm which is main wavelength used in optical communication. Well thickness is changed from 2.3 to 0.8 nm, while barrier thickness was fixed to 4.5 nm. Strong ISBT at 1.55 µm was observed at well thickness of 1.0 nm. Thinner well thickness than 1.0 nm induced red-shift of ISBT wavelength, which is attributable to the increase of effective well thickness for 2nd subband energy level. It was also found that the absorption magnitude of this study is comparable with that of MBE system and significantly improved than that of other groups using MOVPE system. This is due to the sufficient carriers in well even at low temperature of 770°C by using PI method. According to the secondary ion mass spectroscopy (SIMS) measurement, GaN layer grown by PI method at 770°C showed almost same level of carbon concentration with that grown at 950°C. This indicates that PI method is effective in reducing carbon incorporation, especially at low temperature region.

12:00 PM Lunch

12:30-5:30 PM Virginia City Historical Tour (Available at an additional charge)

1:00-4:15 PM Tahoe Queen Lake Cruise (Available at an additional charge)

Thursday Invited Talks

Thursday AM
May 27, 2010

Room: Lakeside Ballroom
Location: Hyatt Regency Lake Tahoe

Session Chair: Kentaro Onabe, University of Tokyo, Tokyo, Japan

8:30 AM Invited

InGaN Based True Green Laser Diodes on Novel Semi-Polar {20-21} GaN Substrates: *Masaki Ueno*[1]; Yusuke Yoshizumi[1]; Yohei Enya[1]; Takashi Kyono[1]; Masahiro Adachi[1]; Takamichi Sumitomo[1]; Shinji Tokuyama[1]; Takatoshi Ikegami[1]; Koji Katayama[1]; Takao Nakamura[1]; [1]Sumitomo Electric Industries, Ltd.

The realization of InGaN based green laser diodes (LDs) has been desired as light sources in mobile projectors. While those on conventional c-plane, new non-polar m-plane, a-plane, and semi-polar (11-22) planes have been actively developed, problems in piezoelectric fields or inferior crystal quality have hampered the increase in lasing wavelength. Very recently, it was reported that the lasing wavelength on c-plane reached to 515 nm at long last. Thus we explored most appropriate planes for true green LDs. We discovered novel {20-21} planes as a consequence. In this paper, we present the high crystal quality and homogeneity in InGaN quantum wells (QWs) on {20-21} planes with the 531 nm true green pulsed lasing and the 520 nm CW operation. LD structures were grown on {20-21} freestanding GaN substrates by metal organic vapor phase epitaxy (MOVPE). Gain-guided and ridge-waveguide lasers were fabricated with 600 micron long cavities and coated mirror facets. The crystal quality and emission characteristics of {20-21} green InGaN LDs were investigated. Uniform and defect-free QWs with abrupt interfaces were observed by transmission electron microscopy. The lattice matching condition to {20-21} GaN substrates was confirmed by X-ray-reciprocal-space mapping, which indicates advantages utilizing InAlGaN cladding layers to reduce internal strains. Microscopic photoluminescence image exhibited highly homogeneous and remarkably few non-radiative active regions. This homogeneity was also confirmed by full width at half maximum of electroluminescence peaks at 520nm, which is about 35 nm and narrowest among those on polar, non-polar, and semi-polar planes ever reported. This result indicates high In homogeneity and small band tail states even at green region, thus it demonstrated the superiority of {20-21} planes for green laser diodes.The 531nm true green lasing under pulsed operation and the 520 nm CW operation were realized in those InGaN LDs on {20-21} planes. The lasing wavelength of 531 nm is same as that made by second harmonic generation (SHG) green lasers. The threshold current, threshold current density, threshold voltage, and slope efficiency for CW operated 520 nm LDs were 95 mA, 7.9 kA/cm2, 9.4 V, and 0.1 W/A, respectively.

9:00 AM Invited

Wurtzite–Zinc Blende Transition in InAs Nanowires: *Jonas Johansson*[1]; Kimberly Dick[1]; Philippe Caroff[2]; Maria Messing[1]; Jessica Bolinsson[1]; Knut Deppert[1]; Lars Samuelson[1]; [1]Lund University; [2]CNRS

Semiconductor nanowires made of materials with zinc blende crystal structure often contin a high density of stacking defects and more or less random inclusions of wurtzite structure. In order to reproducibly fabricate electronic and optoelectronic devices it is of paramount importance to be able to control the nanowire crystal structure. We have recently reported extraordinary polytypic control of gold seeded InAs nanowires with diameter and growth temperature as control parameters [P. Caroff et al, Nature Nanotech. 4 (2009) 50]. In this presentation, however, we will focus on the cross-over from wurtzite to zinc blende crystal structure as the nanowire diameter is increased. The nanowires were grown by low-pressure metal-organic vapor phase epitaxy (MOVPE) at 420–480°C, using aerosol fabricated, size-selected gold particles with diameters between 10 and 150 nm as seed particles. Trimethyl indium and arsine were used as precursors at a V/III ratio of 130.When increasing the nanowire diameter, a transition from pure wurtzite (thin wires) to a zinc blende dominated crystal structure (thick wires) is observed. At 420°C, the cross-over diameter for this smooth transition is about 110 nm. At 480°C, the cross-over diameter is significantly smaller, about 70 nm. We explain these results with classical nucleation theory combined with Poissonian statistics. A new monomolecular layer can either nucleate in the ordinary ABC stacking orientation, resulting in zinc blende. Alternatively, it can nucleate in fault orientation, resulting in twinning for an isolated fault plane, or in wurtzite formation for an uninterrupted sequence of fault planes. By comparing the nucleation rates of ordinary and fault planes, we can predict the fraction of wurtzite as a function of the nanowire diameter and the supersaturation. The strong diameter dependence is handled by including the Gibbs-Thomson effect in the chemical potential. This approach leads to much larger (almost an order of magnitude), and thus more realistic, cross-over diameters than what has previously been theoretically predicted.

9:30 AM Break

Nitrides (Devices)

Thursday AM
May 27, 2010

Room: Lakeside Ballroom
Location: Hyatt Regency Lake Tahoe

Session Chairs: David Bour, Applied Materials, Santa Clara, CA, USA; Michael Heuken, Aixtron AG, Herzogenrath, Germany

10:00 AM

Growth of the Active Zone in Nitride Based Long Wavelength Laser Structures: *Uwe Rossow*[1]; Holger Jönen[1]; Moritz Brendel[1]; Alexander Dräger[1]; Torsten Langer[1]; Lars Hoffmann[1]; Heiko Bremers[1]; Andreas Hangleiter[1]; [1]TU Braunschweig

While GaN based optoelectronic devices such as blue or white LEDs or blue/violet lasers are commercially available, emission wavelengths >500nm are desirable for many applications. This requires InGaN active layers with high In concentrations $x_{In} \geq 0.30$. One problem is a degrading material quality and an reduced stability against processes at high temperatures, e.g. growth for efficient p-type doping of the upper waveguide, cladding or contact layers. Another problem is the resulting piezoelectric fields in the quantum wells which dramatically reduce the oscillator strength. Very recently first electrically pumped lasers in the long wavelength region have been reported by companies Nichia, Osram, Rohm, and Sumitomo. However, homogeneous indium incorporation with high optical quality is still a challenge and degradation can easily occur when growth temperatures are raised too quickly to high levels in the growth process after the active region. In this contribution we discuss these issues for a range of different InGaN/GaN MQW structures grown by MOCVD with a focus on possible laser applications. We achieved InGaN-QW structures with Indium concentrations as high as $x_{In} \geq 0.40$ showing well defined PL peaks at low and room temperature with no sign of phase separation. FWHM of the PL peaks can be described by random fluctuations of the local indium concentration. The quality of the layer structures is reasonably good for $x_{In} \leq 0.40$ indicated by presence of superlattice peaks in HRXRD and interfaces in TEM images but is degrading quickly for higher indium concentrations. Such structures are quite sensitive to the temperature profile chosen after the growth of the QW. In order to improve the quality of the GaN barriers much higher temperatures are desirable than those of the InGaN-QW. It turned out that the temperature profile in the first 20nm is most critical and if chosen properly in upper parts of the laser structures i.e. waveguide and cladding the influence is much less pronounced and temperatures more than 300°C above the QW temperature can be tolerated. We demonstrate that for optimized structures optical gain can beobtained from a single quantum well for wavelengths beyond 490nm.

10:20 AM

Performance Characteristics of AlInGaN Laser Diodes Depending on Electron Blocking Layer and Waveguide Layer Designs Grown by Metalorganic Chemical Vapor Deposition: Jianping Liu[1]; Yun Zhang[1]; Zachary Lochner[1]; Seong-Soo Kim[1]; Jeomoh Kim[1]; *Jae-Hyun Ryou*[1]; Shyh-Chiang Shen[1]; P. Yoder[1]; Russell Dupuis[1]; Kewei Sun[2]; Alec Fischer[2]; Fernando Ponce[2]; [1]Georgia Institute of Technology; [2]Arizona State University

AlInGaN-based blue and green laser diodes (LDs) are of interest for applications in full-color displays. We investigated the effect on the performance characteristics of LDs of two device design elements: (1) the profile of the electron blocking layer (EBL) by comparing typical constant alloy composition AlGaN EBL and a graded-composition EBL, and (2) the use of optical waveguide layers (WGLs) of GaN and InGaN. We used a graded Al composition (grading from the InGaN last QW to the AlGaN EBL) in the $Al_xGa_{1-x}N$ EBL instead of a onstant Al composition used in conventional EBL design. As a result, the device performance shows a reduced threshold current density as well as a greater slope efficiency for LDs using a graded-composition EBL. We believe the graded EBL mitigates the polarization field caused by the differential of spontaneous and piezoelectric polarization between last GaN barrier and AlGaN EBL in order to suppress the parasitic electron accumulation. Due to the smaller difference of refractive index between AlGaN and GaN materials as the wavelength increases, the optical confinement of the waveguide becomes smaller in blue and longer-wavelength LDs. We use InGaN layers for the WGL in blue and longer-wavelength LDs to utilize the larger refractive index contrast for InGaN compared to GaN. The effects of the InGaN waveguide layers on the optical properties are investigated by comparing LDs with GaN and InGaN WGLs. The advantage of enhanced radiative recombination efficiency using InGaN WGLs was observed in addition to improved optical confinement. The spontaneous EL peak intensity at 50 mA for the LDs with $In_{0.03}Ga_{0.97}N$ waveguide layers is 80% higher than that of the LDs with GaN waveguide layers. Moreover, the FWHM of the EL at 50 mA for the LDs with $In_{0.03}Ga_{0.97}N$ waveguide layers is 27.8 nm, 6 nm lower than that of the LDs with GaN waveguide layers. LDs with $In_{0.03}Ga_{0.97}N$ waveguides lase (pulsed) at λ=454.6 nm at 300K. The threshold current density Jth is 3.3kA/cm^2 and the threshold voltage is 5.9V. The use of these waveguide designs in the development of longer-wavelength (green) LDs will also be discussed.

10:40 AM

GaN-Based Laser Structure Using 3D Semipolar InGaN Quantum Wells Embedded in Planar AlGaN Cladding Layers: *Thomas Wunderer*[1]; Johannes Biskupek[2]; Andrey Chuvilin[2]; Ute Kaiser[2]; Yakiv Men[3]; Junjun Wang[1]; Frank Lipski[1]; Stephan Schwaiger[1]; Kamran Forghani[1]; Ferdinand Scholz[1]; [1]Institute of Optoelectronics, Ulm University; [2]Central Facility of Electron Microscopy, Ulm University; [3]Institute of Electron Devices and Circuits, Ulm University

Non- and semipolar group III-nitrides providing reduced piezoelectric fields are promising candidates for improved device performance due to an increased overlap of the electron and hole wave functions within the quantum wells (QWs). Nevertheless, a main problem is still limiting the use of non- or semipolar material for industrial production: On foreign substrates with conventional size just inferior material quality compared to c-plane growth can be achieved up to now. Non-radiative recombination is then compensating the advantage of the reduced fields and leads to bad performance of such devices. On the other hand high quality material can be obtained by cutting pieces from HVPE grown c-plane GaN in the desired direction. However, the limited sample size and its high price are still limiting factors for any mass production. By the use of selective area epitaxy three dimensional (3D) GaN structures can be obtained with side facets providing semipolar surfaces. High semipolar material quality can be achieved on low-cost full 2 inch or larger c-oriented sapphire wafers. It was shown that InGaN/GaN MQWs or even complete light emitting device (LED) structures can be realized by growing the respective layers on these facets.Now, we successfully reduced the size of the 3D GaN structures in order to implement the semipolar QWs in a conventionally grown, well working laser structure. Therefore, the mask period of the structures has been reduced to a lateral dimension of just 240nm using electron beam lithography and sputter coating of SiO2 deposited on the lower AlGaN cladding layer. Then, the active area consisting of an InGaN QW has been grown on the 3D GaN structures and planarized by GaN grown under 2D conditions. The GaN layers, representing a waveguide layer, and the selectively grown semipolar QW with a zigzag shape have been embedded in planar AlGaN cladding layers as known from standard devices. Detailed structural analyses including TEM as well as optical properties will be presented. The strong semipolar InGaN luminescence is influenced by light-matter coupling originating from the SiO2-GaN grating which could potentially be used in a distributed feedback device.

11:00 AM

Blue-Violet Boron-Based Distributed Bragg Reflectors for VCSEL Application: *Mohamed Abid*[1]; Tarik Moudakir[2]; G. Orsal[3]; Simon Gautier[4]; Aotmane En Naciri[5]; Anne Migan-Dubois[6]; Zakaria Djebbour[6]; Abdallah Ougazzaden[1]; [1]Georgia Institute of Technology/GT-Lorraine-UMI 2958 Georgia Tech-CNRS; [2]UMI 2958 Georgia Tech-CNRS; [3]Laboratoire Matériaux Optiques, Photonique et Système (LMOPS); [4]Laboratoire Matériaux Optiques, Photonique et Système (LMOPS), UMR CNRS 7132, University of Metz and Supelec; [5]Laboratoire de Physique des milieux denses (LPMD), Université Paul Verlaine-Metz; [6]Laboratoire de Génie Electrique de Paris, UMR 8507 CNRS; SUPELEC; University Paris-Sud 11, University Pierre et Marie Curie

In this work, we have demonstrated unique optical properties of BGaN materials enabling the development of innovative DBR technologies for VCSELs in the Blue-Violet spectral range. In this range, compared to edge emitting lasers, VCSELs have several advantages, noticeably their small cavity size which allows high quality structures. Yet, achieving highly reflective DBR remains a major challenge. Current AlGaN materials based mirrors have small refractive index contrasts. In addition, they suffer from strain relaxation and dislocation generation. Though, in this study, we propose a new scheme of DBR employing a new material system BGaN that can provide simultaneously high reflectivity and high structural quality. In order to investigate the optical properties of BGaN materials, we have grown, in a low-pressure MOVPE reactor, systematic series of BGaN samples with different boron compositions varying from 0 to 1.3% on AlN/Sapphire substrates. The AlN template enables the optical characterization of BGaN layers, which would otherwise experience an overlap with the bandgap and lattice parameters of conventional GaN/Saphhire substrates. We have been able to extract the refractive index, the absorption coefficient and the bandgap of the $B_xGa_{1-x}N$ materials using both spectroscopic ellipsometry and light transmission/reflection measurements at room temperature. For all the compositions of BGaN alloys, we have obtained an excellent agreement between experimental and simulated curves. The resulted dispersion curves showed a high contrast between GaN and BGaN materials. For instance, for 1% of boron, the BGaN/GaN multilayer structure has a refractive index contrast of more than which is equivalent to this of AlGaN/GaN with Al=22%. Moreover, the lattice mismatch between $B_{0.01}Ga_{0.99}N$ and GaN is only 0.2% which leads to good structural quality of BGaN/GaN DBRs.In conclusion, we propose a new scheme of DBR using the new material BGaN that can provide an effective solution for the development of UV VCSELs. We have demonstrated the large refractive index contrast of BGaN/GaN. As a result, with BGaN/GaN system, a fewer number of periods are needed to reach a high DBR reflectivity. The small percentage of boron results in nearly lattice-matched structures that could enable the growth of high quality active region for VCSELs.

11:20 AM

Electroluminescense from InGaN Quantum Dots, in a Monolithically Grown GaN/AlInN Cavity: *Heiko Dartsch*[1]; Christian Tessarek[1]; Malte Fandrich[1]; Stephan Figge[1]; Timo Aschenbrenner[1]; Carsten Kruse[1]; Detlef Hommel[1]; [1]University of Bremen

InGaN quantum dots (QDs) and their implementation into the micro cavity of a vertical distributed Bragg reflector (DBR)-resonator structure are the key elements to achieve room temperature single photon emission required for quantum cryptography. We present an electrically driven structure based on a monolithically GaN/AlInN cavity with a single quantum dot layer grown by MOVPE. The device was grown on c-plane sapphire substrate with a GaN buffer layer. The QDs are imbedded into a GaN cavity surrounded by a 40 fold GaN/AlInN DBR below and a 10 fold GaN/AlInN DBR on top. AlInN with an indium content of 18% was used as low index material which is lattice matched to the high index GaN layers. As doping of such super-lattices is difficult whilst maintaining high reflectivity, the device was realized with an intra-cavity contact scheme. For this reason a thick 5-λ cavity was used which is Si doped in its upper half and Mg doped below the QD-layer. The QD-layer itself was grown by self organization in a 2-step growth scheme which provides reliable QD-based emission. Planar device structures were made as well as pillar structures where contacts to the both sides of the cavity were applied by focused ion beam etching and electron beam activated deposition of platinum. The center wavelength of both DBRs is located near 510nm which is at the spectral position of the low energy tail of the quantum dot ensemble. This ensures to have only few QDs in resonance with the cavity mode which is essential for single photon emission. The 40 fold bottom GaN/AlInN DBR shows a reflectivity of 97%. For the whole planar cavity structure a peak reflectivity of 92% can be observed. This presentation will discuss both growth and optical parameters of the device.

11:40 AM

Indium Compositional Dependence of the Two-Dimensional Electron Gas in $In_xAl_{1-x}N$/AlN/GaN Heterostructure Field-Effect Transistors: *Suk Choi*[1]; Hee Jin Kim[1]; Zachary Lochner[1]; Bravishma Narayan[1]; Yun Zhang[1]; Shyh-Chiang Shen[1]; Jae-Hyun Ryou[1]; Russell Dupuis[1]; [1]Georgia Institute of Technology

HFETs based on InAlN/GaN have been proposed as an alternative of AlGaN/GaN HFETs. In this work, two-dimensional electron gas (2-DEG) engineering in InAlN/AlN/GaN heterostructure filed-effect transistors (HFETs) is described. By using nearly in-plane lattice-matched InAlN barriers containing ~18% In composition on top of GaN, the lattice-mismatch strain and any strain-induced layer quality depreciation can be minimized. In addition, a larger density of 2-DEG and higher carrier mobility than those of AlGaN/GaN HFETs are expected. At the same time, strain and polarization field engineering by changing the mole fraction of InAlN cap layer is possible and this is the main focus of this study. If the In composition in InAlN barrier layer decreases below 18%, tensile strain in the layer will produce piezoelectric field which is parallel to (aligned in the same direction) the spontaneous polarization field. As a result, the overall built-in potential increases and a higher 2-DEG density can be obtained with negative shift of threshold voltage. On the contrary, if the In composition of the barrier layer increases beyond the lattice-matching regime, the barrier produces compressive strain, and the piezoelectric field (that is antiparallel to the spontaneous polarization) will compensate the spontaneous polarization field and reduce the overall built-in potential and 2DEG density. The threshold voltage is expected to be shifted toward positive voltages. Therefore, it can be expected that InAlN/GaN HFETs with compressively strained barrier layers will have a potential to exhibit enhancement-mode operation. In the present study, we report novel method for the engineering of the 2-DEG in the HFETs with InAlN cap layer in order to explore the feasibility of enhancement-mode operation in InAlN/GaN HFET devices. The shift of threshold voltage with different In composition in InAlN barrier layer was demonstrated both theoretically and experimentally. The threshold voltages were measured to be ~-3V ~-1.25V and -0.1V for the HFETs with $In_{0.18}Al_{0.82}N$, $In_{0.22}Al_{0.78}N$, and $In_{0.25}Al_{0.75}N$, respectively. High quality InAlN/GaN HFET structures with various In composition were grown and fabricated. The characterization of material and epitaxial structures and HFET devices will be reported.

12:00 PM Lunch

Nanowires

Thursday AM
May 27, 2010

Room: Regency C&F
Location: Hyatt Regency Lake Tahoe

Session Chairs: Takashi Fukui, Hokkaido University, Sapporo, Japan; George Wang, Sandia National Laboratories, Albuquerque, NM, USA

10:00 AM

Epitaxial Growth of Ensembles of Indium Phosphide Nanowires on Amorphous Surfaces: Structural, Electrical, Optical Characterization, and Device Applications: *Andrew Lohn*[1]; Sagi Matthai[2]; Xuema Li[2]; V. J. Logeeswaran[3]; M. Saif Islam[3]; Takehiro Onishi[1]; Joseph Straznicky[2]; Shih-Yuan Wang[2]; R. Stanley Williams[2]; Milo Holt[1]; Nobuhiko Kobayashi[1]; [1]University of California Santa Cruz; [2]Hewlett Packard Laboratories; [3]University of California Davis

A novel method for the growth of indium phosphide (InP) nanowires has been demonstrated. Compound semiconductor nanowires are frequently grown by metal-organic chemical vapor deposition (MOCVD) via the vapor-liquid-solid (VLS) mechanism using lattice-matched single-crystal substrates as a template for the epitaxial growth of nanowires as in epitaxial growth of thin films. For the case of nanowire growth, lattice-matching conditions are expected to be significantly relaxed and it is conceivable that atomic ordering having lateral dimension comparable to that of the base of the nanowire itself is sufficient to induce epitaxial growth of nanowires. In our demonstration, amorphous hydrogenated silicon (a-Si:H) deposited on quartz substrates was used as a template surface for the growth of InP nanowires by MOCVD. The a-Si:H layer possesses short-range atomic ordering which enables the nanowires to nucleate and grow on amorphous surfaces. The InP nanowires are found to have either zincblende or wurtzite lattice, and these two types of nanowires co-exist as is commonly seen in group III-V compound semiconductor nanowires grown via the VLS mechanism on single-crystal surfaces. Growth on amorphous surfaces, however results in many characteristics that are not commonly observed on single-crystal surfaces. In the VLS mechanism, nanowires grow dominantly in <111> directions, however the lack of long-range ordering on the amorphous template surfaces results in <111> directions randomly oriented with respect to the surface normal and thus randomly oriented nanowires. Random orientation has distinctive implications for these optically active nanowires including the abolition of geometric selection rules for Raman scattering. Photoluminescence at various temperatures suggests the presence of complex photo-excited carrier dynamics within an ensemble of InP nanowires.At high areal densities, randomly oriented nanowires have a tendency to fuse together during growth, creating regions of physical interaction where interesting optical and electrical behavior can be observed. Various devices that employ randomly oriented nanowires with non-traditional architecture can be envisioned and are demonstrated in the form of photoconductors and photodetectors. The proposed growing technique of InP nanowires offers a route to significantly reduce substrate costs and a simple means of integrating group III-V compound semiconductors with other material platforms such as silicon.

10:20 AM

Alternative Seed Particle Material for Epitaxial Growth of III/V Nanowires: *Karla Hillerich*[1]; Maria Messing[1]; Bengt Meuller[1]; Kimberly Dick[1]; Jonas Johansson[1]; Knut Deppert[1]; [1]Lund University

Nanowires are 1D structures with diameters in the nanometer range and a high aspect ratio. The limited dimensions change the electrical and optical properties and allow new material combinations. This has led to several devices, such as wrap gate field-effect transistors, light-emitting diodes, solar cells and biosensors. Although nanowires have successfully been grown epitaxially with a high crystalline quality for years, there are still open questions remaining on the growth mechanism. Nanowires are mostly grown by the so-called vapor-liquid-solid mechanism: A metal nanoparticle serves as a seed, where the growing material preferentially deposits. An alloy is formed and the material precipitates at the interface between the metal particle and the substrate due to supersaturation, resulting in nanowire growth. At nanowire growth conditions the growth rate is highly anisotropic, i.e. the crystal grows much faster in the axial direction than in the lateral direction. The influence of the particle and its properties on the growth is still under discussion. Gold has been successfully used as seeding material for years. However, gold is known to cause deep traps in silicon and complicates the integration of nanowires into the existing silicon technology. For silicon and germanium nanowires other metals like aluminum and copper have successfully served as seeds. For III-V nanowires, however, only a few reports on different seed particle materials are known. We investigated the growth of III-V materials from alternative catalyst materials by MOVPE. We report epitaxial growth of InP nanowires from copper particles the first time. We will present the growth behavior in dependence of temperature and molar fractions as well as investigations on the incorporation of the precursors into the seeding particle. Compared to growth from gold seed particles the growth temperature is low and the growth rate surprisingly fast. Another surprising result is the presence of phosphorous in the particle after growth, which has never been observed for gold seeds. The use of copper as seed particle material opens up new parameter regimes and helps to understand the growth mechanism.

10:40 AM

Growth and Doping of InP Nanowires: *Andrey Lysov*[1]; Christoph Gutsche[1]; Ingo Regolin[1]; Kai Blekker[1]; Zi-An Li[1]; Marina Spasova[1]; Werner Prost[1]; Franz Josef Tegude[1]; [1]Center for Nanointegration Duisburg-Essen

Semiconductor III-V nanowires are attractive candidates for future nanophotonic applications. InP nanowires have recently received attention for use in nanowire based photodiodes and LEDs [1,2,3]. This contribution reports about the growth and doping of InP nanowires with alternative not gaseous precursors and their influence on the nanowire morphology. Nanowires were produced by low pressure (50 mbar) metallorganic vapour-phase epitaxy (MOVPE) using tertiarybutylphosphine (TBP) as group-V, while trimethylindium (TMIn) as group-III source. As doping sources diethylzinc (DEZn) und tetraethyltin (TESn) were used. Colloidal Au-nanoparticles and thin Au-layers deposited on the (111)B InP were used as templates for the nanowire growth. Before growth an annealing step of 5 min. at 600°C under TBP atmosphere was carried out. The growth temperature and the V/III ratio were varied in the ranges between 395°C – 430°C and 20 - 200 respectively. InP nanowires grown from colloidal nanoparticles show a strong dependence of morphology on V/III ratio at a definite growth temperature. For the growth temperature of 410°C appearance of an unintentional nanowire shell and the kinking of nanowires was observed. Two temperature growth regime turned out to be necessary to produce untapered nanowires without kinking. When growing from an annealed gold layer untapered nanowires with extremely high aspect ratios (> 1000) occur for the wide range of V/III ratios ($50 < V/III < 200$) and growth temperatures ($395°C < T < 430°C$). Electrical investigations of untapered InP nanowires grown under supply of DEZn (p-type) and TESn (n-type) have revealed currents in a μA range flowing through single wires. This indicates three orders of magnitude higher conductivity, than in nominally undoped samples, where current in pA range are typical. The combination of already achieved p- and n- doping in a single nanowire should lead in further steps to the preparation of axial and radial pn-junctions with high current densities in single nanowires. [1] C. Novotny et al. 2008 Nano Lett., 8 (3), pp. 775–779 [2] Ethan D. Minot et al. 2007 Nano Lett., 7 (2), pp. 367–371[3] M. T. Borgström et al. 2008 Nanotechnology, 19, 445602.

11:00 AM

Determination of Diffusion Lengths in Nanowires: *Jessica Bolinsson*[1]; Anders Gustafsson[1]; Niklas Sköld[2]; Lars Samuelson[1]; [1]Lund University; [2]Toshiba Research Europe Ltd

Low-dimensional semiconductor structures including nanowires (NWs) have a great potential for use in future optical devices such as light-emitting diodes and solar cells. It is important for device performance and of fundament interest to understand the transport properties of NWs, in particular the diffusion of minority carriers, electron-hole pairs, and excitons. There are many ways of determining the diffusion lengths in semiconductors, where e.g. optical methods based on photoluminescence include spatially and time resolved as well as pump-probe investigations. However, one of the most useful methods is cathodoluminescence (CL) imaging in the scanning electron microscope (SEM). We demonstrate a scheme to study the diffusion lengths in NWs using local variations in the emission from single NWs. We have used two different geometries, homogeneous GaAs NWs and axial GaAs/InGaAs/GaAs and GaAs/AlGaAs heterostructures.The NW samples in this study were grown by MOVPE, on (111)B GaAs substrates. Gold particles with 40 or 50nm in diameter were used as seeds for the core of the NWs and in most cases the nanowires were capped with an AlGaAs shell. We have used CL imaging to determine the diffusion lengths in these nanowires by recording intensity profiles either from the interface between the substrate and the nanowire or at the edges of segments in nanowires containing axial heterostructures. Diffusion lengths of 100-900nm were recorded, where the largest contribution to the reduction as compared with bulk is attributed to surface recombination in uncapped NWs. The longest diffusion lengths (900 nm) are observed in AlGaAs-capped GaAs NWs and the shortest in uncapped GaAs NWs.

11:20 AM

Fabrication and Characterization of InAs Tubular Channel FETs Using Core-Shell Nanowires Grown by SA-MOVPE: *Takuya Sato*[1]; Junichi Motohisa[1]; Eiichi Sano[1]; Shinjiro Hara[1]; Takashi Fukui[1]; [1]Hokkaido University

Semiconductor nanowires have been attracting a great deal of attention as novel nanoscale materials with a high degree of freedom in realizing various one-dimensional structures and devices. Especially, the advantages of surrounding gate FETs using III-V nanowires have been intensity addressed, in which higher electron mobility and immunity in short-channel effects is promising for replacing conventional FETs used in Si-CMOS technology. We previously reported on the lateral InGaAs nanowire FETs and pointed out some issues for their performance improvement. Here we propose and fabricate nanowire FETs with tubular channel structure, which utilizes InP-core and InAs-shell heterostructures. This structure has potential advantages of high on-off ratio as well as small subthreshold slope, as compared to nanowire FETs with the same diameter. Firstly, we grew InP-core/InAs-shell nanowires on InP (111)A substrates by selective-area MOVPE method. The growth condition required for InP-core was high temperature (590^{o}C) and low V/III ratio (15) to promote the growth in the vertical direction without lateral growth. The growth of InAs-shell was carried out at 400^{o}C, which was required to proceed the growth uniformly around InP-core, while at higher growth temperature, nanowires were bent due to non-uniform growth and strain originating from lattice-mismatch. The diameter of the InP-core and thickness of InAs-shell is 80 nm and 10 nm, respectively. After the growth, the nanowires were transferred to a SiO_2-coated Si substrate with alignment mark. Ohmic contacts and a top gate were formed by EB lithography, metal evaporation, and the lift-off technique. For ohmic contacts, O_2 plasma ashing and wet chemical etching based on buffered hydrofluoric acid were carried out to remove remained resist and native oxide layer from the surface prior to metal evaporation. Al_2O_3 was used as gate dielectric deposited by atomic layer deposition at 300^{o}C.We confirmed modulation of source-drain current by top-gate bias and characteristics of an n-channel FET. On-off ratio and subthreshold slope were roughly 10^4 and 360mV/dec, respectively. Although the results are still preliminary, improvement of the device performance is possible, for instance, by the optimization of the thickness of Al_2O_3 insulating layer and surface treatment before its deposition, and so on.

11:40 AM

InAs/GaSb Heterostructure Nanowires for Tunnel FETs: *Mattias Borg*[1]; Kimberly Dick[1]; Henrik Nilsson[1]; Bahram Ganjipour[1]; Claes Thelander[1]; Lars-Erik Wernersson[1]; [1]Lund University

The InAs/GaSb heterojunction is potentially an ideal heterostructure for tunnel field effect transistors (FETs), due to the type II broken band alignment. By growing the InAs/GaSb heterostructure in the shape of nanowires, optimal electrostatics can be accomplished via wrap-gate formation at the heterointerface. With the aim of building nanowire tunnel FETs we have studied the MOVPE growth of Au-nucleated InAs/GaSb nanowire heterostructures. The InAs/GaSb heterostructure is challenging from a growth point of view since both the anion and cation are simultaneously switched at the interface, and the manner in which the switching is performed is important for the composition of the grown heterojunction.[1] Furthermore, the physics of broken band heterostructures is intriguing, and the nanowire geometry gives a opportunity to probe and control the electric potential at the interface through the use of gate electrodes.[2] In this work, InAs/GaSb heterostructures are realised using MOVPE by growing InAs nanowires followed by a thin insert of GaAs or InSb, and finishing with a GaSb segment. The growth was also performed in the reverse way, with GaSb grown first. The effect of the seed particle chemistry on the yield of epitaxial nanowires and the interfacial composition and abruptness is investigated by SEM and XEDS. A memory effect of In and Sb is found to be significant and up to 15% In and 6% Sb is detected in the subsequently grown segments. Additionally, the influence of growth parameters on the nanowire and seed particle composition was evaluated. Finally, electrical characterization of individual InAs/GaSb heterojunctions is performed by breaking off nanowires and depositing them on a n+ Si substrate and defining metal contacts using EBL. Either the Si substrate is used as a gate, or partial wrap-gates are defined, separated from the nanowires with a thin, high-k oxide. [1] Booker et al. J. Cryst Growth 145, p.778 (1994)[2] Thelander et al., Solid State Comm., 131, p.573 (2004).

12:00 PM Lunch

Novel Materials

Thursday PM
May 27, 2010

Room: Regency C&F
Location: Hyatt Regency Lake Tahoe

Session Chairs: Thomas Kuech, University of Wisconsin - Madison, Madison, WI, USA; Tien-Chang Lu, National Chiao Tung University, Taiwan

---

1:30 PM

Ordered Planar Arrangements of MnAs Nanoclusters by Selective-Area Metal-Organic Vapor Phase Epitaxy for Lateral Magneto-Resistive Devices: *Shinjiro Hara*[1]; Shingo Ito[2]; Kohei Morita[2]; Keita Komagata[2]; Takashi Fukui[2]; [1]Hokkaido University and JST-PRESTO; [2]Hokkaido University

Magneto-nanoelectronic devices using magneto-resistive effects have been extensively demonstrated on semiconductor wafers by low-temperature molecular beam epitaxy and conventional top-down fabrication techniques. We have demonstrated the build-up fabrication of ferromagnetic MnAs nanoclusters (NCs) position-controlled on {111} semiconductor wafers by selective-area metal-organic vapor phase epitaxy (SA-MOVPE). [1, 2] Using our technique, it is possible to realize magnet tunnel junctions in a vertical and/or lateral geometry, and to tune magnetic properties of the NCs and the NC ensemble by controlling size, shape, position and arrangement of the ferromagnetic MnAs NCs. [3] In this paper, we report the structural and magnetic characterizations for the elongated MnAs NC arrays on AlGaAs nanopillar buffer layers grown by SA-MOVPE on pre-patterned SiO_2-masked GaAs (111)B and Si (111) wafers. The formation of NC pairs with narrow spatial gaps between the NCs is demonstrated for lateral magneto-resistive device applications. To form the MnAs NCs with a high degree of uniformity, the growth temperature of 825^{o}C and the V/Mn ratio of 1125 were chosen. Typical elongated MnAs NCs grown on GaAs (111)B wafers measured about 300 nm in width and 630 nm in length, and had a single magnetic domain after applying the external magnetic fields. It was concluded from the electron beam diffraction patterns and the lattice images characterized by transmission electron microscopy that the MnAs NCs had hexagonal NiAs-type crystal structures, and that their *c*-axes were parallel to the <111>B directions of the zinc-blende-type AlGaAs nanopillars. It is crucial for realizing a lateral magneto-resistive device using the NC pairs that each of the NCs has an elongated shape with a different size to control their magnetized directions and coercive forces. By designing and optimizing the initial SiO_2-mask openings formed by electron beam lithography on the wafers, we fabricated the elongated MnAs NC pairs with a spatial gap of 5 to 10 nm between the NCs and the NC arrangements of various kinds. [1] S. Hara *et al*., J. Cryst. Growth 310, 2390 (2008): [2] S. Ito *et al*., Appl. Phys. Lett. 94, 243117 (2009): [3] M. T. Elm *et al*., J. Appl. Phys. *in press.*

1:50 PM

Effect of Growth Parameters on Mg$_x$Zn$_{1-x}$O Films Grown by Metalorganic Chemical Vapor Deposition: *Kharouna Talla*[1]; Julien Dangbégnon[1]; Magnus Wagener[1]; Johannes Botha[1]; [1]Nelson Mandela Metropolitan University

The need for efficient emitters and detectors operating deeper in the ultraviolet, has encouraged band gap engineering of ZnO. In particular, ZnO can be alloyed with MgO to form the ternary compound Mg$_x$Zn$_{1-x}$O, which has a band gap tuneable (in principle) between 3.37 eV and 7.8 eV, and which offers the possibility to create quantum heterostructures within this very promising II-VI system. Although Mg$_x$Zn$_{1-x}$O has been successfully grown by metalorganic chemical vapor deposition (MOCVD), a thorough understanding of the influence of the various MOCVD growth parameters on the quality of the material has not been attained. In this study, Mg$_x$Zn$_{1-x}$O films are deposited on c-plane sapphire, glass, Si (100) and Si (111) by MOCVD, using ((MeCp)$_2$Mg), diethyl zinc ((C$_2$H$_5$)$_2$Zn) and either tertiary-butanol or oxygen gas as Mg, Zn and oxygen sources, respectively. A comparison of Mg$_x$Zn$_{1-x}$O grown on different substrates is made in terms of magnesium incorporation and film quality. The effect of using oxygen gas, instead of tertiary-butanol, on the composition of the grown films is also considered. The growth temperature is varied between 300°C and 500°C, while the VI/II ratio in the gas phase is varied between 15 and 120 in order to optimise the optical and structural properties of the material. For this purpose, photoluminescence spectroscopy, UV transmission spectroscopy and x-ray diffraction measurements are used. Highly c-axis orientated films are observed for growth temperatures below 380°C, while the Mg content in the layers increases with increasing VI/II ratio. To date, the room temperature band gap has been increased to 3.9 eV, with strong room temperature excitonic emission dominating over the entire composition range achieved. The full-width at half-maximum of around 50 meV compares excellently to the value of 100 meV achieved by molecular beam epitaxy [1]. No additional optically active deep levels are deduced with the incorporation of Mg. Detailed photoluminescence studies between 77 K and 300 K are presented in order to correlate alloy inhomogeneities with exciton localisation. [1] Y. Nishimoto et al., Applied Physics Express 1 (2008) 091209.

2:10 PM

MOCVD Growth of Epitaxial Cugase$_2$ Layers on GaAs by a CuSe-Assisted Continuous Two Phase Process: *Levent Gütay*[1]; Jes Larsen[1]; Susanne Siebentritt[1]; [1]University of Luxembourg

We have grown epitaxial thin film CuGaSe$_2$ layers by MOVPE on GaAs substrates. CuGaSe$_2$ is the highest band gap member of the chalcopyrite Cu(In,Ga)Se$_2$ family (CIGSe). CIGSe is successfully used as absorbers in thin film solar cells. In this study we concentrate on the growth dynamics of CuGaSe$_2$, especially the time dependent formation of the secondary Cu$_x$Se (x~1.8) phase on the layer surface. CuGaSe$_2$, like all chalcopyrites, is very tolerant with respect to stoichiometry deviations. It forms a compensated semiconductor when Cu-poor ([Cu]/[Ga] < 1), and a stoichiometric phase when Cu-rich ([Cu]/[Ga] > 1), where the excess copper forms a Cu$_x$Se phase on the surface. Both compositions Cu-poor and Cu-rich grow epitaxially on GaAs. The growth has been observed by optical in-situ reflectance and ex-situ scanning electron microscopy (SEM) and photoluminescence (PL) measurements. The analyzed samples are from various process durations, the longest one being 4 hours, resulting in Cu-rich samples. The partial pressures of the metallorganics are constant during the whole process. The formation of Cu$_x$Se crystals can be devided into 3 stages: i) A Cu-poor CuGaSe$_2$ layer is growing, Ga droplets appear on the surface, due to Ga-diffusion from GaAs substrate. ii) As the CuGaSe$_2$ layer gets thicker less Ga from the substrate reaches the surface. Thus, the Ga-drops disappear and the growth turns to Cu-rich. Formation of Cu$_x$Se phase starts on the surface. iii) Cu$_x$Se crystals form, causing sudden decrease in surface reflectance, continuing to decrease for longer process times. SEM cross sections show Cu$_x$Se-crystals only on the CuGaSe$_2$ surface, independent of process duration. As Cu$_x$Se already starts to form in phase ii), this observation implies a re-consumption of Cu$_x$Se-crystals by continuous phase transition during further layer growth, which we have analyzed in further experiments.As the electronic defect structure of CuGaSe$_2$ is directly influenced by the Cu-excess during growth the investigation of Cu$_x$Se formation during the process is important for understanding defect formation and distribution in the layer. Furthermore, a better understanding of the two phase dynamics in this process will help understanding mechanisms in other two phase systems and the growth of chalcopyrites as such.

2:30 PM

Au-Catalyzed Self Assembly of GeTe Nanowires by MOCVD: *Massimo Longo*[1]; Claudia Wiemer[1]; Olivier Salicio[1]; Marco Fanciulli[2]; Laura Lazzarini[3]; Lucia Nasi[3]; [1]Laboratorio Nazionale MDM, CNR-INFM; [2]Laboratorio Nazionale MDM, CNR-INFM and Dipartimento di Scienza dei Materiali, University of Milano Bicocca; [3]IMEM-CNR

Self assembled GeTe nanowires (NWs) are receiving increasing interest in the field of phase change memories (PCM) applications, because they potentially allow a defect-free scaling down in the fabrication of high performing and low-power memory devices. Contrary to standard CVD techniques employed for the synthesis of chalcogenide-based NWs, in this study the MOCVD process was adopted for the first time to grow GeTe NWs on SiO2/Si substrates. The growth occurred in the presence of the Au metal catalysts species on the SiO2 surface; the metalorganic precursors were tetrakisdimethylaminogermanium and diisopropyltelluride, the process gas was nitrogen. The morphological analysis of the GeTe NW was carried out by Field emission Scanning Electron Microscopy observations; structural and compositional analyses were performed by X-Ray Diffraction (XRD) and Total Reflection X-Ray Fluorescence (TXRF), respectively. Structural and compositional analyses were performed also on single nanostructures by High Resolution Transmission Electron Microscopy (TEM). The NWs exhibited kinks and a random orientation with respect to the substrate surface plane, since they mainly nucleate on other GeTe grains formed during the deposition. The presence of the gold catalyst on the NWs top confirmed that the growth is driven by the Vapor-Liquid-Solid (VLS) mechanism. The typical diameter of the NWs resulted to be around 50 nm and the length up to 4 µm. The structural measurements showed that both the cubic and rhombohedral crystalline phases of GeTe are present in the obtained NWs, whereas the compositional analyses indicated a Ge36Te64 alloy. In particular, TEM observations revealed that the fcc wires are single crystals 110 oriented, presenting small misorientations in the range of 0-5 degrees.

2:50 PM

Dimethylzinc Adduct Chemistry Revisited; MOCVD of ZnO Nanowires Using Oxygen Donor Adducts of Dimethylzinc: *Ravi Kanjolia*[1]; Anthony Jones[2]; Kate Black[2]; S. Ashraf[2]; Paul Chalker[2]; S. Hindley[1]; Paul Williams[1]; Raj Odedra[1]; Peter Heys[1]; [1]SAFC Hitech; [2]University of Liverpool

There has been a significant recent re-awakening of interest in the wide-bandgap semiconductor ZnO which has a variety of applications in short-wavelength photonic and electronic devices. In particular, there has been much recent interest in ZnO nanostructures which have potential applications in UV laser diodes, gas-sensors, and excitonic solar cells. The MOCVD of ZnO films has been extensively studied for more than two decades. Dialkylzinc precursors, such as diethylzinc, [Et2Zn], or dimethylzinc, [Me2Zn], together with oxygen and/or H2O are the conventional precursors for the MOCVD of ZnO. However, these precursors undergo a vigorous homogeneous pre-reaction resulting in the deposition of particulates upstream of the susceptor. To avoid this problem, less reactive oxidants have been investigated, including carbon dioxide, nitrous oxide, nitric oxide and oxygen-containing heterocyclic ligands, such as THF. However, these oxygen sources generally yield very low ZnO growth rates. Although pre-reaction between [R2Zn] compounds and oxygen can be limited by working at very low partial pressures of oxygen, a better solution is to develop Zn precursors which are intrinsically less reactive to oxygen. Over twenty years ago Jones and co-workers showed that the reactivity of [Me2Zn] towards the gas-phase nucleophilic species oxygen, [H2Se] and [H2S] could be significantly reduced by pre-forming an adduct between [Me2Zn] and an oxygen or nitrogen donor ligand such as 1,4-dioxane or triethylamine. In this paper, we re-visit dimethylzinc adduct chemistry and show that as well as preventing the [Me2Zn] / O2 pre-reaction, the use of the adduct precursors [Me2Zn(L)] (L = THF (C4H8O), tetrahydropyran (C5H10O) and furan (C4H4O)) also provides a method for the growth of vertically-aligned ZnO nanowires by liquid injection MOCVD. The ZnO nanowires were deposited in the region of 500°C on Si(111) substrates. The materials and photonic properties of the ZnO films deposited on Si(111) are reported and are compared with the equivalent properties of ZnO films deposited on conducting ITO-coated glass substrates. The effect of molecular structure on ZnO morphology is also investigated by the use of a range of new [Me2Zn(L")] adducts and possible growth mechanisms are discussed.

3:10 PM

Electrical and Optical Characterizations of the n-InAsSb/n-GaSb Heterojunctions: *David Lackner*[1]; Milena Martine[1]; Oliver Pitts[2]; Michael Steger[1]; Albion Yang[1]; Yata Cherng[3]; Wladek Walukiewicz[4]; Michael Thewalt[1]; Patricia Mooney[1]; Simon Watkins[2]; [1]Simon Fraser University; [2]Present Address: CPFC, NRC Institute for Microstructural Sciences; [3]4D Labs, Simon Fraser University; [4]Lawrence Berkeley National Laboratory

InAs$_{0.91}$Sb$_{0.09}$, epitaxially grown on GaSb, has received steady attention in the past few years for optical detectors in the 3-5 micron range. Attempts to increase the detection wavelength by increasing the Sb mole fraction have been hindered by the lack of lattice-matched substrates. We propose a InAsSb/InAs strain balanced superlattice structure (SLS) grown on GaSb. We recently have demonstrated that this is a powerful approach by PL measurements on SLS structures with Sb compositions ranging from 14% to 27%. For the latter composition, a PL energy corresponding to a wavelength of 10 µm is detected. However in order to incorporate this into a detector, a heterojunction between the GaSb substrate and the InAsSb is formed. Due to the extreme staggered band offset, unusual electrical properties are found. In this work we studied the electrical properties of an n-InAsSb/n-GaSb heterojunctions as a function of the GaSb doping concentration. Because of the staggered type II band alignment, strong electron accumulation occurs on the InAsSb side. For low GaSb doping, depletion occurs on the GaSb side resulting in a Schottky-like junction as previously reported[1]. As the GaSb doping increases, the built-in voltage as well as depletion width decreases as shown using self-consistent simulations. For GaSb doping levels above 5×10^{17} cm^{-3}, the junction loses its rectifying properties due to tunneling. Under zero and reverse bias voltage the photoresponse of these diodes is solely due to the photovoltaic effect in the GaSb depletion region. For forward bias voltages > 400 mV we also observed a photoconductive response from the InAsSb layer. The proposed physical mechanism is quite different from the one suggested in a recent paper[2]. [1] Srivastava et al. Appl. Phys. Lett. 49, 41 (1986)[2] Y. Sharabani, et al. Proc. SPIE, 2008, vol. 6940, p. 69400D.

3:30 PM Break

Arsenides, Phosphides

Thursday PM — Room: Lakeside Ballroom
May 27, 2010 — Location: Hyatt Regency Lake Tahoe

Session Chairs: Jean Decobert, Alcatel-Thales III-V Lab, Marcoussis, France; Masakazu Sugiyama, University of Tokyo, Tokyo, Japan

1:30 PM

GaP Nucleation on Si(001) Substrates for III/V Device Integration: *Kerstin Volz*[1]; Andreas Beyer[1]; Wiebke Witte[1]; Jens Ohlmann[1]; Bernardette Kunert[2]; Wolfgang Stolz[1]; [1]Philipps University Marburg; [2]NAsP III/V

Integration of active III/V devices on Silicon substrates would tremendously increase the functionality of this semiconductor material. In order to realize true monolithic integration, a defect-free nucleation layer is of outmost importance. As CMOS industry nowadays focuses on exactly oriented (001) Si substrates, the integration of a III/V semiconductor based device structure, employing either lattice relaxed III/V layers for high electron mobility devices or the pseudomorphically strained, active direct-band gap material Ga(NAsP) for optic devices, also has to be pursued on this substrate type. High-efficiency, Si-based solar cells can however also be deposited on off-cut substrates. The III/V nucleation layer we use is GaP-based due to the similar lattice constants of GaP and Si. Besides the known challenges of III/V on IV heteroepitaxy, like charge neutrality of the interface, cross-diffusion of dopants and slight differences in lattice constant and thermal expansion coefficient, nucleation on Si furthermore poses the challenge of the formation of antiphase domains. These form as the Si surface is covered with monoatomar steps. Prior to the deposition of the heteroepitaxial III/V layer, a 500nm thick Si-buffer is grown by VPE using silane. The growth and post-growth annealing conditions of this layer are optimized to maximize the number of double steps on the Si-surface with respect to the monoatmar steps for exactly oriented as well as 2° and 6° offcut Si-substrates. The GaP layer is grown with triethylgallium (TEGa) and the more efficiently decomposing metal organic group-V-source tertiarybutyl phosphine (TBP). The MOVPE growth conditions of thin GaP layers on Si substrate have been varied systematically, e.g. growth temperature, TBP/TEG vapour phase ratio and sequence of the first III/V coverage layer. Main investigation techniques for the III/V layers on the Si substrates are transmission electron microscopy, atomic force microscopy as well as high resolution X-ray diffraction. Under optimized growth conditions a two dimensional GaP-nucleation is achieved, which facilitates the deposition of high quality III/V device materials on Si substrates. There is a strong correlation between the development of antiphase boundaries and the III/V growth conditions, the Si-surface pre-treatment and the wafer miscut, which will also be discussed in detail.

1:50 PM

Improvement of GaAs MIS Characteristics with the Optimum Thickness of AlP *In Situ* Passivation Layer: *Yuki Terada*[1]; Yukihiro Shimogaki[1]; Mitsuru Takenaka[1]; Shinichi Takagi[1]; Yoshiaki Nakano[2]; Masakazu Sugiyama[1]; [1]Department of Electrical Engineering and Information Systems, School of Engineering, The University of Tokyo; [2]Research Center for Advanced Science and Technology, The University of Tokyo

Suppression of interfacial states is essential for the III-V metal-insulator-semiconductor (MIS) transistors with high electron mobility (In)GaAs channel. Since arsenic oxide is the major origin of interface states between a channel and a gate dielectric, surface oxidation of a III-V layer should be avoided. We have developed *in situ* GaAs surface passivation with AlP epitaxial layer. The AlP layer almost converted to Al$_2$O$_3$ upon air-exposure, forming a part of a gate dielectric. We here discuss the effect of AlP thickness on the interface state density of in GaAs/Al$_2$O$_3$ gate stack. A series of GaAs epitaxial layers with different thicknesses of AlP passivation layer were prepared by MOVPE. A buffer layer of n-GaAs with the thickness of 500nm was grown on an n-GaAs (001) substrate. *In situ* H$_2$S treatment was carried out in order to remove excess As from the GaAs surface. We then grew AlP passivation layer at 500°C with the growth period of 1, 10, 30 and 60 seconds. The growth period of AlP had significant effect on the layer structure after the MOVPE and air exposure. As analyzed by angle-resolved-XPS, a 0.5-nm-thick Al$_2$O$_3$ layer existed on GaAs when the growth period was 10 seconds. Longer period of AlP growth resulted in residual AlP layer between Al$_2$O$_3$ and GaAs. A 10-nm-thick Al$_2$O$_3$ layer was deposited on those layers with ALD, followed by Cr/Au evaporation, in order to obtain a gate stack. Photoluminescence of GaAs, which is a measure of interface state density, was three times stronger with the AlP growth period of 10 seconds than the gate stack without the AlP passivation. Longer growth period of AlP resulted in weaker intensity. C-V characteristics of the gate stack were also the best with the AlP growth period of 10 seconds: the frequency dispersion of accumulation capacitance was the smallest, suggesting reduced density of interface states. Even though we preserved the AlP-passivated layer for 1 night before succeeding ALD, no significant degradation was observed in C-V characteristics. Therefore, 0.5-nm-thick AlP was the optimum: too thin layer exhibited insufficient passivation, while too thick layer resulted in residual AlP and increased interface states.

2:10 PM

Atomic Layer Epitaxy of Ternary In$_X$Ga$_{1-X}$As Layers on InP Substrates Using Metalorganic and Hydride Precursors: *Yong Huang*[1]; Jae-Hyun Ryou[1]; Russell Dupuis[1]; [1]Georgia Institute of Technology

Atomic layer epitaxy (ALE) growth of ternary InGaAs nearly lattice-matched to InP substrates (x$_{In}$~0.53) has not been fully explored unlike the ALE growth of binary GaAs, InAs, InP, GaN, and AlN layers and ternary AlGaAs and InxGa1-xAs (x$_{In}$<0.2) (on GaAs substrates) layers. In the present study, growth parameters for ALE of ternary InGaAs layers on InP substrates using metalorganic and hydride precursors, such as trimethylindium (TMIn), trimethylgallium (TMGa), and arsine (AsH$_3$), is described. In this work, the incorporation kinetics of In and Ga Group-III elements for the ALE growth of InGaAs was investigated by varying growth parameters, including the growth temperature, metalorganic and hydride precursor exposures, Group-III precursor ratio, and hydrogen purge time between exposures. By separating the growth rate of InGaAs into InAs and GaAs components, it was found that the incorporation of In and Ga strongly depends on the source exposure time, H$_2$ purge conditions, and growth temperature. At 500°C the growth rate of InAs is determined by the metalorganic source supply duration and the growth rate of GaAs is determined by the AsH3 exposure duration. With increasing H$_2$ purge time, Ga incorporation is enhanced. At an elevated temperature of 550°C the incorporation of both In and Ga is dependent on metalorganic source exposure, while at a low temperature of 400°C the In and Ga incorporation is limited by the AsH$_3$ exposure. A growth model was proposed in order to explain the growth kinetics of

InGaAs ALE at 500°C, which involves metal In and $GaCH_3$ adsorbates as the In and Ga species on the growing surface, respectively.

2:30 PM

InAs/InAsP Quantum Wells on $InAs_yP_{1-y}$(Sb) Metamorphic Buffer Layers for Mid-IR Emission: *J. Kirch*[1]; L.J. Mawst[1]; K. Radavich[1]; J. Konen[1]; T.F. Kuech[1]; [1]University of Wisconsin at Madison

Metamorphic buffer layers (MBLs) have been reported by many groups as a means to produce a low defect density "virtual substrate" with a chosen lattice constant. However, the resulting surface morphology of the MBL is generally cross-hatched along the orthogonal <110> directions. High doping levels of Te ($1x10^{19}$ cm^3) have led to significantly reduced crosshatching and improved surface roughness for $InAs_yP_{1-y}$ MBL compositionally graded from InP to $InP_{0.68}As_{0.32}$[1], although MBLs employing high As-contents were not evaluated. $GaAs_ySb_{1-y}$ MBLs on GaAs substrates have also been previously reported [2], and show reduced surface roughness compared with $In_xGa_{1-x}As$ MBLs. Here we investigate two techniques to reduce surface roughness of $InAs_yP_{1-y}$/InP MBLs; 1) the incorporation of Sb and 2) the use of chemical-mechanical polishing (CMP). The luminescence of InAs QW structures grown on the MBLs are also evaluated for mid-IR emission. The MBL structures studied here were grown on (100) InP substrates by OMVPE, using conditions similar to our previous report [3] which demonstrated RT PL emission near 3 µm from InAs QWs employing $InP_{0.8}Sb_{0.2}$ claddings and an $InAs_{0.66}P_{0.34}$ SCH grown on the $InAs_yP_{1-y}$ MBL. However, a high density of hillocks was typically observed from the growth of the $InP_{0.8}Sb_{0.2}$, which tend to align with the underlying cross-hatched surface morphology. Incorporating a few percent Sb into the $InAs_yP_{1-y}$/InP MBLs is found to reduce the surface roughness (from ~15nm to 4-9nm RMS), and allows for the growth of low hillock density $InP_{0.8}Sb_{0.2}$. InAs QW SCH structures grown on top of the $InAs_yP_{1-y}$(Sb) MBL exhibit higher PL intensity (30-60% higher) compared with our previously reported structures. The use of CMP after the growth of $InAs_yP_{1-y}$ MBL with a 0.5 µm-thick $In_{0.85}Ga_{0.15}As$ capping layer, indicates that the cross-hatching morphology is nearly eliminated if ~0.5-0.6µm is removed. Additional work is required on the growth of QW structures on the MBLs subjected to CMP treatment. 1. J. G. Cederberg and S. R. Lee, APL, 91, 201915(2007). 2. H. Y. Liu, et al., APL, 92, 111906(2008). 3. J. Kirch, et al., 14th workshop on OMVPE, AUGUST 9-14, 2009, LAKE GENEVA, WISCONSIN. Acknowledgement: This work is funded by ARO MURI W911NF-05-1-0262 (Dr. John Prater).

2:50 PM

Growth of InAs/GaAs Quantum Dots on Germanium-on-Insulator-on-Silicon (GeOI) Substrate by MOCVD with High Optical Quality at Room Temperature in the 1.3 µm Band: *Mohan Rajesh*[1]; Denis Guimard[1]; Damien Bordel[1]; Masao Nishioka[1]; Emmanuel Augendre[2]; Laurent Clavelier[2]; Yasuhiko Arakawa[1]; [1]The University of Tokyo; [2]CEA-LETI

Monolithic integration of QD lasers on silicon at the telecommunication wavelength of 1.3 µm would be a major step towards the realization of high-speed optical interconnects. Fabrication of III-V-based lasers on silicon by direct epitaxial growth has been particularly challenging because of the lattice mismatch and the polar/non-polar nature of the III-V/IV system. There has been a limited number of reports on the growth of InAs/GaAs QDs on Si [1,2], or SiGe/Si substrates [3]. Electroluminescence at 1.3 µm was recently demonstrated from QDs grown on graded SiGe/Si [3]. However, for lasing action at 1.3 µm, high density InAs QDs with narrow peak linewidth and high optical quality at room temperature (RT) are required. The germanium-on-insulator-on-silicon (GeOI) substrate has been proposed as a potential platform for the monolithic integration of III-V devices with silicon [4], because it is both lattice-matched to GaAs via the top Ge layer and compatible with silicon CMOS technology. To date, no optical source has been demonstrated on GeOI though. Here, we report the growth of GaAs layers on GeOI with high structural quality and low surface roughness (RMS of 1 nm). We show that the introduction of a single QD layer within the GaAs buffer layer totally suppresses the propagation of APDs to the surface. We demonstrate the achievement of high density InAs QDs on GaAs/GeOI with RT emission at 1.3 µm, narrow peak linewidth of 33 meV and identical optical quality as that of QDs grown on GaAs substrate, which were used for the fabrication of low-threshold InAs/GaAs QD lasers by MOCVD at 1.3 µm [5]. This study is an important step towards the monolithic integration of QD lasers at 1.3 µm on Si substrate. References: [1] J. Yang et al., IEEE Trans. Electron Dev. 54, (2007) 2849. [2] L. Li et al., Appl. Phys. Lett. 92, (2008) 263105. [3] H. Tanoto et al., Appl. Phys. Lett. 95, (2009) 141905. [4] S. G. Thomas et al., IEEE Electron Device Lett. 26, (2005) 438. [5] D. Guimard et al., Appl. Phys. Lett. 94, (2009)103116.

3:10 PM

Effect of In-Situ $CBrCl_3$ Etching on the Structural Properties of InAs/GaAs Quantum Dots for Controlling Size and Density: *Atsushi Koizumi*[1]; Kazuo Uchida[1]; Shinji Nozaki[1]; [1]The University of Electro-Communications

Since a low-density of semiconductor quantum dots (QDs) manifested emission of single photons, there has been a rapidly growing interest in the low-density QDs for a solid-state, electrically pumped single-photon source. The thermal treatment performed in MOVPE growth is one of the commonly used techniques to control the InAs size and density. However, it is difficult to precisely control the etching rate because of the growth interruption required to change temperature. Although carbon tetrahalogenides, such as CBr_4, CCl_4, and $CBrCl_3$, have been widely used as carbon precursors for p-type GaAs and related compound semiconductors in the MOVPE growth, it should be noted that these precursors can also cause etching, the etching rate and time can be accurately controlled by adjusting the parameters of $CBrCl_3$ supply. We have studied the in-situ $CBrCl_3$ etching of the InAs dots, aming for controlling the size and density in the MOVPE reactor just after the growth of the InAs dots on GaAs and obtained a low density of the InAs dots for possible application to single photon sources. The InAs/GaAs structures were grown on semi-insulating (001) GaAs substrates by low-pressure MOVPE. After the growth of a GaAs buffer layer, the InAs was grown at 500°C for 30 s followed by the in-situ $CBrCl_3$ etching at 500°C in arsine ambient. The etching time was varied to 0 (without supplying $CBrCl_3$), 15 and 30 s. The size and density obtained InAs dots were measured by atomic force microscopy.The average height and density of the InAs dots without $CBrCl_3$ etching were 23.3 nm and 4×10^9 cm^{-2}, respectively. With the increased etching time, the density of InAs dots decreased to 1×10^9 and 2×10^8 cm^{-2} for $CBrCl_3$ etching times of 15 and 30 s, respectively. The average height of InAs dots for 15 s etching was 25.5 nm, which is almost same that for no $CBrCl_3$ etching, and it decreased to 16.4 nm with the further increased etching time to 30 s. These results suggest that the in-situ $CBrCl_3$ etching can decreased all InAs dots and effectively remove smaller InAs dots.

3:30 PM Break

Poster Session II

Thursday 4:00-6:00 PM	Room: Regency Ballroom
May 27, 2010	Location: Hyatt Regency Lake Tahoe

Please see pages 45-51 for the posters.

6:30 PM Reception (Lakeside Ballroom)

7:30 PM Banquet (Lakeside Ballroom)

Friday Invited Talks

Friday AM
May 28, 2010

Room: Lakeside Ballroom
Location: Hyatt Regency Lake Tahoe

Session Chair: Euijoon Yoon, Seoul National University, Seoul, Korea

---

8:30 AM Invited
Growth and Characterization of Polar and Nonpolar Nitride Quantum Well Structures: *Menno Kappers*[1]; M.A. Moram[1]; C. McAleese[1]; R. Hao[1]; T.Y. Chang[1]; Y. Zhang[1]; C.J. Humphreys[1]; T.J. Badcock[1]; C.A. Taylor[1]; S. Hammersley[1]; P. Dawson[1]; [1]University of Cambridge

Opto-electronic devices based on group-III nitrides are taking a growing market share with applications such as in laser reading/writing on DVD discs, LED traffic lights and displays, back-lighting of LCD displays, while white LEDs will gradually replace lighting in our homes and offices. The efficiencies of light-emitting structures based on InGaN quantum wells are truly remarkable considering the high density of dislocation threading through the active region. The internal quantum efficiency (IQE) of InGaN/GaN and InGaN/AlInGaN QW structures as measured by temperature-dependent photoluminescence measurements can exceed 70% at room temperature in the blue part of the visible spectrum, but the IQE values of structures designed to emit in the ultra-violet and the green spectral regions are much less. There is still no consensus on the exact mechanism(s) that govern this fall-off in IQE but the strong internal polarisation fields along the polar [0001] growth direction may play an important role. The resulting reduced electron and hole wave function overlap can lead to reduced light output when non-radiative pathways are available, and the effect becomes worse with the higher fields, resulting from increased strain in higher-indium-content layers necessary for green emission. We will describe the optical properties and microstructure of polar InGaN/GaN QWs designed to emit in the green part of the spectrum that were prepared using diffent growth procedures. Growth along nonpolar crystal directions is a way of avoiding the effects of the strong polarization-induced electric fields along the [0001] growth direction. Unfortunately, when nonpolar GaN is grown heteroepitaxially on sapphire or SiC, the resulting thin films have a high defect density and, in particular, a high density of stacking faults (typically high-105 cm-1) and their associated partial dislocations (typically high-1010 cm-2). We will discuss defect reduction methods and the structural and optical properties of a-plane (11-20) InGaN/GaN QW structures as a function of defect density and alloy composition and compare their IQE values at room temperature with structures grown on polar growth directions c-plane.

9:00 AM Invited
Various Embedded Structures of InGaN LED Employing Selective MOCVD Growth: *Chang-Hee Hong*[1]; Hyung Gu Kim[1]; [1]Chonbuk National University

The InGaN-based light emitting diodes (LEDs) with various embedded structures such as periodic deflector, overcut deflector and air-gap reflector etc. were fabricated by a selective MOCVD growth and wet etching process to increase light output power. The geometrical shape of embedded structures can be served to enhance the light extraction efficiency due to the effect of scattering or suppressing of total internal reflection in facilitating the multiple chances of photon to escape. Especially the air-gap embedded structures in GaN LED layer promise to enhance the light output power compared to other embedded LED structures.

9:30 AM Break

Nitrides III

Friday AM
May 28, 2010

Room: Lakeside Ballroom
Location: Hyatt Regency Lake Tahoe

Session Chairs: Marie-Antoinette Poisson, Alcatel-Thales III-V Lab, Marcoussis, France; Markus Weyers, Ferdinand Braun Institute, Berlin, Germany

---

10:00 AM
GaN Heteroepitaxy on High Index Silicon Substrates: *Roghaiyeh Ravash*[1]; Jürgen Bläsing[1]; Armin Dadgar[1]; Thomas Hempel[1]; Peter Veit[1]; Alois Krost[1]; [1]Otto-von-Guericke Universität Magdeburg, FNW/IEP/AHE

Due to the lack of GaN homosubstrates, the growth of GaN-based devices is usually performed on heterosubstrates as sapphire or SiC. These substrates are either insulating or expensive, and both unavailable in large diameters. Meanwhile, silicon can meet the requirements for a low price and thermally well conducting substrate and also enabling the integration of optoelectronic devices with Si-based electronics. Up to now, the good matching of hexagonal GaN with the 3-fold symmetry of Si(111) greatly promotes the c-axis orientated growth of GaN on this surface plane. A large spontaneous polarization oriented along the c-axis exists in such hexagonal structure because of a large ionicity factor of the covalent metal-nitrogen bond and the noncentrosymmetry of the wurzitic material. In addition, these materials show a strong piezoelectric polarization in this crystalline growth direction enhancing or reducing the overall polarization field strength. Particularly in quantum wells the electric field induces separation of electrons and holes and reduces the radiative emission efficiency leading to low efficiencies for thick quantum wells. In contrast, the attention to the growth of non-polar, ((1-100) m-plane and (11-20) a-plane) or semi-polar ((10-11)-, (10-12)-, (10-13)-plane) GaN based epitaxial structures has been increased recently because of reducing the effect of the polarization fields in these growth directions. However, basal plane and prismatic stacking faults are common defects in such non-polar material degrading device performance. Therefore we studied GaN epilayers grown by metalorganic vapor phase epitaxy on silicon substrates with different orientations, e.g. on Si(211), Si(711). The search for suitable and promising substrate orientations was performed by a variation of the growth parameters as temperature, seeding layer thickness, etc.We investigated the crystallographic structures of GaN grown on Si by X-ray analysis and scanning electron microscopy. The impact of symmetry of Si surface on GaN crystallites texture was studied. We observed that AlN seeding layer growth time plays a significant role in obtaining different GaN textures. Applying a ~ 4 nm AlN seeding layer we obtain a single crystalline GaN epilayer on Si (211).

10:20 AM
On the Anisotropic Wafer Curvature of GaN-Based Heterostructures on Si(110) Substrates Grown by MOVPE: Christof Mauder[1]; Ian Booker[1]; Hassan Boukiour[1]; Lars Rahimzadeh Khoshroo[1]; Joachim Woitok[2]; Michael Heuken[3]; Holger Kalisch[1]; Rolf Jansen[1]; *Dirk Fahle*[1]; [1]RWTH Aachen University; [2]PANalytical B.V.; [3]AIXTRON AG

We highlight the challenges of GaN growth on (110)-oriented Si substrates with respect to the balancing of substrate-induced anisotropic strain. For growth on Si, an AlN nucleation layer is typically used. The epitaxial orientation of AlN on Si(110) is [11-20] || [001] and [1-100] || [1-10] with a lattice mismatch of 19.0% and 0.7%, respectively. However, to understand the resulting strain state after growth, one has to take into account the 5:4 lattice matching relationship between AlN and Si(111) which is also valid for the mismatch of AlN on Si(110) along the [11-20] direction. This misfit reduces the effective lattice mismatch for AlN to -1.3% in [11-20]. Although the close matching in both directions is advantageous for achieving low defect densities, the opposite signs of the two mismatch values lead to problems with strain management. The reason is the thermal mismatch between nitrides and Si which leads to tensile strain during cool down. To compensate for this, compressive strain is required. However, AlN grows on Si(110) with tensile strain in [1-100]. For a simple growth scheme with 1 µm GaN on top of a 40 nm AlN buffer layer, this situation is reflected in the aspherical wafer curvature measured by X-ray diffraction omega scans. While for the growth on Si(111), the wafer is concavely bent with a curvature of ~140 km^{-1} in both directions, the same layer stack on Si(110) causes a bowing of 300 km^{-1} and 150 km^{-1} in [1-100] and [11-20], respectively. We may note that the latter approach causes cracking, predominantly occurring parallel to the

[11-20] direction. In contrast, the layer on Si(111) is crack-free. An almost complete reduction of the bending anisotropy on Si(110) can be achieved by the insertion of a 400 nm thick AlGaN buffer layer with ~17% Al mole fraction. Both crystal quality and surface roughness are not strongly affected by the introduction of this buffer layer. We conclude that the ternary alloy itself is responsible for the reduction of anisotropy in lattice mismatch. Thus, an optimized layer stack including an AlGaN film is needed to grow high-quality, crack-free films on Si(110) substrates.

10:40 AM

Reduction of Threading Dislocations in GaN on In-Situ Meltback-Etched Si Substrates: *Hiroyasu Ishikawa*[1]; Keita Shimanaka[2]; [1]Shibaura Institute of Technology; [2]Nagoya Institute of Technology

We report the novel growth technique of GaN on Si substrates using a conventional horizontal MOCVD method. Using metal droplets, which are formed by supplying metalorganic gasses, Si substrates can be meltback-etched under the droplets, resulting in craters. Both deep and shallow craters are favorable to reduce threading dislocations (TDs) as follows; 1) Deep craters can be used as lateral growth region, 2) shallow craters are also useful to bend TDs as well as the growth on shallowly patterned sapphire substrates . Moreover, this process can be carried out through the MOCVD reactor. Metal droplets were formed by feeding only metalorganic gasses at 500°C under atmospheric pressure. Trimethylgallium (TMG), trimethylindium (TMI) and trimethylaluminium (TMA) were used to form Ga, In and Al droplets. Then, the reactor pressure was set at 100 Torr and a 50-nm-thick AlN interlayer and a 1-µm-thick GaN layer were grown on the meltback-etched Si (MES) substrate at 1080°C. The Si substrate was heated at 1080°C to initiate meltback etching by metal droplets for 10-30 min. Interference optical microscope observations reveal mirror-like and mirror surfaces using Ga and In droplets, whereas the one using Al droplets was cloudy. A careful examination result shows as follows; pits with a density of $0.7\text{-}1\text{x}10^7$ cm^{-2} on the surface using Ga droplets, polycrystalline GaN using Al droplets, and feartureless surface using In droplets. The lateral growth can be expected around the pits on GaN on the MES substrate using Ga. Al droplets are likely to remain on the Si surface, forming the continuous film after melting during the increase in temperature; In droplets are likely to evaporate before creating craters. Ga has intermediate values, and hence Ga is suitable for our aim. Transmission electron microscope (TEM) observations reveal that all types of the TDs have bent in to a direction parallel to the growing surface, leading to significant reduction of TDs around the craters. It is found that the AlN interlayer is grown on the craters and most of the TDs around the craters have bent toward pits, not toward the centers of craters.

11:00 AM

Effect of Indium Incorporation on Optical and Structural Properties of M-Plane InGaN/GaN MQW on LiAlO$_2$ Substrates: Christof Mauder[1]; Benjamin Reuters[1]; Kwang-Ru Wang[2]; Achim Trampert[2]; Mikalai Rzheutskii[3]; Evgenii Lutsenko[3]; Gennadi Yablonskii[3]; Joachim Woitok[4]; Michael Heuken[5]; Holger Kalisch[1]; Rolf Jansen[1]; *Dirk Fahle*[1]; [1]RWTH Aachen University; [2]Paul-Drude-Institut für Festkörperelektronik; [3]National Academy of Sciences of Belarus; [4]PANalytical B.V.; [5]AIXTRON AG

We report about the optical and structural characterisation of m-plane InGaN/GaN multiple quantum well structures (MQW) with different indium fractions between 7 and 42% as determined by high-resolution X-ray diffraction (HRXRD). All samples were grown on 2-inch LiAlO$_2$ substrates in AIXTRON MOVPE reactors. The heterostructures show superlattice oscillations in HRXRD symmetric 2Theta/Omega-scans and were further investigated by polarization-dependent room-temperature (RT) photoluminescence (PL) spectroscopy. As expected, lower MQW growth temperatures lead to an increase of indium fraction and PL peak position wavelength. Higher PL peak full width half maximum values of ~200-300 arcsec at RT are found for indium fractions above 15%. Also, the degree of polarization at RT changes from ~0.4 to ~0.8 when the indium content is varied from 7 to 42%. As probable reason for both effects, larger strain for higher In contents results in a higher energy separation between the uppermost valence subbands in InGaN. Furthermore, the PL peaks show good stability when the excitation intensity is varied by two orders of magnitude. While a comparable c-plane MQW exhibits a peak energy shift of 287 meV, only a slight energy shift dependent on indium fraction between 5 and 67 meV is detected for the m-plane heterostructures. A clustering mechanism is assumed to be responsible for this remaining peak shift. Atomic force microscopy reveals fine stripes on the surface of all MQW samples which are not visible for the underlying GaN buffer layer. These stripes are oriented in the (0001) plane of GaN and their density doubles from $\sim 1\cdot 10^5$ cm^{-1} to $\sim 2\cdot 10^5$ cm^{-1} when more indium is incorporated. As most likely reason, higher indium fractions lead to greater strain between barrier and well, inducing the generation of basal plane stacking faults (BSF) in the MQW. The BSF are assumed to affect the surface morphology by creating the striation pattern. An investigation by transmission electron microscopy is ongoing to confirm this theory. However, we think an improved strain management in nonpolar InGaN/GaN MQW is necessary to achieve high-performance long-wavelength light-emitting diodes.

11:20 AM

Spatially-Resolved Study of Luminescence and In Incorporation in GaN and High-In Content InGaN/GaN Nanowires: *George Wang*[1]; Qiming Li[1]; [1]Sandia National Laboratories

Given the strong interest in III-nitride-based nanowires for optoelectronic and energy applications, a better understanding of their optical properties and structure-composition is required, particularly at nanoscale spatial resolutions, which could shed light into issues such as the nature and distribution of radiative defects and alloy compositional variations. Here, we present a spatially-resolved, correlated study of luminescence and composition in GaN, Al(Ga)N/GaN, and InGaN/GaN core-shell nanowires grown by metal-organic chemical vapor deposition. For GaN nanowires, a surface layer exhibiting strong yellow luminescence (YL) near 566 nm in the nanowires was directly revealed by high resolution, cross-sectional cathodoluminescence (CL) imaging, compared to weak YL in the bulk. In contrast, other defect related luminescence near 428 nm (blue luminescence) and 734 nm (red luminescence), in addition to band-edge luminescence (BEL) at 366 nm, were observed in the bulk of the GaN nanowires but were largely absent at the surface. As the nanowire width approaches a critical dimension, the surface YL layer completely quenches the BEL. The surface YL is attributed to the diffusion and piling up of mobile point defects, likely isolated gallium vacancies, at the surface during growth. AlGaN/GaN and AlN/GaN core-shell nanowires were observed to exhibit stronger BEL and weaker YL as compared with bare GaN nanowires, which may relate to the passivation of nanowire surface states. InGaN/GaN core-shell nanowires were also investigated by correlated CL and cross-sectional scanning TEM (STEM). Dislocation-free InGaN layers with up to ~40% indium incorporation were achieved on GaN nanowires. The indium composition distribution in the InGaN layers were qualitatively correlated to the strain energy density distribution as calculated by finite element analysis models. The observed high indium incorporation and high crystalline quality in the heteroepitaxial InGaN layers is attributed to strain-relaxed growth on the nanowires. Sandia is a multiprogram laboratory operated by Sandia Corporation, a Lockheed Martin Company, for the United States Department of Energy under contract DE-AC04-94AL85000.

11:40 AM

Growth of AlGaN and AlN on Patterned AlN/Sapphire Templates: *Viola Kueller*[1]; Arne Knauer[1]; Frank Brunner[1]; Ute Zeimer[1]; Hernan Rodriguez[1]; Michael Kneissl[2]; Markus Weyers[1]; [1]Ferdinand-Braun-Institut Berlin; [2]Technical University of Berlin

UV-transparent and low defect density AlN and AlGaN buffer layers are required for UV- light emitting diodes (LEDs). However, typical threading dislocation densities of heteroepitaxial AlN are still in the range of 10^{10} cm^{-2}. One method to reduce the dislocation density is epitaxial lateral overgrowth (ELO). In this study, maskless epitaxial overgrowth of AlGaN on structured AlN templates was performed and the impact of stripe orientation on the lateral growth of AlGaN was studied. 700 nm thick AlN templates were grown on c-plane sapphire by MOVPE in an AIX2400G3HT 11x2" reactor. The FWHM of the XRD rocking curves (10-12 reflection) was about 1000 arcsec. The AlN/sapphire templates were then patterned into stripes by inductively-coupled plasma etching. The structure, a stripe pattern with 1.5 µm wide bars and a period of 3 µm, was etched 1.4 µm deep into the sapphire. Subsequently, AlGaN and AlN growth has been performed on the patterned templates. Two stripe orientations have been investigated: parallel to the [1-100] and parallel to the [11-20] direction. Cross-sectional secondary electron microscopy images of AlGaN grown on a stripe pattern in [1-100] direction show that coalescence occurs after 1.8 µm vertical growth. We also observe AlGaN growth on the exposed sapphire surface until the coalescence prevents the precursors from reaching the grooves between the stripes. Spectrally resolved cathodoluminescence (CL) investigations at 80 K show that the Al-content is dependent on the growth facet and varies between 30% in the sidewalls and 50% on the c-facet. AlGaN grown on a stripe pattern in [11-20] direction coalesces after 1.2 µm vertical growth, but the surface is facetted and rough. The CL spectrum at 80 K exhibits luminescence at several distinct wavelengths, hence many facets are involved during the overgrowth of a stripe pattern in [11-20] direction. AlN layers grown on patterned substrates show a smoother surface morphology for stripes oriented in [1-100] direction compared to stripes in [11-20] direction. The FWHM (10-12 reflection) of the AlN template and the overgrown AlN is reduced from 1000 arcsec to 500 arcsec, respectively, indicating a reduced dislocation density via this method.

Nanostructures

Friday AM
May 28, 2010

Room: Regency C&F
Location: Hyatt Regency Lake Tahoe

Session Chairs: Jeff Cederberg, Sandia National Laboratories, Albuquerque, NM, USA; Jonas Johansson, Lund University, Lund, Sweden

10:00 AM

Continuous-Flow MOVPE Growth of Position-Controlled Gan Nanorods: *Werner Bergbauer*[1]; Martin Strassburg[2]; Christopher Kölper[2]; Norbert Linder[2]; Sönke Fündling[3]; Shunfeng Li[3]; Hergo-Heinrich Wehmann[3]; Andreas Waag[3]; Claudia Roder[4]; Jonas Lähnemann[4]; Achim Trampert[4]; [1]OSRAM Opto Semiconductors GmbH; Institut für Halbleitertechnik, TU Braunschweig; [2]OSRAM Opto Semiconductors GmbH; [3]Institut für Halbleitertechnik, TU Braunschweig; [4]Paul-Drude-Institut für Festkörperelektronik

Controlled growth of GaN nanorods (NRs) containing optically highly efficient defect free quantum discs with tuneable emission wavelength[1] or core shell heterostructures[2] is promising to improve light emitting devices in future. In comparison to MBE and HVPE, catalyst free MOVPE growth of NRs still requires quite delicate growth modes, such as pulsed MOVPE growth[3], to achieve homogenous NR arrays. In our work, GaN NRs were grown using continuous flux MOVPE on a large volume production tool. NRs with InGaN/GaN heterostructures as well as n- and p-doped GaN NRs using silicon and magnesium have been grown catalyst free. Position control of NRs was enabled by a SiO$_2$ masking layer on bare c-plane sapphire substrates. Small and dense substrate pattern were obtained by nanoimprint lithography (NIL) realizing characteristic NR diameters down to 220 nm. A significant influence of H$_2$ fraction within the H$_2$/N$_2$ carrier gas mixture on nanostructure morphology was identified. Using an increasing hydrogen fraction as morphactant within the carrier gas enables transformation from pyramidal shaped GaN nanostructures to GaN NRs. Additionally lateral growth rate was suppressed effectively by adding supplementary hydrogen enabling typical aspect ratios around 7:1. High growth rates up to 25µm/h were observed and hold for time and cost saving efficient growth process of nitride based LEDs. To evaluate structural quality and optical properties SEM, TEM and cathodoluminescence (CL) measurements were applied, respectively. The dependence of lateral growth rate on the pitch was analyzed by statistical evaluation from top view SEM images. The mean diameter of NR decreases significantly for all carrier gas compositions with decreasing pitch. Sapphire surface roughness and side wall properties of mask openings were identified as origin of defect generation in the lower part of the NRs by TEM analyses. Position and amount of In incorporation could be designated by different emission energies to polar and semipolar planes using room temperature CL measurements on the edge of cleaved NR samples. ***[1]A. Kikuchi et al.; Japanese Journal of Applied Physics 43, pp.L1524-L1526, 2004. [2]F. Quian et al.;Nano Letters, Vol.4, No.10, 1975-1979, 2004. [3]S.D. Hersee et al.; Nano Letters, Vol.6, No.8, 1808-1811, 2006.***

10:20 AM

Selective Growth of High-Quality GaN Nanowires without Using a Pulsed Method: *Kihyun Choi*[1]; Munetaka Arita[2]; Yasuhiko Arakawa[3]; [1]Institute of Industrial Science, University of Tokyo; [2]Institute for Nano Quantum Information Electronics, University of Tokyo; [3]Institute of Industrial Science, Institute for Nano Quantum Information Electronics, University of Tokyo

Semiconductor nanowires have great potential to realize highly efficient optoelectronic devices partly because of their unique nature such as possibility of eliminating dislocations. Recently, we have developed catalyst-free metalorganic chemical vapor deposition (MOCVD) growth of self-assembled GaN nanowires [1]. However, considering practical use, precise control of positions and dimensions of the nanowires is crucial. Although selective area growth of GaN nanowires using the pulsed MOCVD in which material sources are alternatively supplied has been reported [2], its complexity causes some difficulties in optimization and/or stabilization of growth parameters. Here, we report a simple selective area MOCVD growth of GaN nanowires, in which all sources are simultaneously, continuously supplied. A 40-nm thick SiO$_2$ was first deposited on GaN/sapphire (0001) using rf-sputtering, then patterned by electron-beam lithography and reactive ion etching. We prepared circular openings with diameters ranging from 100 nm to 1 µm. Finally, regrowth of GaN was carried out in an MOCVD reactor at a temperature between 950°C and 1050°C in 76 Torr without using any interruption or modulation of source gas supply. Trimethylgallium (TMG) and NH$_3$ were supplied as group III and V sources, respectively. Similarly as we have found previously in the catalyst-free self-assembled growth of GaN nanowires [1], by reducing flow rates of source gases under low V/III ratio, we succeeded to grow columnar crystals with six smooth {1-100} facets along [0001] direction. Nanowires grown for 8 minutes on 100 nm diameter openings have 100 nm ± 10 nm in diameter and 940 nm ± 80 nm in length. Interestingly, it is revealed that the optimum NH$_3$ flow rate depends on the diameter of the pattern: the larger the diameter is, the more reduced NH$_3$ flow rate is required. It is suggested that effective source supply rates at smaller openings are lower than those at larger openings. These results will certainly contribute to build up nitride nanowire-based devices by a rather simple method. This work was supported by Special Coordination Funds for Promoting Science and Technology. [1] M. Arita *et al.*, in preparation[2] S. D. Hersee *et al.*, Nano Lett. 6, 1808 (2006).

10:40 AM

Multiple Vertically Stacked Quantum Dots, Quantum Wires and Quantum Wells of III-Nitrides by MOVPE Nano Selective Area Growth: *Wui Hean Goh*[1]; Gilles Patriarche[2]; Peter Bonanno[1]; Simon Gautier[3]; Tarik Moudakir[4]; Mohamed Abid[1]; Gaëlle Orsal[3]; Andrei Sirenko[5]; Zonghou Cai[6]; Anthony Martinez[2]; Abderrahim Ramdane[2]; Luc Le Gratiet[2]; David Troadec[7]; Ali Soltani[8]; Abdallah Ougazzaden[1]; [1]Georgia Institute of Technology/GT-Lorraine, UMI 2958 Georgia Tech-CNRS; [2]Laboratoire de Photonique et de Nanostructures, CNRS 20; [3]Laboratoire Matériaux Optiques, Photonique et Micro-nano Systèmes, UMR CNRS 7132, Université de Metz et Supélec; [4]UMI 2958 Georgia Tech-CNRS; [5]Department of Physics, New Jersey Institute of Technology; [6]Advanced Photon Source; [7]Institut d'Electronique, de Microélectronique et de Nanotechnologie ; [8]Institut d'Electronique, de Microélectronique et de Nanotechnologie

The bandgap of (Al,Ga,In)N semiconductors extends from 0.7-6.2 eV making them potential candidates for optoelectronic devices covering the whole visible spectrum. However, the optical efficiency of these semiconductors are constrained by the piezoelectric effect in these highly strained materials. One way to circumvent this problem is by growing GaN along non-polar or semi-polar planes. On the other hand, it is proposed that the presence of quantum dots in the InGaN active region result in high external quantum efficiency despite the high treading dislocation. In this work, we have grown up to twelve vertically stacked quantum dots, quantum wires, and semi-polar plane quantum wells of III-nitrides by selective area growth (SAG). E-beam nanolithography were used to prepare the mask with hole and stripe-shaped openings of ~100nm. To investigate the quality of the quantum structure, the nanostructures were processed by focused ion beam and characterized by high resolution scanning transmission electron microscopy (HR-STEM). High angle dark field HR-STEM images show a uniform and well defined AlGaN layers with thickness of ~0.5nm along {1-1.1} plane, indicating high quality growth. These layers were used as markers to understand the growth mechanism of nanodots in SAG. On the apex of the nanodots forms the quantum dots of ~3nm diameter with uniform size and composition along the growth. Energy dispersive x-ray analysis shows aluminum incorporation of 5%-8% on the apex of nanostructures compared to 2% on the {1-1.1} facets. This high contrast of incorporation along c-plane enhances carrier confinement in the case of InGaN alloys. Bright field HR-STEM shows some stacking faults in the nanostructure but no noticeable treading dislocations. Synchrotron submicron beam x-ray diffraction measurements corroborate the STEM results, showing aluminum incorporation of 8.5% in the nano-SAG AlGaN structures compared to 5.3% in the unmasked area. This phenomenon is attributed to surface migration and lateral vapor phase diffusion.In summary, we propose a novel method to grow quantum dots, quantum wires and quantum wells of GaN-based materials by nano-SAG with high quality and small feature size. The SAG mechanism of nanodots has been clarified by using markers and HR-STEM cross-section analysis.

11:00 AM

Structural and Optical Properties of Site-Controlled InAs/InP Quantum Dots Grown by Selective Area MOVPE Growth for Single Photon Source Applications: *Noelle Gogneau*[1]; Luc Le Gratiet[1]; Bruno Fain[1]; Gilles Patriarche[1]; Ludovic Largeau[1]; Gregoire Beaudoin[1]; David Elvira[1]; Richard Hostein[1]; Alexios Beveratos[1]; Isabelle Robert-Philip[1]; Isabelle Sagnes[1]; [1]LPN-CNRS

The development of single photon sources emitting at 1.55 µm based on InAs/InP quantum dots (QDs) is essential for quantum communication, in particular for long distance quantum cryptography. To realize efficient sources, the coupling of the QDs emission with the cavity modes and therefore the positioning of the QDs within a microcavity are required. Although, the Stranski-Krastanow growth mode is the widely used method to synthesis QDs, it does not allow the precise localization of the QDs on the surface, which is a crucial issue for the development of reproducible sources. In this work, we demonstrate a new approach of Nano Selective Area Growth (NSAG) to precisely localized InAs/InP QDs by low-pressure Metalorganic Vapour Phase Epitaxy (MOVPE). This approach is based on partial patterning of substrates by using Hydrogen Silsesquioxane negative resist, in only one step (e-beam insulation) avoiding mask etching and resist removal before growth. Furthermore, the peculiar nano-patterning uses two MOVPE properties, the growth inhibition and the very long diffusion length of the actives species on the dielectric mask. Hence, the growth is perfectly localized on the surface, leading to the growth of site-controlled QDs. By combination of Scanning Electron Microscope (SEM), Atomic Force Microscope (AFM) and High Resolution Scanning Transmission Electron Microscope (STEM), we demonstrate the synthesis of 40 nm large localized InAs/InP QDs with high structural properties. In addition, the dimensions of the nano-patterning being lower than the diffusion length of the actives species, we establish a controllable growth rate and thus an adjustable QD height in the nanometer scale. Hence, we demonstrate the modulation of the wavelength emission of site-controlled QDs, in the 1 µm – 1.7 µm range. Finally, we exhibit that the site-controlled InAs/InP QDs can be embedded with the InP capping layer. The planarized structure presents a very flat top surface characterized with atomic steps and a rough mean scare of the order of 1.2 nm, which is crucial for the fabrication of good microcavities localized on the nanostructures.

11:20 AM

Distribution and Number Control of 1.55-µm InAs Quantum Dots on Truncated InP Pyramids Grown by Selective Area Metal Organic Vapor Phase Epitaxy: *Hao Wang*[1]; Jiayue Yuan[1]; Peter J. Veldhoven[1]; Richard Nötzel[1]; [1]Eindhoven University of Technology

Self-organized quantum dots (QDs) have brought enhanced performance to lasers and optical amplifiers due to their discrete energy states, which is of particular importance for operation in the 1.55-µm telecom wavelength region. These devices rely on QDs grown in the Stranski-Krastanow (SK) mode which are distributed randomly on the substrate surface. For advanced quantum functional devices, however, precise position and number control of a few down to a single QD is required. This can be realized by pre-defined QD nucleation on truncated pyramids formed by selective area growth in dielectric mask openings.Here we report the control of distribution and number of InAs QDs on truncated InP pyramids grown by selective area metal organic vapor phase epitaxy (MOVPE). The top surface of the InP pyramids is composed of a (100) facet and naturally formed {103} and {115} facets aside. The arrangement of the facets and their relative sizes are determined by the shape of the pyramid base (e.g., square, circular, triangular) defined by the mask opening together with the competition of surface energy and edge energy to minimize the total energy of the pyramid. The facet arrangement allows the precise position and distribution control of the QDs due to preferential nucleation on the {103} and {115} facets providing optimal strain relief. The QD number, related to the specific shape of the pyramid top surface, is reduced by the shrinking size during growth. Well defined positioning of four, three, two, and single QDs is realized. Finally the emission from single QDs is observed at 1.55 µm after optimization of the growth parameters.

11:40 AM

High Optical Quality and Versatility of Pyramidal Site Controlled Quantum Dots Grown by MOVPE: *Valeria Dimastrodonato*[1]; Lorenzo Mereni[1]; Robert Young[2]; Gediminas Juska[1]; Emanuele Pelucchi[1]; [1]Tyndall National Institute, University College Cork; [2]Lancaster University

In the last decade Quantum Dots (QDs) have been important in the development of fundamental physics studies and a broad gamut of optoelectronics applications. Their optical properties are ideal for quantum information and computing applications, where reproducibility with high uniformity, tailoring of the optical properties and high spectral purity are highly desirable. Site control techniques overcome difficulties, typical of self-assembled QDs, related to randomness of the growth mechanism, leading to more uniform and reproducible optical features. Nevertheless, because of contaminants incorporated during the pre-growth processing, site controlled systems, grown both by MetalOrganic Vapor Phase Epitaxy (MOVPE) and Molecular Beam Epitaxy, in general perform poor spectral qualities. Moreover, for MOVPE grown structures, intrinsic limits, due to employed sources and reactor environment issues, can narrow the possibilities toward the achievement of high optical quality. We present a nearly ideal system offering both uniformity and high quality of exciton emission spectra from pyramidal site controlled QDs, grown by MOVPE on GaAs (111)B substrates, pre-patterned with 7.5µm pitch pyramidal recesses. The dots nucleate in situ, as result of a self-limiting profile formation, and defect free interfaces are guaranteed. Optimization of growth conditions, a careful handling and a constant contamination monitoring of the reactor revealed to be key parameters toward a record spectral purity. Excitons emitted from InxGa1-xAs /GaAs dots present linewidths with a Full Width at Half Maximum of 18µeV and inhomogeneous broadening of 2.3meV. Our QDs offer the possibility of reducing/controlling strain effect in the confined structure: no built-in strain affects the dot formation and the (111)B substrate permits obtaining symmetrical structures. Strain engineering can be achieved, for example, through low Nitrogen incorporations in the dot layer: it ideally allows extending the pyramidal QD emission wavelengths and a broad-range tuning of optical properties. As an example, first micro-photoluminescence measurements conducted on site controlled diluted InGaAsN QDs, with Nitrogen incorporations <<1%, revealed a surprising anti-binding behavior of the biexciton state (determined by power dependence, whilst a more accurate fine structure splitting characterization is still ongoing), opening appealing perspectives toward the control of excitonic features and, for example, in the field of energetically indistinguishable photons.

Poster Session I

Tuesday, 4:00-6:00 PM Room: Regency Ballroom
May 25, 2010 Location: Hyatt Regency Lake Tahoe

P1.1 Effect of Growth Pressure on Coalescence Thickness and Crystal Quality of GaN Deposited on 4H-SiC: Piotr Caban[1]; Wlodek Strupinski[1]; Jan Szmidt[2]; Deniz Caliskan[3]; Ozgur Kelekci[3]; Ekmel Ozbay[3]; [1]Institute of Electronic Materials Technology; [2]Warsaw University of Technology; [3]Bilkent University

The application potential of III-N compounds, in particular GaN, is widely known. Such unique properties as high thermal stability and high breakdown voltage material make this wide gap nitride a good candidate for the opto-electronic devices. Most gallium nitride based epitaxial structures are grown on sapphire as relatively low cost substrates material, however, it does not meet the requirement of higher thermal conductivity necessary for high power applications. A good solution is the replacement of sapphire with silicon carbide, which successfully fulfils this condition. This paper presents the results of GaN growth pressure on crystal quality and surface roughness of epilayer grown on silicon carbide at 50mbar, 125mbar and 200mbar. The coalescence thickness in case of GaN growth were analyzed using atomic force microscopy (AFM). In order to confirm the quality of the GaN epilayers in power applications, AlGaN/AlN/GaN/SiC HEMT transitors were fabricated. Gallium nitride epilayers were grown by low pressure MOVPE technique on (0001) – oriented 4H-SiC substrates. AlN was deposited as a wetting layer between GaN and SiC to avoid surface cracks. GaN epilayers were characterized using HRXRD measurement. GaN grown at 200mbar displayed better crystal quality than that grown in lower pressure. Atomic force microscopy showed that the increase of the GaN growth pressure improves smoothness of the epilayers surface. It was demonstrated that GaN island coalescence mechanism exerted major impact on the surface roughness. Systematic investigations were performed on 3D - 2D growth modes changes. GaN growth performed at different pressures was being interrupted after 1, 6, 10, 15 minutes and surface morphology by AFM was being studied to explain the material characteristics. Moreover, Etched Pits Density was examined by the defect-selective etching of GaN surface in molten NaOH–KOH eutectic. In order to determine the influence of GaN buffer growth pressure on the device performance, AlGaN/AlN/GaN–based heterostructures were deposited on SI 4H-SiC substrates. The growth conditions of AlGaN-barrier were the same for all the structures. The only difference was GaN growth pressure. The HEMT structures were processed and characterized.

P1.2 Thickness Dependence of Optical and Crystal Properties of Semipolar (11-22) GaN Grown on m-Plane Sapphire without Low Temperature Buffer Layer: Hyun Sung Park[1]; Geun Ho Yoo[1]; Hyoung Jin Lim[1]; Ok Hyun Nam[1]; *Sung-Nam Lee*[1]; [1]Korea Polytechnic University

GaN-based light emitting devices are mainly grown on c-plane GaN templates. However, conventional c-plane GaN-based devices have been suffered from the quantum confinement stark effect due to the existence of strong piezoelectric and spontaneous polarization. To solve the limits of physical problems in III-nitrides, a lots research groups have studied in the growth of nonpolar and semipolar GaN-based optoelectronic devices for polarization-reduced heterostructure. However, there are a few issues to grow high quality nonpolar and semipolar GaN on sapphire substrates due to the huge difference of anisotropic lattice and thermal mismatch. In this study, we introduced the novel growth technique and the thickness dependence of optical and crystal properties of semipolar GaN.Semipolar (11-22) GaN growth procedure was consisted of 0.05 μm-thick GaN with N2 atmosphere and 2.0 μm-thick GaN with H2 atmosphere at 1050 C without low temperature GaN buffer layer by using metalorganic chemical vapor deposition. To clarify the growth mode, we prepared semipolar (11-22) GaN/m-sapphire with different film thickness from 0.05 to 2.0 μm. From surface analysis, the quasi 3-dimensional surface structure toward [11-2-3] was evolved at an initial growth stage (< 0.1 μm). Above film thickness of 0.5 μm, arrowhead-like surface structure was developed and planarized with increasing the film thickness. From room temperature photoluminescence (PL) measurement, PL intensity of bandedge emission was drastically increased up to 1.0 μm, and then gradually increased above a thickness of 1.0 μm. With increasing the film thickness, the increase of PL intensity was inversely proportional to the full width at half maximum (FWHM) of high-resolution X-ray diffraction. It implied that optical property was significantly dependent upon crystal defects of semipolar GaN. Particularly, within a thickness of 0.1 μm, FWHM with incident beam of [1-100] was decreased much more than that of [11-2-3]. It indicated that defects related to [1-100] were drastically decreased by initial growth stage, having a faster growth rate of [1-100] than [11-2-3] in our growth condition. From these results, we concluded that 2-dimensional growth was dominant above 0.1 μm and the optical quality was significantly enhanced due to the improvement of crystal quality.

P1.3 Formation of Self-Assembled GaN Nanorings by Metalorganic Vapor Phase Epitaxy: *Urusa Alaan*[1]; Fanyu Meng[1]; Subhash Mahajan[1]; [1]Arizona State University

Self-assembled GaN nanorings were deposited without a template by MOVPE on *c*-plane sapphire substrates using an AIXTRON 200 RF horizontal reactor. First, gallium droplets were formed on the substrate by flowing 50-sccm of trimethyl gallium into the reactor at 570°C and 300-mbar for 30 seconds and hydrogen was used as a carrier gas. To form the rings, the temperature and pressure were raised to 900°C and 700-mbar, respectively. Ammonia was subsequently injected into the reactor for 2 minutes, using either hydrogen or nitrogen as a carrier gas. The as-grown deposits were cooled in ammonia to prevent their decomposition during the cycle down to room temperature. SEM, TEM and XRD analyses revealed that the rings are wurtzitic, single-crystalline and epitaxial with sapphire. For the above growth parameters, the Ga droplets have a radius of 58-nm and are uniformly distributed with a density of 40 droplets per square micron. The rings are coarse and non-uniform with a radius of approximately 300-nm. There are roughly 5.4 rings per square micron. TEM weak-beam dark-field imaging shows that the rings are highly strained. Photoluminescence spectra indicate yellow luminescence from the rings that were grown in nitrogen, but not in hydrogen; this may be caused by gallium vacancies. The GaN rings form as a result of a volume contraction in the Ga droplets. The density of GaN (6.15-g/cm^3) is greater than that of Ga (5.91-g/cm^3), and so the same number of Ga atoms occupies less volume in GaN. We argue that GaN nucleates first at the triple points along the droplet edges and grows preferentially from these sites. The diffusion time for nitrogen to reach the centers of the droplets are longer, resulting in “holes” as the gallium atoms are consumed. This explanation was confirmed by a volumetric comparison between the droplets and the rings. This work was supported by the Fulton Undergraduate Research Initiative (FURI) of the Ira A. Fulton School of Engineering, Arizona State University in Tempe, AZ 85287-8706.

P1.4 Effect of Ammonia Flow Rate and 70 MeV Si Ion Irradiation Induced Defects on Structural, Optical, Electrical and Device Characteristics of GaN: *Suresh Sundaram*[1]; Balaji Manavaimaran[1]; Baskar Krishnan[1]; [1]Anna University

Gallium Nitride (GaN) is an important semiconductor material for optoelectronics in the UV-Visible-IR range and also for high power and high temperature electronics for future applications. But the defects in this material hinder such progress in these fields. Dedicated studies on the understanding of defects, and their effect on devices characteristics are extremely important to improve the performance GaN based devices. In the present investigation effect of growth parameters on the device characteristics of Pd/n-GaN schottky diodes and 70 MeV Si ion irradiation induced changes in properties of GaN epilayers were discussed. Concentration of the compensating defects and the threading dislocation was found to increase with increase of V/III ratio. Current-Voltage (I-V) barrier height varies from 0.75 eV to 0.98 eV. The ideality factor and leakage current decreases with increase in V/III ratio. Large variation in the slope of the lines of A^2/C^2 vs. V plot was observed. I-V-T measurements revealed that the ideality factor and reverse leakage current increases with temperature confirming that the conduction mechanism is through trap assisted tunnelling process or deep center hopping conduction. The formation of nanoclusters on the surface of Gallium Nitride (GaN) epilayers due to irradiation with 70 MeV Si ions with the fluences of 1x10E10, 1x10E11 and 1x10E12 ions/cm^2 at the liquid nitrogen temperature (77 K) has been discussed. Atomic force microscopy image reveals formation of nanoclusters on the surface of the irradiated samples. As the ion fluence was increased, the RMS roughness also increases from 0.6 nm to 1.1 nm due to the surface modification induced by irradiation. X-ray photoelectron spectroscopy (XPS) studies confirm that the nanoclusters on the surface are composed of GaN. The effect of V/III ratio and swift ion beam induced lattice defects on the nonideal behaviour of GaN schottky diodes and surface morphology respectively were studied and a possible mechanism responsible for the variations has been discussed.

P1.5 Temperature Dependence of Electron Transport Properties in $Al_xGa_{1-x}N/In_yGa_{1-y}N$/GaN Heterostructures: *Jie Song*[1]; Fujun Xu[1]; Zhenlin Miao[1]; Chengcheng Huang[1]; Xinqiang Wang[1]; Zhijian Yang[1]; Bo Shen[1]; [1]Peking University

GaN-based high electron mobility transistors (HEMTs) with the $In_xGa_{1-x}N$ channel are advantageous over those with conventional GaN channels by theoretical calculation due to the smaller electron effective mass and stronger polarization in the $In_xGa_{1-x}N$ channel. The different directions of piezoelectric polarization in $Al_xGa_{1-x}N$ barrier and $In_xGa_{1-x}N$ channel will lead to complex varieties of carrier transport properties with increasing temperature. Thus the study of temperature dependence of carrier transport properties of $In_xGa_{1-x}N$ channel HEMTs is very important. In this study, $Al_xGa_{1-x}N/In_yGa_{1-y}N$/GaN heterostructures were grown on 2-inch (0001) sapphire substrates by means of metal-organic chemical vapor deposition (MOCVD). The Hall mobility and sheet carrier density are determined as 918 cm^2/Vs and 1.1×10^{13} cm^{-2}, respectively, at room temperature. The temperature dependence of carrier transport properties of $Al_{0.25}Ga_{0.75}N/In_{0.03}Ga_{0.97}N$/GaN and $Al_{0.25}Ga_{0.75}N$/GaN heterostructures has been contrastively investigated. It is found that the electron Hall mobility in $Al_{0.25}Ga_{0.75}N/In_{0.03}Ga_{0.97}N$/GaN heterostructures is higher than that in $Al_{0.25}Ga_{0.75}N$/GaN ones at temperatures higher than 250°C even if the mobility in the former is much lower than that in the latter at room temperature. More importantly, the carrier sheet density in $Al_{0.25}Ga_{0.75}N/In_{0.03}Ga_{0.97}N$/GaN heterostructures decreases with increasing temperature above 250°C. This is different entirely from that in $Al_xGa_{1-x}N$/GaN ones, where the carrier sheet density increases with increasing temperature above 250°C. It is believed that a carrier depletion layer is formed at $In_yGa_{1-y}N$/GaN heterointerface due to the antiparallel piezoelectric polarization between $In_yGa_{1-y}N$ channel and $Al_xGa_{1-x}N$ barrier in $Al_xGa_{1-x}N/In_yGa_{1-y}N$/GaN heterostructures, which effectively suppresses the parallel conduction originated from thermal stimulation in underlying i-GaN layer at high temperatures.

P1.6 Defect Reduction of Semi-Polar GaN Grown on Nanoporous GaN Templates Prepared by Photo Enhanced Electrochemical Etching: Dong-Hun Lee[1]; *Ok-Hyun Nam*[1]; Jong-Jin Jang[1]; Bo-Hyun Kong[2]; Hyung-Koun Cho[2]; Jung Hwan Hwang[1]; Kwan Hyun Lee[1]; [1]Korea Polytechnic University; [2]Sungkyunkwan University

Group III-nitride semiconductors have emerged as the materials for growth of light emitting devices. Currently, GaN devices are predominantly grown in the (0001) c-plane orientation. However, in case of using polar substrate, an important physical problem of nitride semiconductors with the wurtzite crystal structure is their spontaneous electrical polarization. For this reason, we introduced semi-polar GaN growth on m-plane sapphire to overcome this problem. However, it is difficult to obtain high quality semi-polar GaN directly grown on sapphire substrate because of very high defect density. We modified the surface of semi-polar GaN by photo-enhanced electrochemical etching to make many nano-sized pores. Si-doped GaN was used as an etching substrate with optimized etching condition and its doping concentration was 3 x1019 cm-3 measured by Hall measurement. Undoped semi-polar GaN was re-grown on porous GaN templates prepared by different etching conditions to investigate the effect of different etched surface morphologies. Surface morphology of re-grown semi-polar GaN on nanoporous GaN template was enhanced by surface modification. Cross-section and plane-view TEM images showed the reduction of threading dislocations and basal stacking faults at the re-grown interface. Photoluminescence and high resolution X-ray diffraction measurements also showed that crystallinity of re-grown GaN was improved by the defect reduction. Experimental details will be discussed at the conference.

P1.7 Growth Mechanism of (11-22) Semi-Polar GaN on m-Sapphire by MOCVD: Jang Jong Jin[1]; Lee Kwan-Hyun[1]; Hwang Jung-Hwan[1]; *Nam Ok-Hyun*[1]; [1]Korea Polytechnic University

III-nitrides have attracted much attention for optoelectronic device applications whose emission wavelengths range from green to ultraviolet light due to their wide band gap. Currently, GaN devices are predominantly grown in the (0001) c-plane orientation. While these devices are the easiest to produce with repeatable results, they are influenced by spontaneous and piezoelectric polarization effects at interfaces within the active layers, decreasing device efficiency and luminescent output due to the quantum confined stark effect (QCSE). Color stability is poor in c-plane light-emitting diodes, where the emission wavelength changes with drive current. The piezoelectric-fields can be reduced by growth of GaN on semi- or nonpolar surface planes. It is expected that nonpolar or semi-polar GaN will lead to an improvement in efficiency of GaN based optoelectronic devices beyond the physical limits of c-plane GaN. In this study, we have investigated the properties of GaN buffer layer with different thickness, from 30 to 90nm and the influence of GaN buffer layer thickness on the (11-22) semi-polar GaN on m-sapphire. Their surface morphologies and crystal properties were studied OM(Optical Microscope), AFM(Atomic Force Microscope), PL(Photoluminescence), DXRD(Double crystal X-ray diffraction). The experiments were carried out in the 3x2” commercial metal-organic chemical vapor deposition (MOCVD) system. The molar flow rates of TMGa and NH3 were kept at 75umol/min and 0.25mol/min, respectively. The buffer layers were all deposited at 1050° to thickness of nominally 30~90nm. AFM study showed various buffer layer morphologies with different growth time on m-plane sapphire. Surface roughness of buffer layer was the lowest value of about 8.3nm, which is probably due to the formation the most uniform nucleation compared with the different buffer layer thickness. DXRC showed that FWHM value perpendicular to m-axis increases with increasing buffer thickness. However, the FWHM value parallel to m-axis decreases with increasing buffer thickness, which indicates that the crystalline quality of the c-plane slightly improves with increasing buffer thickness. Further study is underway to investigate the growth mechanism of semi-polar GaN.

P1.8 Electrical Properties in Cubic GaN Films Grown on GaN Buffer Layers by AP-MOVPE: *Heber Vilchis*[1]; Victor Sánchez[1]; Arturo Escobosa[1]; [1]Centro de Investigación y Estudios Avanzados (CINVESTAV-IPN)

Epitaxial cubic gallium nitrided films were synthesized by atmospheric pressure metalorganic vapor phase epitaxial (AP-MOVPE) on gallium nitride buffer layer obtained by nitridation of gallium arsenide. Even though the GaN buffer present cubic and hexagonal phase the upper film only present cubic phase, this was verified by photoluminescence and HR-XRD measurement and pole diagrams. Hall measurements by Van Der Pauw method indicate that the films have an average density of $5x10^{19}$ cm^{-3} and the mobility of carrier is between 1 and 10 cm^2/Vs at room temperature. This is due to the contribution from the different scattering mechanisms which are analyzed in this work. The resistivity of cubic GaN is in the range from $1.5x10^{-2}$ to $3.4x10^{-3}$ ohm-cm and I-V curves show it is constant in a wide range of voltage from -10 V to 10 V without damage the material. Au, Al, Ti/Au and Ti/Al were deposited by thermal evaporation for obtain Ohmic contacts. The specific contact resistances (ρc) were determined using the linear transfer length method (TLM), for Al $\rho c = 6.3x10^{-2}$ ohm cm^2 improve with Au $\rho c = 7.5x10^{-3}$ ohm cm^2 but the best result is with Ti/Au $\rho c = 2.1x10^{-5}$ ohm cm^2. HR-XRD and pole diagrams results confirm the cubic GaN films are monocrystalline. Photoluminescence, hall and I-V measurements indicate that the cubic GaN films have good electrical properties but is necessary improve them in order to fabricate electrical or optoelectronic devices, also we prove that Ti/Au metallization present a low contact resistance for c-GaN.

P1.9 GaN Quantum Dots in p-AlGaN/GaN Superlatices without Intentional Wetting Layer: *Ding Li*[1]; Rui Li[1]; Lei Li[1]; Lei Wang[1]; Ningyang liu[1]; Lei Liu[1]; Xiaodong Hu[1]; Guoyi Zhang[1]; [1]Peking University

The GaN quantum dots with density of 106 to 109 cm-2 were formed in p- AlGaN/GaN superlatices with Al content increasing from 0.1 to 0.3 without intentional wetting layer by MOCVD growth. They are 40 nm in width and 1.4 nm in height confirmed by AFM measurement at the surface and Resonant Raman Scattering in Optics. The strain distributions were analyzed both reciprocal space mapping and grazing incidence diffraction by X-ray diffraction. The strain from the AlN interlayer between the superlattices and undoped GaN were the main cause for the formation of GaN quantum dot with the assistance of Mg doping.

P1.10 Nitride Compounds of InGaN Grown by SMI H-MOVPE: Shangzhu Sun[1]; L. Provost[1]; Gary Tompa[1]; *Bruce Willner*[1]; [1]Structured Materials Industries, Inc.

InGaN is one of the key compound semiconductor materials used for the fabrication of GaN-based blue, green, white LEDs and blue laser diodes. Most of the existing LEDs reply on MOCVD to produce the quantum well structures for the InGaN emitters [1, 2, 3]. In order to grow high quality InGaN-based active layers, a low InGaN growth temperature (<750°C) is required due to its low thermal stability relative to the GaN material. However, at low growth temperature in the MOCVD system, the amount of reactive nitrogen available for growth from NH3 is very low and indium droplet formation can occur. Therefore, a very high NH3 partial pressure is required to avoid nucleation of indium liquid on the surface. However, using high NH3 is not only costly, but also increases H2 by product from NH3 decomposition. The H2 can reverse the InGaN deposition reaction, which will reduce the growth rate and material quality. SMI has modified its rotating disc reactor system to operate with both metal-HCl and metal-organic/HCL precursors [4]. Our Hydride-Metal Organic Vapor Phase Epitaxy (H-MOVPE) system has been used to deposit the nitride compounds in the same reactor chamber. In this work, we will describe the H-MOVPE system and report on initial growths of InGaN layers at low growth temperature and low V/III ratio. Also the effects of HCl/TMIn+TMGa ratio and growth temperature on growth rate are presented.

P1.11 MOCVD Growth and the Transport Properties of Lattice-Matched In0.18Al0.82N/GaN Heterostructures with the AlN Interlayer: *Zhenlin Miao*[1]; Fujun Xu[1]; Ning Tang[1]; Tongjun Yu[1]; Jie Song[1]; Chengcheng Huang[1]; Xinqiang Wang[1]; Zhijian Yang[1]; Bo Shen[1]; [1]Peking University

Recently, InxAl1-xN/GaN heterostructures are attracting more and more attentions because it can be lattice matched to GaN at x~0.18 which would eliminate the device reliability issues related to the strain in AlxGa1-xN/GaN heterostructures. Furthermore, owing to the large spontaneous polarization difference between InxAl1-xN and GaN layers, lattice-matched InxAl1-xN/GaN heterostructures exhibit a high two dimensional electron gas (2DEG) density of the order of 2.0×1013cm-2, which is higher than that of conventional AlxGa1-xN/GaN ones, and can realize the devices with higher power density. In this study, an In0.18Al0.82N/GaN heterostructure with the AlN interlayer were grown on 2-inch (0001) sapphire substrates by means of low-pressure metal-organic chemical vapor deposition (MOCVD). After GaN layer grown by the conventional two-step growth methods with H2 as carrier gas, In0.18Al0.82N layer was grown at lower temperature with N2 as carrier gas. The thickness of the AlN interlayer is found playing an important role in the transport properties of the 2DEG. By optimizing the thickness of the AlN interlayer, the heterostructures with the 2DEG mobility and density of 1230 cm2/Vs and 2.2×1013 cm-2, respectively, at room temperature have been obtained. Furthermore, the magnetotransport properties of lattice-matched In0.18Al0.82N/GaN heterostructures were investigated by means of magnetoresistance measurements at low temperatures and high magnetic fields. Strong Shubnikov–de Haas (SdH) oscillations with the double periodicity are observed clearly. The 2DEG density at the first and the second subbands are determined as 1.9×1013 cm-2 and 1.7×1012 cm-2, respectively. The energy distance between two subbands is determined to be 188 meV. These results imply that the triangular quantum is much deeper in lattice-matched In0.18Al0.82N/GaN heterostructures than AlxGa1-xN/GaN ones and the 2DEG is distributed more close to the heterointerface. As a result, the interface roughness scattering is very strong in InxAl1-xN/GaN heterostructures. It is except to further improve the transport properties by increasing the interface quality.

P1.12 Growth and Characterization of GaN Layer Using InN Interlayer and Sapphire Substrate: *Keon-Hun Lee*[1]; Sung Hyun Park[1]; Jong Hack Kim[1]; Nam Hyuk Kim[1]; Min Hwa Kim[1]; Hyunseok Na[2]; Yasushi Nanishi[3]; Euijoon Yoon[4]; [1]Seoul National University; [2]Dajin University; [3]Seoul National University (WCU program), Ritsumeikan University; [4]Seoul National University (WCU program, MSE)

GaN layer grown on sapphire substrate contains considerable strain because of difference in lattice constants and thermal expansion coefficients. Owing to the large difference between conventional growth temperature of GaN layer over 1000°C and room temperature, strain (~10^{-4}) is applied to the GaN layer on sapphire substrates, which causes wafer bowing. It is generally known that the amount of wafer bowing is 20~30 micro meter when using 2 inch sapphire substrates. We grew InN interlayer between GaN layer and sapphire substrate. It is expected that InN interlayer is decomposed to metallic indium or indium-containing phases during high temperature (HT) GaN growth, which will eventually help relax the residual thermal strain in GaN layer. InN layer was grown on 2 micro meter thick sapphire c-plane using a metal-organic vapor deposition (MOCVD) system. Trimethylindium (TMIn), Trimethylgallium (TMGa) and ammonia were used as indium, gallium and nitrogen sources, respectively. InN layers with various thickness (10~100 nm) was grown on c-plane sapphire substrate. Then, low temperature (LT) GaN layer was grown on InN layer to protect InN layer from direct exposure to hydrogen flow during HT GaN growth and/or violent decomposition during temperature ramp-up before HT GaN growth. Thick HT GaN layer (a few micro meter thick) was continuously grown on LT GaN/InN/sapphire template. GaN, InN and sapphire related peaks were detected by X-ray diffraction measurement. Strong GaN (002) and sapphire (006) peaks were observed at 34.5 and 41.7°, respectively. InN and metallic indium signals were below the detection level. Microstructure of the epilayer-substrate interface was investigated by transmission electron microscopy (TEM). From the cross sectional high angle annular dark field TEM image, the growth of columnar structured LT GaN was observed. Growth of HT GaN layer on LT GaN layer with good crystallinity was also confirmed. The decomposition of InN layer and diffusion process of indium atoms were analyzed using secondary ion mass spectrometry. The relaxation of compressive strain in GaN layer was analyzed by photoluminescence and Raman measurement.

P1.13 Low Dislocation Densities GaN Epi-Layer on Nano-Scale Patterned Si(001) Substrate: *Chieh-Chih Huang*[1]; C. H. Kuo[2]; S. J. Chang[1]; C. H. Ko[3]; Clement H. Wann[3]; Y. C. Cheng[4]; W. J. Lin[4]; S. P. Chang[1]; [1]Institute of Microelectronics and Department of Electrical Engineering, Center for Micro/Nano Science and Technology, Advanced Optoelectronic Technology Center, National Cheng Kung University; [2]Department of Optics and Photonics, National Central University; [3]Taiwan Semiconductor Manufacturing Company; [4]Materials and Electro-Optics Research Division, Chung Shan Institute of Science and Technology

We report the growth of high quality GaN epi-layer on Si(001) nano- patterned substrate, which was 40nm strip patterns along <100> facet. It was found that the epi-layer prepared on nano-patterned Si(001) substrate exhibits stronger hexagonal phase. It was also found that threading dislocation observed from GaN prepared on 40nm patterned Si(001) substrate was significantly decreased. Furthermore, it was found that we can get almost strain release GaN epitaxial layer using the 40nm patterned Si(001) substrate.

P1.14 Evolution and Control of Dislocations in GaN Grown on Patterned Sapphire Substrate by Metal Organic Vapor Phase Epitaxy: *Yue Bin Tao*[1]; Tong Jun Yu[1]; Zhi Yuan Yang[1]; Ding Li[1]; Chuan Yu Jia[1]; Zhi Zhong Chen[1]; Xiang Ning Kang[1]; Zhi Jian Yang[1]; Guo Yi Zhang[1]; [1]Peking University

In this paper, GaN epi-layers grown on commercially available Patterned sapphire substrate (PSS) by Metal Organic Vapor Phase Epitaxy in a Thomas Swang reactor were investigated. The pattern of the sapphire substrate is cone-shaped bump with 1.9 µm height, 3.0 µm diameter at bottom and approximate 1µm interval. All wafers were grown by three stages: (a) initial stage of 20nm buffer layer, (b) middle stage of 2µm un-doped GaN layer and (c) finial stage of 1.5µm un-doped GaN layer. The growth conditions in the initial stages are the same for epi-layers. The growth temperature and pressure during the middle and final growth stages were changed to control the dislocation behavior. Voltage dependence of monochromatic cathodoluminescence (CL) was applied to investigate the dislocation behavior. Less amount of dislocations were observed in CL images, when the penetration depth of electron became shorter by changing the accelerating voltage from 30kv to 5kv. Further, it was shown that many dislocations were generated on the top of the cone-shape region, interval region and the coalescence region, while there was almost no TD in the slope region of the cone-shaped bump. It is well known that the dislocations would bend in the process of the island-island coalescence or disappear at the interface of layer. We tried to control the behaviors of dislocations by varying the lateral rate and vertical rate at different stages of GaN growth. When the growth pressure was changed from 200 torr to 100 torr during the final stage, the less dislocations were observed in CL images and the full width at half maximum (FWHM) s for (002) and (102) planes in X ray diffraction (XRD) curves decreased to 203 and 228 arcsec from 260 and 312 arcsec, respectively. Furthermore, when the growth temperature was decreased from 1040°C to 1000°C during middle stage, the dislocation distribution was obviously changed. The dislocation in the interval regions of patterns disappeared. The atomic force microscope (AFM) and photoluminescence (PL) measurements were also performed to assess the material quality. From the micro analysis, the process of dislocations' evolution was deduced.

P1.15 The Optical Properties and Morphology of Selective Area Growth of GaN on R-Plane Sapphire: *Bong Kyun Kang*[1]; Sam Mook Kang[1]; Keun Man Song[1]; Dae Ho Yoon[1]; [1]Sungkyunkwan University

III-nitride based semiconductors have attracted as the high performance light emitting devices, solar-blind ultraviolet detectors, and high power, high temperature devices. In case of high performance light emitting devices, commercially InGaN/GaN multi quantum wells (MQWs) on the c-plane polar GaN is grown by using (0001) sapphire substrates. However, the grown c-orientation of GaN on hetero-substrates has strong electric field due to internal piezoelectric polarization, which lead to reduce the internal quantum efficiency due to obstacle recombination and spatial separation of electron and hole wavelength. The non-polar GaNs such as m-plane or a-plane have been fabricated to eliminate these polarization effects. As grown GaN on hetero-substrate, the high density of threading dislocation (TD) and misfit dislocation happen in GaN film. The selective area growth technique (SAG), epitaxial lateral overgrowth (ELOG) can be use to prevent from propagating and inducing TDs and misfit dislocations. In case of SAG technique, the changing pattern of mask can fabricate truncated pyramidal, pyramidal stripes structure without etching methods at Si (111) and sapphire (0001). Thus, device and structure which don't exist damage by dry etching can be made and improved quality of crystallinity and optical property. In this study, We observed the a-plane GaN by SAG. The GaN structures on the r-plane sapphire are fabricated by metal organic vapor deposition (MOCVD). The characteristics of non-polar GaN structures were investigated by field emission scanning electron microscopy (FE-SEM), X-ray diffraction (XRD), cathodo luminescence (CL) and transmission electron microscopy (TEM). We observed morphology, crystallinity and optical property from these analysis methods.

P1.16 Study of MOCVD Growth of InGaAsSb/AlGaAsSb/GaSb Heterostructures Using Two Different Aluminium Precursors TMAl and DMEAAl: *Marek Wesolowski*[1]; Wlodek Strupinski[1]; Marcin Motyka[2]; Grzegorz Sek[2]; Ewa Dumiszewska[1]; Piotr Caban[1]; [1]ITME; [2]Wroclaw Institute of Technology

The antimonide laser heterostructures growth technology using MBE epitaxy is currently well-developed, while MOVPE method is still being improved. It is known that the crucial issue is oxygen contamination of aluminium containing waveguides and claddings. The solution would be the preparation of proper aluminum precursor. In the study we present the results of metal-organic epitaxy of In- and Al-containing layers and quantum well structures composing antimonide lasers devices. Special emphasis was put on aluminum precursor and its relation to AlGaSb and AlGaAsSb materials. We optimised the GaSb substrate thermal treatment to obtain high quality GaSb homoepitaxial layers. The crystalline quality of layers grown with different Al precursors were compared and very good structural quality films were obtained. These materials in particular exhibited very high sensitivity to V/III ratio and also to the growth temperature. The results suggested substantial influence of precursors pre-reactions on the epitaxial process. Oxygen contamination was resolved by SIMS, which confirmed its dependence on the precursor choice. Process parameters relation to the oxygen level was examined. Good quality InGaAsSb layers were obtained even within the predicted miscibility gap, when arsenic content reached highly above 10% values. InGa(As)Sb/AlGa(As)Sb quantum wells were grown and their optical properties were characterised by photoluminescence and photoreflectance spectroscopy. Type-I quantum wells showed a fundamental optical transition in 1.9 – 2.1micr range in room temperature. The epitaxial technology of the structures was subject to an optimisation procedure. The quality and parameters of particular layers and heterostructures were analysed to predict their functionality in laser devices.

P1.17 Surface Morphology of InGaAsN Epilayer Lattice-Matched to GaAs Substrates Grown by MOVPE: *Wu Tzung-Han*[1]; Yan-Kuin Su[1]; Yu-Jen Wang[1]; [1]Institute of Microelectronics and Advanced Optoelectronic Technology Center, National Cheng Kung University

In the recent years,InGaP/GaAs/ InGaAsN/Ge (1.8/ 1.42/ ~1/ 0.7eV) heterostructures have attracted much attention. With a 1.0 eV InGaAsN subcell, the efficiency of tandem solar cell would exceed a further growth. Due to the different crystal structures such as zinc-blende structure or wurtzite structure, there exists a miscibility gap with phase separation in (In)GaAs and GaN; It is a challenge to grow high quality InGaAsN film with high nitrogen incorporation lattice-matched to GaAs substrate. To achieve 1eV band gap energy of InGaAsN material, the In content and N content are confirm in 8% and 3% separately. In this study, we have grown InGaAsN films in various growth conditions by AIX200 metalorganic chemical vapor phase epitaxy (MOVPE) using trimethylgallium (TMGa), tertiarybutylarsine (TBAs), dimethylhydrazine (DMHy), and trimethylindium (TMIn). At first we fixed the flow rates of TMIn, TBAs and TMGa to keep the In content, then, we grew InGaAsN layers with different DMHy/V ratios at the growth temperature 600°C, 575°C, and 550°C individually; we distinguished the lattice-matching from the peak splitting in x-ray diffraction results. In this work, we grew the InGaAsN film lattice-matched ($\Delta a/a < 800$ ppm) to GaAs substrates successfully. The AFM results reveal the surface morphology of InGaAs and InGaAsN film grown on GaAs substrates, and the surface roughness of InGaAsN got smaller in lower growth temperature. The morphology of InGaAsN surface is strongly associated with growth temperature and N content. The morphology with a root mean square (rms) roughness as low as 0.284 nm over 3×3μm was achieved from the growth temperature 550°C and DMHy/V ratio 0.95.

P1.18 The Importance of Low-Angle Misorientation on the Optical Properties of InGaAs/AlInAs Quantum Wells: Robert Young[1]; *Lorenzo Mereni*[1]; Nikolay Petkov[1]; Gabrielle Knight[1]; Valeria Dimastrodonato[1]; Paul Hurley[1]; Greg Hughes[1]; Emanuele Pelucchi[1]; [1]Tyndall National Institute

Recent MOVPE growth studies on the (Al)GaAs/GaAs material system have shown that small misorientations in the range 0 to 0.6° on the GaAs substrate have a dramatic impact on the optical and transport properties of the grown layers[1], allowing record MOVPE-grown material properties to be achieved. In this work we investigate whether a similar dependence is present in the InP-lattice matched InGaAs/InAlAs materials system, which is of tremendous importance to the optoelectronics industry. A structure containing three InGaAs/InAlAs quantum wells, with nominal widths of 2, 5 and 15nm, was grown on a series of InP substrates with misorientations from (100) towards the (111)A planes ranging from 0° to 0.6°. The neutral exciton linewidth of photoluminescence (PL) at low temperature was used as a figure of merit to initially optimise the growth conditions and finally to comparatively assess the quality of the quantum wells. We found that this procedure for growth optimisation lead to a reduction in PL linewidth by a factor of >2 and that quantum wells grown on wafers offcut by 0.4° consistently gave the narrowest peaks, with the optimal linewidth of just 4.25 meV found from a 15nm quantum well. This is the smallest value yet to be reported in this material system. We proceed to examine the surface morphology of the grown structures by atomic force microscopy (AFM). The optimal low-angle misorientation of 0.4° is found to coincide with the transition from step-flow to heavy step-bunching, a result which is consistent with the previous growth study of GaAs quantum wells[1]. [1] E. Pelucchi, N. Moret, B. Dwir, D. Y. Oberli, A. Rudra, N. Gogneau, A. Kumar, E. Kapon, E. Levy, A. Palevski, J. Appl. Phys. 99 (2006) 093515.

P1.19 Tellurium Doping of InGaP for Tunnel Junctions in Triple Junction Solar Cells: *Chris Ebert*[1]; Z. Pulwin[1]; D. Byrnes[1]; A. Paranjpe[1]; W. Zhang[1]; [1]Veeco Turbodisc

Triple junction solar cells (TJSC) offer the highest efficiency devices for space and terrestrial applications today with MOCVD material growth optimized for best device performance. In particular, tunnel junction interconnects in the monolithically grown solar cell on germanium need to be optimized for best electrical and optical characteristics. InGaP doped with tellurium offers excellent material characteristics for the n side of the tunnel junction between the middle and top cell of the TJSC device. Unfortunately, tellurium is a difficult dopant to incorporate in InGaP [1] and the large compressive strain in the InGaP due to the large atomic size of Te leads to poor surface morphology. For an adequate tunnel junction, a sharp dopant profile with high carrier concentration (≥1E19/cm^3) is required in a 200 to 300 Angstrom thick layer to minimize series resistance and maximize tunneling current. Here we report on a series of designed experiments (DOE) utilizing MOCVD growth parameters such as growth temperature, V/III ratio, TMIn/TMGa molar ratio, plus an evaluation of pre-growth tellurium delta doping to improve dopant incorporation. InGaP material parameters were optimized based on Hall tests, x-ray, AFM, and surface morphology. SIMS data was also evaluated to understand dopant profiles for the InGaP layer. High quality Te:InGaP with carrier concentrations (≥1E19/cm^3) are acheived with excellent surface morphology and sharp dopant profile at a growth temperature of 580°C,V/III inlet ratio of 7.5,TMIn/TMGa molar flow ratio of 0.77. These growth conditions provide AFM rms surface roughness of 4 Angstroms and x-ray strain of 0.15%. SIMS measurement of tellurium in InGaP show a sharp dopant profile but require a pre-growth delta doping step and a post growth pause with elevated temperature. Results from these tests establish process conditions for MOCVD growth of high quality Te:InGaP tunnel junctions in TJSC materials. [1] I. Garcia, et.al., J Crystal Growth 298 (2007) 794-799.

P1.20 InAs Quantum Dot Growth on Planar InP (100) by Metal Organic Vapor Phase Epitaxy with a Thin GaAs Interlayer: Jiayue Yuan[1]; *Hao Wang*[1]; Peter J. Veldhoven[1]; Richard Nötzel[1]; [1]Eindhoven University of Technology

InAs quantum dots (QDs) were grown on planar InP (100) by metal organic vapor phase epitaxy (MOVPE) with a thin GaAs interlayer beneath the QDs. With increasing GaAs interlayer thickness the QD size reduces and the photoluminescence (PL) intensity increases, before it decreases. It increases 2.7 times for 2 ML GaAs and 2 times for 3 ML GaAs as compared with 1ML GaAs, and the PL peak blueshifts from 1750 nm (1 ML GaAs) to 1700 nm (2 and 3 ML GaAs), accompanied with QD density decrease. This reveals suppression of A/P exchange during InAs growth by the GaAs interlayer, previously shown on InGaAsP, resulting in better QD quality, before it drops for too large GaAs thickness, i.e., tensile strain. With increasing growth temperature from 490° to 500° and to 515°, for 1 ML GaAs, the PL peak redshifts from 1765 nm to 1800 nm and to 1780 nm with similar PL intensity, indicating increasing As/P exchange, resulting in the bigger QDs, and the onset of As/P intermixing. For decreasing TBA supply from 3 sccm to 1 sccm and to 0.5 sccm, and 1 ML GaAs, the QD PL peak blueshifts from 1765 nm to 1603 nm and to 1443 nm with PL intensity drop to 80% for 1 sccm TBA supply and 24% for 0.5 sccm TBA supply as compared with 3 sccm TBA supply, showing decreased QD quality at low TBA supply. Finally, the PL intensity increases 1.4 times for 180 sccm TMI supply (1.8 ML InAs) as compared with 200 sccm TMI supply (2 ML InAs), for TBA supply of 3 sccm and 1 ML GaAs, confirming better QD quality for larger group V/III ratio. Hence, high quality InAs QDs on InP (100) are achieved with wide wavelength range and emission at 1.55 µm with 1.5 sccm TBA supply, 2 ML GaAs, and 180 sccm TMI supply.

P1.21 High Growth Rate of InGaAs and InGaP Materials for Triple Junction Solar Cells: *Wei Zhang*[1]; Chris Ebert[1]; Devon Dyer[1]; Ziggy Pulwin[1]; Dong Lee[1]; Ajit Paranjpe[1]; [1]Veeco

High throughput is important to reduce the MOCVD production cost of triple junction solar cells (TJSC) in the application of concentrated photovoltaic systems (CPV) and to keep it competitive compared with other PV technologies. InGaAs and InGaP that are lattice-matched to Ge substrate are the main component layers of the TJSC structure and their growth rates mostly determine the throughput. Proper design of the MOCVD reactor is key to prevent the gas phase pre-reaction, which would limit the growth rates of these materials. Here we show high growth rates of InGaAs and InGaP with excellent material quality can be achieved in large scale MOCVD reactors. InGaAs nucleation on Ge with a growth rate of 20 µm/hr was obtained with excellent X-ray and low haze after InGaAs layer strain was optimized. To further explore the growth rate range, the dependence of the growth rate of GaAs on TMGa flow rates was investigated and growth rates as high as 25 µm/hr was obtained. No growth rate “roll off” or decrease was observed with the increased TMGa flow and instead a linear dependence is obtained as measured by in-situ monitoring and feedback control of the OM source concentration. It’s shown that TMGa concentration actually dropped at very high flow rate but was compensated with in-situ feedback control, which is important to the precise control of composition at such very high growth rate. High quality InGaP with a growth rate as high as 4.1 µm/hr was grown at 640°C. Excellent material quality and uniformity was shown with the results from microscopy, X-ray and photoluminescence. High growth rate of V/III materials with excellent material quality continue to improve throughput of MOCVD production of TJSC materials.

P1.22 Growth and Characterization of Heavily Selenium Doped GaAs Using MOVPE: *Andre Maaßdorf*[1]; Marc Hoffmann[1]; Marcus Weyers[1]; [1]Ferdinand-Braun-Institut

Heavily n-type doped GaAs is particularly of interest for the realization of tunnel junction diodes. Unlike p-type doping in GaAs:C, where doping concentrations up to 10^{20} cm^{-3} can be achieved, n-type doping in GaAs is limited well below 10^{19} cm^{-3}. However, using silicon for n-type doping in GaAs is particularly limited to doping concentrations of $4x10^{18}$ cm^{-3} due to the solubility limit, which is caused by the amphoteric incorporation behavior of silicon in GaAs. This work is thus focused on n-type doping in GaAs using selenium alternatively. Our investigations are based on single layer GaAs:Se samples, grown on s.i.-GaAs substrates. Epitaxy was done in a 5x4” planetary MOVPE reactor (AIX2400G3). Thermal annealing of selected samples was carried out separately in this machine also, under As-rich conditions at 730°C. The standard precursors TMGa, AsH_3 and Si_2H_6 as well as ditertiary-butylselenide (DTSe) as selenium source where used. The samples were characterized using LT-PL, XRD-, SIMS- and Hall-measurements. We started our investigations by focusing on a series of samples with varying DTSe partial pressure (p_{DTSe}). Comparing SIMS and Hall data of these samples shows almost complete donor activation up to selenium concentrations of $8x10^{18}$ cm^{-3}. When increasing p_{DTSe} further the electrical donor activation drops continuously. Based on 10K-PL measurements we studied several samples near the activation drop. Several below gap emission peaks could be observed, some of which are known and are supposedly related to the formation of gallium vacancies as well as vacancy complexes. While as-grown samples appear to be compressively strained according to our XRD measurements, the strain is slightly reduced after annealing, but remains compressive. Comparing the covalent atomic radii of gallium and arsenic with selenium one would expect the strain to be tensile instead. We therefore assume the compressive strain to be caused by selenium being incorporated as interstitial at selenium concentrations above $8x10^{18}$ cm^{-3}. Furthermore we observed a donor-acceptor-pair transition (DAP) in the PL spectra of samples after annealing with an atomic selenium concentration of almost 10^{20} cm^{-3}. The nature of this DAP remains unclear up to now and is subject to further investigations.

P1.23 Cadmium Doping of InAs and InAsSb Epilayers: *Viera Wagener*[1]; Magnus Wagener[1]; Reinhardt Botha[1]; [1]Nelson Mandela Metropolitan University

The interest in InAs and InAsSb materials is driven by the need for devices operating in the near-infrared range of the electromagnetic spectrum. In recent years, molecular-beam epitaxial growth has been the technique of choice for the deposition of these materials as high quality layers have been achieved. In this paper, atmospheric pressure metalorganic vapour phase epitaxy is used to produce undoped and cadmium-doped epitaxial InAs and InAsSb epilayers. Trimethylindium, tertiarybutylarsine, trimethylanitomony and dimethylcadmium are used as precursors. In order to facilitate electrical and optical measurements, the growth is performed on both GaAs (semi-insulating) and InAs substrates misoriented by 2º from (001) towards (111)B. It is well know that electrical measurements of InAs are complicated by a surface electron accumulation layer. This has prevented earlier attempts in measuring the true doping concentration of p-type thin films. Recent work by Wagener et al. [1], however, demonstrated the accurate determination of the transport properties of p-type InAs by means of temperature dependent thermoelectric measurements. Despite the large lattice mismatch to GaAs (~7%), we have achieved high material quality for undoped InAs (300K mobility > 10,000 cm2/V.s) using a low temperature buffer layer. Although p-type material is traditionally attained by zinc doping, the high diffusivity of Zn is known to influence device characteristics. Voronina et al. [2] have achieved p-type conduction using Mg as a dopant. Despite changing the Mg mole fraction by a few orders of magnitude, p-type conduction was only measured for layers with carrier concentration exceeding 1E18 /cm3. In this work, Cd-doping of InAs and InAsSb is investigated. The cadmium doping properties, e.g. the incorporation efficiency has been studied for epilayers deposited using various growth parameters, such as the growth temperature, V/III ratio, etc. To our knowledge, this is the first report of p-type doping of thin film InAs across a large range of concentrations, from as low as 2E15 /cm3, up to 1E18 /cm3. [1]M. C. Wagener, V. Wagener, and J.R. Botha, Appl. Phys. Lett. 94 (2009)262106. [2]T. I. Voronina, T.S. Lagunova, S.S. Kizhayev, S.S. Molchanov, B.V. Pushnyi and Yu. P.Yakovlev, Semiconductors 38 (2004) 537.

P1.24 Design and Simulation of a Multi-Showerhead MOVPE Reactor: *Ran Zuo*[1]; Jingsheng Chen[1]; Haiqun Yu[1]; [1]Jiangsu University

With the requirement of mass production for LED epitaxial wafers, there is an urgent need for the enlargement of MOVPE reactors that can produce multi-wafers and wafers of larger area. Current MOVPE reactors can not be simply scaled-up with traditional design, since with susceptor diameter increasing, both the flow path and gas residence time will increase. Consequently, the problems of reactant depletion along the flow path, the non-uniformity of gas concentration from reactor center to edge, the flow non-stability at the outer edge, and the parasitic gas phase reaction will all become worse. In order to solve the problems in traditional design, a novel multi-showerhead MOVPE reactor is designed. In this reactor both the inlet and outlet are located on top of the chamber and the multiple showerheads are aligned above the susceptor with a nozzle attached to each showerhead, each facing to a substrate wafer. The reactants are sprayed to the wafer from the multi-showerhead above the substrate to form the stagnation flow, and the exhaust gas flows upwards around each showerhead to the top outlet. Under each showerhead, the growth condition for each wafer is almost the same, no longer depends on the susceptor radius. Thus the uniformity of the film growth can be greatly improved without the susceptor rotation. For the new reactor design, a numerical simulation for GaN MOVPE growth was conducted, including radiation effect and major gas phase and surface chemical reactions. The velocity, temperature and concentration fields, the growth rate along the radial direction, and the parasitic deposition on the walls are all predicted. The effects of reactor geometry on the uniformity of the film growth are especially studied, and the optimized reactor design is proposed.

P1.25 Influence of Strain Reducing Layer Type on Electroluminescence and Photoluminescence of InAs/GaAs QD Structures: Alice Hospodková[1]; Jirí Pangrác[1]; Jirí Oswald[1]; Pavel Hazdra[2]; Karla Kuldová[1]; Jan Vyskocil[1]; *Eduard Hulicius*[1]; Tomislav Šimecek[1]; [1]Institute of Physics CAS; [2]Czech Technical University, Faculty of Electrical Engineering

InAs/GaAs QDs are promising structures for active region of telecommunication lasers. The QD luminescence wavelength can be redshifted by introduction of $In_xGa_{1-x}As$ or $GaAs_{1-y}Sb_y$ strain reducing layer (SRL) covering QDs [1]. While MBE prepared QDs are already used in laser structures [2], MOVPE prepared QD devices exhibit considerable blue shift of electroluminescence (EL) maximum or lasing wavelength in comparison to their photoluminescence (PL) position. PIN QD structures were prepared by low pressure MOVPE in a RAS LayTec equipped AIXTRON 200 machine, using Stranski–Krastanow growth mode on n-type Si doped GaAs (for EL) and SI GaAs (for PL) substrates. TMGa, TEGa, TMIn, AsH_3,TBA and TESb were used as precursors for the growth of GaAs, InAs, $GaAs_{1-y}Sb_y$ and $In_xGa_{1-x}As$ layers. The first GaAs buffer layer was grown at 650 °C then the temperature was decreased to 490°C for the growth of the GaAs second buffer layer; InAs QD layer; undoped thin $In_xGa_{1-x}As$ or $GaAs_{1-y}Sb_y$ SRL and 5 nm GaAs capping layer; then the temperature was increased to 650°C for the growth of the the rest of the structure: undoped GaAs ; p type C doped GaAs; p^+ type C doped GaAs layers. We present the structure with negligible shift between PL and EL maxima. InGaAs and GaAsSb SRLs were used to shift the luminescence maximum towards telecommunication wavelengths 1.3 or 1.55 µm. EL results of QD structures with both types of strain reducing layers will be presented and compared with their PL properties. We will focus on the shift of EL maxima. Comparison of luminescence from higher excited state for samples with InGaAs, GaAsSb or without any SRL will be discussed. [1] A. Hospodková, E. Hulicius, J. Pangrác, J. Oswald, J. Vyskocil, K. Kuldová, T. Šimecek, P. Hazdra, O. Caha, J. Crystal Growth (2009) doi:10.1016/j.jcrysgro.2009.10.057. [2] D. Bimberg, N.N. Ledentsov, J. Phys. Condens. Matter. 15 (2003) R1063.

P1.26 InAs/GaAs QD Capping in Kinetically or Diffusion Limited Growth Regime: *Alice Hospodková*[1]; Jirí Pangrác[1]; Jan Vyskocil[1]; Jirí Oswald[1]; Pavel Hazdra[2]; Karla Kuldová[1]; Eduard Hulicius[1]; Ondrej Caha[3]; [1]IOP ASCR; [2]FEE CTU; [3]ICMP MU

InAs/GaAs QD properties can be significantly influenced by the growth condition of QD capping layers. InAs/GaAs QD structures have to be prepared and capped at temperatures near 500 °C. At these temperatures the cracing efficiency of standard MOVPE precursors (arsin and TMGa) is poor. This changes the diffusion limited to kinetically limited growth regime for higher TMGa concentration, when the epitaxial surface is covered by methyl groups [1]. At kinetically limited growth regime the growth rate dependence on concentration of group III metalorganics in the reactor is sublinear due to their incomplete decomposition . The characteristic surface reconstruction can be recognized by RAS spectra [2]. When QDs are capped by strain reducing InGaAs layer, the composition and thickness of ternary layer can be considerably changed under kinetically limited growth [1]. We will discuss how both types of growth regime can influence QD photoluminescence properties. QD structures were prepared by low pressure MOVPE in a RAS LayTec equipped AIXTRON 200 machine, using Stranski–Krastanow growth mode on SI GaAs substrates. TMGa or TEGa, TMIn, and AsH_3 or TBA were used as precursors for the growth of GaAs, InAs, and $In_xGa_{1-x}As$ layers. The first GaAs buffer layer was grown at 650°C then the temperature was decreased to 490°C for the growth of the main part of the structure: second GaAs buffer layer, InAs QD layer, thin $In_xGa_{1-x}As$ strain reducing layer (in some structures) and capping layer. The growth regime of the capping process was changed by TMGa or arsine reactor concentration and by the type of precursors, the growth temperature was held constant. RAS spectra were used to distinguish the growth regime; time resolved RAS was used for the GaAs growth rate determination. X-ray diffraction was used for the determination of the ternary layer composition and x-ray reflection for layer thickness measurement. [1] G. Saint-Girons, I. Sagnes, G. Patriarche, Phys. Rev. B 73 (2006) 045308. [2] M Pristovsek, M. Zorn, M. Weyers, Journal of Cryst. Growth, 262 (2004) 78.

P1.27 On the Luminescence of Au-Catalyst Grown GaAs-AlGaAs Core-Shell Nanowires and Its Dependence on MOVPE Conditions: *Paola Prete*[1]; Ilio Miccoli[2]; Fabio Marzo[2]; Nico Lovergine[2]; Giancarlo Salviati[3]; Laura Lazzarini[3]; [1]IMM-CNR; [2]Università del Salento; [3]IMEM-CNR

The luminescence of free-standing GaAs/AlGaAs core-shell nanowires grown by Au-catalyzed MOVPE on (111)B-GaAs is reported, using trimethylgallium, trimethylaluminium (TMAl), and tertiarybutylarsine (TBAs) as precursors, and colloidal Au nanoparticles as catalysts. (111)B-aligned and kink-free GaAs nanowires were grown between 400°C and 440°C, with average diameters in the 50÷70 nm range and lengths up to ~10 µm. AlGaAs shells with thickness in the 70÷160 nm interval were overgrown at a temperature in the 650°C-700°C range by conventional MOVPE. Also, the precursors V:III molar ratio in the vapor was varied between 4:1 and 30:1 by changing the molar flow rate of TBAs. The Al composition in the shell was measured by energy dispersion X-ray spectroscopy analyses performed on single core-shell nanowires in a transmission electron microscope operated in Z-contrast imaging mode, and turned out to be $x_{Al}=0.32$; a higher carbon signal was also detected within the nanowire core than in the shell, ascribed to increased carbon segregation during VLS growth. Photoluminescence (PL) spectra recorded from dense (10^8-10^9 nanowire/cm^{-2}) arrays of core-shell nanowires showed that the GaAs core emission is dominated by a broad band in the 1.49-1.51 eV range. Previous high resolution cathodoluminescence measurements performed on single core-shell nanowires demonstrated that the GaAs core emissions shift in energy (within few tens of meV) with respect to each others [1], an effect ascribed to a varying built-in electric field at the core–shell hetero-interface. Decreasing the precursor V:III ratio from 30:1 to 4:1 during AlGaAs shell growth alone also leads to broadening and red-shift of the GaAs emission, demonstrating that such energy shift is an interface-driven effect, and further ascribable to the build-up of a space-charge induced electric field at the core-shell hetero-interface. The latter effect is explained as due to the electrical compensation of unintentional impurities on either sides of the hetero-interface, namely C in GaAs and Si in AlGaAs, the latter ascribed to background contamination in TMAl. Study of the nanowire PL emission as function of VLS temperature further allowed to investigate C incorporation during Au-catalyzed self-assembly. [1] P. Prete et al., J. Cryst. Growth 310 (2008) 5114.

P1.28 Au-Catalyzed MOVPE Growth of Vertically-Aligned GaAs Nanowires on GaAs/(111)Si Hetero-Substrates: Ilio Miccoli[1]; *Nico Lovergine*[1]; Paola Prete[2]; [1]Università del Salento; [2]IMM-CNR

The growth of III-V nanowires on Si could pave the way to the direct integration of the high-electron mobility and optically active III-V materials with well established Si microelectronic technology. Perspective NW-based nano-devices (such as nano-scale LEDs, LASERs, FETs, and solar cells) require the controlled heteroepitaxial growth of III-V nanowires on Si. Recent studies have shown that vertically-aligned GaAs nanowires on (111)Si substrate are difficult to obtain with high yield, while growth along (111)-equivalent or even undefined directions is commonly observed. We report on the MOVPE growth and characterization of GaAs nanowires on hetero-structured substrate, the latter composed of a thin (10-100 nm) GaAs buffer epilayer grown on Si(111). The early nucleation behavior and epitaxy of GaAs on (111)Si have been rarely studied before. In the present work GaAs buffer layers were grown on (111)Si substrate [pre-treated under tertiarybutylarsine (TBAs)] by a common two-step procedure consisting in the low (400°C) temperature growth of a nucleation layer, followed by a second layer grown at higher (625-700°C) temperatures. X-ray diffraction analyses and field emission scanning electron microscopy observations have shown that the growth of the nucleation layer occurs in the form of flat epitaxial nanoislands, whose lateral growth leads to the progressive coverage of the Si substrate, until a compact epilayer is obtained. Relatively flat GaAs (111)-oriented buffers layers are then obtained upon growth of the second high temperature step. Dense arrays of (111)-oriented (i.e., in the direction normal to the substrate surface plane) GaAs nanowires were thus grown onto these hetero-structured GaAs/Si substrates using trimethylgallium, TBAs, and colloidal Au nanoparticles as catalysts. Growth temperatures were in the 400-450°C interval. As-grown nanowires show hexagonal cross sections, as well as axial and sidewall growth rates consistent to those expected in the case of epitaxial VLS growth on (111)B-GaAs substrates. This suggests that the underlying GaAs buffer layer is also oriented (111)B onto (111)Si. These results open a promising road towards controlling the heteropitaxy of GaAs nanowires on Si.

P1.29 Alternative Technique for the Preparation of InAs Nanowires on (110) GaAs Using LP-MOVPE: Kamil Sladek[1]; Andreas Penz[1]; *Hilde Hardtdegen*[1]; Kilian Floehr[2]; Marcus Liebmann[2]; Christian Bloemers[1]; Haci Günel[1]; Thomas Schaepers[1]; Markus Morgenstern[2]; Detlev Gruetzmacher[1]; [1]Research Center Juelich; [2]RWTH Aachen University

Undoped InAs nanowires are prospective building blocks for field effect and spinelectronic transistors due to their high conductivity and large spin orbit coupling allowing carrier transport as well as spin manipulation. In order to control their properties, it is desirable to be able to produce wires of uniform diameter and large aspect ratio. Up to now two preparation approaches have been largely employed: the one is to use a metal particle such as gold and to grow wires via the vapor liquid solid method. These wires exhibit a diameter close to the particle dimension. The second is to use the openings in a mask - typically of SiO_2 or Si_3N_4 - to predefine the position and the diameter of the wires by selective area metal organic vapor phase epitaxy (SA-MOVPE). In this contribution we will present an alternative approach which is based on the surface modification of GaAs substrates by means of reactive ion etching. It was found that the morphological, structural and electrical properties differ from those produced by our normal SA-MOVPE-procedure using the same growth parameters. Field effect transistors were prepared. Details of the preparation and growth process as well as the electrical characteristics of these wires will be presented.

P1.30 The Study of InAs/InGaAs Dot-in-a-Well Structures for Quantum Dot Infrared Photodectectors by Metal Organic Chemical Vapor Deposition: *Jungsub Kim*[1]; Changjae Yang[1]; Jaeyel Lee[1]; Sehun Park[1]; Seung-kyu Ha[2]; Won Jun Choi[2]; Yasushi Nanishi[3]; Euijoon Yoon[4]; [1]Department of Materials Science and Engineering, Seoul National University ; [2]Nano-Device Research Center, Korea Institute of Science and Technology; [3]Department of Photonics, Ritsumeikan University and Hybrid Materials Program (WCU), Department of Materials Science and Engineering, Seoul National University; [4]Department of Materials Science and Engineering, Seoul National University and Hybrid Materials Program (WCU), Department of Materials Science and Engineering, Seoul National University

Theoretically, the quantum dot infrared photodetectors (QDIPs) have a high responsivity, high operation temperature and low dark current due to their carrier confinement effect. To realize these benefits, the density and size of QDs should be manipulated on purpose and the non-defective growth of QDs is required. Previously, we reported the suppression of abnormally large island formation and the enhancement of emission efficiency by using periodic arsine interruption [1]. To tune the density and size of QDs, the InGaAs layer has been used as a buffer layer and capping layer of QDs, so called InAs/InGaAs dot-in-a-well (DWELL) structure [2]. InAs QDs were grown on the different InGaAs buffer layers by using post growth interruption (GI) and observed by atomic force microscopy (AFM). The post GI means that the growth step in which the supply of all sources is paused after the QD deposition. The density of QDs decreased and their heights increased with increasing the time of the post GI in all cases of InGaAs buffer layers. The reduction rate of the density was faster in the case of low In content of the buffer layer. This implies the mechanism of material diffusion on the QD surface is subject to the condition of InGaAs buffer layer. As a result of low temperature photoluminescence (PL) at 14 K, the Ga diffusion from InGaAs buffer layer is dominant in case of high In content. For QDIP application, we grew n-type GaAs/intrinsic DWELL/n-type GaAs structures. After the fabrication of devices with a simple mesa structure, dark current depending on the bias and temperature was measured. We found that the growth temperature of n-doped top contact layer (TCL) should be lower than 600°C. If not, the emission efficiency was severely reduced in PL measurement and dark current increased. Recent experimental results and discussion will be addressed. [1] Y. Lee, E. Ahn, J. Kim, P. Moon, C. J. Yang and E. Yoon, Appl. Phys. Lett. 90 033105 (2007). [2] J. Kim, C. J. Yang, U. Sim, E. Yoon, Y. Lee, W. J. Choi, J. the Korean Phys. Soc. 52 s34 (2008).

Poster Session II

Thursday, 4:00-6:00 PM   Room: Regency Ballroom
May 27, 2010   Location: Hyatt Regency Lake Tahoe

P2.1 MOVPE Technology for LEDs on 200 mm Diameter (111) Silicon: *Adam Boyd*[1]; Olaf Rockenfeller[1]; Simon Thomas[2]; Christof Sommerhalter[3]; Bernd Schineller[1]; Johannes Kaeppeler[1]; Michael Heuken[1]; [1]AIXTRON AG; [2]AIXTRON Ltd.; [3]AIXTRON Inc.

One advantage of the use of silicon as a substrate is the availability of low cost large diameter substrates, achieving an LED production cost reduction through an increased number of chips per wafer without an equivalent increase in processing costs. The challenge to grow on large diameter substrates is primarily due to the temperature uniformity from the large and varying wafer bow throughout the process which is required to achieve high material quality and a low bow at the end of the process. In this study a Crius® vertical close coupled showerhead reactor was used with a single 200 mm wafer configuration. GaN and full InGaN/GaN LED structures were grown on 725 µm thick (111) silicon utilising an AlN/AlGaN buffer layer. The wafer temperature profile over the entire susceptor was monitored in-situ by Argus®, which incorporates an array of 24 dual wavelength pyrometers across the radius of the susceptor. Based on this, the temperature profile throughout the process was optimized by varying concentric heater zones. The wafer curvature was monitored using a two-beam deflectometer at 60º intervals on the wafer at a radius of 35 mm, giving information about the strain and curvature uniformity during the process. Reflectivity was also measured, yielding the accurate thickness of the component layers and an indication of the surface morphology during the process. Using these techniques 1.3 µm GaN:Si(3.3×10^{18}cm^{-3}) was grown crack free (except outer 9 mm), with a final bow of < 100 µm, and x-ray diffraction full width at half maximums of 550 arcsec and 1000 arcsec for the 002 and 102 reflexes respectively. State of the art uniformities were achieved, including thickness standard deviation of $\sigma = 1.2\%$ of the n-GaN structure, and photoluminescence peak wavelength standard deviation of $\sigma = 1$ nm of a full LED structure incorporating a 5 period InGaN/GaN MQW with mean wavelength of 465 nm (measured ex-situ using Nanometrics rpm Vertex, with 4 mm edge exclusion).

P2.2 Growth by MOCVD of AlInGaN Structures for Optoelectronic Devices on 6 Inch Substrates: Assadullah Alam[1]; Christof Sommerhalter[2]; Bernd Schineller[1]; *Michael Heuken*[1]; [1]AIXTRON AG; [2]AIXTRON Inc.

The reduction of the production cost of optoelectronic devices is a paramount driving factor for the industry. Consequently, MOCVD processes and tools have to contribute to the cost reduction effort. For example, switching from a configuration of 42x2 inch to 6x6 inch for an AIX 2800G4 HT MOCVD equipment an increase in productivity of 28.6% is achieved. After extensive numerical modelling to design the 6x6 inch configuration in he AIX 2800G4 HT platform the tool was benchmarked using layer materials commonly used in LED production. For instance, AlGaN layers in LED structures are used as electron blocking layers and for strain management. Layers containing 18% and 50% Al/Ga-ratio were grown at a growth temperature of 1100°C on 6 inch at 100 mbar and 50 mbar. X-ray diffraction scans exhibited uniformities of ±2.2% and ±1.4% for the 18% and 50% layers, respectively, indicating good compositional uniformity. Based on experience from up-scaling from 2 inch to 4 inch diameter bow compensation becomes more difficult for larger wafers. To investigate the influence of the substrate thickness on the growth results 6 inch sapphire substrates with thickness of 1.0 mm and 1.3 mm were used. As expected, In-situ curvature measurements from a 2 beam deflectometer revealed considerable differences in the bow for the high temperature GaN buffer, i.e. 170/km curvature for a 1 mm and 85/km for a 1.3 mm thick substrate, respectively. This clearly indicates that a thicker substrate is more resistant to bow. However, when cooling down to MQW growth temperature the bows of the two wafers were found to be almost identical, yielding comparable temperature profiles on the surface which are a prerequisite for uniform In-incorporation.Consequently, the 5 period InGaN MQW structures grown on top of the aforementioned GaN buffers yielded similar photoluminescence wavelength standard deviations s_{λ} of 2.4 nm for a mean wavelength of 449.4 nm for the 1.3 mm thick substrate and $s_{\lambda} = 2.8$ nm at a mean wavelength of 452.9 nm for the 1 mm thick substrate. Further results will be presented.

P2.3 Reduced Anisotropy in a-GaN Crystalline Quality by Metalorganic Chemical Vapor Deposition: *Keun-Man Song*[1]; Jong-Min Kim[1]; Dong-Hun Lee[1]; Won-Kyu Park[1]; Chul-Ki Ko[1]; Sung-Min Hwang[2]; Dae-Ho Yoon[3]; [1]Korea Advanced Nano Fab Center; [2]Korea Electronics Technology Institute; [3]Sungkyunkwan University

Recently, advanced progresses in III-nitride semiconductors are mainly based on the polar [0001] direction of GaN, which contains a strong internal electric fields in the quantum wells (QWs). As a result, a spontaneous and piezoelectric field limit the performance of optoelectronic devices. To overcome this problem, one of the promising substitutions is nonpolar or semipolar III-nitride semiconductors. However, it is difficult to obtain high quality nonpolar or semipolar GaN and related alloys with a smooth surface, since the layers contain numerous nonradiative recombination centers owing to lattice and thermal expansion mismatch between a-GaN and substrate. The a-GaN exhibited that the planar anisotropic characteristic of the growing surface direction due to anisotropic strain and adatom diffusion length, resulting in structural, surface morphological, optical, and electrical anisotropy. In order to achieve a high crystalline quality of a-GaN grown on r-sapphire with a flat surface, controlling the growth mode for 3D faceted islands is considered important process. However, there are only a few studies regarding initial growth condition for 3D nucleation process correlating crystalline anisotropy and quality of a-GaN. In this study, the effect of initial growth pressure on crystalline and anisotropic quality of a-GaN grown by metalorganic chemical vapor deposition (MOCVD) was investigated. The a-GaN samples were characterized by scanning electron microscopy (SEM), X-ray diffraction (XRD), Photoluminescence (PL). Nonpolar a-GaN epilayer were grown directly on an r-sapphire substrate without low temperature GaN or high temperature AlN buffer. The high temperature a-GaN was grown by two step growth pressure, which consisted of initial nucleation growth with varied growth pressure and subsequently lateral growth with low growth pressure for coalescence at 1040°C. We found that initial growth pressure for nucleation growth plays an important role in growing a-GaN with enhanced anisotropy and crystalline quality.

P2.4 Influence of Reactor Pressure on the Phase Stability of Indium-Rich In$_{1-x}$Ga$_x$N Epilayers: *Max Buegler*[1]; Ramazan Atalay[1]; Sampath Gamage[1]; Indika Senevirathna[1]; Jielei Wang[1]; Muhammad Jamil[2]; Ian Ferguson[2]; Ramon Collazo[3]; Zlatko Sitar[3]; Nikolaus Dietz[1]; [1]Georgia State University; [2]UNC Charlotte; [3]North Carolina State University

While significant progress in the growth of high quality group III-nitride epitaxial layers has been made during the last decades, the integration of indium rich InGaN epilayers into wide band gap group III-nitrides is still very challenging due to the lower disassociation temperature of indium-rich InGaN alloys compared to that of GaN. A further challenge is the large difference between the lattice constants of the binaries InN and GaN (~11%), which results in induce lattice strain and contributes to the observed compositional instabilities in InGaN layers integrated in gallium-rich heterostructures. This contribution discusses the potential of high-pressure Chemical Vapor Deposition (HPCVD) to improve the phase stability in InGaN layers, utilizing high pressures nitrogen gas to stabilize the In$_{1-x}$Ga$_x$N growth surface and effectively suppressing the thermal decomposition process above the growth surface. Growth conditions and characterization results are presented for single-phase In$_{1-x}$Ga$_x$N epilayers ($x < 0.6$) grown under at different reactor pressures and growth temperatures. X-ray diffraction, optical transmission spectroscopy, and Raman spectroscopy are used to analyze the structural and optical properties of the epilayers. The findings were linked to the surface morphological properties of the In$_{1-x}$Ga$_x$N layers.

P2.5 Defect Dependence of Optical and Crystal Properties on InGaN/GaN Multiple-Quantum Well Grown on Nonpolar a-Plane (11-20) GaN Templates: *Sung-Nam Lee*[1]; Kyoung-Kook Kim[1]; Ok-Hyun Nam[1]; [1]Korea Polytechnic University

Recently, one of most important issues is the enhancement of light output power in GaN-based light emitting diodes (LEDs) to commercialize as a lighting source. However, there are a few critical technical issues to increasing light output power. Among some problems, the luminous efficiency of c-plane GaN-based LEDs has been significantly influenced by intrinsic spontaneous and piezoelectric polarization effects. Therefore, a lots research groups have focused on non-polar GaN-based LEDs. In this study, we investigated the effect of optical and crystal qualities on InGaN/GaN quantum well structure grown on a-plane (11-20) GaN/r-sapphire. Nonpolar a-plane (11-20) GaN templates were grown by introducing the novel growth method without low temperature GaN buffer layer. And then, InGaN/GaN 5-period quantum wells (QWs) structures were grown on two a-plane GaN templates (sample A and B). The full width at half maximums (FWHMs) of X-ray ω-rocking curves of sample A and B were 460 and 850 arcsec, respectively. From X-ray diffraction (XRD) ω/2θ measurements, the satellite peak of InGaN QWs grown on sample A was well developed, while that of InGaN QWs grown on sample B was not observed. It implied that the interfacial quality of QWs could be enhanced by a-plane GaN with high crystal quality. Photoluminescence (PL) spectra showed that the emission intensity of QW grown on sample A was 2 times higher than that of QWs on sample B. From XRD and PL measurements, one can see that interfacial quality could affect the optical qualities of InGaN QWs. Additionally, by comparing InGaN 0th peak of XRD ω/2θ scans, we observed higher indium composition in the InGaN QWs grown on sample B than sample A. It was consistent with a longer wavelength and a broader emission of InGaN QWs grown on sample B. It can be explained by high In incorporation and the generation of defects at the region of dislocations during the growth of InGaN. Therefore, we could suggest that the interfacial quality and the In incorporation of InGaN QWs were significantly affected by the crystal quality of a-plane GaN template.

P2.6 Influence of Substrate Temperature on Structural and Optical Properties of InN Epilayer Grown by RF-MOMBE with GaN Buffer Layer: *Wei-Chun Chen*[1]; Shou-Yi Kuo[2]; Fang-I Lai[3]; Chien-Nan Hsiao[1]; [1]Instrument Technology Research Center, National Applied Research Laboratories; [2]Department of Electronic Engineering, Chang Gung University; [3]Department of Electrical Engineering, Yuan-Ze University, Taiwan

This work reports on the correlation structural and optical properties of radio frequency metal-organic molecular beam epitaxy (RF-MOMBE) grown InN epilayer on GaN(0001)/c-sapphire. In this paper, we discussed effect of growth temperatures on the structural and optical properties of InN. The InN films has been characterized in detail using X-ray diffraction (XRD), field emission scanning electron microscopy (FE-SEM), transmittance electron microscopy(TEM), electrical and optical properties were performed by Hall Effect system and photoluminescence (PL) measurements. XRD results indicated InN films were along c-axis highly orientation growth and lattice constant about 0.57 nm. SEM images exhibit the InN were growth by two-dimensional mode and thickness about 700 nm. Specially, InN was high growth rate ~ 1.5 μm/hr disposition on substrates by our system. Optical measurements on the films revealed a luminescence feature near-infrared emission peak centered at 0.75 eV. The films used here were nominally undoped with electron concentrations measured from high 10^18 to mid-10^19 cm-3 that mobility measured from 30 to 464 cm/V-s.

P2.7 Effect of Moisture in Ammonia on LED Device Performance and Impurity Control through Liquid Extraction Total Vaporization Delivery and Purification Technologies: Hirotaka Mangyo[1]; Joe Vininski[1]; *Mark Raynor*[1]; Robert Torres[1]; Yoshihiko Kobayashi[2]; Takuya Ikeda[2]; Hiroyuki Ono[2]; Kazutada Ikenaga[2]; Koh Matsumoto[3]; [1]Matheson Tri-Gas, Inc.; [2]Taiyo Nippon Sanso Corporation; [3]TN EMC Ltd

Oxygenated impurities are particularly detrimental in GaN MOCVD. Incorporation of oxygen into nitride layers from water vapor (moisture) in the ammonia not only lowers the brightness of LEDs but also affect process yield. Therefore it is important to understand at what level critical impurities affect devices and how the concentration of the impurities change during delivery of the ammonia, in order to implement effective impurity control technologies. In this work, InGaN/GaN multi-quantum well LED structures were grown at 740ºC using TMG, TMI and 5N grade ammonia. Moisture was added to the ammonia at concentrations from 12.5 ppb to 2500 ppb using a dilution manifold and gas standard to investigate its effect on the device electroluminescence (EL). The moisture concentration was found to significantly affect the EL intensity. At 12.5 ppb moisture, EL intensity was close to that of the background. However at 100 ppb moisture, a ~30% decrease in relative intensity was observed and at 1000 ppb, the EL dropped to ~15% of the original intensity. The results indicate that H2O levels in ammonia should be minimized as other device structures may be even more sensitive than the structure used in this study. The concentration of moisture delivered in ammonia can vary greatly depending on the delivery conditions. Water partitions between the vapor and liquid phases and increasing moisture is observed as gas phase is withdrawn from the source, especially close to and after the phase-break point. Further, moisture levels are affected by the flow rate and temperature of the ammonia when delivered via gas phase. In contrast, liquid extraction with total vaporization (LETV) of the ammonia results in a stable but higher moisture concentration as liquid is withdrawn from the vessel. Testing of an LETV delivery system shows consistent moisture levels as a unit was consumed down to 97%, at flow rates of 750 slpm and greater. As discussed above moisture must be controlled to low and sub-ppb levels in delivered ammonia for MOCVD. Introduction of purification technologies should be implemented for process consistency and will also be discussed in this paper.

P2.8 Optical Properties of Non-Polar GaN Nanorod Arrays on r-Plane Sapphire with Embedded $In_xGa_{1-x}N$/GaN Multiple Quantum Wells: Jinchai Li[1]; *Hueimin Huang*[1]; Wei-Wen Chan[1]; Tien-Chang Lu[1]; Hao-chung Kuo[1]; Shing-chung Wang[1]; [1]NationalChiao Tung University

Non-polar (a-plane) GaN nanorod arrays with embedded $In_xGa_{1-x}N$/GaN (x=0.09, 0.14, 0.24, and 0.3) multiple quantum wells (MQWs) grown on r-plane sapphire have been fabricated successfully by self-assembled Ni nanomasks and subsequent inductively coupled plasma reactive-ion etching. Optical properties are investigated by means of temperature-dependent and polarization-dependent photoluminescence (PL). Similar to the as grown samples, low- (PL) and high-energy (PH) PL peaks, related to localized states and quantum wells, respectively, also can be observed at low temperature after nanorod formation. However, the intensity-ratio of PL and PH decreases by a factor of 35%, 60%, 65%, and 49% for nanorod samples with In compositions of 0.09, 0.14, 0.24, and 0.3, respectively, indicating the reduction of localized states. This argument is verified from the smaller activation energies for high temperature region in the nanorod samples as compare with that in the as-grown samples. Furthermore, the polarization-dependent PL reveals that the degree of polarization (DOP) decreases slightly by 11% and 7% in the nanorod samples with In-composition of 0.09 and 0.14, respectively, while increases significantly by 79% and 27% in the nanorod samples with In-composition of 0.24 and 0.30, respectively. Such behaviors may be attributed to the competition between the DOP-reduction effect by strain relaxation and DOP-enhancement effect by the reduction of localized radiative centers. These results suggest that the nanorod fabrication can be an effective way to fabricate long-wavelength GaN-based LEDs with higher DOP.

P2.9 Impact of Gradient Temperature on the Growth of InN by MOCVD: Tzu Tao Yuan[1]; Ping Yu Kuei[1]; Mu Jen Lai Lai[2]; Yi Cheng Cheng[3]; Ta ching Li[3]; Wei Chun Chang[1]; [1]Chung Cheng Institute of Technology/National Defense University; [2]Chang Gung University; [3]Chung Shan Institute of Science and Technology

In our study, the single crystalline InN nanorods have been developed and they were grown by a two step process using our home-made low-pressure metal-organic chemical vapor deposition (LP-MOCVD). The technology of gradient temperature growth was applied to the two step process. It was observed by SEM that when the growth temperature of InN increases from 560 to 640°, the width and the density of the InN nano-rods change from 86 to 211 nm and from 4.85 to 0.76μm-2, respectively. The RMS roughness of surface morphology was mapped as a function of growth temperature and the result of the AFM measurement was consisted with the trend of SEM observation. It was obtained that the growth window of preferable temperature of InN growth was between from 580 to 600° by Hall measurement on our MOVCD system. The InN nano-rods were single-crystalline structure by XRD spectra with the InN diffraction peak at 31.38° of hexagonal (0002) plane. The mechanism of forming InN nano-rods is attributed to the enhancement of 1D growth when the InN growth rate is hastily increased. The results suggest that the two step process with gradient temperature growth is a promising technique for the fabrication of InN nano-rods structured without using catalyst, nano-template and halide conditions by MOCVD.

P2.10 Growth of InN Layer on Sapphire Substrate by MOCVD and the Effect of Two-Step Growth on Its Structural Properties: *Keon-Hun Lee*[1]; Hee Jin Kim[2]; Hyunseok Na[3]; Tae-Yeon Seong[4]; Euijoon Yoon[5]; [1]Seoul National University; [2]Georgia Institute of Technology; [3]Daejin University; [4]Korea University; [5]Seoul National University (WCU program, MSE)

InN films were grown on (0001) sapphire substrates by a metal-organic chemical vapor deposition system. Trimethylindium (TMIn) and ammonia were used as indium and nitrogen sources, respectively. In case of typical one-step InN growth, flat surface was obtained by well-controlled substrate nitridation and low TMIn flow rate even though It is generally known that 3-D evolution at the initial stage of InN growth due to the large lattice mismatch between InN and sapphire (~29%). However, low TMIn flow rate necessarily results in slower growth rate of InN layer. For this reason, two-step InN growth was adopted to increase the growth rate of InN layer while maintaining flat surface and metallic indium-free growth. First 40 nm InN layer was grown under low TMIn flow rate (2.07 μmol/min), which led to flat surface. Then TMIn flow rate was raised (to 4.14 μmol/min) for second 40 nm InN layer, which corresponds to the V/III ratio of 80,000. The surface of 80 nm InN was mirror-like by optical microscopy inspection. The phase and crystallinity of grown InN films were analyzed by X-ray diffraction (XRD) measurement. From the (0002) X-ray symmetrical rocking curves measurement of one-step InN samples which are 40 nm-thick, as the TMIn flow rate decreased, decrease of the full width at half maximum from 980 to 800 arcsec was observed for TMIn flow rate of 4.14 and 2.07 μmol/min, respectively. Six peaks at every 60 degree indicating 6-fold symmetry were detected for every sample from XRD (10-14) phi-scan measurement. The effect of two-step growth on the surface morphology was examined by atomic force microscopy. 40 nm InN films were grown under TMIn flow rate of 4.14 μmol/min on sapphire and flat 40 nm InN template. For the sample grown with two-step method, the surface morphology showed smooth feature without bright spots. Even though the total thickness of the sample grown on InN template was thicker, the root mean square roughness represented comparable value for both samples. It indicates that second InN layer tends to grow homo-epitaxially on underlying first InN template due to relieved lattice mismatch on flat InN surface.

P2.11 Influence of Buffer Layers on the Microstructure of MOVPE-Grown a-Plane InN: Masihhur Laskar[1]; Tapas Ganguli[2]; Abdul Kadir[1]; A. A. Rahman[1]; Nirupam Hatui[1]; M.R. Gokhale[1]; A. P. Shah[1]; *Arnab Bhattacharya*[1]; [1]Tata Institute of Fundamental Research; [2]Raja Ramanna Centre for Advaced Technology

We report a comprehensive study of structural, electrical, optical and morphological properties of a-plane InN grown on r-plane sapphire using different buffer layers: GaN, AlN, and low-temperature InN. Even for the same epilayer growth conditions, the buffer layer has strong influence on the microstructure and hence the electrical and optical properties of a-plane InN. About 0.2μm-thick epilayers were grown in a 3x2” close-coupled showerhead reactor using TMIn, NH3 precursors and N_2 carrier gas. All the epilayers are uniform, mirror like over the entire 2”-wafer. In a separate study, we determined the optimum conditions for the growth of a:InN in our showerhead reactor to be T=550°C, P=500 Torr, V/III~11000. Keeping the growth parameters constant, we have deposited InN using different buffer layer (BL) schemes - 1μm-thick GaN BL, low-temperature InN nucleation layer, and a 3-stage AlN BL. The results show that the AlN BL significantly improves the crystalline quality, gives higher mobility and lower background carrier concentration compared to the GaN and InN BLs. We observe that the in-plane anisotropy in the mosaicity of the a-plane InN is strongly influenced by the buffer layer. Microstructural parameters measured from Williamson-Hall plots reveal different in-plane tilt values along the c- and m-directions. From the reciprocal space map of the symmetric (11-20) plane with different orientation of scattering planes (along c- or m-directions) we observe that the InN-epilayers have a Nagai-tilt which arises because of large lattice mismatch between InN and AlN and possibly due to a miscut in the substrate. This tilt is along the c-axis. The best crystalline quality of a-plane InN obtained using AlN buffer layers has a symmetric (11-20) ω-fwhm of 2760 arcsec and 3074 arcsec along [0001] and [-1100] direction respectively, and asymmetric (10-11) ω-fwhm of 4030 arcsec with 11K PL peak at 1760 nm, mobility of 342 cm^2 /Vs, carrier concentration $6.8x10^{18}$ cm^{-3} at room temperature and an RMS roughness ~14 nm over a 3μm × 3μm area. To the best of our knowledge these values are among the best reported for MOVPE-grown a-InN so far.Data for these results can be viewed online at www.tifr.res.in/~arnab/a_InN_AlN.pdf

P2.12 Internal Quantum Efficiency Measurement in InGaN/GaN UV LEDs with Patterned Sapphire Substrate by Electroluminescence Method: *Chao-Hsun Wang*[1]; C. H. Chiu[1]; C.C. Ke[1]; H.C. Kuo[1]; T.C. Lu[1]; S.C. Wang[1]; [1]National Chiao Tung University

1. Introduction: III-nitride based light emitting diodes (LEDs) have attracted much attention in ultraviolet (UV) range because of their tremendous potential in applications like white light sources [1], environmental cleaning, bio-medical examination. For UV LEDs, the internal quantum efficiency (IQE) is more sensitive to the dislocation density. Therefore, using patterned sapphire substrate (PSS) technique to lower the dislocation density is very important for IQE improvement. Though PSS had been proven as an effective method, the exact improvement number in IQE is still not clear. In this study, two methods to measure the IQE of UV LEDs with/without PSS had been proposed by electroluminescence (EL). The details of the theory and results will be discussed. 2. Results and conclusion:We prepared two samples grown on conventional and PSS samples with wavelength at 400 nm [2]. The EQE at 20 mA for PSS and non-PSS LEDs are 43% and 28%, respectively.

The 53.6% enhancement in EQE was believed due to the increasing in both IQE and extraction efficiency. From the results, the slop of efficiency decrement was similar between both samples, which mean the existing of dislocation density will not affect the efficiency droop performance at high injection current. The efficiency is defined as the collected photon number divided by the injected carrier numbers and all normalized to its maximum efficiency. Assume the emitted pattern and collected solid angle remains constant through whole measurement period, the curve could be viewed as the IQE variation [3]. Basically, the non-radiative centers would be suppressed as the environment temperature decreased, which means a higher efficiency is expected at low temperature. However, as observed, the fewer activated hole concentration and poorer hole mobility at low temperature caused an efficiency reduction. These two phenomenons compete with each other while we cooling down the environment temperature. As a result, we observed a maximum peak at about 77 K during whole temperature dependent efficiency measurement period. By normalizing the peak number, we could get the EL IQE. The most important thing we cared about is the IQE number at 20 mA injection at room temperature of these two samples. The IQE for PSS and conventional LED were 56.3 and 44.6% in EL method, respectively, and the difference in IQE is 11.7 % in EL method. This significant improvement can be attribute to better crystal quality with PSS.

P2.13 Characterization of a-Plane GaN Layers Grown on Patterned r-Sapphire Substrate by MOCVD: Geun Ho Yoo[1]; Hyun Sung Park[1]; Dong Hun Lee[1]; Hyoung Jin Lim[1]; Seung A Lee[1]; *Ok Hyun Nam*[1]; Bo Hyun Kong[2]; Hyung Koun Cho[2]; [1]Korea Polytechnic University/KPU LED Center; [2]Sungkyunkwan University/School of Advanced Materials Science and Engineering

GaN and other related □-Nitride based semiconductors have attracted significant attention for optoelectronic device applications covering the ultraviolet and full visible ranges of the electromagnetic spectrum due to their wide band-gap. The vast majority of these devices are grown parallel to the [0001] c-axis of the wurtzite GaN crystal structure. However, the intrinsic spontaneous and extrinsic piezoelectric polarizations which are always present in GaN-based heterostructure grown with the orientation of basal plane of wurzite structure can degrade electronic and optical properties. Recently, there were many interests in the growth of non-polar GaN for opto-electronic device structures free of polarization induced electric fields. However, non-polar optoelectronic devices directly grown on r-plane sapphire substrates usually contain a high threading dislocation (TD) density. In this study, a-plane GaN layers were grown on hemispherical patterned r-sapphire substrates by metal organic chemical vapor deposition (MOCVD) in order to reduce defects and enhance extraction efficiency of light. We employed the size of pattern with 300 nm, 2 μm and 3 μm to investigate growth mechanism and reduction of defects. We studied the growth behavior with the process parameters such as temperature, pressure and TMGa flow rate. The PL intensity of a-plane on PSS was over 20times higher than that of conventional a-plane GaN. The FWHM of Double Crystal Rocking Curve (DCRC) of a-GaN template on PSS showed about 673 and 683 arcsec in parallel and vertical direction to c-axis, respectively. TEM observation confirmed that defect reduction of nonpolar a-GaN on PSS was achieved through a lateral growth on the hemispherical pattern. TEM measurement also showed that basal staking fault and threading dislocation density of a-GaN grown on PSS decreased about 10 times than conventional a-GaN grown on planer r-sapphire substrate. Additional results will be reported in the conference.

P2.14 Photoluminescence Studies of Indium Nitride Films Grown on Oxide Buffer by Metalorganic Molecular-Beam Epitaxy: Fang-I Lai[1]; Woei-Tyng Lin[1]; Wei-Chun Chen[2]; Chien-Nan Hsiao[2]; *Shou-Yi Kuo*[3]; Yu-Kai Liu[4]; Ji-Lin Shen[4]; [1]Department of Electro-Optical Engineering, Yuan-Ze University; [2]Instrument Technology Research Center, National Applied Research Laboratories; [3]Department of Electronic Engineering, Chang Gung University; [4]Department of Physics, Chung Yuan Christian University

We have investigated the optical properties of InN films grown on oxide buffer by metalorganic molecular-beam epitaxy. The structural and optoelectrical properties of InN films were investigated by X-ray diffraction, scanning and transmission electron microscopy, Hall-effect and temperature-dependence photoluminescence (PL) measurements. Strong dependence of dislocation densities and optoelectrical properties upon V/III flux ratio is observed. Near-infrared emission peaks between 0.74 eV and 0.78 eV were observed. While decreasing the V/III flux ratio, the PL emission peak red-shifted related to Moss-Burstein effect. In addition, the PL spectra show an abnormal behavior with increasing temperature. The temperature-dependence PL spectra exhibit blue-shift as the temperature increased up to 100K and then red-shift. We suggest that the abnormal temperature-dependent photoluminescence might be ascribed to the fluctuation in stoichiometry and crystallographic defects.

P2.15 Experimental Determination of the Diffusion Lengths of Trimethylindium and Related Species during Selective Area MOVPE Growth of InP: *Noelle Gogneau*[1]; Gilles Patriarche[1]; Gregoire Beaudoin[1]; Luc Le Gratiet[1]; Christian Ulysse[1]; Isabelle Sagnes[1]; [1]LPN-CNRS

Recently, the Selective Area Growth (SAG) technique was pushed to the nanoscale level, in order to precisely position the growth of a single quantum dot (QD). Such growth localization is only possible by the combination of metalorganic vapour phase epitaxy (MOVPE) growth and the use of dielectric patterns. In fact, due to the growth inhibition on dielectric masks, the active species diffuse, thus enabling selective deposition in the openings. However, it results in a modulation of the film thickness in the vicinity of the masked edges, leading to a variation of the properties of the active layer. It is therefore crucial to understand and control these effects as a function of the pattern dimensions.In this work, we experimentally determined the diffusion lengths of Trimethylindium (TMIn) and related species (subsequent decomposition from TMIn to dimethylindium (DMIn), then to monomethylindium (MMIn), and finally, to element In) during the SAG growth of InP at low temperature (around 500°C) compatible with InAs/InP QD growth conditions. Each species has a corresponding diffusion length, depending on the diffusion coefficient and the reaction constant of the given specie. The mask pattern consists of two parallel dielectric stripes of width Wm aligned along the [110] direction of a (100) InP substrate and spaced by an opening of width Wo (between 0.25 and 160μm). The profiles of the overgrowth at the mask edge were studied by SEM, AFM and optical interferometer microscope. A diffusion length of 260, 40, 2 and 0.5μm for TMIn, DMIn, MMIn, and In respectively was measured. We associate TMIn, and DMIn diffusion to gas phase diffusion process and MMIn and In atoms diffusion to surface migration process. When the pattern size is comparable to surface diffusion length, the surface diffusion process is dominant, while for higher pattern size, the vapour phase diffusion process becomes dominant. We have developed a peculiar nano-patterning with dimensions lower than the In adatom diffusion length (< 500nm) which allows a reproducible growth of site-controlled InAs/InP QDs, with controllable height and width (5 and 50nm respectively). Similar measurements of In under Arsine should be undertaken to complete the study.

P2.16 Atomic Layer Deposition of LaAlO$_3$ Heterostructures: *Nick Sbrockey*[1]; Marc Aranguren[2]; Jonathan Spanier[2]; Gary Tompa[1]; [1]Structured Materials Industries, Inc.; [2]Drexel University

Oxide heterostructures, consisting of a polar oxide such as LaAlO$_3$ and a non-polar oxide such as SrTiO$_3$, offer a novel route to fabricating high speed, nano dimension devices. Atomic Layer Deposition (ALD) has several advantages for fabricating these structures, including excellent control of film thickness, uniformity and stoichiometry. Reliable control of these parameters will be imperative for ultimate device fabrication. This paper describes the development of ALD processes for LaAlO$_3$ films on both silicon and SrTiO$_3$ substrates, using trimethyl aluminum and lanthanum i-propylcyclopentadienyl for the metal precursors, and water as the oxidizer. Excellent control of film thickness and uniformity was demonstrated in the 300C to 400C temperature range, consistent with ALD processes for similar materials. Control of the La/Al stoichiometry in the films was achieved by adjusting the La source temperature, and by the relative number of La to Al vapor source pulses. The LaAlO$_3$ films were amorphous in the as-deposited state, as evidence by the lack of x-ray diffraction peaks. The films crystallized on annealing at 900C.

P2.17 Synthesis of ZnO-Based Semiconductors by Vectored-Flow Epitaxy: *Vishnukanthan Venkatachalapathy*[1]; Mareike Trunk[1]; Tianchong Zhang[1]; Alexander Azarow[1]; Matthew Branch[2]; Glyn Jones[2]; Augustinas Galeckas[1]; Andrej Kuznetsov[1]; [1]University of Oslo; [2]EMF Semiconductor Systems Ltd.

Synthesis of ZnO-based semiconductors, including pure ZnO as well as alloying with MgO and CdO, was mastered by metal organic vapor phase epitaxy (MOVPE) employing so called vectored flow epitaxy utilizing separate injection/exhaust of group II and VI precursors maximising reagent cracking and minimizing harmful pre-reactions. Firstly, the injector positioning in the chamber was investigated by simulations choosing optimal precursor distribution over the rotating platen holding samples. Further, the synthesis was studied as a function of growth temperature (250-500 ^{o}C), chamber pressure (600 and 700 torr), rotation rate (30-120 rpm), II/VI ratios (0.1-1.0), bubbler temperatures as well as nature of precursors and substrates. Diethylzinc (DEZn) and tertiary butanol (t-BuOH) were used as Zn and

O reagents, while dimethylcadmium (DMCd) and Bis(cyclopentadienyl)magnesium (Cp_2Mg) were used for introducing Cd and Mg doping. A host of structural, electrical and optical properties were monitored while this report highlights controlling structural quality by x-ray diffraction (XRD), chemical composition by Rutherford backscattering spectroscopy (RBS), and optical properties by photoluminescence (PL). Specifically, investigating the influence of the growth pressure/temperature we evaluate the FWHM of the characteristic (002) rocking curve peaks and thus determine our fundamental growth parameters. Moreover, the influence of the DEZ and t-BuOH decomposition on the introduction of intrinsic defects was investigated and correlated with Zn rich/lean conditions. Further, researching wurtzite-cubic phase separation issues in Zn (Cd,Mg)O alloys we found an interesting balance for single-phase film manufacturing by tuning pyrolysis conditions and II/VI ratios resulting in different abundance of reagents in the reaction zone.

P2.18 Growth of Highly (00l) Oriented Thin Films of V2O5 and V6O13 Phases by MOCVD: *Ujwala Ail*[1]; S. Shivashankar[1]; A. Umarji[1]; [1]Indian Institute of Science

The oxides of vanadium are technologically important because of their diverse physical and chemical properties. The richness of the system is due to the presence of various stable oxidation states and also of different ordered and disordered defect structures giving rise to a wide range of stoichiometry of the lattice, viz., the existence of the homologous series (VnO2n-1 and VnO2n+1) [1]. These phases undergo semiconductor-to-metal transition at temperatures ranging from 80 K to 435 K, accompanied by a jump in electrical conductivity and also in magnetic susceptibility. They have been examined widely for use as catalyst, cathode material for solid state batteries, electrochromic devices, electronic and optical switches, gas sensors, etc. Here we report the Metalorganic Chemical Vapor deposition (MOCVD) of highly (00l) oriented thin films of V2O5 and V6O13 on amorphous, fused silica, and thermally oxidized Si substrates. Given the well known narrow range of stability of many of the vanadium oxides, it is necessary to discover and maintain the precise CVD conditions to grow thin films of V2O5 and V6O13. Since precise control of the deposition parameters is extremely important to stabilize desired phases during MOCVD, an attempt was made to tailor the V/O ratio, by controlling the molar ratio of the metal precursor to oxygen fed into the reaction chamber. This was done using the knowledge of vapor pressure and partial pressure of the precursor (vanadyl acetylacetonate) under the chosen deposition conditions. This method is based on Langmuir equation and uses the raising temperature thermogravimetric data of the metal precursor carried out both at atmospheric pressure [2], and at low pressures characteristic of the actual MOCVD process. The films obtained were highly oriented along (00l) direction as characterized by X-ray Diffraction. Scanning Electron Microscopy and pole figure analysis as well as the details of the thermal study and film deposition will be presented. [1] G. Anderson, Acta Chem.. Scand, 8, (1954), 1599. [2] G. V. Kunte, S. A. Shivashankar, A. M. Umarji, Meas. Sci. Technol, 19, (2008), 025704.

P2.19 MOCVD Growth of ZnO/ZnS Core-Shell Nanowires Arrays for Photovoltaic Applications: Shangzhu Sun[1]; Elane Coleman[1]; *Bruce Willner*[1]; Aurelien Du Pasquier[2]; Gary Tompa[1]; [1]Structured Materials Industries, Inc.; [2]Rutgers the State University of New Jersey

ZnO nanowires have received considerable attention for their application in photovoltaic devices, owing to the ease of growing arrays of high crystalline quality and well controlled length and shape nanowires. Furthermore, the ability to grow them on ZnO-based transparent conducting oxides makes the system even more attractive for the photovoltaic application. Large contact area and fast electron mobility normal to the plane in ZnO nanowires are especially advantageous for the combination with organic semiconductors, where exciton diffusion length is a limiting factor. Since ZnO is an n-type semiconductor with a wide bandgap of 3.3 eV, visible light absorption must be provided by an associated p-type semiconductor. Hybrid photovoltaic devices have been demonstrated using poly (3-hexylthiophene) (P3HT) as light absorber and hole transport phase [1]. Dye sensitized solar cells have also been demonstrated using ZnO nanotips grown on GZO substrates [2]. Another approach is to design n-core/p-shell structures using a core of ZnO nanowires and a shell of ZnS, where both can be grown by MOCVD. Bandgap control is achieved through the staggered type II heterojunction, where the effective bandgap at the junction can be calculated as the difference between the valence band level of ZnS, and the conduction band level of ZnO [3]. This talk will present initial MOCVD growth results of ZnO-ZnS core-shell nanostructures characterized via SEM, XRD and UV-vis spectroscopy. Their application in photovoltaic devices of the type GZO/ZnO-ZnS/Ag and GZO/ZnO-ZnS/P3HT/Ag will be discussed as well.

P2.20 MOCVD of Nanocrystalline Zinc Oxide for Power Field Effect Transistors: *Bruce Willner*[1]; Shangzhu Sun[1]; Gary Tompa[1]; [1]Structured Materials Industries, Inc.

Zinc oxide (ZnO) is an attractive material for high-speed high power devices. With a wide bandgap of 3.37eV and an exciton binding energy of 59 meV, ZnO has been found to have a high breakdown field of $5 * 10^6$ V/cm, slightly higher than GaN and SiC, and a high carrier saturation velocity. Semiconducting thin films of ZnO have been produced on silicon by metal organic chemical vapor deposition (MOCVD). The film qualities, including crystal size, can be controlled through the deposition parameters, providing high quality material, allowing material optimization for performance devices, and allowing well controlled deposition of more complex layer structures through parameter control. A MOCVD tool, designed specifically for ZnO deposition, was used to deposit high quality ZnO films for device fabrication. The lower deposition temperatures of ZnO (400-600°C), compared with other wide bandgap semiconductors, allows deposition on a greater variety of substrates. MOCVD is a highly scalable technique which can provide uniform, pin-hole-free deposition over large areas, excellent for the precision fabrication of RF power devices and large scale production. ZnO deposition with thickness variation of under 3% across an 8”diameter substrate have been achieved. The material and fabrication costs for ZnO are estimated to be approximately 1/8 that of GaN or SiC. Bottom gate device structures were fabricated using SiO_2 as the gate dielectric. Fabricated devices demonstrated field effect mobilities of greater than 25 cm^2/Vs. Devices with on-off ratios of $>10^{10}$ and enhancement mode operation were achieved. Post fabrication annealing improved device performance.

P2.21 Vertically Grown ZnO Nanowires on Silicon Substrate: *Ebraheem Azhar*[1]; Shangzhu Sun[2]; Jhih-Hong Peng[1]; Bruce Willner[2]; Sandwip Dey[1]; Gary Tompa[2]; Hongbin Yu[1]; [1]Arizona State University; [2]Structured Materials Industries

ZnO and its various nanoscale structures have many unique properties that could have promising applications in electronics, optoelectronics, and sensing. The ability to grow these structures using metal-organic chemical vapor deposition (MOCVD) technique will facilitate the large scale production for their potential applications. It is therefore important to control and understand the growth of ZnO nanostructures using such a technique. Vertically aligned ZnO nanopillars and wires have been demonstrated to grow on GaN/Al2O3 template as well as on ZnO substrates. This is in contrast to the often observed growth on Si(001) and Si(111) where first the formation of a layer can be observed on which the nucleation of the poorly aligned nanopillars starts. It is suggested that this is due to the large lattice mismatch between ZnO and Si compared to the almost perfectly lattice matching to GaN/Al2O3. In this work, we show by using MOCVD and appropriate growth conditions and procedures, vertically aligned ZnO nanowires can be formed on Si(100) substrate. ZnO nanowires were grown using DEZn and oxygen in an inert carrier gas at substrate temperatures ranging from 450 to 550°C. Field-emission SEM was used to characterize ZnO nanowire samples in both planar and cross-sectional geometry, and indicating the vertical alignment of ZnO nanowires with respect to Si (100) substrate. X-ray diffraction was used to characterize crystal orientation of ZnO nanowires. All the strong peaks can be readily indexed to hexagonal wurtzite ZnO with cell constants comparable to the reported data. The strong intensity of (0 0 2) peak relative to other peaks exhibits high c-axis growth orientation of the ZnO nanowires. MOCVD growth of ZnO nanowires with and without Au catalyst seeds were compared, and both cases show vertical growth on Si(100) substrate. In addition, patterned Au seed arrays of various size and spacing are used to modify and study the growth mechanisms of ZnO nanowires on the substrate.

P2.22 Growth and Dielectric Properties of Compositionally Graded BST Films Deposited by MOCVD: *Nick Sbrockey*[1]; S. Alpay[2]; Melanie Cole[3]; T. Kalkur[4]; Jonathan Spanier[5]; Gary Tompa[1]; [1]Structured Materials Industries, Inc.; [2]University of Connecticut; [3]U.S. Army Research Laboratory; [4]University of Colorado at Colorado Springs; [5]Drexel University

Thin films of barium-strontium-titanate (BST) can serve as voltage tunable dielectrics in a variety of RF and microwave devices. Compositionally graded BST films are needed, in order to simultaneously optimize these films for highest permittivity, highest tunability, maximum temperature stability and minimum dielectric loss. Deposition of BST films by metal organic chemical vapor deposition (MOCVD) provides the greatest degree of flexibility to tailor the film composition profile, and achieve the optimum combination of properties. This paper describes deposition of compositionally graded BST films, using a dual liquid injection - flash evaporation, metal organic chemical vapor deposition (MOCVD) technique.

Injecting two separate precursor solutions (one for Ba-Ti oxide and one for Sr-Ti oxide) provides a simple and direct means to adjust the Ba/Sr ratio (and thus the Curie temperature) of the BST film during growth. The dual liquid injection MOCVD technique also avoids potential problems with ligand exchange for Group IIA beta-diketonate precursors. BST films were deposited on Pt coated (100) silicon and Pt coated (1-102) sapphire substrates. The Ba/Sr ratio was graded from 90/10 to 60/40 throughout the film thickness. The films were fabricated into parallel plate capacitor structures for electrical characterization. Dielectric properties of the BST film were measured as a function of temperature and applied DC voltage. Compositionally grading is shown to be an effective technique to optimize both the dielectric properties and temperature stability of MOCVD deposited BST films.

P2.23 Trace Impurity Detection in Electronic Grade Arsine by Cavity-Enhanced Direct Frequency Comb Spectroscopy: Kevin Cossel[1]; Florian Adler[1]; Kris Bertness[2]; Michael Thorpe[1]; Jun Feng[3]; *Mark Raynor*[3]; Jun Ye[1]; [1]JILA; [2]National Institute of Standards and Technology; [3]Matheson Tri-Gas, Inc.

The presence of trace levels of contaminants in process gases such as arsine is undesirable as they can result in unintentional doping and lattice defects in III-V compound semiconductors. In particular oxygen incorporation in alloys such as AlGaAs forms a deep recombination level resulting in decreased photoluminescence efficiency and carrier lifetimes. A primary source of oxygen is trace water vapor, which has been shown to impact device performance at 10 ppb or less. Water vapor can be introduced from several sources such as the gas cylinder or a contaminated gas distribution system. In addition other impurities including carbon dioxide, hydrocarbons and hydrogen sulfide must be controlled. Consequently, development of sensitive analytical methods to measure and improve gas purity is important. Cavity-enhanced direct frequency comb spectroscopy (CE-DFCS) has recently been developed and investigated for detection of multiple gas species at trace levels. This novel technique offers a unique combination of high bandwidth, rapid data acquisition, high sensitivity and high resolution, which is unavailable with conventional systems. Previous investigations have focused on proof-of-principle experiments with analytes in an inert gas matrix [1]. In this work, we present the application of CE-DFCS for impurity detection in electronic grade arsine in a previously unexplored spectral region (1.75-1.95 μm) where absorption bands of multiple important impurities were expected to overlap with a transparent region in the arsine absorption spectrum. A gas handling system was designed and used to spike contaminants into arsine at known concentrations. Arsine was found to be a strongly absorbing matrix gas with an extremely congested and broadband spectrum which rendered trace detection of impurities, such as methane, carbon dioxide and hydrogen sulfide, exceptionally difficult. However identification and quantification of trace water, using lines that were isolated from the arsine absorption features, was possible using the CE-DFCS system. A minimum detection concentration of 31 ppb water vapor in arsine was achieved. These and other results will be discussed in this presentation. [1] M.J. Thorpe, D. Balslev-Clausen, M.S. Kirchner and J. Ye, Cavity enhanced optical frequency comb spectroscopy: application to human breath analysis, Opt. Express 16, 2008, 2387-2397.

P2.24 Record Spectral Purity of GaAs/AlGaAs Quantum Wells: Relevance of a Consistent Tool to Monitor MOVPE Reactor Quality: *Valeria Dimastrodonato*[1]; Lorenzo Mereni[1]; Robert Young[2]; Gediminas Juska[1]; Emanuele Pelucchi[1]; [1]Tyndall National Institute, University College Cork; [2]Lancaster University

MetalOrganic Vapor Phase Epitaxy (MOVPE) has revealed to be a crucial growth technique in terms of process parameters control, throughput, ability to precisely and rapidly vary alloy compositions. High quality remains a critical issue though, especially in comparison to Molecular Beam Epitaxy (MBE). Well resolved near-band emission measurements and Hall investigations on (Al)GaAs epitaxial layers and two-dimensional electron gases have been extensively conducted with the goal to study the contamination impact on optical and transport properties. Different III/V sources have been also suggested to minimize C and O incorporation. Nonetheless a large disparity regarding the material quality still remains within MOVPE community and no efficient and reproducible approach toward a high purity reactor environment has been delineated yet. We present a high quality 15nm thick GaAs/AlGaAs Quantum Well (QW) structure, grown on GaAs (100) 0.2° misoriented substrate, with record spectral purity: low temperature μPhotoLuminescence characterizations of the neutral exciton emission revealed a Full Width at Half Maximum of 412μeV, approaching the lowest published MBE value of ~300μeV for similar systems. Most importantly our structure represents a consistent tool to efficiently monitor impurities inside the reactor and understand the critical parameters limiting the achievement of high purity in MOVPE processes. Key feature which needs to be examined and then controlled is the hydride purification system. In particular we studied the impact on the optical properties of our QW of the performances of two different commercially available AsH3 purifiers, both claiming H20 and O2 purification levels below 1ppb. Our analysis highlights the relevance of a proper activation/conditioning procedure of the employed purifiers: although both of them delivered extremely low contamination levels, different periods of activation were necessary to attain level of purity «1ppb (concerning H20), essential for reaching spectral features as pure as those of our QWs. Moreover the purity achieved in our reactor enables the possibility to grow other III/V material systems, such as pyramidal site controlled InGaAs/GaAs Quantum Dots, whose spectral purity becomes comparable with some of the best MBE grown structures.

P2.25 The Characterization of *p*-GaAs/*i*-InGaAsN/*n*-GaAs Hetero-Junction Solar Cell with Various DMHy Flow Rates: *Wu Tzung-Han*[1]; Yan-Kuin Su[1]; Yu-Jen Wang[1]; [1]Institute of Microelectronics and Advanced Optoelectronic Technology Center, National Cheng Kung University

In this study, we have grown *p*-GaAs/*i*-InGaAsN/*n*-GaAs double heterojunction solar cell (DHJSC) by AIX200 metalorganic chemical vapor deposition (MOCVD). InxGa1-xAs1-yNy films were grown by trimethyl-indium (TMIn), trimethylgallium (TMGa), ter-tiarybutylarsine (TBAs), and dimethyl-hydrazine (DMHy). InGaAsN films were grown on n-type GaAs substrate orientated 2° off (100) towards <110>. The lattice matched InGaAsN films were grown at the growth temperature 550°C with DMHy flow rate 3.5×10^{-3} mol/min and 3.8×10^{-3} mol/min, respectively. The FHWM from x-ray diffraction results showed the crystal quality of intrinsic InGaAsN absorption layer, the FHWM decreases with higher DMHy flow rate. We selected the suitable parameters to grow intrinsic InGaAsN absorption layers at 550°C of double heterojunction *p-i-n* solar cell. The conversion efficiency of DHJSCs increases form 1.78% to 2.33% with lower DMHy flow rate. The open circuit voltage of DHJSCs increase from 0.29 V to 0.35 V and the short circuit current of DHJSCs increase from 11.56 mA/cm^2 to 13.56 mA/cm^2.

P2.26 Structural Characterization of OMVPE Grown $In_{1-x}Mn_xAs$ Epitaxial Layers: *Stanislav Hasenohrl*[1]; Edmund Dobrocka[1]; Jan Soltys[1]; Jozef Novak[1]; Pavol Strichovanec[1]; Ivo Vavra[1]; [1]Institute of Electrical Engineering, Slovak Academy of Sciences

The $In_{1-x}Mn_xAs$ epitaxial layers were grown with the aim to prepare diluted magnetic semiconductor layers (DMS). A set of $In_{1-x}Mn_xAs$ epitaxial layers was prepared using a low pressure OMVPE reactor AIX 200. The growth temperature and the reactor pressure were set to 500ºC and 70 mbar respectively. The deposition rate was in the range of 0.1 μm/h; layer thickness was 300 nm. The As and In precursors were arsine (AsH_3) and trimethylindium (TMIn). The source of Mn was bis(monomethylc yclopentadienyl) manganese ($(MeCp)_2Mn$). Substrates were undoped semiinsulating GaAs wafers with (100) exact orientation. The content of Mn in the layers (x_{Mn}) was varied. It was set by changing the partial pressure ratio $p(MeCp)_2Mn/pTMIn$ in the reactor from 0 up to 0.68. The highest value led to a layer with $x_{Mn}=0.13$. $In_{1-x}Mn_xAs$ epitaxial films were prepared also by the atmospheric pressure OMVPE using tricar bonyl(methylcyclopentadienyl)manganese (TCMn) source [1]. Compared to TCMn, using $(MeCp)_2Mn$ requires more than 5 times higher Mn source vapour pressure in the reactor to achieve the comparable Mn concentration in the layer. The manganese concentration in the layers was determined using high resolution X ray diffraction (HRXRD). Layer mismatch determined by HRXRD was used for calculation of x_{Mn} from Vegard`s law providing that the lattice parameter of the hypothetical zincblende MnAs is 0.601 nm [2]. The Mn content in the layers was verified by energy dispersive X ray (EDX) microanalysis. Magnetic properties of layers were measured using a superconducting quantum interference device (SQUID). Layers with x_{Mn} higher than 0.04 exhibited ferromagnetism up to the room temperature. The Curie temperature T_c was approximately 343 K. Contrary to $In_{1-x}Mn_xAs$ epitaxial films described in [1] which were phase pure up to $x_{Mn}=14$ (corresponding Mn/In ratio in the gas phase 0.12), in our films (although they were grown in the “single phase” region of the schematic phase diagram from [1]) hexagonal precipitates are observed by the detailed HRXRD analysis. These precipitates are not seen in the electron diffraction pattern taken during their characterization in the transmission electron microscope (TEM). In our contribution we will report on structural properties of set of layers with variable x_{Mn}.

P2.27 Vapor Pressure of Erbium, Neodymium and Magnesium Based Organometallic Precursors: Pavel Morávek[1]; Michal Fulem[1]; Jirí Pangrác[2]; Kvetoslav Ružicka[1]; Eduard Hulicius[2]; *Tomislav Šimecek*[2]; Vlastimil Ružicka[1]; Boris Kozyrkin; [1]Institute of Chemical Technology; [2]Institute of Physics, CAS

Metalorganic Vapor Phase Epitaxy (MOVPE) and other epitaxial techniques use a broad variety of organometallic precursors. The correct and exact knowledge of the essential physical and chemical parameters is necessary for precise technological application of these materials during technological processes. In particular volatility data and a detailed vapor pressure equation is essential for controlled precursor dosimetry and thermodynamic analysis of MOVPE growth. Over the last decade our laboratories have been involved in systematic measurements of vapor pressure of new as well as recently available high quality precursors used for MOVPE. The vapor pressure data of various precursors of Ga, Al, Sb, Zn, Si, In, Y, Zr and Ge were determined in our previous works. In this work we report the vapor pressure data of several erbium, neodymium and magnesium precursors measured by the static method. The following precursors were studied: tris(2,2,6,6-tetramethylheptane-2,5-dionato)erbium; tris(isopropylcyclopentadienyl)erbium; tris(2,2,6,6-tetramethylheptane-2,5-dionato)neodymium; tris(isopropylcyclopentadienyl)neodymium; bis(cyclopentadienyl)magnesium; bis(methylcyclopentadienyl)magnesium; bis(ethylcyclopentadienyl)magnesium; bis(isopropylcyclopentadienyl)magnesium. The stability of the studied precursors, which can significantly affect vapor pressure measurements, is discussed.

A

Abid, M 23, 29, 37
Adachi, M 28
Adler, F 50
Ail, U 49
Alaan, U 39
Alam, A 45
Ali, M 11
Allerman, A 8
Alliman, D 27
Alpay, S 49
Arakawa, Y 34, 37
Aranguren, M 48
Argut, I 20
Arita, M 37
Aschenbrenner, T 29
Ashraf, S 32
Atalay, R 46
Augendre, E 34
Azarow, A 48
Azhar, E 49

B

Babcock, S 11
Barrigon, E 12
Bazarevskiy, D 14
Beaudoin, G 17, 38, 48
Behmenburg, H 8
Bender, D 27
Bergbauer, W 37
Bertness, K 50
Bertram, F 20, 21, 22
Beveratos, A 38
Beyer, A 13, 33
Bhattacharya, A 9, 47
Biefeld, R 11, 23
Bimberg, D 15
Biskupek, J 29
Black, K 32
Blaesing, J 21
Bläsing, J 35
Blecker, K 19
Blekker, K 30
Bloeck, U 22
Bloemers, C 44
Blokhin, S 15
Boca, A 18
Bolinsson, J 28, 31
Bonanno, P 37
Booker, I 35
Borasio, M 25
Bordel, D 34
Borg, M 31
Borghs, G 9
Borkenhagen, B 22
Botha, J 32
Botha, R 22, 43
Bougrov, V 11
Boukiour, H 35
Bour, D 28
Boyd, A 45
Brammertz, G 12
Branch, M 48
Bremers, H 28
Brendel, M 28
Brien, D 24
Brox, O 26
Brückner, S 13, 22
Brueckner, S 12
Brunner, F 13, 25, 36
Buegler, M 46
Bugge, F 26
Byrnes, D 42

C

Caban, P 39, 42
Caha, O 44
Cai, Z 37
Caliskan, D 39
Canizares, C 10
Cao, J 21
Caroff, P 28
Carron, R 10
Caymax, M 12
Cederberg, J 27, 37
Chalker, P 32
Chan, W 47
Chang, J 18
Chang, S 21, 41
Chang, W 47
Chang-Hasnain, C 19
Chatterjee, S 15
Chen, J 43
Chen, P 15
Chen, R 19
Chen, W 46, 48
Chen, Z 41
Cheng, K 9
Cheng, S 21
Cheng, Y 41, 47
Cherkashin, N 14
Cherng, Y 33
Chernikow, A 15
Chiang, B 21
Chiu, C 47
Cho, H 40, 48
Choi, K 37
Choi, S 14, 29
Choi, W 45
Christen, J 20, 21, 22
Chu, H 11, 20
Chuang, L 19
Chuvilin, A 29
Clavelier, L 34
Cockburn, J 26
Cole, M 49
Coleman, E 18, 49
Collazo, R 46
Coltrin, M 24
Commin, P 26
Cossel, K 50
Creighton, J 21, 24
Cross, K 27

D

Dadgar, A 21, 35
Dangbégnon, J 32
Dapkus, P 11, 20
Dartsch, H 29
Dauelsberg, M 24
Daum, W 22
Decobert, J 11, 33
Degroote, S 9
Deng, D 15
Deppert, K 28, 30
Derluyn, J 9
Deura, M 12
Dey, S 49
Dick, K 28, 30, 31
Dietz, N 46
Dimastrodonato, V 21, 38, 42, 50
Dinh, D 20
Djebbour, Z 29
Dobrich, A 12, 13, 22
Dobrocka, E 50
Doescher, H 12
Döscher, H 13, 22
Dräger, A 28
Drechsel, P 25
Dudley, P 10
Dumiszewska, E 42
Du Pasquier, A 49
Dupuis, N 11
Dupuis, R 14, 20, 28, 29, 33
Dwir, B 10
Dyer, D 43

E

Ebert, C 15, 42, 43
Eichfelder, M 15, 16, 26
Einfeldt, S 13
Elvira, D 38
En Naciri, A 29
Enya, Y 28
Erbert, G 26
Ermer, J 18
Escobosa, A 40

F

Fahle, D 35, 36
Fain, B 38
Fanciulli, M 32
Fandrich, M 29
Favaloro, T 18
Fekete, D 10
Feneberg, M 8
Feng, J 50
Ferguson, I 46
Fetzer, C 18
Figge, S 29
Figiel, J 24
Fischer, A 14, 28
Floehr, K 44
Forghani, K 8, 29
Fujan, K 8
Fukui, T 17, 19, 30, 31
Fulem, M 51
Fündling, S 37

G

Galeckas, A 48
Galiana, B 12
Gallo, P 10
Gamage, S 46
Ganguli, T 9, 47
Ganjipour, B 31
Garreau, A 11
Garrod, T 10
Gautier, S 23, 29, 37
Geisz, J 17
Germain, M 9
Germann, T 15
Giesen, C 8
Gogneau, N 17, 38, 48

Goh, W 37
Gokhale, M 9, 47
Gradkowski, K 21
Gruetzmacher, D 44
Guillamet, R 11
Guimard, D 34
Günel, H 44
Gustafsson, A 31
Gütay, L 32
Gutsche, C 19, 30
Gutt, R 8

H

Ha, S 45
Haberland, K 13, 25
Hader, J 15
Hangleiter, A 28
Hannappel, T 12, 13, 17, 22
Hara, S 17, 19, 31
Hardtdegen, H 8, 44
Hasenohrl, S 26, 50
Hassanet, S 27
Hatui, N 47
Hazdra, P 44
Hebert, P 18
Heinle, U 8
Hempel, T 21, 35
Hertkorn, J 8
Heuken, M 8, 28, 35, 36, 45
Heyns, M 12
Heys, P 32
Hillerich, K 30
Hindley, S 32
Hiruma, K 17, 19
Hoffmann, L 28
Hoffmann, M 43
Hoffmann, V 13
Holt, M 30
Hommel, D 29
Hong, C 35
Hong, W 18
Hospodková, A 44
Hostein, R 38
Hsiao, C 46, 48
Hsu, H 21
Hu, X 40
Huang, C 40, 41
Huang, H 47
Huang, S 21
Huang, Y 33
Hughes, G 42
Hulicius, E 19, 44, 51
Hurley, P 42
Huyet, G 21
Hwang, J 40
Hwang, S 46
Hytch, M 14

I

Iga, R 9
Ikeda, T 46
Ikegami, T 28
Ikenaga, K 46
Inoue, Y 9
Ishikawa, H 36
Islam, M 30
Ito, S 31

J

Jakomin, R 17
Jamil, M 46
Jang, J 40
Jansen, R 8, 35, 36
Jetter, M 8, 15, 16, 22, 26
Jha, S 10, 11
Jia, C 41
Johansson, J 28, 30, 37
Johnson, E 17
Jönen, H 28
Jones, A 32
Jones, G 48
Jong Jin, J 40
Jung-Hwan, H 40
Juska, G 38, 50

K

Kadir, A 47
Kaeppeler, J 45
Kaiser, U 8, 29
Kalisch, H 8, 35, 36
Kalkur, T 49
Kanazawa, S 9
Kang, B 41
Kang, S 41
Kang, X 41
Kanjolia, R 32
Kapon, E 10
Kappers, M 24, 35
Katayama, K 28
Kazmierski, C 11
Ke, C 47
Kelekci, O 39
Kennedy, K 26
Kessler, C 16
Kim, H 14, 29, 35, 47
Kim, J 28, 41, 45, 46
Kim, K 46
Kim, M 41
Kim, N 41
Kim, S 10, 14, 28
King, R 18
Kirch, J 10, 34
Klein, M 8
Klein, O 8
Kleinschmidt, P 12, 22
Knauer, A 13, 36
Kneissl, M 13, 20, 24, 36
Knight, G 42
Ko, C 41, 46
Ko, W 19
Kobayashi, N 18, 30
Kobayashi, Y 46
Koch, S 15
Koizumi, A 34
Koleske, D 24
Kölper, C 37
Komagata, K 31
Kondo, Y 12
Konen, J 34
Kong, B 40, 48
Kozyrkin, B 51
Kremzow, R 20
Krishnan, B 39
Krost, A 21, 35
Kruse, C 29
Krysa, A 26
Kryzhanovskaya, N 14
Kuan, T 11
Kuboya, S 25
Kuech, T 10, 11, 31, 34
Kuei, P 47
Kueller, V 36
Kuldová, K 44
Kunert, B 15, 24, 33
Kunst, M 22
Kunze, M 8
Kuo, C 41
Kuo, H 21, 47
Kuo, S 46, 48
Kuznetsov, A 48
Kwan-Hyun, L 40
Kyono, T 28

L

Lackner, D 33
Lähnemann, J 37
Lai, F 46, 48
Lai, M 47
Langer, T 28
Largeau, L 17, 38
Larrabee, D 18
Larsen, J 32
Laskar, M 9, 47
Lau, K 13, 14, 15
Lau, M 18
Lazzarini, L 32, 44
Ledentsov, N 15
Lee, D 40, 43, 46, 48
Lee, J 45
Lee, K 40, 41, 47
Lee, S 20, 39, 46, 48
Le Gratiet, L 37, 38, 48
Leute, R 8
Leys, M 9, 12, 14
Li, D 40, 41
Li, J 47
Li, L 40
Li, Q 25, 36
Li, R 40
Li, S 37
Li, T 47
Li, X 30
Li, Z 30
Liebmann, M 44
Lilienkamp, G 22
Lim, H 39, 48
Lin, W 41, 48
Linder, N 37
Lipsanen, H 11
Lipski, F 8, 20, 21, 29
Liu, J 28
Liu, L 40
liu, N 40
Liu, X 17, 18
Liu, Y 48
Lochner, Z 28, 29
Logeeswaran, V 30
Lohn, A 30
Longo, M 32
Loo, R 12
Lott, J 15
Lovergine, N 44
Lu, T 21, 31, 47
Lundin, W 11, 14
Lutsenko, E 36

Lysov, A 19, 30

M

Maaßdorf, A 43
Mahajan, S 39
Manavaimaran, B 39
Mangyo, H 46
Martine, M 33
Martinez, A 37
Marzo, F 44
Mason, N 12
Matsumoto, K 46
Matthai, S 30
Mauder, C 35, 36
Mauguin, O 17
Mawst, L 10, 34
Medjdoub, F 9
Men, Y 29
Meng, F 39
Mereni, L 21, 38, 42, 50
Messing, M 28, 30
Metzner, S 20, 21, 22
Meuller, B 30
Meuris, M 12
Meyer, A 8
Miao, Z 40, 41
Miccoli, I 44
Michler, P 8, 15, 16, 22, 26
Migan-Dubois, A 29
Mitsuhara, M 9
Miyoshi, T 8
Moewe, M 19
Mogilatenko, A 26
Moloney, J 15
Mooney, P 33
Morávek, P 51
Morgenstern, M 44
Morita, K 31
Motohisa, J 17, 19, 31
Motyka, M 42
Moudakir, T 23, 29, 37
Mukai, T 8
Mutig, A 15

N

Na, H 41, 47
Nagahama, S 8
Nakamura, T 28
Nakano, Y 12, 13, 18, 26, 27, 33
NAM, O 48
Nam, O 39, 40, 46
Nanishi, Y 41, 45
Narayan, B 29
Narukawa, Y 8
Nasi, L 32
Neuschl, B 8
Ng, K 19
Nguyen, D 12
Nikolaev, A 14
Nilsson, H 31
Nishioka, M 34
Noltemeyer, M 21
Nötzel, R 38, 42
Novak, J 26, 50
Nozaki, S 34

O

Odedra, R 32
Odnoblyudov, M 11
Ohlmann, J 13, 33
Ok-Hyun, N 40
Onabe, K 25, 28
Onishi, T 18, 30
Onitsuka, R 18
Ono, H 46
Orsal, G 23, 29, 37
Oswald, J 44
Ougazzaden, A 17, 23, 29, 37
Ozbay, E 39

P

Pangrác, J 44, 51
Pantzas, K 23
Paranjpe, A 42, 43
Parekh, A 18
Park, H 39, 48
Park, I 14
Park, S 14, 41, 45
Park, W 46
Passow, T 8
Patriarche, G 23, 37, 38, 48
Pelucchi, E 21, 38, 42, 50
Peng, J 49
Penz, A 44
Petkov, N 42
Pitts, O 33
Pohl, U 15
Poisson, M 35
Ponce, F 14, 28
Prete, P 44
Pristovsek, M 20, 24
Prost, W 19, 30
Provost, L 40
Pulwin, Z 42, 43
Püsche, R 24

R

Radavich, K 34
Rahimzadeh Khoshroo, L 35
Rahman, A 9, 47
Rajesh, M 34
Ramdane, A 37
Ravash, R 35
Raynor, M 46, 50
Regolin, I 19, 30
Reiffers, M 26
Reischle, M 15, 16
Reuters, B 36
Revin, D 26
Rey-Stolle, I 12
Richard, O 12
Riechert, H 25
Robert-Philip, I 38
Roblin, C 17
Roca I Cabarrocas, P 17
Rockenfeller, O 45
Roder, C 37
Rodriguez, H 36
Romanov, A 11
Rösch, R 20
Rossbach, R 15, 16, 26
Rossow, U 24, 28
Rudra, A 10, 15
Ružicka, K 51
Ružicka, V 51
Ryou, J 14, 28, 29, 33
Rzheutskii, M 36

S

Sagnes, I 17, 38, 48
Sagol, B 22
Sakharov, A 14
Salehzadeh, O 20
Salicio, O 32
Salviati, G 44
Samuelson, L 28, 31
Sánchez, V 40
Sano, E 31
Sano, M 8
Sato, T 9, 31
Savas, Ö 24
Sbrockey, N 48, 49
Schaepers, T 44
Schenk, T 25
Schineller, B 45
Schlegel, J 24
Scholz, F 8, 20, 21, 29
Schön, O 24
Schulz, W 15, 16, 26
Schulze, J 15
Schwaiger, S 8, 20, 21, 29
Schwarzburg, K 22
Segal, A 24
Sek, G 42
Seki, Y 25
Selvamanickam, V 18
Senevirathna, I 46
Seong, T 47
Shah, A 9, 47
Shakouri, A 18
Shchukin, V 15
Shen, B 40, 41
Shen, J 48
Shen, S 28, 29
Shimanaka, K 36
Shimogaki, Y 27, 33
Shivashankar, S 49
Siebentritt, S 32
Sijmus, B 9
Šimecek, T 44, 51
Sirenko, A 37
Sitar, Z 46
Sizov, V 14
Sköld, N 31
Sladek, K 44
Soltani, A 23, 37
Soltys, J 50
Sommerhalter, C 45
Song, J 40, 41
Song, K 41, 46
Sopanen, M 11
Spanier, J 48, 49
Spasova, M 30
SpringThorpe, A 26
Steger, M 33
Stellmach, J 24
Stewart, L 11, 20
Stolz, W 9, 13, 15, 24, 33
Strassburg, M 37
Straznicky, J 30
Strichovanec, P 50
Stringfellow, G 8
Strupinski, W 39, 42
Su, Y 21, 42, 50
Sugita, K 13

Sugiyama, M 12, 13, 18, 27, 33
Suihkonen, S 11
Sumitomo, T 28
Sun, K 14, 28
Sun, S 40, 49
Sundaram, S 39
Supplie, O 13, 22
Svensk, O 11
Szabó, N 22
Szmidt, J 39

T

Tachikawa, T 25
Takagi, S 12, 33
Takenaka, M 12, 33
Talalaev, R 24
Talla, K 32
Tanemura, T 18
Tang, N 41
Tao, Y 41
Tegude, F 19, 30
Telek, P 26
Terada, Y 33
Tessarek, C 29
Thelander, C 31
Thewalt, M 33
Thieu, Q 25
Thomas, S 45
Thonke, K 8
Thorpe, M 50
Tischer, I 8
Tokuyama, S 28
Tomioka, K 17, 19
Tompa, G 18, 40, 48, 49
Törmä, P 11
Torres, R 46
Trampert, A 36, 37
Tran, T 19
Tränkle, G 13
Troadec, D 23, 37
Trunk, M 48
Tsao, J 8, 19
Tsatsulnikov, A 14
Tzung-Han, W 42, 50

U

Uchida, K 34
Ueno, M 28
Ulysse, C 48
Umarji, A 49
Usov, S 14

V

Valkovskiy, G 14
Vavra, I 26, 50
Veit, P 35
Veldhoven, P 38, 42
Venkatachalapathy, V 48
Vilchis, H 40
Vininski, J 46
Volz, K 13, 15, 21, 24, 33
Vyskocil, J 44

W

Waag, A 37
Wächter, C 8, 22
Wagener, M 22, 32, 43
Wagener, V 22, 43
Waldmueller, I 27
Walukiewicz, W 33
Wang, C 24, 47
Wang, G 12, 25, 30, 36
Wang, H 38, 42
Wang, J 29, 46
Wang, K 36
Wang, L 40
Wang, S 30, 47
Wang, X 40, 41
Wang, Y 13, 15, 42, 50
Wanke, M 27
Wann, C 41
Watkins, S 9, 20, 33
Wehmann, H 37
Wernersson, L 31
Wesolowski, M 42
Weyers, M 13, 25, 26, 35, 36, 43
Wiedmann, M 10, 11
Wiemer, C 32
Wieneke, M 21
Wiesner, M 15
Williams, P 32
Williams, R 30
Willner, B 40, 49
Witte, H 21
Witte, W 33
Woitok, J 35, 36
Wunderer, T 20, 21, 29

X

Xu, F 40, 41

Y

Yablonskii, G 36
Yagovkina, M 14
Yakovlev, E 14, 24
Yang, A 33
Yang, C 21, 45
Yang, J 27
Yang, Z 40, 41
Ye, J 50
Yeh, T 11, 20
Yoder, P 14, 28
Yoo, G 39, 48
Yoon, D 41, 46
Yoon, E 35, 41, 45, 47
Yoshimura, M 19
Yoshizumi, Y 28
Young, R 38, 42, 50
Yu, H 43, 49
Yu, N 15
Yu, T 41
Yuan, J 38, 42
Yuan, T 47

Z

Zavarin, E 14
Zeimer, U 26, 36
Zettler, J 13
Zettler, T 12, 25
Zhang, G 40, 41
Zhang, T 48
Zhang, W 42, 43
Zhang, Y 28, 29
Zhong, Z 13
Zou, X 15
Zuo, R 43

Notes

ICMOVPE wishes to thank the following sponsors and exhibitors:

(as of April 27, 2010)

Air Force Office of Scientific Research
AIXTRON
Akzo Nobel
Army Research Office
Dockweiler Chemicals GmbH
Dow
GHO Adventures
Johnson Matthey
Jordan Valley Semiconductor
K-Space Associates, Inc
Kyocera Industrial Ceramics Corp
LayTec GmbH
Lehighton Electronics, Inc
Matheson Tri-Gas
Noah Precision
Office of Naval Research
ORS Limited
Power+Energy, Inc
PVA TePla AG
SAFC HiTech
Sandia National Laboratory
STR Group
Structured Materials, Inc
Taiyo Nippon Sanso Corp
Valence Process Equipment, Inc
Veeco
Wafer Technology
WEP

TMS

Your Professional Partner for Career Advancement

EXPANDING YOUR HORIZONS

Get involved with the **Electronic, Magnetic, & Photonic Materials Division (EMPMD**) of TMS! Members actively promote technical exchange and assist in professional development through programming, publications, continuing education, mentorship, and professional recognition. **EMPMD** addresses the synthesis and processing, structure, properties, and performance of electronic, photonic, magnetic and superconducting materials, as well as the materials used in packaging and interconnecting such materials in device structures. **EMPMD** consists of 10 committees, including the Electronic Materials Committee, which sponsored this conference.

To become a member of TMS, apply online at **www.tms.org/Society/membership.html.**

ABOUT TMS

The Minerals, Metals & Materials Society (TMS) is a professional organization that encompasses the entire range of materials and engineering, from minerals processing and primary metals production to basic research and the advanced applications of materials. If at any time before, during or after the event you would like to offer suggestions or comments, your input is always welcome.

TMS
EMPMD
Electronic, Magnetic
& Photonic Materials
Division

www.tms.org

BE MATERIALS MINDED

TMS is committed to environmental responsibility as we fulfill our mission to promote global science and engineering by going green at our headquarters, conferences and through membership communication.

Be materials-minded. M *Join* TMS *in reducing, reusing and recycling.*

ICMOVPE-XV Program Grid

	Sunday PM	Monday AM	Monday PM	Tuesday AM	Tuesday PM	Wednesday AM	Thursday AM	Thursday PM	Friday AM
Lakeside Ballroom	Welcome Reception 7:00-9:00 PM	Opening Remarks 8:00-8:20 AM Plenary Session 8:20-9:50 AM Nitrides I 10:20 AM-Noon	In Situ Monitoring and Process Control 1:30-3:30 PM Nitrides (LEDs) 4:00-5:20 PM	Tuesday Invited Talks 8:30-9:30 AM Energy Technology (Solid State Lighting, PV, Thermoelectrics, etc) 10:00 AM-Noon	Nitrides (Nonpolar and Semipolar) 1:30-3:30 PM Panel Discussion: The Role of III-Vs in SSL and Terrestrial PV 6:30-9:30 PM	Wednesday Invited Talks 8:30-9:30 AM Nitrides II 10:00 AM-Noon	Thursday Invited Talks 8:30-9:30 AM Nitrides (Devices) 10:00 AM-Noon	Arsenides, Phosphides 1:30-3:30 PM Conference Reception 6:30-7:30 PM Conference Banquet 7:30-9:30 PM	Friday Invited Talks 8:30-9:30 AM Nitrides III 10:00 AM-Noon
Regency ABDE		Continental Breakfast 7:00-8:00 AM Coffee Break 9:50-10:20 AM	Coffee Break 3:30-4:00 PM Exhibitor's Reception 5:30-6:30 PM	Continental Breakfast 7:00-8:30 AM Coffee Break 9:30-10:00 AM	Coffee Break 3:30-4:00 PM Poster Session I 4:00-6:00 PM	Continental Breakfast 7:00-8:30 AM Coffee Break 9:30-10:00 AM	Continental Breakfast 7:00-8:30 AM Coffee Break 9:30-10:00 AM	Coffee Break 3:30-4:00 PM Poster Session II 4:00-6:00 PM	Continental Breakfast 7:00-8:30 AM Coffee Break 9:30-10:00 AM
				Exhibits 9:30 AM-5:00 PM		Exhibits 10:00 AM-1:00 PM	Exhibits 10:00 AM-5:00 PM		
Regency CF		Arsenides, Phosphides, Antimonides and Dilute Nitrides 10:20 AM-Noon	Patterned and Selective Area Growth 1:30-3:30 PM Devices I 4:00-5:20 PM	Heteroepitaxy - Nanostructures 10:00 AM-Noon	Characterization 1:30-3:30 PM	Devices II 10:00 AM-Noon	Nanowires 10:00 AM-Noon	Novel Materials 1:30-3:30 PM	Nanostructures 10:00 AM-Noon
Regency Foyer	Registration 3:00-9:00 PM	Registration 7:00 AM-5:00 PM		Registration 8:00 AM-5:00 PM		Registration 8:00 AM-1:00 PM	Registration 8:00 AM-5:00 PM		Registration 8:00 AM-Noon